Metabolomics and dereplication-based isolation of novel bioactive natural products from marine sponge-associated actinomycetes

Metabolomik und Dereplikations-basierte Isolierung von neuen bioaktiven Naturstoffen aus marinen, Schwamm-assoziierten Actinomyceten

Doctoral thesis for a doctoral degree
at the Graduate School of Life Sciences,
Julius-Maximilians-Universität Würzburg,
Section: Infection and Immunity

submitted by

Cheng Cheng

from

Tianjin, China

Würzburg, June, 2016

Submitted on:

Members of the *Promotionskomitee*:

Chairperson: Prof. Dr. Thomas Müller

Primary Supervisor: Prof. Dr. Ute Hentschel Humeida

Supervisor (Second): Prof. Dr. Martin J. Mueller

Supervisor (Third): Dr. RuAngelie Edrada-Ebel

Supervisor (Fourth): Dr. Usama Ramadan Abdelmohsen

Date of Public Defence:

Date of Receipt of Certificates:

Affidavit

I hereby confirm that my thesis entitled "Metabolomics and dereplication-based isolation of novel bioactive natural products from marine sponge-associated actinomycetes" is the result of my own work. I did not receive any help or support from commercial consultants. All sources and / or materials applied are listed and specified in the thesis.

Furthermore, I confirm that this thesis has not yet been submitted as part of another examination process neither in identical nor in similar form.

Würzburg, 6th Jun 2016
Place, Date Signature

Eidesstattliche Erklärung

Hiermit erkläre ich an Eides statt, die Dissertation "Metabolomik und Dereplikations-basierte Isolierung von neuen bioaktiven Naturstoffen aus marinen, Schwamm-assoziierten Actinomyceten" eigenständig, d.h. insbesondere selbständig und ohne Hilfe eines kommerziellen Promotionsberaters, angefertigt und keine anderen als die von mir angegebenen Quellen und Hilfsmittel verwendet zu haben.

Ich erkläre außerdem, dass die Dissertation weder in gleicher noch in ähnlicher Form bereits in einem anderen Prüfungsverfahren vorgelegen hat.

Würzburg, 6th Jun 2016
Ort, Datum Unterschrift

Acknowledgments

I would like to express my deepest gratitude to all those who helped me to make this thesis possible.

First, I would like to thank my supervisor **Prof. Dr. Ute Hentschel Humeida** for providing me with the opportunity to work on this exciting project, for being patient in teaching me my work and for supporting me even beyond the confines of my studies. I am extremely thankful that I have been able to complete my Ph.D. thesis under her excellent supervision.

My great appreciation also goes out to my committee member, **Dr. Usama Ramadan Abdelmohsen**, who has always been very kind and patient in supporting my work, encouraging me, and providing me valuable suggestions, as well as accurate and tight guidance on my experiments and academic work.

I would offer my special thanks to **Dr. RuAngelie Edrada-Ebel** for giving me the opportunity to join in the SeaBioTech project and to implement the metabolomics analysis in the University of Strathclyde. My gratitude also goes to **Dr. Lynsey MacIntyre, Dr. Christina Viegelmann**, and **Dr. Tong Zhang** for their kind help on metabolomics data processing and sample measurements in the University of Strathclyde.

I would like to acknowledge **Prof. Dr. Martin J. Mueller** for providing me the chance to measure my samples in the Department of Pharmaceutical Biology, Würzburg University, and **Dr. Markus Krischke**, **Dr. Agnes Fekete**, **Dr. Stefan Schäbler,** and **Ms. Maria Lesch** for their support on mass spectrometry measurement and analysis.

I am grateful to **Dr. Matthias Grüne** for the NMR measurements in the Department of Organic Chemistry, Würzburg University, and his vital comments on compound structure elucidation.

For the sponge collections and bioassay screening, I would like to thank all the members in WP2 and WP3 within the SeaBioTech project, and **Ms. Antje Fuß** in the Missionsärztliches Institut Würzburg, especially for the antitrypanosomal screening. My gratitude also goes to **Dr. Eman Maher Othman**, **Prof. Dr. Helga Stopper**, **Anastasija Reimer**, **Dr. Vera Kozjak-Pavlovic**, **Prof. Dr. Thomas Rudel**, **Srikkanth Balasubramanian**, **Dr. Tobias Oelschläger** for their help and support in the bioactivity testings of the isolated compounds.

I would like to thank **Ms. Christine Gernert** for her patience and kindness in teaching me the procedure of the DNA extraction and amplification.

My appreciation also goes to my labmates **Hannes Horn** for the support on phylogenetic analysis and German translation, **Dr. Lucas Moitinho-Silva**, **Dr. Lucía Pita Galán**, **Beate Slaby**, **Dr. Kristina Bayer**, and **Martin Jahn** for the friendship and happy time we spent together.

I am thankful to the **SeaBioTech** and the **SFB630** project for the financial support and **GSLS Würzburg University** for providing me the chance to participate in a variety of excellent workshops and transferable skills courses during my Ph.D. study.

Lastly, I would like to thank my parents for their endless love and support throughout my life and wish to offer my best regards and blessings to all of those who supported me in any respect during the completion of the project.

DEDICATION

THIS DISSERTATION IS DEDICATED TO

MY FAMILY

Table of Contents

Summary

Marine sponge-associated actinomycetes are considered as promising source for the discovery of novel biologically active compounds. Metabolomics coupled multivariate analysis can efficiently reduce the chemical redundancy of re-isolating known compounds at the very early stage of natural product discovery. This Ph.D. project aimed to isolate biologically active secondary metabolites from actinomycetes associated with different Mediterranean sponges with the assistance of metabolomics tools to implement a rapid dereplication and chemically distinct candidate targeting for further up-scaling compounds isolation.

This study first focused on the recovery of actinomycetes from marine sponges by various cultivation efforts. Twelve different media and two separate pre-treatments of each bacterial extract were designed and applied to facilitate actinomycete diversity and richness. A total of 64 actinomycetes were isolated from 12 different marine sponge species. The isolates were affiliated to 23 genera representing 8 different suborders based on nearly full-length 16S rRNA gene sequencing. Four putatively novel species belonging to the genera *Geodermatophilus*, *Microlunatus*, *Rhodococcus*, and *Actinomycetospora* were identified based on a sequence similarity <98.5% to validly described 16S rRNA gene sequences. 20% of the isolated actinomycetes was shown to exhibit diverse biological properties, including antioxidant, anti-*Bacillus* sp., anti-*Aspergillus* sp., and antitrypanosomal activities.

The metabolomics approaches combined with the bioassay results identified two candidate strains *Streptomyces* sp. SBT348 and *Streptomyces* sp. SBT345 for further up-scaling cultivation and compounds isolation. Four compounds were isolated from *Streptomyces* sp. SBT348. Three of these compounds including the new cyclic dipeptide petrocidin A were previously highlighted in the metabolomics analyses, corroborating the feasibility of metabolomics approaches in novel compounds discovery. These four compounds were also tested against two pathogen microorganisms since the same activities were shown in their crude extract in the preliminary bioassay screening, however none of them displayed the expected activities, which may ascribe to the insufficient amount obtained. *Streptomyces* sp. SBT345 yielded 5 secondary metabolites, three of which were identified as new natural products, namely strepthonium A, ageloline A and strepoxazine A. Strepthonium A inhibited the production of Shiga toxin produced by enterohemorrhagic *Escherichia coli* at a concentration of 80 µM, without interfering with the bacterial growth. Ageloline A exhibited antioxidant activity and inhibited the inclusion of *Chlamydia trachomatis* with an IC_{50} value of 9.54 ± 0.36 µM. Strepoxazine A displayed antiproliferative property towards human promyelocytic HL-60 cells with an IC_{50} value of 16 µg/ml.

These results highlighted marine sponges as a rich source for novel actinomycetes and further exhibited the significance of marine sponge-associated actinomycetes as promising producers of novel biologically active compounds. The chemometrics coupled metabolomics approach also demonstrated its feasibility and efficacy in natural product discovery.

Zusammenfassung

Schwamm-assoziierte Actinomyceten stellen eine vielversprechende Quelle für die Entdeckung neuer, biologisch aktiver Verbindungen dar. Metabolomik gekoppelte multivariate Datenalyse kann die erneute Isolation bekannter chemischer Verbindungen in einem frühen Stadium drastisch reduzieren und der Entdeckung neuer Naturstoffe dadurch effizienter machen. Das Ziel dieser Arbeit war es, biologisch aktive Sekundärmetabolite aus Actinomyceten, welche mit Mittelmeerschwämmen assoziiert sind, zu isolieren. Mithilfe von Werkzeugen aus der Metabolomik soll eine schnelle Dereplikation sowie gezielte Auswahl an chemischen Verbindungen implementiert werden um diese nachfolgend und in hohem Durchsatz isolieren zu können.

Diese Promotions-Arbeit konzentriert sich zunächst auf die Isolation von Actinomyceten aus marinen Schwämmen mittels verschiedener Kultivierungsmethoden. Zwölf verschiedene Medien sowie zwei unterschiedliche Vorbehandlungen der bakteriellen Extrakte wurden angewendet, um die Kultivierung diverser Actinomyceten zu ermöglichen. Insgesamt konnten damit 64 Actinomyceten aus 12 unterschiedlichen Schwämmen isoliert worden. Mithilfe der Sequenzierung von 16S rRNA Sequenzen konnten diese bakteriellen Isolate 23 Gattungen und 8 Unterordnungen zugewiesen werden. Aufgrund von Sequenzähnlichkeiten <98.5% wurden 4 neue Arten identifiziert, welche zu den folgenden Gattungen gehören: *Geodermatophilus*, *Microlunatus*, *Rhodococcus* and *Actinomycetospora.* 20% der isolierten Actinomyceten wurde gezeigt, die verschiedene biologische Eigenschaften aufweisen, einschließlich antixocidativer, antibakterieller, Fungiziden Eigenschaften sowie ihrer anti-Trypanosomen -Aktivitäten.

Mithilfe metabolomischer Methoden und Bioassays konnten zwei bakterielle Stämme, *Streptomyces* sp. SBT348 und *Streptomyces* sp. SBT345, für deren Kultivierung und Isolierung chemischer Verbindung identifiziert werden. Aus dem Stamm *Streptomyces* sp. SBT348 konnten vier neue Verbindungen isoliert werden, darunter ein neues, zyklisches Dipeptid Petrocidin A. Drei dieser Verbindungen, einschließlich Petrocidin A, wurden bei der Datenanalyse der Metabolomik hervorgehoben. Das bestätigte die Durchführbarkeit metabolomischer Methoden für die Entdeckung neuer Verbindungen. Allerdings zeigte keine Verbindung die erwarteten Aktivitäten. Das könnte darauf zurückgeführt werden, dass die erhaltenen Mengen unzureichend waren. In *Streptomyces* sp. SBT345 konnten fünf Sekundärmetabolite identifiziert werden, von welchen drei - Strepthonium A, Ageloline A und Strepoxazine A - als neue Naturstoffe identifiziert werden konnten. Durch Strepthonium A in einer Konzentration von 80 µM konnte die Produktion des Shiga-Toxins in *Escherichia coli* gehemmt werden, ohne dessen bakterielles Wachstum zu beeinflussen. Ageloline A wirkte

antioxidativ und hemmte *Chlamydia trachomatis* mit einem IC_{50} Wert von 9.54 ± 0.36 µM. Strepoxazine A zeigte eine wachstumshemmende Wirkung gegenüber HL-60 Zellen (humane Promyelozytenleukämie-Zellen) bei einem IC_{50} Wert von 16 µg/ml.

Die Ergebnisse zeigen auf, dass marine Schwämme viele bisher unbekannte Actinomyceten beherbergen. Diesen Actinomyceten ist eine hohe Bedeutung beizumessen, da sie eine vielversprechende Quelle für neue, biologisch aktive Verbindungen darstellen. Es konnte ebenfalls gezeigt werden, dass der methodische Ansatz via chemometrischer und metabolomischer Methoden gut durchführbar und effizient ist und daher für die Entdeckung von Naturstoffen sehr gut geeignet ist.

中文摘要

基于代谢组学和去重复分析的海绵寄生放线菌二级代谢活性产物的分离与鉴定

海绵寄生菌富含各样具有生物活性的二级代谢产物。多变量分析结合的代谢组学方法在天然产物分离的初级阶段可有效帮助减少对已知分子的重复分离。此博士课题旨于借助代谢组学分析方法快速鉴定地中海海绵相关放线菌的二级代谢产物的组成，并定向分离具有生物活性的新型结构分子。

此课题首先致力于应用多种培养方法分离地中海海绵中寄生的放线菌。为了促进分离放线菌的多样性和对新种的发现，本课题应用了 12 种不同培养基，并且对其海绵提取的菌液进行高温预处理，从 12 种不同种地中海海绵中分离得到 64 株放线菌。根据 16S rRNA 基因测序，这 64 株放线菌从属于 23 个菌属，8 个亚目。其中有 4 株从属于 *Geodermatophilus*，*Microlunatus*，*Rhodococcus*，和 *Actinomycetospora*，基于和现有的 16S rRNA 基因库比对，其相似性小于 98.5% 被初步鉴定为新种。此研究中 20% 分离得到的放线菌显示有不同的生物活性，包括抗氧化，抗菌(*Bacillus* sp. 和 *Aspergillus* sp.)，以及抗锥虫活性。

代谢组学分析结合生物活性检测结果最终选定 *Streptomyces* sp. SBT348 和 *Streptomyces* sp. SBT345 进行大批量培养及活性分子分离。四个分子包括一个新的分子 petrocidin A 从 *Streptomyces* sp.SBT348 中分离，其中有 3 个分子(包括 petrocidin A)在代谢组学分析中被预测，进一步证实了代谢组学方法在新分子发现的应用中的可行性。基于 *Streptomyces* sp.SBT348 粗提取物的抗菌活性，同样的抗菌实验被用于这 4 个分子，但并没有显示任何活性，原因可能归咎于较低的产量所导致的在抗菌实验中的用量较低。五个分子，包括三个新的天然产物（strepthonium A，ageloline A，和 strepoxazine A）从 *Streptomyces* sp. SBT345 中分离。其中 strepthonium A 以 80 μM 的浓度抑制猪源肠出血性大肠杆菌产生的志贺毒素的产量。Ageloline A 显示有抗氧化活性并以 IC_{50} 9.54 ± 0.36 μM 的浓度抑制砂眼衣原体 *Chlamydia trachomatis* 形成。Strepoxazine A 以 IC_{50} 16 μg/mL 的浓度抑制人早幼粒白血病 HL-60 细胞的增生。

此研究结果进一步展示了海绵寄生菌的多样性以及新菌种的丰富性。海绵寄生放线菌展示了其在对新的具有活性的分子的发现方面的重要性。此外，化学计量学结合的代谢组学进一步证明了其在开发天然产物应用中的可行性及有效性。

Chapter 1
Introduction

1.1 Natural products

Nature has been a valuable treasure of therapeutic and medicinal agents for thousands of years. Natural products played a predominant role in ancient medicinal systems, like the traditional Chinese herbal medicines and the Egyptian traditional medicines, of which the application dates back to more than 3000 years ago (Hao and Jiang, 2015; Sarker and Nahar, 2012). "*Shennong Bencaojing (Classic of Herbal Medicine)*" is the earliest pharmacy monograph handed down from the ancient China. This book could date back to the Qin-Han period (1^{st}-2^{nd} century BC) and first describes a total of 365 medicinal natural products from which 252 are of plant origin, 67 are from animals, and 46 are from minerals (Luo et al., 2010). Another prominent Chinese medicinal classic "*Bencao Gangmu (Compendium of Materia Medica)*" records 1892 Chinese medicines, most of which, especially the herbal medicines, are still in common use today in the Chinese medical system (Hao and Jiang, 2015). Artemisinin, the notable anti-malarial drug discovered by Youyou Tu who won the 2015 Nobel Price, was isolated from the Chinese medicinal herb Qinghao (*Artemisia annua*) which was recorded in the book "*Handbook of Prescriptions for Emergency Treatments"* compiled by Hong Ge in Jin period (2^{nd} century AC) (Tu, 2011). A vast number of modern drugs have been derived or designed from natural products (Eder et al., 2014). However, the increasing drug resistance made many of the currently used therapeutics no longer effective (Bock and Lengauer, 2012; Hughes and Andersson, 2015). The development and discovery of new drugs or innovative therapeutic treatments against the exacerbating drug-resistance still remains severe and yet to be attempted. Marine source harboring an affluent unexplored biological entities attracted natural product scientists to seek for unique and novel molecules from, for example, the deep sea sediments, marine algae, marine invertebrates, and their associated microbes (Harvey et al., 2015; Molinski et al., 2009; Rutledge and Challis, 2015). Marine sponges and their associated microorganisms were brought into the front with an impressive record of a considerable number of novel compounds, as well as their multitude biological activities (Abdelmohsen et al., 2014a; Norris and Perkins, 2016; Roue et al., 2012). Interestingly, the medical property of sponge was also recorded in the ancient Chinese medical book "*Bencao Tujing (Illustrated Classics of Materia Medica)"* and used in the treatment of aconuresis and spermatorrhea (Xie et al., 1975), additionally supporting the potentials and significance of marine sponges in medicinal researches. In this Ph.D. thesis work, my attempt in exploring novel chemical structures for pharmaceutical development will focus on marine sponge-associated actinomycetes. In the following introduction, I will start with the biology of

marine sponges and their microbial symbionts, then discuss the actinomycetes with a particular focus on marine sponge-associated actinomycetes and their bioactive properties, and finally present the metabolomics techniques and statistical approaches in the context of natural products discovery.

1.2 Marine sponge microbiology

Sponges (phylum Porifera) are one of the oldest multicellular animals (Metazoa) with current fossil records dating back to the time of the Precambrian-Cambrian boundary (Antcliffe et al., 2014; Hentschel et al., 2012). More than 6,000 species of sponges have been described and they were found to inhabit a wide variety of marine and freshwater systems, such as tropical reefs where abundant population aggregate, the deep sea, polar region, as well as freshwater rivers and lakes. The phylum Porifera is classified into *Hexactinellida* (glass sponges), *Calcarea* (calcareous sponges), and *Demospongiae* (demosponges), of which the last class *Demospongiae* is described with the most comprehensive and diverse species and covers an estimated 85% of all known living species (Brusca and Brusca, 1990; Hooper and Van Soest, 2002) and they encompass various forms in different shapes, colors and sizes (**Fig.1.1**). Sponges are sedentary filter-feeders capable of absorbing and pumping constant volumes of seawater through their bodies to remove wastes and to sustain food intake, examples of which include prokaryotic microorganisms including archaea, bacteria, and unicellular algae, eukaryotes such as fungi, as well as nano- and pico-eukaryotes and even viruses, (Hadas et al., 2006; Thacker and Freeman, 2012; Webster et al., 2012). It has been estimated that a 1 kg sponge can pump up to 24,000 liters of water in a single day (Taylor et al., 2007). Seawater is passed through the small inhalant pores (up to approximately 50 mm) named ostia into the choanocytes chambers where the surface is formed by specialized flagellated cells termed choanocytes. Choanocytes filter the water and transfer up to 96% of microbial cells (Reiswig, 1971; Wehrl et al., 2007) into the mesohyl interior where the archaeocytes cells are located and conduct phagocytosis of the food particles. Near-sterile water is then expelled via the exhalant ostia or osculum within the whole sponge body (Hentschel et al., 2012).

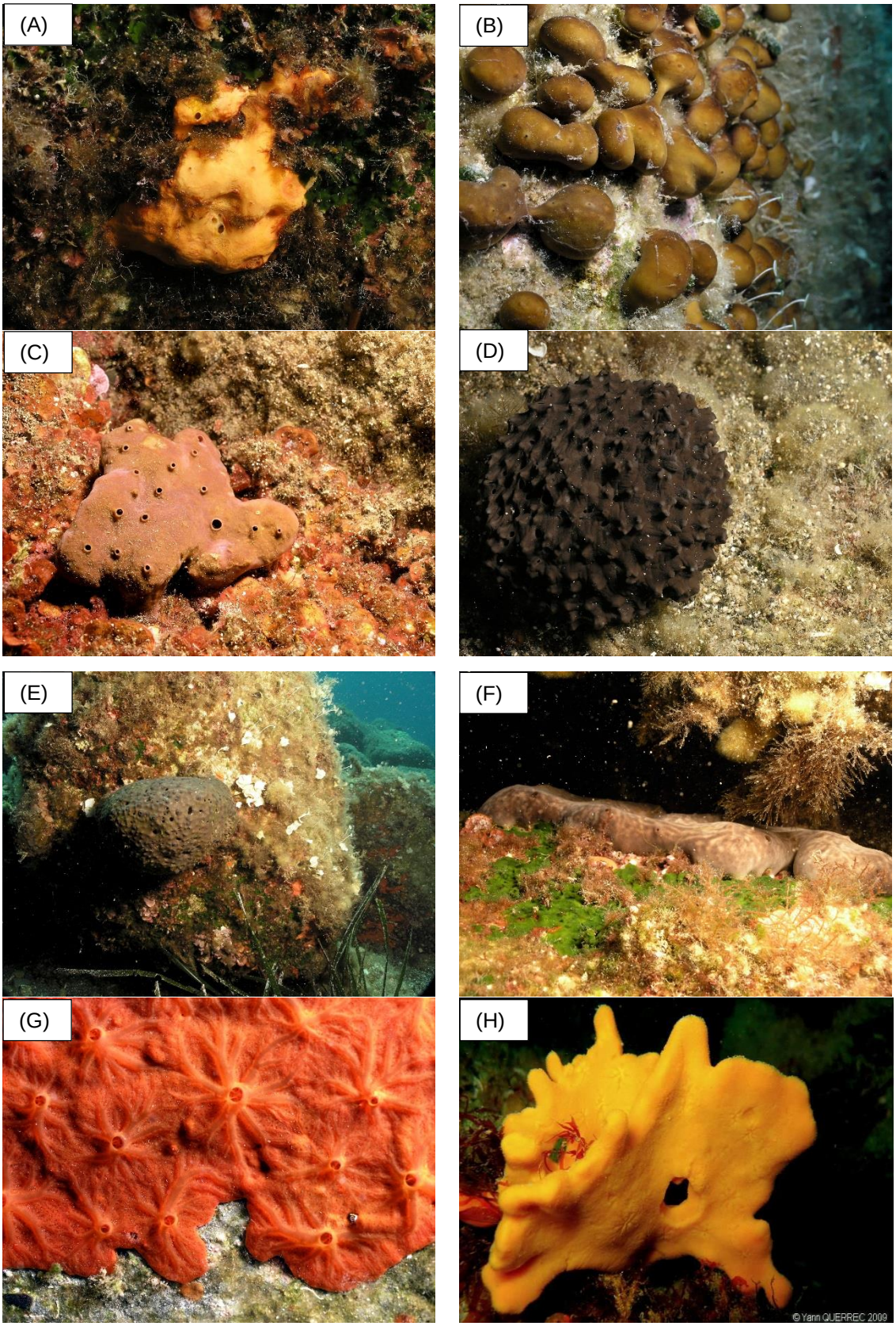

Fig. 1.1 Demosponges: (A) *Agelas oroides*; (B) *Chondrilla nucula*; (C) *Petrosia ficiformis*; (D) *Sarcotragus spinosulus*; (E) *Sarcotragus foetidus*; (F) *Chondrosia reniformis*; (G) *Spirastrella cunctatrix* (underwater photography by Dr. Thanos Dailianis. Sponges that were under investigation in this Ph.D. thesis); (H) *Axinella damicornis* (underwater photography by Yann Querrec)

The complex microbial consortia of sponges were initially investigated through microscopy (Vacelet and Donadey, 1977; Wilkinson, 1978). With the development of molecular techniques, several culture-independent approaches have been established and applied to gain insights into the diversity of the massive bacterial communities, such as 16S rRNA gene library construction, denaturing gradient gel electrophoresis (DGGE), fluorescence in situ hybridization (FISH) and recently a more cost-effective method tag-encoded FLX amplicon pyrosequencing which has been utilized on 32 sponges by Schmitt *et al*. to probe their symbiont bacteria (Hardoim and Costa, 2014; Head et al., 1998; Hentschel et al., 2002; Simister et al., 2012). Phylogenetic studies and direct cultivation have recently recovered members of at least 32 different bacterial phyla from sponges, including the candidate phyla such as phylum *Poribacteria, which is almost sponge-exclusive***,** as well as the most commonly cultivable phyla such as *Acidobacteria*, *Actinobacteria*, *Chloroflexi*, *Cyanobacteria*, *Bacteriodetes*, *Gemmatimonadetes*, *Spirochaetes* and *Proteobacteria* (Schmitt et al., 2012; Taylor et al., 2007).

Highly diverse symbionts of eukarya and archaea have also been identified with the association of marine sponges by the molecular- and culture-dependent studies (Jin et al., 2014; Rodriguez-Marconi et al., 2015). However, compared with the booming investigations concerned with sponge bacteria, the studies of eukarya and archaea symbionts are still in their infancy. Two phyla of fungi and nine phyla of protists have recently been reported to reside within the sponge tissues from eleven sponge species by He *et al.* using 454 pyrosequencing (He et al., 2014). A study from Wiese *et al.* has shown an isolation of 81 fungal isolates affiliating 21 genera from Marine Sponge *Tethya aurantium*, in which a putatively new *Phoma* species was first isolated (Wiese et al., 2011). Two major archaeal phyla *Euryarchaeota* and *Thaumarchaeota* were described from a deep-sea marine sponge *Inflatella pellicula*, of which *Thaumarchaeota* was observed to dominate in Arctic sponges and Irish deep-sea environments (Jackson et al., 2013). Three archaea of *Crenarchaeota thermoprotei*, Marine Group I, and *Thaumarchaeota incertae sedis* have been detected in sponges *Spirastrella insignis* and *Callyspongia confoederata* using a newly developed electrical retrieval method developed by Koyama et al. (Koyama et al., 2015).

With the application of ‘omics’ approaches, the mystery of the function of symbionts within sponges is being gradually illuminated. Functions of the symbiont community attributed to mutual and commensal interactions with the host have been proposed to contribute to nutrient acquisition (Vacelet et al., 1995; Wilkinson, 1992), metabolic waste processing (Beer and Ilan; Bewley et al., 1996), sponge skeleton stabilization (Rutzler, 1985), protection of the host from environmental stress (such as changes in temperature and osmotic pressure and contact with

toxins) (Liu et al., 2012) and chemical defense from attacks from parasites and pathogens (Proksch, 1994; Unson et al., 1994). The gamma proteobacterial symbionts (Moitinho-Silva et al., 2014) were found to undergo methylotrophy, a metabolic procedure to utilize single carbon compounds as the energy source (Chistoserdova et al., 2009). A metaproteogenomic study from Liu et al. has identified the specific transport functions between sponges and their symbionts by observing the expression tripartite ATP-independent periplasmic transporter, which was found to transport the typical sponge metabolites such as halogenated aromatics and dipeptides (Liu et al., 2012). A close link has also been observed between bacterial and archaeal symbionts and their sponge hosts with respect to the nitrogen metabolism through the detection of related functional genes and enzymes (Bayer et al., 2008; Liu et al., 2012; Radax et al., 2012; Schlappy et al., 2010; Taylor et al., 2007). The functional genes related to the environmental stress were noted to be more abundant in the sponge-associated bacteria than the surrounding seawater bacteria (Thomas et al., 2010). The role of sponge symbionts regarding such functions was further demonstrated physiologically through the observation of the expression of chaperones and proteases from symbionts associated with the same sponge species (Liu et al., 2012). Secondary metabolites produced by sponges and their symbionts are also overlapping and bear a resemblance (Piel, 2004), which led to the development of the hypothesis that considers the symbionts as the true producers of defective chemicals (Piel, 2004; Proksch, 1994). The defecting roles of sponge symbionts were preliminarily identified through the detection of biosynthetic genes of host-origin defense compounds and proteins from the symbiotic microbes (Flatt et al., 2005; Proksch et al., 2010; Selvin, 2009; Thacker and Freeman, 2012; Wilson et al., 2014). However, the study of chemical interactions within sponge microcosms is still at a primary stage, and many mysteries remain to be explored and solved.

1.3 Actinomycetes

1.3.1 Actinomycete diversity

Actinomycetes are a group of gram-positive bacteria whose GC-content can be up to 70% (Goodfellow and Williams, 1983; Korn-Wendisch and Kutzner, 1992). They belong to the phylum *Actinobacteria*, which represents one of the 18 major lineages currently described within the kingdom bacteria (Ventura et al., 2007). Actinomycetes exist abundantly in terrestrial and marine environments, such as soil, sediment from the deep sea (Choi et al., 2016), plants (Pawlowski and Demchenko, 2012; Rodrigues et al., 2015), insects (Berlanga, 2015; Kurtboke et al., 2015) and marine invertebrates (Abdelmohsen et al., 2014a; Mahmoud and Kalendar, 2016), as well as extreme environments, such as the cryophilic region (Van Goethem et al., 2016), and hyper-arid desert soil (Crits-Christoph et al., 2016). They are generally anaerobic bacteria noted for a filamentous and branching growth pattern and present diverse colony morphologies, such as a tough leathery texture, a dry or folded appearance, aerial mycelium,

substrate mycelium and diffusible pigments (Waksman, 1950). Actinomycetes are commonly referred to the order *Actinomycetales* which is included in the subclass *Actinobacteridae*. Thirty-nine families have been described with the representatives of *Actinomycetaceae*, *Actinoplanaceae*, *Dermatophilaceae*, *Frankiaceae*, *Mycobacteriaceae*, *Micromonosporaceae*, *Nocardiaceae*, and *Streptomycetaceae* (Garrity et al., 2004). As one of the major consortia of the soil microbial community, actinomycetes play a crucial role in the decomposition of biomaterials of dead plants and animals and are thus responsible for geosmins, the characteristic "wet earthy odor" (Waksman, 1950). More than 10400 actinomycetes 16S rRNA sequences have been obtained from marine systems through culture-dependent isolation (Abdelmohsen et al., 2014a) and a total of 20 novel genera of actinomycetes were reported from marine habitats between 2007 and mid-2013 (Subramani and Aalbersberg, 2013). Representative genera include *Streptomyces*, *Nocardiopsis*, *Nocardia*, *Micromonospora*, *Rhodococcus*, *Salinispora*, *Arthrobacter*, *Microbacterium*, *Micrococcus*, etc. of which the first six species were found to be significantly productive in biologically active compounds (Abdelmohsen et al., 2014a; Blunt et al., 2015; Lane and Moore, 2011). Some members such as *Mycobacterium*, *Corynebacterium* and *Nocardia* can also cause diseases on human (Hall, 2008), animals (Huaman et al., 2016), and plants (Locci, 1994).

1.3.2 Sponge-associated actinomycetes

Marine sponges were found to contain more actinomycetes in comparison to other marine invertebrates, such as corals, tunicates and bryozoans (Hentschel et al., 2003; Selvin et al., 2010; Zhang et al., 2006). The diversity of marine sponge-associated actinomycetes was studied by Abdelmohsen *et al*. among others. A total of 60 genera of actinomycetes had been reported from marine sponges until 2013 (**Fig 1.2**) (Abdelmohsen et al., 2014a). The suborder *Micrococcineae* represented the highest ratio and covered almost half of all the genera, followed by *Streptosporanginaeae*, and *Corynebacterineae* which covered 7 genera, as well as *Micromonosporineae* and *Pseudonocardineae* which covered 6 and 5 genera, respectively. Among them, genera *Actinokineospora*, *Actinomadura*, *Knoellia*, *Nonomuraea, Amycolatopsis*, *Pseudonocardia*, *Saccharomonospora*, *Saccharopolyspora*, and *Verrucosispora* are rare genera recovered from the natural environment, and this finding indicates a real potential of drug discovery from sponge-associated actinomycetes. With the growing number of studies concerning marine sponge-associated microorganisms, numbers of novel actinomycete species have continuously increased (Hames-Kocabas and Uzel, 2012; Kwon et al., 2006; Supong et al., 2013). Most new representatives are *Streptomyces spongiicola* sp. nov. that have been isolated from an unidentified marine sponge obtained from the coast of Sanya City, China (Huang et al., 2015), *Marmoricola aquaticus* sp. nov. isolated from the sponge *Glodia corticostylifera* which was collected from São Paulo, Brazil (de Menezes et al., 2015),

Actinokineospora spheciospongiae sp. nov. recovered from the Red Sea sponge *Spheciospongia vagabunda* (Kampfer et al., 2015) and *Rubrobacter aplysinae* sp. nov., derived from the Mediterranean sponge *Aplysina aerophoba* (order Verongida) collected from Rovinj, Croatia (Kampfer et al., 2014).

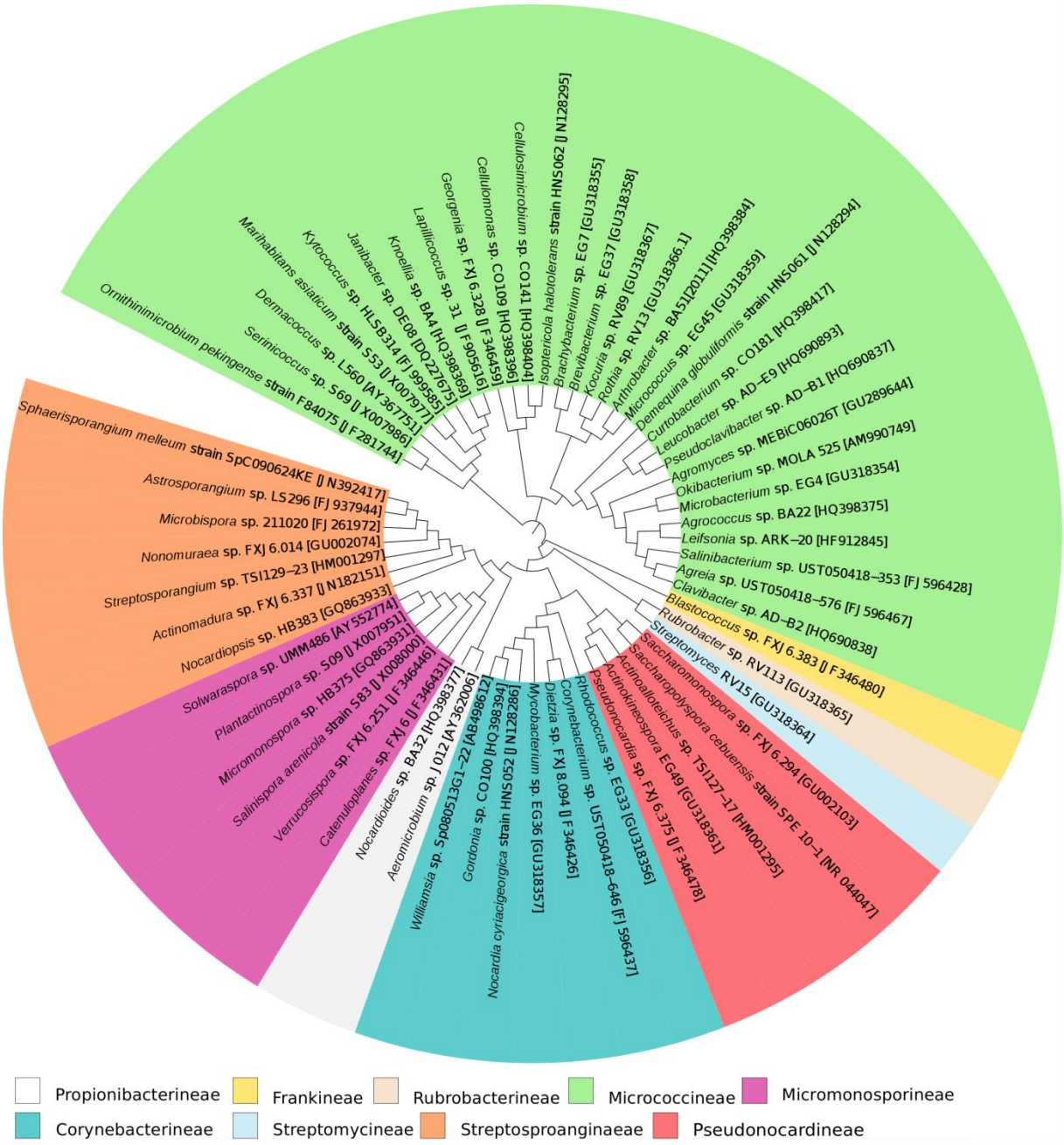

Fig. 1.2 Maximum likelihood phylogenetic tree based on 16S rRNA gene sequences of sponge-associated actinomycete genera derived from literature and NCBI database (Abdelmohsen et al., 2014a).

Several protocols have been established to facilitate the recovery rate of rare and novel actinomycetes from marine sponges. The bacterial extracts were subjected to heat shock treatment and the medium was supplemented with antibiotics (cycloheximide, nystatin) in order to reduce the number of fungi and seawater' bacteria which was usually represented by Gram-negative bacteria (Takizawa et al., 1993; Webster et al., 2001). In order to stimulate spore germination, samples were pretreated with UV radiation and high-frequency waves which resulted in the isolation of unexpected genera *Glycomyces and Knoellia* (Bredholdt et al., 2007). The sponge extracts were also supplemented to the medium in order to simulate the original host nutrient. The sponge-sparked medium has successfully recovered a new species *Rubrobacter aplysinae* sp. nov. from marine sponge *Aplysina aerophoba* (Kampfer et al., 2014). Nutrient-resisted medium, such as oligotrophic medium or agar only, was applied to enhance the growth of oligotrophic bacteria (Olson et al., 2000). Zengler *et al*. developed a new cultivation method by encapsulating single cells through gel microdroplets to enable bacterial cells to grow at environmental concentrations (Zengler et al., 2002). Other approaches that 'trick' cells to grow in their natural environment were deployed using diffusion chambers (Kaeberlein et al., 2002), microbial traps (Gavrish et al., 2008), or isolation chips (Ling et al., 2015). These in vivo approaches were initially applied in soil or sediments samples (Bollmann et al., 2007; Lewis et al., 2010), but also recently developed for marine sponges (Jung et al., 2014; Steinert et al., 2014).

1.3.3 Bioactive compounds from marine sponge-associated actinomycetes

It has long been known that actinomycetes produce a significant number of secondary metabolites with a variety of biological activities. Since the discovery of penicillin in 1928 (Vladimir, 1983), more than 45% bioactive secondary metabolites that have been obtained from microbes are produced by actinomycetes (Selvameenal et al., 2009). The predominant genus *Streptomyces* produces approximately 5,000 antibiotics occupying about half of the known antibiotics that are produced by the whole actinomycete consortia (Subramani and Aalbersberg, 2012). Due to the increasing quest for the development of novel efficient therapeutic agents, the search of rare and new actinomycetes is a central goal of drug discovery. Marine sponges which have been shown to hold a potential source of novel actinomycetes are considered as one promising source of novel chemical entities. A good record of a multitude of novel secondary metabolites (Abdelmohsen et al., 2012b; Grkovic et al., 2014) has been made by marine sponge-associated actinomycetes with diverse biological activities, such as antimicrobial (Eltamany et al., 2014; Hentschel et al., 2001), antiparasitic (Abdelmohsen et al., 2014b; Viegelmann et al., 2014), immunomodulatory (Tabares et al., 2011), antichlamydial (Reimer et al., 2015), antioxidant (Grkovic et al., 2014), and anticancer (Simmons et al., 2011; Yi-Lei et al., 2014) activities. One hundred and twenty compounds have been reported from marine actinomycetes in the MarinLit database till 2015 (J. Blunt, University of Canterbury), of which 19% were isolated from marine sponge-associated actinomycetes. Co-cultivation of microbes and supplementary chemical and molecular elicitors was used to facilitate or stimulate the production of novel secondary metabolites (Abdelmohsen et al., 2015; Dashti et al., 2014; Pimentel-Elardo et al., 2015; Schaberle et al., 2014; Wang et al., 2014; Wu et al., 2015b). The bioactive compounds derived from sponge-associated actinomycetes are represented by several classes, including polyketides, isoprenoids, alkaloids, phenazines, peptides, and others (Abdelmohsen et al., 2014a; Abdelmohsen et al., 2012a; Blunt et al., 2013; Fenical and Jensen, 2006; Solanki et al., 2008; Subramani and Aalbersberg, 2012; Tiwari and Gupta, 2012). Below I have listed prominent examples of novel biologically active secondary metabolites that have been isolated from marine sponge-associated actinomycetes within the recent five years.

Mayamycin is a new benz[a]anthracene derivative isolated from *Streptomyces* sp. strain HB202 cultured from the marine sponge *Halichondria panicea*. Mayamycin displayed significant cytotoxic activity against eight human cancer cell lines (HepG2, HT-29, GXF251L, GXF251L, MAXF401NL, MEXF462NL, PAXF1657L, RXF486L) and antibiotic capacities including methicillin-resistant *Staphylococcus aureus* with the IC_{50} value of 2.5 μM (Schneemann et al., 2010). Tetracenoquinocin and 5-iminoaranciamycin are two new

anthracyclines isolated from the culture of *Streptomyces* sp. Sp080513GE-26 associated with the marine sponge *Haliclona* sp. Tetracenoquinocin exhibited weak cytotoxicities against HeLa and HL-60 cells with IC_{50} values of 120 and 210 μM, respectively (Motohashi et al., 2010). Bendigoles D-F are three new keto sterols isolated from a novel actinomycete *Actinomadura* sp. SBMs009 derived from the marine sponge *Suberites japonicus*. Bendigole D exhibited cytotoxicity against the L929 (mouse fibroblast) cell line and an inhibiting effect against GR-translocation. Bendigole F displayed a potent inhibitor effect against NF-κB nuclear translocation (Simmons et al., 2011).

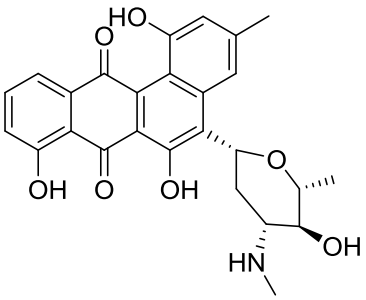

Mayamycin

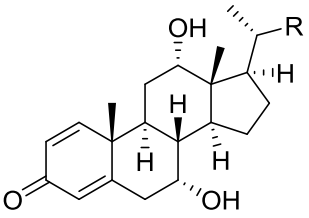

Bendigole D: R = COOH
Bendigole E: R = $COCH_3$
Bendigole F: R = CH_2CH_2COOH

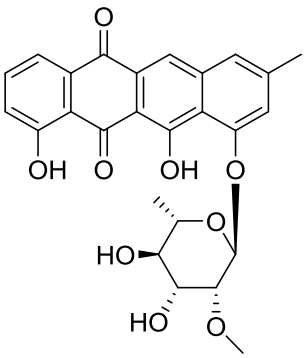

Tetracenoquinocin

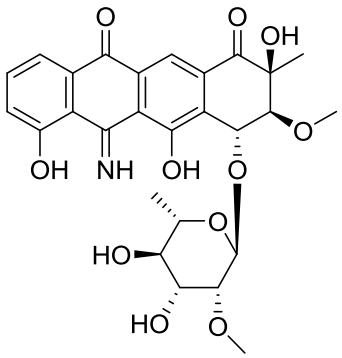

5-iminoaranciamycin

Four new tetromycin derivatives, tetromycins 1-4, were isolated from *Streptomyces axinellae* Pol001(T) cultivated from the Mediterranean sponge *Axinella polypoides* and showed antitrypanosomal activity and time-dependent inhibition of cathepsin L-like proteases (Pimentel-Elardo et al., 2011).

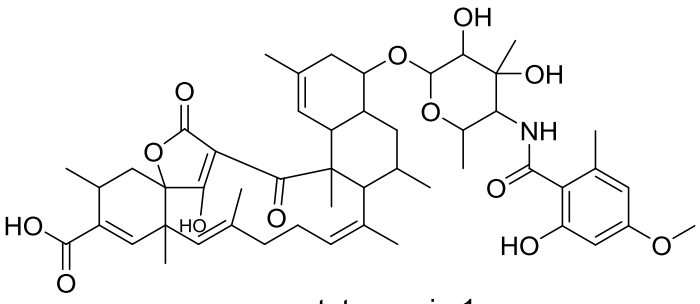

tetromycin 1

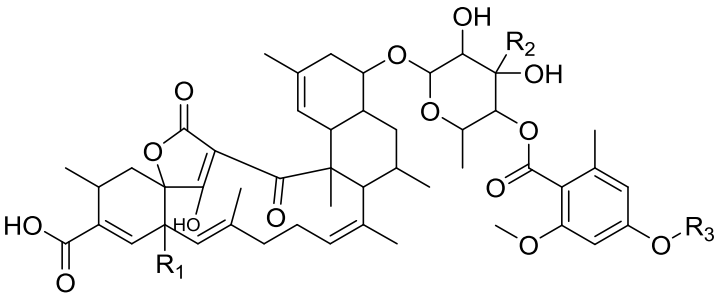

tetromycin 2: $R_1 = CH_3$, $R_2 = H$, $R_3 = CH_3$
tetromycin 3: $R_1 = H$, $R_2 = H$, $R_3 = H$
tetromycin 4: $R_1 = CH_3$, $R_2 = H$, $R_3 = H$

Two new compounds of kijanimicin derivatives, lobophorin C and D, were isolated from *Actinomycetal* Strain AZS17 cultured from marine sponge *Hymeniacidon* sp. collected from coastal waters of the East China Sea. Lobophorin C and D exhibited potent cytotoxic activity against the human liver cancer cell line 7402 and breast cancer cells MDA-MB 435 respectively (Wei et al., 2011). Three new trichostatin analogues, JBIR-109, JBIR-110, and JBIR-111, were isolated from the marine sponge-derived *Streptomyces* sp. strain RM72 and showed a moderate inhibitory effect against histone deacetylase 1 at IC_{50} valued of 48, 74, and 57 μM, respectively (Hosoya et al., 2012).

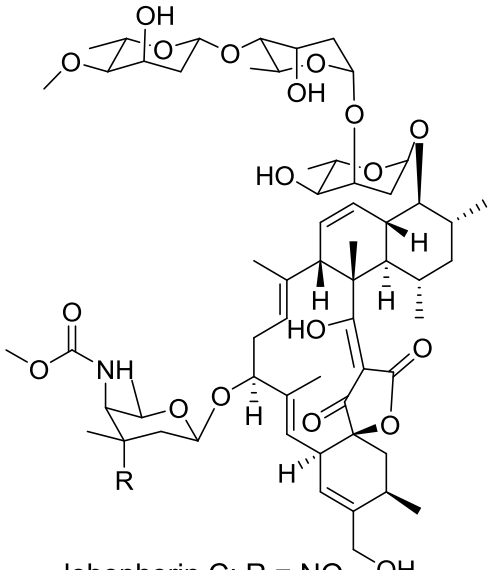

lobophorin C: R = NO_2
lobophorin D: R = NH_2

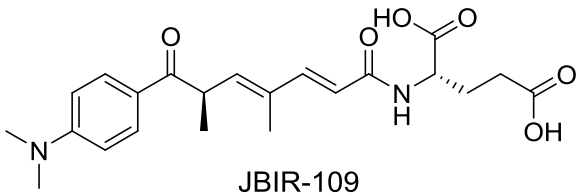

JBIR-109

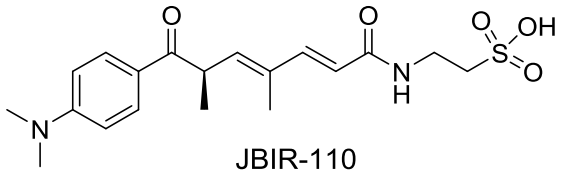

JBIR-110

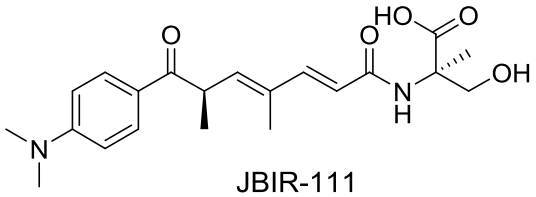

JBIR-111

Nocatriones A and B are two new tetracenedione derivatives isolated from *Nocardiopsis* sp. KMF-002 which was derived from an unidentified marine sponge. Nocatrione A at 10 µM showed a down regulation of MMP-1, a protein that degrades collagen in dermal tissue (Kim et al., 2014). Three new streptophenazines I-K have been identified from *Streptomyces* strain HB202 which was isolated from the sponge *Halichondria panicea* from the Baltic Sea. Streptophenazine K showed moderate antibacterial activity against *Staphylococcus epidermidis* and *Bacillus subtilis* with IC_{50} values at 14.5 and 21.6 µM, respectively. All compounds (streptophenazines I-K) also exhibited inhibitory activities against enzyme phosphodiesterase (PDE 4B) which is the target protein for the treatment of inflammatory diseases such as COPD (Chronic Obstructive Pulmonary Disease) (Kunz et al., 2014). Actinosporins A-D are four new O-glycosylated angucyclines isolated from a novel marine sponge-associated actinomycete *Actinokineospora* sp. EG49 which was cultivated from the Red Sea sponge *Spheciospongia vagabunda*. Actinosporin A displayed anti-parasite activity against *Trypanosoma brucei brucei* with an IC_{50} value of 15 µM. Actinosporins C and D showed a remarkable antioxidant and protective ability from the genomic damage caused by hydrogen peroxide in the human promyelocytic (HL-60) cell line at 1.25 µM (Abdelmohsen et al., 2014b; Grkovic et al., 2014).

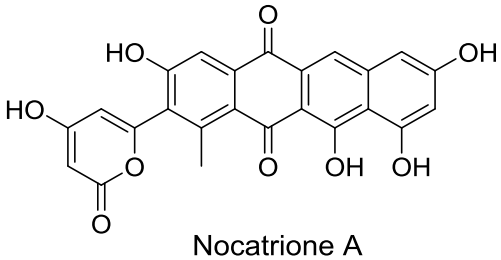

Nocatrione A

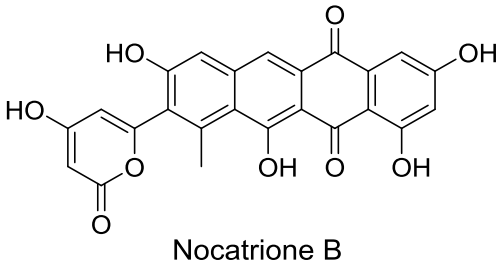

Nocatrione B

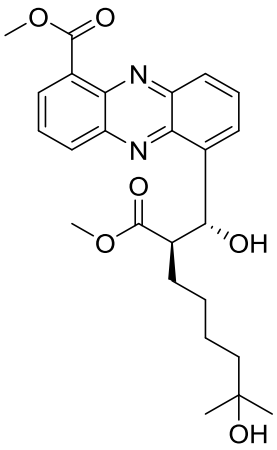

Streptophenazine I

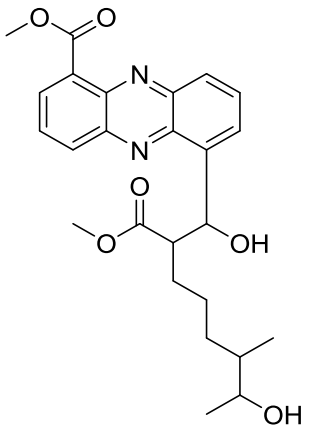

Streptophenazine J

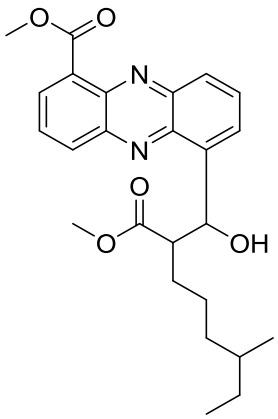

Streptophenazine K

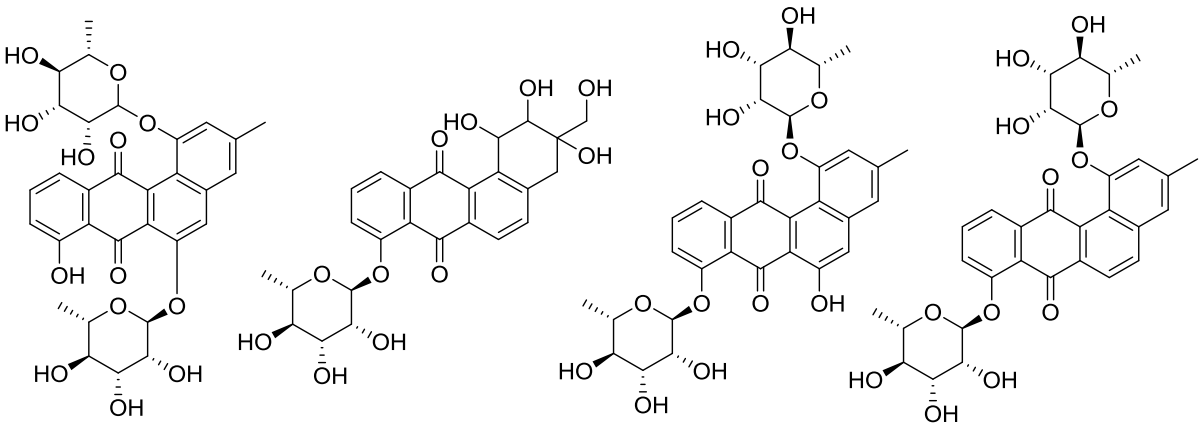

Actinosporin A Actinosporin B Actinosporin C Actinosporin D

A new analogue of echinomycin, quinomycin G, and a new cyclic dipeptide, cyclo-(l-Pro-4-OH-l-Leu), were isolated from *Streptomyces* sp. LS298 associated with the marine sponge *Gelliodes carnosa*. Quinomycin G displayed moderate antibacterial activities against *Staphylococcuse pidermidis*, *S. aureus*, *Enterococcus faecium*, and *E. faecalis* with the MIC values ranging from 16 to 64 g/mL and potent anti-tumor activities against the Jurkat cell line (human T-cell leukemia) with an IC_{50} value of 0.414 M (Zhen et al., 2015).

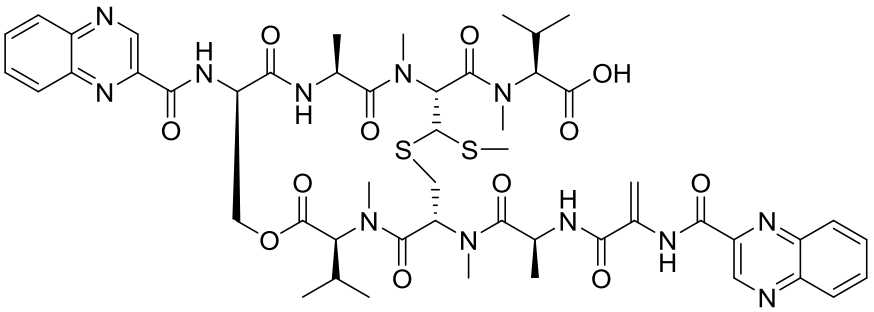

Quinomycin G

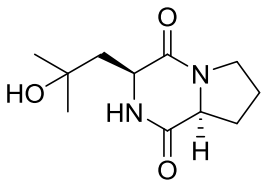

cyclo-(l-Pro-4-OH-l-Leu)

1.4 Utility of metabolomics tools for natural product discovery

Metabolomics refers to a comprehensive and simultaneous determination of the level of metabolites within a given the metabolome and the documentation of the changes over time as a consequence of stimulus or genetic manipulation (Lindon et al., 2006). The first paper describing the quantitative metabolic profiling of human metabolites was developed by Pauling et al. in 1971 using Gas-Liquid Partition Chromatography for the quantification of urine metabolites (Pauling et al., 1971). In 1984, Nicholson et al. reported the application of ^{1}H NMR for detecting changes of metabolites in fasting and diabetic subjects (Nicholson et al., 1984). However, the term metabolomics was only coined in 1998 in the paper "Systematic functional analysis of the yeast genome" where the word metabolome was also first used, followed by the terms genome, proteome, and transcriptome (Oliver et al., 1998). Following mass spectrometry, which allows for the direct identification of compounds, comprehensive metabolite profiling of samples was implemented and first described in the application of gas chromatography/mass spectrometry by Fiehn et al. for the investigation of gene function in plants (Fiehn et al., 2000). Chemometrics was also introduced to permit the evaluation of large data sets and the tracking of significant changes in connection with specific parameters (Nicholson and Lindon, 2008). The first metabolomics web database METLIN was developed in 2005 by Siuzdak's group at the Scripps Research Institute (Smith et al., 2005) and currently covers over 242,000 metabolites. METLIN became the largest repository of tandem mass spectrometry data with over 72,200 data updated in 2016 (METLIN, Scripps Center for Metabolomics). Following the completion of the first draft of the human metabolome, the Human Metabolome Data Base was released in 2007, providing a comprehensive coverage of the human metabolome (Wishart et al., 2013; Wishart et al., 2009; Wishart et al., 2007).

The employment of metabolomic techniques in natural products was followed by biomedical and agricultural researches (Harvey et al., 2015), where metabolomics was primarily established to look for biomarkers in diagnostic research (Harrigan, 2002; Schlotterbeck et al., 2006), and profiling nutrients in vegetables (Fraser et al., 2000). Representative examples of the use of metabolomics in natural products could be exemplified by the application of these tools in the quality control of Traditional Chinese Medicine (TMC), where the chromatographic fingerprints and monographs of TCM have already been established (Liu et al., 2016; Pelkonen et al., 2012). The toxic and therapeutic effects of TCM on complex biological systems have also been investigated with the aid of metabolomics in several medical studies (Wang et al., 2005; Youns et al., 2010; Zhao et al., 2012). A novel HPLC-coupled chemometric method was developed by Li. et al. in order to facilitate the quantification of specific compounds within overlapping profiles of co-eluting compounds in Chinese patent medicines (Li et al., 2013).

Chemometric analysis-guided metabolite profiling has also been applied in the comparison of TCM constituents from different botanical origins (Sun et al., 2013) and preparation procedures (Guo et al., 2015; Wishart et al., 2013). Metabolomics has also been involved in characterizing the real-time transformation of intermediate, by-products and degradants in order to monitor and maintain the production of desired compounds during fermentation in metabolomics engineering (Toya and Shimizu, 2013; Wasylenko and Stephanopoulos, 2015).

Bioassay-guided fractionation has generally been used in isolating individual biologically active compounds in natural product discovery. However, this conventional isolation method has frequently been challenged by the repeated isolation of known compounds, the failed isolation of trace compounds and sometimes the loss of activity during fractionation and isolation (Inui et al., 2012). The blindness of detailed chemical information prior to isolation is the crucial defect associated with traditional natural product discovery. Metabolomics can determine the different active compounds in complex mixtures without comprehensive fractionation or prior isolation of the individual compound while still offering a linkage to structural information; therefore, there is a growing interest in the application of tools of metabolomics in novel natural product discovery.

Chromatography-integrated mass spectrometry (MS) and nuclear magnetic resonance (NMR) are the primary and typical tools utilized in metabolomics profiling. A strategy using MS and NMR-based chemical dereplication and multivariate analyses has been developed (**Fig. 1.3**) and demonstrated an efficient procedure to assist the discovery and isolation of new biologically active compounds (Abdelmohsen et al., 2014b; Forner et al., 2013; Harvey et al., 2015; Hou et al., 2012; Macintyre et al., 2014; Tawfike et al., 2013; Wu et al., 2015a). In this strategy, liquid chromatography-coupled high-resolution MS (LC-HRMS) is conventionally utilized to initially assess and dereplicate secondary metabolites of natural products' crude extracts based on the high-resolution *m/z* values in metabolites database. The commonly used natural products databases are MarinLit (Blunt J.W., University of Canterbury), AntiBase (Laatsch H., Wiley-VCH Verlag GmbH & Co. KGaA), and Dictionary of Natural Products (Hampton Data Services. Ltd). ^{1}H NMR and 2D NMR were also involved in probing the chemical structure of secondary metabolites in a complex mixture prior to the chromatographic step (Bringmann and Lang, 2003; Cheng et al., 2015; Wu et al., 2015a). Dereplication of the known compounds in the crude mixtures reduces the possible redundancy caused by the re-isolation of known compounds and additionally provides an overview of potential chemical entities for each sample.

The LC-MS and NMR data can be subjected to multivariate analyses, where the similarities and differences of secondary metabolites in a group of samples can be revealed. This chemometric approach was introduced to prioritize candidate object from a massive collection of samples, e.g. microorganism collection (Cheng et al., 2015; Forner et al., 2013; Hou et al., 2012; Macintyre et al., 2014; Samat et al., 2014), and to assist in cultural optimization which aims to facilitate the production of novel secondary metabolites (Abdelmohsen et al., 2014b; Grkovic et al., 2014; Tawfike et al., 2013). Principal component analysis (PCA) is one of the most widely used multivariate analyses methods. It is an "unsupervised" statistical procedure designed to determine the most principal element(s) or structure of a massive data set so that it is possible to identify the patterns in data; thus, highlighting their differences and similarities (Eriksson et al., 2006). Given this principle, PCA was applied to reveal the differences and similarities of secondary metabolites amongst groups of samples in terms of their *m/z* values (LC-MS data) or chemical shifts (NMR data), and further suggested candidates that exhibiting distinct or unique chemical properties (Cheng et al., 2015; Forner et al., 2013). Studies of Hou et al., Macintyre et al., and Samat et al. are currently reported examples utilizing this approach for candidate prioritization in marine-derived bacteria and plant extracts (Hou et al., 2012; Macintyre et al., 2014; Samat et al., 2014).

There is another type of statistical approach termed "supervised", in which discriminations of variables (e.g. *m/z* for MS, or chemical shifts for NMR) are identified based upon known classification (Eriksson et al., 2006). The supervised statistical methods are represented by partial least squares-discriminant analysis (PLS-DA) and orthogonal partial least squares-discriminant analysis (OPLS-DA). They are commonly used when PCA analysis cannot provide proper separation of samples among different classes (Bylesjö et al., 2006). OPLS-DA can only process the sample set classified within two groups but provide enhanced interpretability than PLS-DA (Worley and Powers, 2013). Give this concept, OPLS-DA was used to look for the latent relationship between spectral data and biological states by dividing the sample set into "active" and "inactive" and further discriminating the potentially biologically active compounds from the inactive ones (Cheng et al., 2015; Xie et al., 2015).

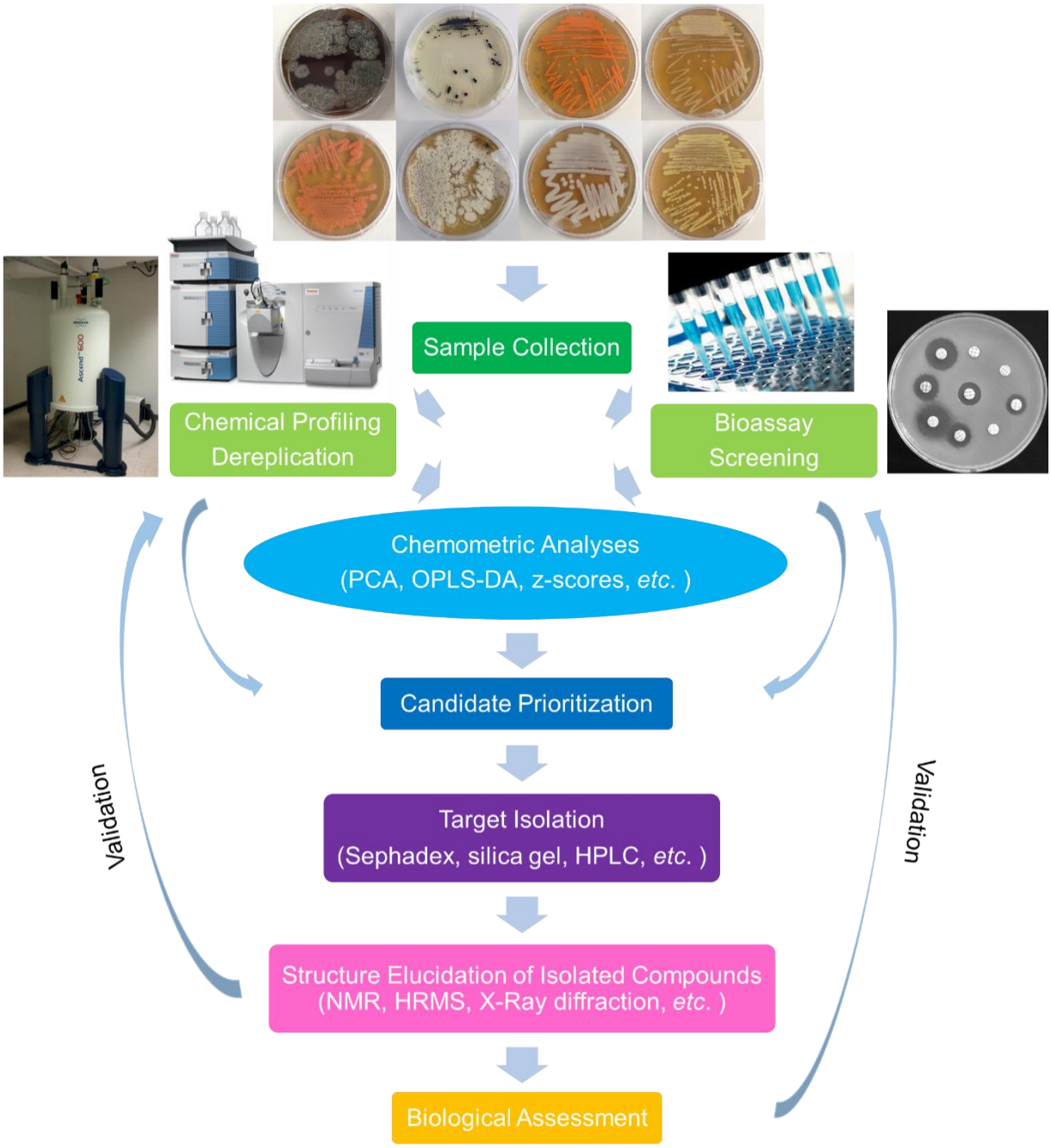

Fig. 1.3 Flowchart of metabolomics tools and biological states based natural product discovery

There are also some previously described examples of the successful identification of new compounds without any chromatographic step. Ancistrogriffithine A is one representative identified from the extract of *Ancistrocladus griffithii* using the hyphenated techniques LC-MS/LC-NMR/LC-CD Triad in the group of Bringmann (Bringmann et al., 2001). TC-705A and TC-705B are two new indole alkaloids characterized by Schroeder et al. using a library developed with 2D NMR spectra of crude fungal extracts (Schroeder et al., 2007).

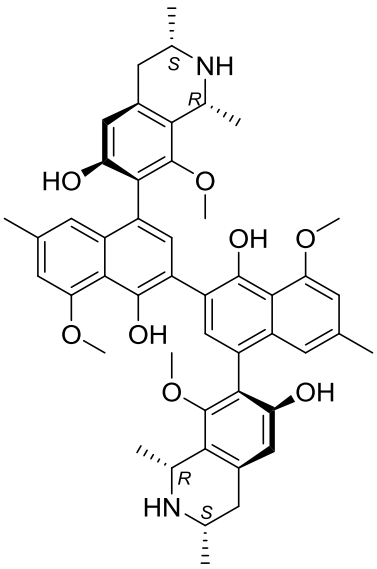

Ancistrogriffithine A

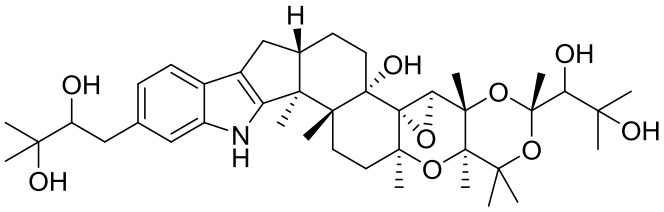

TC-705A

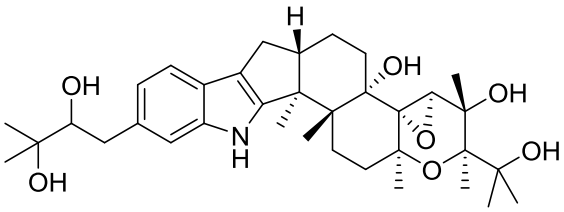

TC-705B

1.5 Scope of the study

Marine sponge-associated microorganisms exhibit great potential in producing natural products with diverse medicinal and pharmaceutical properties. In this Ph.D. thesis, I aimed to apply metabolomics tools to search for and isolate novel biologically active compounds from marine sponge-associated actinomycetes. The experimental tasks were divided into three parts as follows:

The first task (Chapter 2) involved the cultivation of actinomycetes from marine sponges with a particular focus to improve the novel taxa isolation using different modified media. Furthermore, the taxonomic identification of the recovered strains using nearly full-length 16S rRNA gene sequence analysis and bioassay screening of the crude bacterial extracts including antioxidant, antimicrobial, and antitrypanosomal bioassays was performed.

The second task (Chapter 3) aimed at prioritizing candidate strains for up-scaling cultivation and compounds isolation. Preliminary investigation of bacterial secondary metabolites was implemented on a group of selected actinomycetes by HPLC profiling, dereplication study and multivariate statistic approaches, such as PCA and OPLS-DA using LC-MS and NMR data obtained from their crude organic extracts. The nomination of candidate strains for further compounds isolation was based on four criteria, including taxonomic novelty, biological activity, metabolomics uniqueness, and HPLC profiling richness.

The third task (Chapter 4) aimed to isolate and structurally elucidate compounds and test their activities in assays including antioxidant, anti-fungal, anti-Shiga toxin production, anti-cancer, as well as antichlamydial assays.

The experimental chapters are accompanied by an introduction (Chapter 1) and a general discussion (Chapter 5) on the association of actinomycetes with marine sponges, as well as metabolomics based approach of natural products discovery, and their pharmaceutical potential.

1.6 References

Abdelmohsen, U.R., Bayer, K., Hentschel, U., 2014a. Diversity, abundance and natural products of marine sponge-associated actinomycetes. Natural product reports 31, 381-399.

Abdelmohsen, U.R., Cheng, C., Viegelmann, C., Zhang, T., Grkovic, T., Ahmed, S., Quinn, R.J., Hentschel, U., Edrada-Ebel, R., 2014b. Dereplication strategies for targeted isolation of new antitrypanosomal actinosporins A and B from a marine sponge associated-*Actinokineospora* sp. EG49. Marine drugs 12, 1220-1244.

Abdelmohsen, U.R., Grkovic, T., Balasubramanian, S., Kamel, M.S., Quinn, R.J., Hentschel, U., 2015. Elicitation of secondary metabolism in actinomycetes. Biotechnology advances 33, 798-811.

Abdelmohsen, U.R., Szesny, M., Othman, E.M., Schirmeister, T., Grond, S., Stopper, H., Hentschel, U., 2012a. Antioxidant and anti-protease activities of diazepinomicin from the sponge-associated *Micromonospora* Strain RV115. Marine drugs 10, 2208-2221.

Abdelmohsen, U.R., Zhang, G.L., Philippe, A., Schmitz, W., Pimentel-Elardo, S.M., Hertlein-Amslinger, B., Hentschel, U., Bringmann, G., 2012b. Cyclodysidins A–D, cyclic lipopeptides from the marine sponge-derived *Streptomyces* strain RV15. Tetrahedron letters 53, 23-29.

Antcliffe, J.B., Callow, R.H., Brasier, M.D., 2014. Giving the early fossil record of sponges a squeeze. Biological reviews of the Cambridge Philosophical Society 89, 972-1004.

Bayer, K., Schmitt, S., Hentschel, U., 2008. Physiology, phylogeny and in situ evidence for bacterial and archaeal nitrifiers in the marine sponge *Aplysina aerophoba*. Environmental microbiology 10, 2942-2955.

Beer, S., Ilan, M., In situ measurements of photosynthetic irradiance responses of two Red Sea sponges growing under dim light conditions. Marine biology 131, 613-617.

Berlanga, M., 2015. Functional symbiosis and communication in microbial ecosystems. The case of wood-eating termites and cockroaches. International microbiology: the official journal of the Spanish Society for Microbiology 18, 159-169.

Bewley, C.A., Holland, N.D., Faulkner, D.J., 1996. Two classes of metabolites from *Theonella swinhoei* are localized in distinct populations of bacterial symbionts. Experientia 52, 716-722.

Blunt, J.W., Copp, B.R., Keyzers, R.A., Munro, M.H., Prinsep, M.R., 2013. Marine natural products. Natural product reports 30, 237-323.

Blunt, J.W., Copp, B.R., Keyzers, R.A., Munro, M.H.G., Prinsep, M.R., 2015. Marine natural products. Natural product reports 32, 116-211.

Bock, C., Lengauer, T., 2012. Managing drug resistance in cancer: lessons from HIV therapy. Nature reviews cancer 12, 494-501.

Bollmann, A., Lewis, K., Epstein, S.S., 2007. Incubation of environmental samples in a diffusion chamber increases the diversity of recovered isolates. Applied and Environmental microbiology 73, 6386-6390.

Bredholdt, H., Galatenko, O.A., Engelhardt, K., Fjaervik, E., Terekhova, L.P., Zotchev, S.B., 2007. Rare actinomycete bacteria from the shallow water sediments of the Trondheim fjord, Norway: isolation, diversity and biological activity. Environmental microbiology 9, 2756-2764.

Bringmann, G., Lang, G., 2003. Full absolute stereostructures of natural products directly from crude extracts: The HPLC-MS/ MS-NMR-CD 'triad'. Progress in molecular and subcellular biology 37, 89-116.

Bringmann, G., Wohlfarth, M., Rischer, H., Heubes, M., Saeb, W., Diem, S., Herderich, M., Schlauer, J., 2001. A photometric screening method for dimeric naphthylisoquinoline alkaloids and complete on-line structural elucidation of a dimer in crude plant extracts, by the LC-MS/LC-NMR/LC-CD triad. Analytical chemistry 73, 2571-2577.

Brusca, R.C., Brusca, G.J., 1990. Phylum porifera: the sponges. In: Sinauer, A.D. (Ed.) Invertebrates. Sinauer Press, MA, USA, p 179-208.

Bylesjö, M., Rantalainen, M., Cloarec, O., Nicholson, J.K., Holmes, E., Trygg, J., 2006. OPLS discriminant analysis: combining the strengths of PLS-DA and SIMCA classification. Journal of chemometrics 20, 341-351.

Cheng, C., MacIntyre, L., Abdelmohsen, U.R., Horn, H., Polymenakou, P.N., Edrada-Ebel, R., Hentschel, U., 2015. Biodiversity, anti-trypanosomal activity screening, and metabolomic profiling of actinomycetes isolated from Mediterranean sponges. PloS one 10, e0138528.

Chistoserdova, L., Kalyuzhnaya, M.G., Lidstrom, M.E., 2009. The expanding world of methylotrophic metabolism. Annual review of microbiology 63, 477-499.

Choi, H., Koh, H.W., Kim, H., Chae, J.C., Park, S.J., 2016. Microbial community composition in the marine sediments of Jeju Island: next-generation sequencing surveys. Journal of microbiology and biotechnology.

Crits-Christoph, A., Robinson, C.K., Ma, B., Ravel, J., Wierzchos, J., Ascaso, C., Artieda, O., Souza-Egipsy, V., Casero, M.C., DiRuggiero, J., 2016. Phylogenetic and functional substrate specificity for endolithic microbial communities in hyper-arid environments. Frontiers in microbiology 7, 301.

Dashti, Y., Grkovic, T., Abdelmohsen, U.R., Hentschel, U., Quinn, R.J., 2014. Production of induced secondary metabolites by a co-culture of sponge-associated actinomycetes, *Actinokineospora* sp. EG49 and *Nocardiopsis* sp. RV163. Marine drugs 12, 3046-3059.

de Menezes, C.B., Tonin, M.F., Silva, L.J., de Souza, W.R., Parma, M., de Melo, I.S., Zucchi, T.D., Destefano, S.A., Fantinatti-Garboggini, F., 2015. *Marmoricola aquaticus* sp. nov., an actinomycete isolated from a marine sponge. International journal of systematic and evolutionary microbiology 65, 2286-2291.

Eder, J., Sedrani, R., Wiesmann, C., 2014. The discovery of first-in-class drugs: origins and evolution. Nature reviews drug discovery 13, 577-587.

Eltamany, E.E., Abdelmohsen, U.R., Ibrahim, A.K., Hassanean, H.A., Hentschel, U., Ahmed, S.A., 2014. New antibacterial xanthone from the marine sponge-derived *Micrococcus* sp. EG45. Bioorganic & medicinal chemistry letters 24, 4939-4942

Eriksson, L., Byrne, T., Johansson, F., Trygg, J., Vikström, C., 2006. Multi- and megavariate data analysis-basic principles and applications. Umetrics AB Publisher, Sweden, P 39-62.

Fenical, W., Jensen, P.R., 2006. Developing a new resource for drug discovery: marine actinomycete bacteria. Nature chemistry biolology 2, 666-673.

Fiehn, O., Kopka, J., Dormann, P., Altmann, T., Trethewey, R.N., Willmitzer, L., 2000. Metabolite profiling for plant functional genomics. Nature biotechnology 18, 1157-1161.

Flatt, P.M., Gautschi, J.T., Thacker, R.W., Musafija-Girt, M., Crews, P., Gerwick, W.H., 2005. Identification of the cellular site of polychlorinated peptide biosynthesis in the marine sponge *Dysidea* (*Lamellodysidea*) *herbacea* and symbiotic cyanobacterium *Oscillatoria spongeliae* by CARD-FISH analysis. Marine biology 147, 761-774.

Forner, D., Berrue, F., Correa, H., Duncan, K., Kerr, R.G., 2013. Chemical dereplication of marine actinomycetes by liquid chromatography-high resolution mass spectrometry profiling and statistical analysis. Analytica chimica acta 805, 70-79.

Fraser, P.D., Pinto, M.E., Holloway, D.E., Bramley, P.M., 2000. Technical advance: application of high-performance liquid chromatography with photodiode array detection to the metabolic profiling of plant isoprenoids. The Plant journal: for cell and molecular biology 24, 551-558.

Garrity, G.M., Bell, J.A., Lilburn, T.G., 2004. Taxonomic outline of the prokaryotes. In: Bergey's manual of systematic bacteriology. Springer, Berlin, Germany, p 204-301

Gavrish, E., Bollmann, A., Epstein, S., Lewis, K., 2008. A trap for in situ cultivation of filamentous actinobacteria. Journal of microbiological methods 72, 257-262.

Goodfellow, M., Williams, S.T., 1983. Ecology of actinomycetes. Annual review of microbiology 37, 189-216.

Grkovic, T., Abdelmohsen, U.R., Othman, E.M., Stopper, H., Edrada-Ebel, R., Hentschel, U., Quinn, R.J., 2014. Two new antioxidant actinosporin analogues from the calcium alginate beads culture of sponge-associated *Actinokineospora* sp. strain EG49. Bioorganic & medicinal chemistry letters 24, 5089-5092.

Guo, L.X., Li, R., Liu, K., Yang, J., Li, H.J., Li, S.L., Liu, J.Q., Liu, L.F., Xin, G.Z., 2015. Structural characterization and discrimination of Chinese medicinal materials with multiple botanical origins based on metabolite profiling and chemometrics analysis: *Clematidis Radix et Rhizoma* as a case study. Journal of chromatography. A 1425, 129-140.

Hadas, E., Marie, D., Shpigel, M., Ilan, M., 2006. Virus predation by sponges is a new nutrient-flow pathway in coral reef food webs. Limnology Oceanography 51, 1548–1550.

Hall, V., 2008. Actinomyces-gathering evidence of human colonization and infection. Anaerobe 14, 1-7.

Hames-Kocabas, E.E., Uzel, A., 2012. Isolation strategies of marine-derived actinomycetes from sponge and sediment samples. Journal of microbiological methods 88, 342-347.

Hao, Y.F., Jiang, J.G., 2015. Origin and evolution of China Pharmacopoeia and its implication for traditional medicines. Mini reviews in medicinal chemistry 15, 595-603.

Hardoim, C.C., Costa, R., 2014. Microbial communities and bioactive compounds in marine sponges of the family *ircinidae*-a review. Marine drugs 12, 5089-5122.

Harrigan, G., 2002. Metabolic profiling: pathways in drug discovery. Drug discovery today 7, 351-352.

Harvey, A.L., Edrada-Ebel, R., Quinn, R.J., 2015. The re-emergence of natural products for drug discovery in the genomics era. Nature reviews drug discovery 14, 111-129.

He, L., Liu, F., Karuppiah, V., Ren, Y., Li, Z., 2014. Comparisons of the fungal and protistan communities among different marine sponge holobionts by pyrosequencing. Microbial ecology 67, 951-961.

Head, I.M., Saunders, J.R., Pickup, R.W., 1998. Microbial evolution, diversity, and ecology: a decade of ribosomal RNA analysis of uncultivated microorganisms. Microbiol Ecolology 35, 1-21.

Hentschel, U., Fieseler, L., Wehrl, M., Gernert, C., Steinert, M., Hacker, J., Horn, M., 2003. Microbial diversity of marine sponges. Progress in molecular and subcellular biology 37, 59-88.

Hentschel, U., Hopke, J., Horn, M., Friedrich, A.B., Wagner, M., Hacker, J., Moore, B.S., 2002. Molecular evidence for a uniform microbial community in sponges from different oceans. Applied and environmental microbiology 68, 4431-4440.

Hentschel, U., Piel, J., Degnan, S.M., Taylor, M.W., 2012. Genomic insights into the marine sponge microbiome. Nature reviews microbiology 10, 641-654.

Hentschel, U., Schmid, M., Wagner, M., Fieseler, L., Gernert, C., Hacker, J., 2001. Isolation and phylogenetic analysis of bacteria with antimicrobial activities from the Mediterranean sponges *Aplysina aerophoba* and *Aplysina cavernicola*. FEMS microbiology ecology 35, 305-312.

Hooper, J.N.A., Van Soest, R.W.M., 2002. Systema porifera: a guide to the classification of sponges. Kluwer Academic/Plenum Publishers, New York, USA, p 9-13.

Hosoya, T., Hirokawa, T., Takagi, M., Shin-ya, K., 2012. Trichostatin analogues JBIR-109, JBIR-110, and JBIR-111 from the marine sponge-derived *Streptomyces* sp. RM72. Journal of natural products 75, 285-289.

Hou, Y., Braun, D.R., Michel, C.R., Klassen, J.L., Adnani, N., Wyche, T.P., Bugni, T.S., 2012. Microbial strain prioritization using metabolomics tools for the discovery of natural products. Analytical chemistry 84, 4277-4283.

Huaman, M.A., Ribes, J.A., Lohr, K.M., Evans, M.E., 2016. *Mycobacterium marinum* infection after exposure to coal mine water. Open forum infectious diseases 3, ofv205.

Huang, X., Zhou, S., Huang, D., Chen, J., Zhu, W., 2015. *Streptomyces spongiicola* sp. nov. , a novel marine sponge-derived actinomycete. International journal of systematic and evolutionary microbiology 66, 738-743.

Hughes, D.E., Andersson, D.I., 2015. Evolutionary consequences of drug resistance: shared principles across diverse targets and organisms. Nature review genetics 16, 459-471.

Inui, T., Wang, Y., Pro, S.M., Franzblau, S.G., Pauli, G.F., 2012. Unbiased evaluation of bioactive secondary metabolites in complex matrices. Fitoterapia 83, 1218-1225.

Jackson, S.A., Flemer, B., McCann, A., Kennedy, J., Morrissey, J.P., O'Gara, F., Dobson, A.D., 2013. Archaea appear to dominate the microbiome of *Inflatella pellicula* deep sea sponges. PloS one 8, e84438.

Jin, L., Liu, F., Sun, W., Zhang, F., Karuppiah, V., Li, Z., 2014. Pezizomycotina dominates the fungal communities of South China Sea sponges *Theonella swinhoei* and *Xestospongia testudinaria*. FEMS microbiology ecology 90, 935-945.

Jung, D., Seo, E.Y., Epstein, S.S., Joung, Y., Han, J., Parfenova, V.V., Belykh, O.I., Gladkikh, A.S., Ahn, T.S., 2014. Application of a new cultivation technology, I-tip, for studying microbial diversity in freshwater sponges of Lake Baikal, Russia. FEMS microbiology ecology 90, 417-423.

Kaeberlein, T., Lewis, K., Epstein, S.S., 2002. Isolating "uncultivable" microorganisms in pure culture in a simulated natural environment. Science 296, 1127-1129.

Kampfer, P., Glaeser, S.P., Busse, H.J., Abdelmohsen, U.R., Ahmed, S., Hentschel, U., 2015. Actinokineospora *spheciospongiae* sp. nov., isolated from the marine sponge *Spheciospongia vagabunda*. International journal of systematic and evolutionary microbiology 65, 879-884.

Kampfer, P., Glaeser, S.P., Busse, H.J., Abdelmohsen, U.R., Hentschel, U., 2014. *Rubrobacter aplysinae* sp. nov., isolated from the marine sponge *Aplysina aerophoba*. International journal of systematic and evolutionary microbiology 64, 705-709.

Kim, M.C., Hwang, E., Kim, T., Ham, J., Kim, S.Y., Kwon, H.C., 2014. Nocatriones A and B, photoprotective tetracenediones from a marine-derived *Nocardiopsis* sp. Journal of natural products 77, 2326-2330.

Korn-Wendisch, F., Kutzner, H.J., 1992. The family *Streptomycetaceae*. In: The Prokaryotes Springer-Verlag Inc., New York, USA, p 921-995.

Koyama, S., Nishi, S., Tokuda, M., Uemura, M., Ishikawa, Y., Seya, T., Chow, S., Ise, Y., Hatada, Y., Fujiwara, Y., Tsubouchi, T., 2015. Electrical retrieval of living microorganisms from cryopreserved marine sponges using a potential-controlled electrode. Marine biotechnology 17, 678-692.

Kunz, A.L., Labes, A., Wiese, J., Bruhn, T., Bringmann, G., Imhoff, J.F., 2014. Nature's lab for derivatization: new and revised structures of a variety of streptophenazines produced by a sponge-derived *Streptomyces* strain. Marine drugs 12, 1699-1714.

Kurtboke, D.I., French, J.R., Hayes, R.A., Quinn, R.J., 2015. Eco-taxonomic insights into actinomycete symbionts of termites for discovery of novel bioactive compounds. Advances in biochemical engineering/biotechnology 147, 111-135.

Kwon, H.C., Kauffman, C.A., Jensen, P.R., Fenical, W., 2006. Marinomycins A-D, antitumor-antibiotics of a new structure class from a marine actinomycete of the recently discovered genus "*marinispora*". Journal of the American Chemical Society 128, 1622-1632.

Lane, A.L., Moore, B.S., 2011. A sea of biosynthesis: marine natural products meet the molecular age. Natural product reports 28, 411-428.

Lewis, K., Epstein, S., D'Onofrio, A., Ling, L.L., 2010. Uncultured microorganisms as a source of secondary metabolites. Journal of antibiotics 63, 468-476.

Li, Y., Wang, Y., Su, L., Li, L., Zhang, Y., 2013. Exploring potential chemical markers by metabolomics method for studying the processing mechanism of traditional Chinese medicine using RPLC-Q-TOF/MS: a case study of *Radix Aconiti*. Chemistry central journal 7, 36.

Lindon, J.C., Nicholson, J.K., Holmes, E., 2006. The Handbook of Metabonomics and Metabolomics. Elsevier Science, Amsterdam, Netherlands, p 1-33.

Ling, L.L., Schneider, T., Peoples, A.J., Spoering, A.L., Engels, I., Conlon, B.P., Mueller, A., Schaberle, T.F., Hughes, D.E., Epstein, S., Jones, M., Lazarides, L., Steadman, V.A., Cohen, D.R., Felix, C.R., Fetterman, K.A., Millett, W.P., Nitti, A.G., Zullo, A.M., Chen, C., Lewis, K., 2015. A new antibiotic kills pathogens without detectable resistance. Nature 517, 455-459.

Liu, M., Fan, L., Zhong, L., Kjelleberg, S., Thomas, T., 2012. Metaproteogenomic analysis of a community of sponge symbionts. The ISME journal 6, 1515-1525.

Liu, S., Liang, Y.Z., Liu, H.T., 2016. Chemometrics applied to quality control and metabolomics for traditional Chinese medicines. Journal of chromatography. B, Analytical technologies in the biomedical and life sciences 1015, 82-91.

Locci, R., 1994. Actinomycetes as plant pathogens. European Journal of Plant Pathology 100, 179-200.

Luo, Q., Liu, C.H., Gu, M., 2010. Recording of classical prescriptions and materia medica in the Han Dynasty. Zhonghua yi shi za zhi 40, 376-378.

Macintyre, L., Zhang, T., Viegelmann, C., Martinez, I.J., Cheng, C., Dowdells, C., Abdelmohsen, U.R., Gernert, C., Hentschel, U., Edrada-Ebel, R., 2014. Metabolomic tools for secondary metabolite discovery from marine microbial symbionts. Marine drugs 12, 3416-3448.

Mahmoud, H.M., Kalendar, A.A., 2016. Coral-associated actinobacteria: diversity, abundance, and biotechnological potentials. Frontiers in microbiology 7, 204.

Moitinho-Silva, L., Seridi, L., Ryu, T., Voolstra, C.R., Ravasi, T., Hentschel, U., 2014. Revealing microbial functional activities in the Red Sea sponge *Stylissa carteri* by metatranscriptomics. Environmental microbiology 16, 3683-3698.

Molinski, T.F., Dalisay, D.S., Lievens, S.L., Saludes, J.P., 2009. Drug development from marine natural products. Nature reviews drug discovery 8, 69-85.

Motohashi, K., Takagi, M., Shin-Ya, K., 2010. Tetracenoquinocin and 5-iminoaranciamycin from a sponge-derived *Streptomyces* sp. Sp080513GE-26. Journal of natural products 73, 755-758.

Nicholson, J.K., Lindon, J.C., 2008. Systems biology: metabonomics. Nature 455, 1054-1056.

Nicholson, J.K., O'Flynn, M.P., Sadler, P.J., Macleod, A.F., Juul, S.M., Sonksen, P.H., 1984. Proton-nuclear-magnetic-resonance studies of serum, plasma and urine from fasting normal and diabetic subjects. The biochemical journal 217, 365-375.

Norris, M.D., Perkins, M.V., 2016. Structural diversity and chemical synthesis of peroxide and peroxide-derived polyketide metabolites from marine sponges. Natural product reports, doi: 10.1039/C5NP00142K.

Oliver, S.G., Winson, M.K., Kell, D.B., Baganz, F., 1998. Systematic functional analysis of the yeast genome. Trends in biotechnology 16, 373-378.

Olson, J.B., Lord, C.C., McCarthy, P.J., 2000. Improved Recoverability of Microbial Colonies from Marine Sponge Samples. Microbial ecology 40, 139-147.

Pauling, L., Robinson, A.B., Teranishi, R., Cary, P., 1971. Quantitative analysis of urine vapor and breath by gas-liquid partition chromatography. Proceedings of the National Academy of Sciences of the United States of America 68, 2374-2376.

Pawlowski, K., Demchenko, K.N., 2012. The diversity of actinorhizal symbiosis. Protoplasma 249, 967-979.

Pelkonen, O., Pasanen, M., Lindon, J.C., Chan, K., Zhao, L., Deal, G., Xu, Q., Fan, T.P., 2012. Omics and its potential impact on R&D and regulation of complex herbal products. Journal of ethnopharmacology 140, 587-593.

Piel, J., 2004. Metabolites from symbiotic bacteria. Natural product reports 21, 519-538.

Pimentel-Elardo, S.M., Buback, V., Gulder, T.A., Bugni, T.S., Reppart, J., Bringmann, G., Ireland, C.M., Schirmeister, T., Hentschel, U., 2011. New tetromycin derivatives with anti-trypanosomal and protease inhibitory activities. Marine drugs 9, 1682-1697.

Pimentel-Elardo, S.M., Sorensen, D., Ho, L., Ziko, M., Bueler, S.A., Lu, S., Tao, J., Moser, A., Lee, R., Agard, D., Fairn, G., Rubinstein, J.L., Shoichet, B.K., Nodwell, J.R., 2015. Activity-independent discovery of secondary metabolites using chemical elicitation and cheminformatic inference. ACS chemical biology 10, 2616-2623.

Proksch, P., 1994. Defensive roles for secondary metabolites from marine sponges and sponge-feeding nudibranchs. Toxicon: official journal of the International Society on Toxinology 32, 639-655.

Proksch, P., Putz, A., Ortlepp, S., Kjer, J., Bayer, M., 2010. Bioactive natural products from marine sponges and fungal endophytes. Phytochemistry Reviews 9, 475-489.

Radax, R., Rattei, T., Lanzen, A., Bayer, C., Rapp, H.T., Urich, T., Schleper, C., 2012. Metatranscriptomics of the marine sponge *Geodia barretti*: tackling phylogeny and function of its microbial community. Environmental microbiology 14, 1308-1324.

Reimer, A., Blohm, A., Quack, T., Grevelding, C.G., Kozjak-Pavlovic, V., Rudel, T., Hentschel, U., Abdelmohsen, U.R., 2015. Inhibitory activities of the marine streptomycete-derived compound SF2446A2 against *Chlamydia trachomatis* and *Schistosoma mansoni*. Journal of antibiotics 68, 674-679.

Reiswig, M.H., 1971. Particle feeding in natural populations of three marine demosponges. The biological bulletin 141, 568-591.

Rodrigues, R.R., Pineda, R.P., Barney, J.N., Nilsen, E.T., Barrett, J.E., Williams, M.A., 2015. Plant invasions associated with change in root-zone microbial community structure and diversity. PloS one 10, e0141424.

Rodriguez-Marconi, S., De la Iglesia, R., Diez, B., Fonseca, C.A., Hajdu, E., Trefault, N., 2015. Characterization of bacterial, archaeal and eukaryote symbionts from Antarctic Sponges reveals a high diversity at a three-domain level and a particular signature for this ecosystem. PloS one 10, e0138837.

Roue, M., Quevrain, E., Domart-Coulon, I., Bourguet-Kondracki, M.-L., 2012. Assessing calcareous sponges and their associated bacteria for the discovery of new bioactive natural products. Natural product reports 29, 739-751.

Rutledge, P.J., Challis, G.L., 2015. Discovery of microbial natural products by activation of silent biosynthetic gene clusters. Nature reviews microbiology 13, 509-523.

Rutzler, K., 1985. Associations between Caribbean sponges and photosynthetic organisms. Smithsonian Institution Press, 455-466.

Samat, N., Tan, P.J., Shaari, K., Abas, F., Lee, H.B., 2014. Prioritization of natural extracts by LC-MS-PCA for the identification of new photosensitizers for photodynamic therapy. Analytical chemistry 86, 1324-1331.

Sarker, S.D., Nahar, L., 2012. An introduction to natural products isolation. Methods in molecular biology 864, 1-25.

Schaberle, T.F., Orland, A., Konig, G.M., 2014. Enhanced production of undecylprodigiosin in *Streptomyces coelicolor* by co-cultivation with the corallopyronin A-producing myxobacterium, *Corallococcus coralloides*. Biotechnology letters 36, 641-648.

Schlappy, M.L., Schottner, S.I., Lavik, G., Kuypers, M.M., de Beer, D., Hoffmann, F., 2010. Evidence of nitrification and denitrification in high and low microbial abundance sponges. Marine Biology 157, 593-602.

Schlotterbeck, G., Ross, A., Dieterle, F., Senn, H., 2006. Metabolic profiling technologies for biomarker discovery in biomedicine and drug development. The pharmacogenomics journal 7, 1055-1075.

Schmitt, S., Tsai, P., Bell, J., Fromont, J., Ilan, M., Lindquist, N., Perez, T., Rodrigo, A., Schupp, P.J., Vacelet, J., Webster, N., Hentschel, U., Taylor, M.W., 2012. Assessing the complex sponge microbiota: core, variable and species-specific bacterial communities in marine sponges. The ISME journal 6, 564-576.

Schneemann, I., Kajahn, I., Ohlendorf, B., Zinecker, H., Erhard, A., Nagel, K., Wiese, J., Imhoff, J.F., 2010. Mayamycin, a cytotoxic polyketide from a *Streptomyces* strain isolated from the marine sponge *Halichondria panicea*. Journal of natural products 73, 1309-1312.

Schroeder, F.C., Gibson, D.M., Churchill, A.C., Sojikul, P., Wursthorn, E.J., Krasnoff, S.B., Clardy, J., 2007. Differential analysis of 2D NMR spectra: new natural products from a pilot-scale fungal extract library. Angewandte Chemie (International ed. in English) 46, 901-904.

Selvameenal, L., Radhakrishnan, M., Balagurunathan, R., 2009. Antibiotic pigment from desert soil actinomycetes; biological activity, purification and chemical screening. Indian journal of pharmaceutical sciences 71, 499-504.

Selvin, J., 2009. Exploring the antagonistic producer *Streptomyces* MSI051: implications of polyketide synthase gene type II and a ubiquitous defense enzyme phospholipase A2 in the host sponge *Dendrilla nigra*. Current microbiology 58, 459-463.

Selvin, J., Ninawe, A.S., Kiran, G.S., Lipton, A.P., 2010. Sponge-microbial interactions: ecological implications and bioprospecting avenues. Critical reviews in microbiology 36, 82-90.

Simister, R.L., Deines, P., Botte, E.S., Webster, N.S., Taylor, M.W., 2012. Sponge-specific clusters revisited: a comprehensive phylogeny of sponge-associated microorganisms. Environmental microbiology 14, 517-524.

Simmons, L., Kaufmann, K., Garcia, R., Schwar, G., Huch, V., Muller, R., 2011. Bendigoles D-F, bioactive sterols from the marine sponge-derived *Actinomadura* sp. SBMs009. Bioorganic & medicinal chemistry 19, 6570-6575.

Smith, C.A., O'Maille, G., Want, E.J., Qin, C., Trauger, S.A., Brandon, T.R., Custodio, D.E., Abagyan, R., Siuzdak, G., 2005. METLIN: a metabolite mass spectral database. Therapeutic drug monitoring 27, 747-751.

Solanki, R., Khanna, M., Lal, R., 2008. Bioactive compounds from marine actinomycetes. Indian journal of microbiology 48, 410-431.

Steinert, G., Whitfield, S., Taylor, M.W., Thoms, C., Schupp, P.J., 2014. Application of diffusion growth chambers for the cultivation of marine sponge-associated bacteria. Marine biotechnology (New York, N.Y.) 16, 594-603.

Subramani, R., Aalbersberg, W., 2012. Marine actinomycetes: an ongoing source of novel bioactive metabolites. Microbiological research 167, 571-580.

Subramani, R., Aalbersberg, W., 2013. Culturable rare actinomycetes: diversity, isolation and marine natural product discovery. Applied microbiology and biotechnology 97, 9291-9321.

Sun, H., Wang, M., Zhang, A., Ni, B., Dong, H., Wang, X., 2013. UPLC-Q-TOF-HDMS analysis of constituents in the root of two kinds of *Aconitum* using a metabolomics approach. Phytochemical analysis 24, 263-276.

Supong, K., Suriyachadkun, C., Suwanborirux, K., Pittayakhajonwut, P., Thawai, C., 2013. *Verrucosispora andamanensis* sp. nov., isolated from a marine sponge. International journal of systematic and evolutionary microbiology 63, 3970-3974.

Tabares, P., Pimentel-Elardo, S.M., Schirmeister, T., Hunig, T., Hentschel, U., 2011. Anti-protease and immunomodulatory activities of bacteria associated with Caribbean sponges. Marine biotechnology 13, 883-892.

Takizawa, M., Colwell, R.R., Hill, R.T., 1993. Isolation and diversity of actinomycetes in the chesapeake bay. Applied and environmental microbiology 59, 997-1002.

Tawfike, A.F., Viegelmann, C., Edrada-Ebel, R., 2013. Metabolomics and dereplication strategies in natural products. Methods in molecular biology 1055, 227-244.

Taylor, M.W., Radax, R., Steger, D., Wagner, M., 2007. Sponge-associated microorganisms: evolution, ecology, and biotechnological potential. Microbiology and molecular biology reviews : MMBR 71, 295-347.

Thacker, R.W., Freeman, C.J., 2012. Sponge-microbe symbioses: recent advances and new directions. Advances in marine biology 62, 57-111.

Thomas, T., Rusch, D., DeMaere, M.Z., Yung, P.Y., Lewis, M., Halpern, A., Heidelberg, K.B., Egan, S., Steinberg, P.D., Kjelleberg, S., 2010. Functional genomic signatures of sponge bacteria reveal unique and shared features of symbiosis. The ISME journal 4, 1557-1567.

Tiwari, K., Gupta, R.K., 2012. Rare actinomycetes: a potential storehouse for novel antibiotics. Critical reviews in biotechnology 32, 108-132.

Toya, Y., Shimizu, H., 2013. Flux analysis and metabolomics for systematic metabolic engineering of microorganisms. Biotechnology advances 31, 818-826.

Tu, Y., 2011. The discovery of artemisinin (qinghaosu) and gifts from Chinese medicine. Nature medicine 17, 1217-1220.

Unson, M.D., Holland, N.D., Faulkner, D.J., 1994. A brominated secondary metabolite synthesized by the cyanobacterial symbiont of a marine sponge and accumulation of the crystalline metabolite in the sponge tissue. Marine biology 119, 1-11.

Vacelet, J., Boury-Esnault, N., Fiala-Medioni, A., Fisher, C.R., 1995. A methanotrophic carnivorous sponge. Nature 377, 296-296.

Vacelet, J., Donadey, C., 1977. Electron microscope study of the association between some sponges and bacteria. Journal of experimental marine biology and ecology 30, 301-314.

Van Goethem, M.W., Makhalanyane, T.P., Valverde, A., Cary, S.C., Cowan, D.A., 2016. Characterization of bacterial communities in lithobionts and soil niches from Victoria Valley, Antarctica. FEMS microbiology ecology 92.

Ventura, M., Canchaya, C., Tauch, A., Chandra, G., Fitzgerald, G.F., Chater, K.F., van Sinderen, D., 2007. Genomics of Actinobacteria: tracing the evolutionary history of an ancient phylum. Microbiology and molecular biology reviews 71, 495-548.

Viegelmann, C., Parker, J., Ooi, T., Clements, C., Abbott, G., Young, L., Kennedy, J., Dobson, A.D., Edrada-Ebel, R., 2014. Isolation and identification of antitrypanosomal and antimycobacterial active steroids from the sponge *Haliclona simulans*. Marine drugs 12, 2937-2952.

Vladimir, B., 1983. The chemistry and biology of antibiotics. Pharmacochemistry library 5, 594-595.

Waksman, S.A., 1950. The actinomycetes: their nature, occurrence, activities and importance. Chronica Botanica Company. Mass. USA, p 3-21.

Wang, M., Lamers, R.J., Korthout, H.A., van Nesselrooij, J.H., Witkamp, R.F., van der Heijden, R., Voshol, P.J., Havekes, L.M., Verpoorte, R., van der Greef, J., 2005. Metabolomics in the context of systems biology: bridging traditional Chinese medicine and molecular pharmacology. Phytotherapy research 19, 173-182.

Wang, Y., Wang, L., Zhuang, Y., Kong, F., Zhang, C., Zhu, W., 2014. Phenolic polyketides from the co-cultivation of marine-derived *Penicillium* sp. WC-29-5 and *Streptomyces fradiae* 007. Marine drugs 12, 2079-2088.

Wasylenko, T.M., Stephanopoulos, G., 2015. Metabolomic and (13)C-metabolic flux analysis of a xylose-consuming *Saccharomyces cerevisiae* strain expressing xylose isomerase. Biotechnology and bioengineering 112, 470-483.

Webster, N.S., Luter, H.M., Soo, R.M., Botte, E.S., Simister, R.L., Abdo, D., Whalan, S., 2012. Same, same but different: symbiotic bacterial associations in GBR sponges. Frontiers in microbiology 3, 444.

Webster, N.S., Wilson, K.J., Blackall, L.L., Hill, R.T., 2001. Phylogenetic diversity of bacteria associated with the marine sponge *Rhopaloeides odorabile*. Applied and environmental microbiology 67, 434-444.

Wehrl, M., Steinert, M., Hentschel, U., 2007. Bacterial uptake by the marine sponge *Aplysina aerophoba*. Microbial ecology 53, 355-365.

Wei, R.B., Xi, T., Li, J., Wang, P., Li, F.C., Lin, Y.C., Qin, S., 2011. Lobophorin C and D, new kijanimicin derivatives from a marine sponge-associated actinomycetal strain AZS17. Marine drugs 9, 359-368.

Wiese, J., Ohlendorf, B., Blumel, M., Schmaljohann, R., Imhoff, J.F., 2011. Phylogenetic identification of fungi isolated from the marine sponge *Tethya aurantium* and identification of their secondary metabolites. Marine drugs 9, 561-585.

Wilkinson, C.R., 1978. Microbial associations in sponges. I. Ecology, physiology and microbial populations of coral reef sponges. Marine Biology 49, 161-167.

Wilkinson, C.R., 1992. Symbiotic interactions between marine sponges and algae. In: Reisser (ed) Algae and symbioses: plants, animals, fungi, viruses, interactions explored. Biopress Ltd. Bristol, United Kingdom, p 112-128.

Wilson, M.C., Mori, T., Ruckert, C., Uria, A.R., Helf, M.J., Takada, K., Gernert, C., Steffens, U.A., Heycke, N., Schmitt, S., Rinke, C., Helfrich, E.J., Brachmann, A.O., Gurgui, C., Wakimoto, T., Kracht, M., Crusemann, M., Hentschel, U., Abe, I., Matsunaga, S., Kalinowski, J., Takeyama, H., Piel, J., 2014. An environmental bacterial taxon with a large and distinct metabolic repertoire. Nature 506, 58-62.

Wishart, D.S., Jewison, T., Guo, A.C., Wilson, M., Knox, C., Liu, Y., Djoumbou, Y., Mandal, R., Aziat, F., Dong, E., Bouatra, S., Sinelnikov, I., Arndt, D., Xia, J., Liu, P., Yallou, F., Bjorndahl, T., Perez-Pineiro, R., Eisner, R., Allen, F., Neveu, V., Greiner, R., Scalbert, A., 2013. HMDB 3.0--The Human Metabolome Database in 2013. Nucleic acids research 41, D801-807.

Wishart, D.S., Knox, C., Guo, A.C., Eisner, R., Young, N., Gautam, B., Hau, D.D., Psychogios, N., Dong, E., Bouatra, S., Mandal, R., Sinelnikov, I., Xia, J., Jia, L., Cruz, J.A., Lim, E., Sobsey, C.A., Shrivastava, S., Huang, P., Liu, P., Fang, L., Peng, J., Fradette, R., Cheng, D., Tzur, D., Clements, M., Lewis, A., De Souza, A., Zuniga, A., Dawe, M., Xiong, Y., Clive, D., Greiner, R., Nazyrova, A., Shaykhutdinov, R., Li, L., Vogel, H.J., Forsythe, I., 2009. HMDB: a knowledgebase for the human metabolome. Nucleic acids research 37, D603-610.

Wishart, D.S., Tzur, D., Knox, C., Eisner, R., Guo, A.C., Young, N., Cheng, D., Jewell, K., Arndt, D., Sawhney, S., Fung, C., Nikolai, L., Lewis, M., Coutouly, M.A., Forsythe, I., Tang, P., Shrivastava, S., Jeroncic, K., Stothard, P., Amegbey, G., Block, D., Hau, D.D., Wagner, J., Miniaci, J., Clements, M., Gebremedhin, M., Guo, N., Zhang, Y., Duggan, G.E., Macinnis, G.D., Weljie, A.M., Dowlatabadi, R., Bamforth, F., Clive, D., Greiner, R., Li, L., Marrie, T., Sykes, B.D., Vogel, H.J., Querengesser, L., 2007. HMDB: the Human Metabolome Database. Nucleic acids research 35, 521-526.

Worley, B., Powers, R., 2013. Multivariate analysis in metabolomics. Current metabolomics 1, 92-107.

Wu, C., Kim, H.K., van Wezel, G.P., Choi, Y.H., 2015a. Metabolomics in the natural products field-a gateway to novel antibiotics. Drug discovery today: technologies 13, 11-17.

Wu, C., Zacchetti, B., Ram, A.F., van Wezel, G.P., Claessen, D., Hae Choi, Y., 2015b. Expanding the chemical space for natural products by *Aspergillus-Streptomyces* co-cultivation and biotransformation. Scientific reports 5, 10868.

Xie, B., Zhang, Z., Gong, T., Zhang, N., Wang, H., Zou, H., 2015. Application of metabonomic strategy to discover an unreported active ingredient in LiuWeiDiHuang pills suppressing beta-glucuronidase. Analytical and bioanalytical chemistry 407, 609-614.

Xie, Z.W., Fan, C.S., Zhu, Z.Y., 1975. The national compilation of Chinese herbal medicine. People's Medical Publishing House, Beijing, China, p 25-26.

Yi-Lei, N., Yun-Dan, W., Chuan-Xi, W., Ru, L., Yang, X., Dong-Sheng, F., Hong, J., Yun-Yang, L., 2014. Compounds from marine-derived *Verrucosispora* sp. FIM06054 and their potential antitumour activities. Natural product research 28, 2134-2139.

Youns, M., Hoheisel, J.D., Efferth, T., 2010. Toxicogenomics for the prediction of toxicity related to herbs from traditional Chinese medicine. Planta medica 76, 2019-2025.

Zengler, K., Toledo, G., Rappe, M., Elkins, J., Mathur, E.J., Short, J.M., Keller, M., 2002. Cultivating the uncultured. Proceedings of the National Academy of Sciences of the United States of America 99, 15681-15686.

Zhang, H., Lee, Y.K., Zhang, W., Lee, H.K., 2006. Culturable actinobacteria from the marine sponge *Hymeniacidon perleve*: isolation and phylogenetic diversity by 16S rRNA gene-RFLP analysis. Antonie van Leeuwenhoek 90, 159-169.

Zhao, L., Nicholson, J.K., Lu, A., Wang, Z., Tang, H., Holmes, E., Shen, J., Zhang, X., Li, J.V., Lindon, J.C., 2012. Targeting the human genome-microbiome axis for drug discovery: inspirations from global systems biology and traditional Chinese medicine. Journal of proteome research 11, 3509-3519.

Zhen, X., Gong, T., Liu, F., Zhang, P.C., Zhou, W.Q., Li, Y., Zhu, P., 2015. A new analogue of echinomycin and a new cyclic dipeptide from a marine-derived *Streptomyces* sp. LS298. Marine drugs 13, 6947-6961.

Chapter 2
Isolation, biodiversity, and biological activity screening of actinomycetes isolated from Mediterranean sponges

2.1 Materials and methods

2.1.1 Specimen collection

Sponge samples were collected from the islands of Milos and Crete, Greece, located in the eastern Mediterranean Sea. The eastern basin of the Mediterranean Sea is considered to be one of the most oligotrophic regions in the world with relatively warm (~15-25 ^{o}C) and high saline waters (36-40 psu) (Danovaro et al., 2010). The sponges *Agelas oroides*, *Chondrosia* reniformis, Chondrilla *nucula*, *Ircinia variabilis*, *Petrosia ficiformis*, *Spirastrella cunctatrix*, *Sarcotragus spinosulus*, and *Sarcotragus foetidus* were collected in duplicate by SCUBA diving from offshore Pollonia, Milos, Greece (N36.76612º; E24.51530º) at 5-7 m depth in May 2013. The sponge *Acanthella* acuta, *Axinella damicornis*, *Axinella cannabina*, *Agelas oroides*, *Aplysina* sp., *Chondrilla nucula*, *Chondrosia reniformis*, *Dysidea avara*, *Ircinia fasciculata*, *Phorbas tenacior*, *Petrosia ficiformis,* and *Sarcotragus* sp. were collected in duplicate by SCUBA diving from offshore Agios Ioannis, Souda Bay, Crete, Greece (35.47032º N and 24.12508º E) at 3-28 m depth in Nov 2013. Sponges were transferred to plastic bags containing surrounding seawater and transported to the laboratory.

2.1.2 Isolation of sponge-associated actinomycetes

Sponge specimens were rinsed with sterilized seawater which had been filtered by use of a 0.2 µm filter pump to remove seawater bacteria. One cm^3 of inner sponge tissue was excised using an ethanol-sterilized scalpel, homogenized in 10 mL seawater using the ethanol-sterilized mortar and pestle, and transferred to 15 mL sterile centrifuge tube. After 10 min to allow for the settlement of particulate material, the supernatant of the bacterial extract was taken and diluted in sterilized seawater in ten-fold series (10^{-1}, 10^{-2}, 10^{-3}). The duplicate homogenates were heated in the heating block at 90 °C for 10 min to kill the fast growing bacteria and to facilitate the growth of actinobacteria before plating on solid media.

Twelve diverse agar media were used including the basic actinobacterial media M1 (Mincer et al., 2005), ISP 2 (Shirling and Gottlieb, 1966), and Oligotrophic medium (OLIGO) (Olson et al., 2000). The media M1_SE and OLIGO_SE, which were further supplemented with 1% corresponding sponge biomass extract (1 g/mL) (Abdelmohsen et al., 2010), as indicated by the abbreviation "_SE". Nutritionally poor media were generated by preparation with only

artificial seawater (ASW) or natural seawater (NSW) to agar. Efforts to enrich for filamentous actinomycetes were undertaken on M1_F and ISP 2_F which were covered by a layer of soft agar on the top after inoculation (as indicated by the abbreviation "_F"). The media R2A (Reasoner and Geldreich, 1985), MA medium (Reasoner and Geldreich, 1985), and M5 (Zhang et al., 2006) were additionally used to magnify actinomycete diversity. All media were added with nalidixic acid (25 µg/mL) which inhibits many fast growing Gram-negative bacteria (Abdelmohsen et al., 2010) and the antifungal agent cycloheximide (0.2 µm pore size filtered; 100 µg/mL). Media formulations were provided in the Annex section. One hundred µL of bacterial homogenate was spread out on each agar plate in duplicate using sterile glass beads. The plates were then incubated at 30 ˚C and regularly inspected for growth for up to 6 weeks. Actinomycete-like colonies (dry or folded appearance, leathery texture, aerial and/or substrate mycelium, and presence of diffusible pigments) were re-streaked on corresponding agar media until colonies were visually free of contamination. The isolated actinomycetes were prepared in 33% glycerol in ISP 2 broth medium and maintained in cryotubes at - 80 ˚C.

2.1.3 Molecular identification and phylogenetic analysis

16S rRNA gene amplification and sequencing were executed according to Hentschel et al. (Hentschel et al., 2001). The whole genome DNA of each strain was extracted by scrapping few bacterial biomass, suspending in 100 µL sterile water and heating at 90 ˚C for 10 min then cooling down the lysate on ice and centrifugation at 13000 rpm for 10 min. The supernatant containing genome DNA was transferred into a new eppendof for 16S rRNA gene amplification. For some strains that the genome DNA couldn't be extracted using above method, FastDNA spin kit for soil (MP BIomedicals, Germany) was used to obtain the whole genome DNA by following manufacturer's protocol.

Nearly full-length 16S rRNA genes (1542 nucleotide bases) were amplified by polymerase chain reaction (PCR) using primers 27F (5'-GAGTTTGATCCTGGCTCAG-3') and 1492R (5'-GGTTACCTTGTTACGACTT-3'). The reaction mixture consists of 5 µL of 10 X FastDigest Green buffer including 20 mM $MgCl_2$ (Fermentas, Germany), 1 µL of 10 mM dNTPs mixture (Fermentas, Germany), 1 µL of 25 mM of each primer (SIGMA, Germany), 0.19 µL of 5 U/µL DreamTaq DNA olymerase (Thermo Scientific, Germany), 1 µL of template DNA and 41.81 µL sterile water to fill up a final volume of 50 µL. The PCR was performed on a thermal cycler (Biometra, Germany) using the following thermal cycling protocol: the initial denaturation temperature at 95 ˚C for 2 min, followed by 34 cycles of reaction starting another denaturation at 95 ˚C for 0.5 min, then primer annealing at 56 ˚C for 0.5 min and primer extension at 72 ˚C for 1.5 min, as well as the final primer extension at 72 ˚C for 10 min. The reaction was stopped by chilling at 16 ˚C to limit the polymerase activity (Hentschel et al., 2001). 5 µL PCR product

was examined by agarose gel electrophoresis by running the voltage at 300 V for 20 min. 5 µL of 0.5 µg/µL GeneRular 1Kb DNA ladder (Fermentas, Germany) was used as the reference control. The 16S rRNA genes presenting a clear single band around 1500 bases compared to the ladder under the Molecular Imager® Gel Doc™ XR System (Bio-Rad Laboratories, Italy) indicated a successful amplification and were purified using NucleoSpin Gel and PCR Clean-up package (MACHEREY-NAGEL, Germany) following the manufacturer's protocol. The genes that amplified with more than one band were purified by cutting off the right band and extracting from the agarose gel using NucleoSpin Gel and PCR Clean-up package by following the manufacturer's protocol. The concentration of the purified 16S rRNA genes was examined on NanoDrop 2000C Spectrophotometer (Thermo Scientific, Germany) and adjusted to 30 µg/µL. High-quality 16S rRNA genes were sent to LGC Genomics GmbH (Berlin, Germany) for sequencing using forward primer 27F and reverse primer 1492R. Sequences were checked for chimeras using the DECIPHER web service (Wright et al., 2012). The remaining sequences were quality-filtered from both ends with the BWA's trimming algorithm and a quality threshold of 30 (Li and Durbin, 2009). To obtain consensus sequences, a self-written perl script calculating a MUSCLE (MUltiple Sequence Comparison by Log-Expectation) alignment and assessing quality scores on overlap area was performed (Edgar, 2004). Alignments were manually curated if necessary. Contigs of ~1450 bp length of sequences of high quality were searched through a BLAST run against the non-redundant and 16S ribosomal database (Altschul et al., 1990) to identify the nearest related and type strains to the amplified sequence.

The phylogenetic tree generated was based on a multiple alignment with the SINA web aligner (Pruesse et al., 2012). A maximum likelihood tree was constructed with 500 bootstrap repetitions by means of RaxML (Stamatakis, 2014) and finally shown via the iTOL web service (Letunic and Bork, 2007). 98.5 % was used as the thresholds to discriminate between sequences of the same species (Ahn et al., 2011; Hoffmann et al., 2012; Kaur et al., 2012; Menezes et al., 2015).

2.1.4 Bioassay screening

A total of 46 selected bacterial actinomycetes were fermented with shaking at 30 ˚C using 200 mL ISP2 broth medium for 5, 7 and 10 days based on their individual growth. The fermented cultures were filtered using filter paper with a small piece of cotton underneath and the bacterial cells left on the filter paper and cotton were lysed with methanol. The filtrates were extracted twice using 200 mL ethyl acetate and the resulting extracts were dried in vacuo using a rotary evaporator and prepared for bioassay screening.

2.1.4.1 Antioxidant assay

The assay was performed in triplicate and followed protocols from Huang et al. (Huang et al., 2002) and Ganske et al. (Ganske and Dell, 2006) with slight modifications. Briefly, 60 µL of 10nM fluorescein solution in 10mM phosphate buffer (pH7.4) was added to 10 µL standard or sample solution in a microplate. After a 10 minute incubation at 37 °C, the reaction was started by adding 30 µL of 120 mM AAPH (2,2'-Azobis(2-amidinopropane) dihydrochloride) solution. Fluorescence (ex/em 485 nm/520 nm) was recorded every minute for 100 minutes in a microplate reader (POLARstar Optima, BMG Labtech). The area under the fluorescence curve (AUC) was calculated by the normalized curves with the following equation: AUC = (f0/f0+f99/f0) x 0,5 + (f1/f0+ ...+ f98/f0) where f0 was the fluorescence reading at the start of the reaction and f99 was the last measurement. The net AUC was obtained by subtracting the AUC of the blank from that of a sample or standard. This experiment was performed by Dr. Eva Küttner in Matis Ltd. (Reykjavík, Iceland).

2.1.4.2 Antimicrobial assay

The *in vitro* antimicrobial assay was carried out using the standard disc diffusion assay (Inderlied and Salfinger, 1995) against bacteria (*Bacillus* sp*.* and *E. coli*) and fungi (*Aspergillums* sp.). The pathogen cultures were prepared freshly for each assay by growing them in LB broth medium at 37 ◦C for bacteria and 30 °C for fungus overnight under shaking at 175 rpm. The concentration of the overnight cultures were adjusted with LB medium to obtain an optical density of OD_{600} = 0.2 using NanoDrop 2000C Spectrophotometer (Thermo Scientific, Germany). 50 µl of the adjusted pathogen culture was spread out on 120 mm-squared dry LB agar plates and allowed to absorb in the agar for 10 min. The sterile Whatman filter paper (Roth, Germany) discs of 6 mm Ø were impregnated with the crude extracts (5 mg/mL in MeOH, 20 µL/disc) and dried under the fume hood. Loaded discs were placed on the agar plates which were inoculated with the target microorganism in advance and gently taped to ensure the contact with the agar surface. The plates were inverted and incubated at 37 °C for bacteria and 30 °C for fungus for 24 h. The antimicrobial potential was assessed by diameters of the inhibition zone. Chloramphenicol was used as the positive control for bacteria and cycloheximide for fungus, while 100 % methanol was used as the negative control.

2.1.4.3 Antitrypanosomal bioassay

The antitrypanosomal bioassay was performed following Huber and Koella (Huber and Koella, 1993). Briefly, 10^4 trypanosomes per mL of *Trypanosoma brucei brucei* strain TC 221 were cultivated in Complete Baltz Medium. Trypanosomes were tested in 96-well plate chambers against different concentrations of test extracts at 10-200 µg/mL in 1% DMSO to a final volume of 200 µL. For controls, 1% DMSO as well as parasites without any test extracts were used simultaneously in each plate to show no effect of 1% DMSO. The plates were then incubated

at 37 °C in an atmosphere of 5% CO_2 for 24 h. After addition of 20 µL of Alamar Blue, the activity was measured after 48 and 72 h by light absorption using an MR 700 Microplate Reader (Dynatech Engineering Ltd., Willenhall, UK) at a wavelength of 550 nm with a reference wavelength of 650 nm. The IC_{50} values of extracts were quantified by linear interpolation in three independent measurements. This experiment was performed by Ms. Antje Fuss in the Würzburg University (Würzburg, Germany).

2.2 Results

2.2.1 Diversity of sponge-associated actinomycetes

A total of 64 actinomycete isolates were isolated from the Greek collection effort. The bacterial isolates were phylogenetically affiliated to 23 genera, 15 families and 8 suborders (**Table 2.1**) based on nearly complete 16S rRNA genes sequencing (each > 1100 bp in length, **Table 2.2**). In terms of novelty, four bacteria exhibited sequence similarities < 98.5 % compared to other 16S rRNA gene sequences available in the NCBI database. They were affiliated with the genera *Geodermatophilus* (SBT350), *Microlunatus* (SBT365), *Rhodococcus* (SBT367), and *Actinomycetospora* (SBT374) (**Table 2.2**). The sponge *Sarcotragus spinosulus* yielded the highest number of actinomycetes (12), followed by *Petrosia ficiformis* (10), *Spirastrella cunctatrix* (10), *Agelas oroides* (9), *Phorbas tenacior* (5), *Chondrilla nucula* (4), *Ircinia variabilis* (4), *Ircinia fasciculata* (3), *Sarcotragus foetidus* (3), *Axinella damicornis* (2), *Acanthella acuta* (1), and *Aplysina* sp. (1) (**Fig. 2.1**). *Petrosia ficiformis* was remarkable for the high recovery rate of *Streptomyces* isolates (n=5). Actinomycetes were not isolated from *Chondrosia reniformis*, *Dysidea avara*, *Sarcotragus* sp., and *Axinella cannabina*.

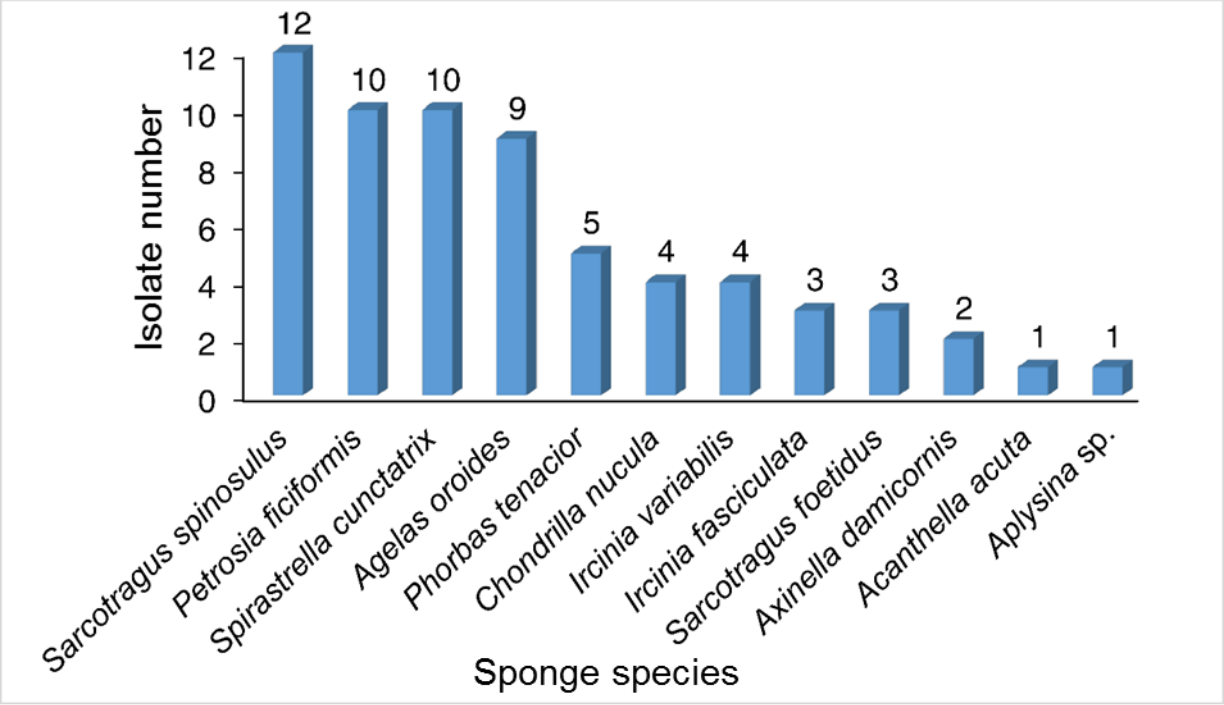

Fig. 2.1 Isolation of actinomycetes from different sponge species

Among the 64 actinomycete isolates, the genera *Micrococcus* (n=11), *Streptomyces* (n=11), and *Micromonospora* (n=9) were numerically dominant which is accordance with previous studies (Abdelmohsen et al., 2010), followed by *Microbacterium* (n=7), *Arthrobacter* (n=3), *Dietzia* (n=3), *Kocuria* (n=2), *Geodermatophilus* (n=2), *Modestobacter* (n=2), as well as an additional 14 genera that were represented by only one isolate (**Fig. 2.2**). Representatives from the genera *Microlunatus*, *Geodermatophilus*, *Modestobacter, Actinomycetospora*, and *Promicromonospora* were, to our knowledge, isolated from marine sponges for the first time. Regarding the medium composition, M1 recovered the highest recovery rate (51.6%) with 33 isolates representing 15 different genera and exhibited the best recovery rates of *Micromonospora* (8 isolates). The ISP2 medium displayed the second best recovery rates (32.8%) with a total of 21 isolates representing 8 different genera. Among them, eight isolates were affiliated to *Streptomyces* sp. One putatively new isolate, *Rhodococcus* sp. SBT367, was recovered from M1_SE medium which was addictive with sponge extract. The other amended media (identified by the label "_F"), prepared to enrich the growth of filamentous *Streptomyces* sp., yieled three *Streptomyces* sp. (SBT344, SBT345, and SBT348). The media Agar_NSW and OLIGO recovered 3 and 4 actinomycetes, respectively, and R2A and M5 yielded one actinomycete species each.

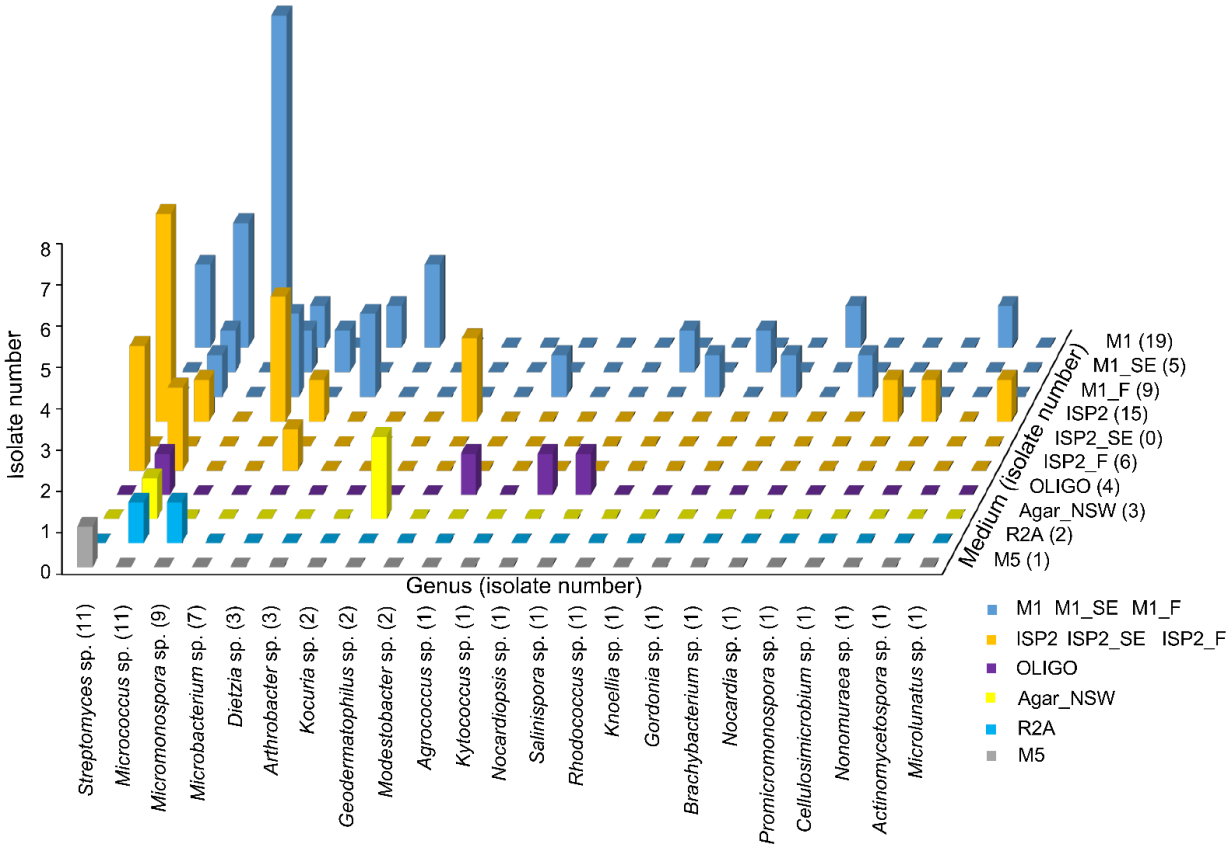

Fig. 2.2 Distribution of actinomycete genera grown on different media compositions

Table 2.1 Phylogenetic affiliation of 64 bacterial isolates from Milos and Crete collection

Order (n=8)	**Family (n=15)**	**Genus (n=23)**	**Total (n=64)**
Micrococcineae			Total 29
	Microbacteriaceae		Total 9
		Microbacterium sp.	7
		Agrococcus sp.	1
	Micrococcaceae		Total 14
		Micrococcus sp.	9
		Arthrobacter sp.	3
		Kocuria sp.	2
	Dermabacteraceae	*Brachybacterium* sp.	1
	Dermacoccaceae	*Kytococcus* sp.	1
	Intrasporangiaceae	*Knoellia* sp.	1
	Promicromonosporaceae		Total 2
		Cellulosimicrobium sp.	1
		Promicromonospora sp.	1
Corynebacterineae			Total 5
	Dietziaceae	*Dietzia* sp.	3
	Nocardiaceae	*Rhodococcus* sp.	1
	Gordoniaceae	*Gordonia* sp.	1
Frankineae	*Geodermatophilaceae*		Total 4
		Modestobacter sp.	2
		Geodermatophilus sp.	2
Streptosporangineae			Total 2
	Nocardiopsaceae	*Nocardiopsis* sp.	1
	Streptosporangiaceae	*Nonomuraea* sp.	1
Micromonosporineae	*Micromonosporaceae*		Total 11
		Micromonospora sp.	9
		Nocardia sp.	1
		Salinispora sp.	1
Streptomycineae	*Streptomycetaceae*	*Streptomyces* sp.	Total 11
Propionibacterineae	*Propionibacteriaceae*	*Microlunatus* sp.	Total 1
Pseudonocardineae	*Pseudonocardiaceae*	*Actinomycetospora atypical* sp.	Total 1

Table 2.2 Isolation and identification of 46 selected bacterial isolates from the Milos and Crete collection (2013)

Isolate Code (Milos)	Sponge Source	Sequence Length	Closest Relative by BLAST	% Sequence Identity
SBT343	*Petrosia ficiformis*	1448	*Streptomyces flavogriseus* strain P.S.461	99.65
SBT344	*Petrosia ficiformis*	1450	*Streptomyces cinereospinus* strain NBRC 15397	99.31
SBT345	*Agelas oroides*	1398	*Streptomyces* sp. 56E35	99.86
SBT346	*Petrosia ficiformis*	1348	*Streptomyces thermocarboxydus*	99.93
SBT347	*Spirastrella cunctatrix*	1178	*Streptomyces* sp. CNR918 PL04	99.66
SBT348	*Petrosia ficiformis*	1152	*Streptomyces atroolivaceus* strain Nt1-5	99.91
SBT349	*Sarcotragus spinosulus*	1339	*Streptomyces* sp. AMS578	98.95
SBT350	*Chondrilla nucula*	1262	*Geodermatophilus obscurus* strain DSM 43160	98.41
SBT351	*Ircinia variabilis*	1257	*Agrococcus jenensis* strain B16	98.89
SBT353	*Sarcotragus spinosulus*	1105	*Dietzia maris* strain RB 30	99.55
SBT354	*Sarcotragus spinosulus*	1186	*Dietzia maris* strain RB 30	99.66
SBT355	*Sarcotragus spinosulus*	1245	*Dietzia maris* strain RB 30	100
SBT356	*Petrosia ficiformis*	1358	*Kocuria* sp. Drb9	99.41
SBT357	*Ircinia variabilis*	1271	*Kocuria rhizophila* strain XFB-BG	100.00
SBT358	*Spirastrella cunctatrix*	1265	*Arthrobacter* sp. MR-17	99.92
SBT359	*Petrosia ficiformis*	1231	*Arthrobacter* sp. Als3	99.84
SBT360	*Agelas oroides*	1253	*Arthrobacter* sp. 19503	99.68
SBT361	*Sarcotragus spinosulus*	1233	*Gordonia terrae* strain 5-Sj-4-3-2-M	99.92
SBT362	*Spirastrella cunctatrix*	1312	*Modestobacter roseus* strain KLBMP 1279	99.39
SBT363	*Sarcotragus foetidus*	1351	*Modestobacter multiseptatus* strain AA826	99.26
SBT364	*Sarcotragus foetidus*	1336	*Nonomuraea* sp. DLS-53	98.74
SBT365	*Spirastrella cunctatrix*	1281	*Microlunatus soli* strain CC-012602	97.97
SBT366	*Chondrilla nucula*	1185	*Nocardiopsis* sp. HB370	99.58
SBT367	*Spirastrella cunctatrix*	1373	*Rhodococcus opacus* strain S106	98.40

Isolate Code (Milos)	Sponge Source	Sequence Length	Closest Relative by BLAST	% Sequence Identity
SBT368	*Spirastrella cunctatrix*	1082	*Salinispora pacifica* strain S54	99.72
SBT370	*Spirastrella cunctatrix*	1205	*Cellulosimicrobium* sp. 20.1 KSS	99.92
SBT371	*Sarcotragus spinosulus*	1170	*Kytococcus* sp. HS24	99.74
SBT372	*Agelas oroides*	1264	*Micromonospora* sp. TCA20016	99.37
SBT373	*Chondrilla nucula*	1193	*Micromonospora* sp. ALFpr19a	99.75
SBT374	*Petrosia ficiformis*	1234	*Actinomycetospora atypica* strain NEAU-st4	98.46
SBT375	*Sarcotragus spinosulus*	1251	*Micromonospora* sp. ALFpr19a	99.84
SBT376	*Sarcotragus spinosulus*	1184	*Brachybacterium* sp. YB056	99.92
SBT380	*Sarcotragus spinosulus*	1306	*Knoellia* sp. S44CA	99.92
SBT381	*Ircinia variabilis*	1267	Uncultured *Geodermatophilus* sp. clone BC100	99.84

Isolate Code (Crete)	Sponge Source	Sequence Length	Closest Relative by BLAST	% Sequence Identity
SBT686	*Ircinia fasciculate*	1287	*Streptomyces* sp. Act53	99.77
SBT687	*Phorbas tenacior*	1232	*Micromonospora* sp. 10-65	99.59
SBT688	*Ircinia fasciculate*	1329	*Streptomyces badius* strain G4-3	99.85
SBT689	*Phorbas tenacior*	1305	*Nocardia araoensis* strain S107	99.54
SBT690	*Ircinia fasciculate*	1260	*Streptomyces* sp. Sn-22	99.92
SBT691	*Phorbas tenacior*	1237	*Streptomyces* sp. Sn-22	100.00
SBT692	*Phorbas tenacior*	1084	*Micromonospora* sp. FXJ6.350	99.82
SBT693	*Phorbas tenacior*	1113	*Micromonospora* sp. S1	99.73
SBT694	*Axinella damicornis*	1262	*Micromonospora* sp. DS3001	99.37
SBT695	*Agelas oroides*	1292	*Micromonospora echinospora* strain T7-15	99.37
SBT696	*Axinella damicornis*	1200	*Micromonospora auratinigra* strain 166210	99.92
SBT697	*Agelas oroides*	1309	*Promicromonospora umidemergens* strain 126185	99.62

2.2.2 Phylogenetic analysis

A total of 46 isolates except those belonging to the genera *Micrococcus* and *Microbacterium* which are usually of non-pharmaceutically interesting were selected from the strain collection based on their characteristic colony morphology and taxonomic relevance for secondary metabolism. A maximum-likelihood tree was constructed and their nearest sequence relatives obtained from a BLAST run were included (**Fig. 2.3**). The two major taxonomic groups *Micromonospora* and *Streptomyces* were collapsed (**Fig. 2.3**) and shown at higher resolution (**Fig. 2.4A** and **2.4B**). The observation that the outer branches were less supported by bootstrap values than the inner ones indicates equivocal solutions on the species level but also a higher accuracy at higher taxonomic ranks. All genera fell into distinct clades, except the genus *Salinispora,* which fell within the *Micromonospora*; albeit with low bootstrap support of 52 (**Fig. 2.4A**). This is reasonable since *Salinispora* and *Micromonospora* are closely related. The isolates SBT354 and SBT355 shaped a distinct clade within the genus *Dietzia* and they may be the same isolate since they were derived from the same *Sarcotragus spinosulus* sample (**Fig. 2.3**). The isolates SBT345 from *Agelas oroides*, and SBT690 from *Ircinia fasciulata*, formed a separate cluster within the genus *Streptomyces*. These isolates may belong to the same species besides the fact that they were obtained from different sponge species and sample sites (**Fig. 2.4B**). Evidence for the novelty of isolates SBT365 and SBT374 is further provided by phylogenetic analysis, showing uncultured bacterial clone sequences as their nearest relatives (**Fig. 2.3**). The 16S rRNA gene sequences of all isolates were deposited in GenBank under the accession numbers KP145919-KP145922 and KP238412-KP238453. The maximum-likelihood tree was constructed by Hannis Horn (Würzburg University, Germany).

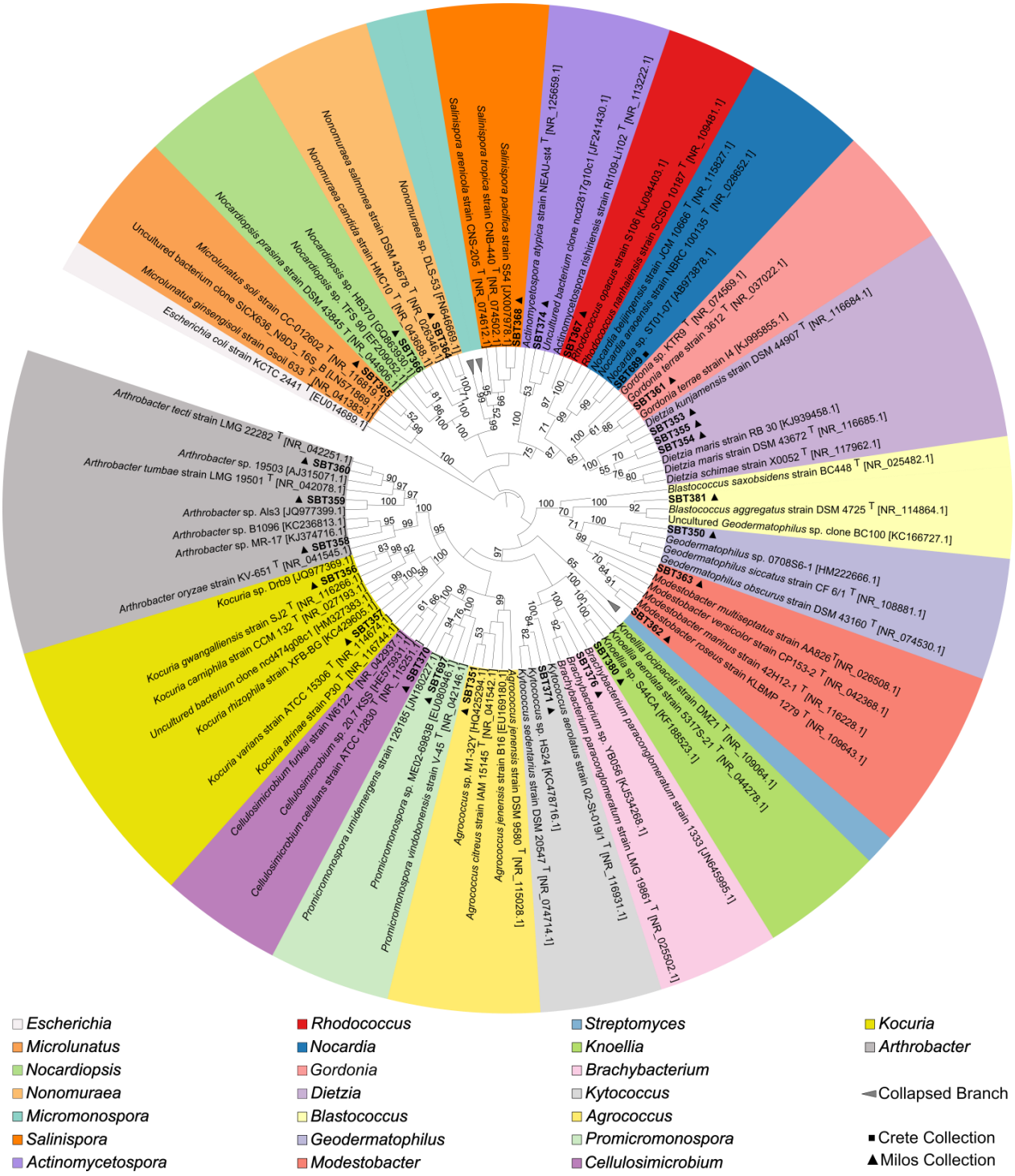

Fig. 2.3 Maximum-likelihood tree of selected actinomycete isolates from the Crete (SBT 686-697) and Milos collection (SBT349-381) as well as their nearest representative strains based on the 16S rRNA gene sequence. The color legend indicates the genus-level of all sequences. The tree is rooted at *Escherichia coli* strain KCTC 2441^{T} which serves as outgroup. All bootstrap values >50 (500 resamples) are given in percent at the nodes of the tree.

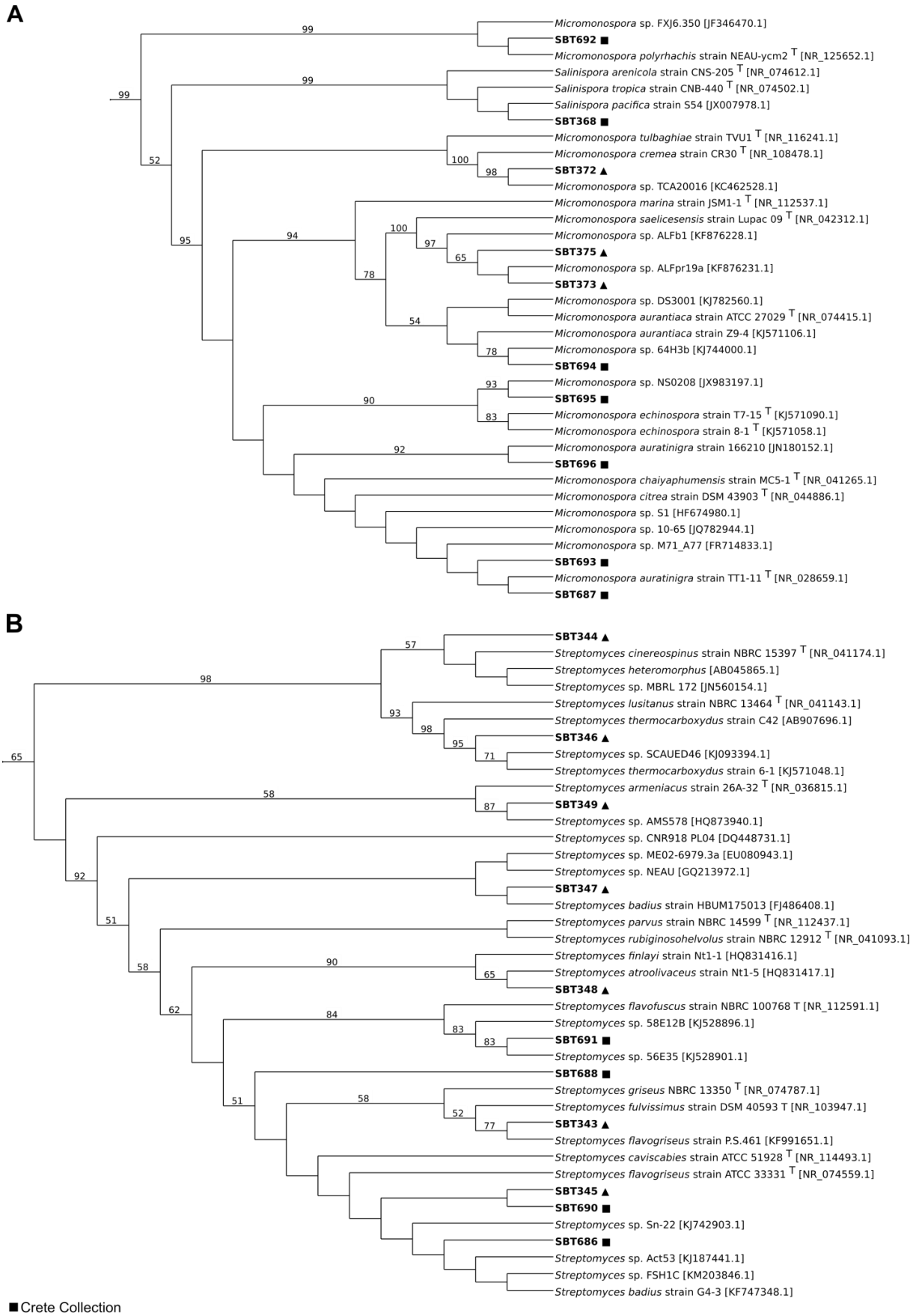

Fig. 2.4 Maximum-likelihood tree of *Micronomospora* (A) and *Streptomyces* (B) isolates from the Crete (SBT6xx) and Milos collection (SBT3xx) as well as their nearest representative strains based on the 16S rRNA gene sequence. The trees are rooted at *Escherichia coli* strain

KCTC 2441^T which serves as outgroup (not shown). All bootstrap values >50 (500 resamples) are given in percent at the nodes of the tree.

2.2.3 Bioassay screening

Out of the 46 tested bacterial extracts, six strains including 4 *Streptomyces* sp., 1 *Micromonospora* sp., and 1 *Kocuria* sp. showed antioxidant activities by showing the AUC values of 875 to 1323 at 100 µg/ml of the crude bacterial extract (**Table 2.3**). None of the collected strains exhibited antimicrobial activities in their broth extracts, with the exception of the solid extract of *Streptomyces* sp. SBT348, which showed 12 mm and 7 mm zones of inhibition against *Bacillus* sp. and *Aspergillums* sp. respectively in the in-house disc diffusion assay. Eight strains belonging to 6 different genera (*Streptomyces*, *Modestobacter, Nonomuraea*, *Rhodococcus*, *Geodermatophilus*, and *Micromonospora*) exhibited activities against *T. brucei brucei* strain TC 221 with IC_{50} values < 20 µg/ml. Among them, three strains of *Streptomyces* sp. SBT344, *Modestobacter* sp. SBT363, and *Nonomuraea* sp. SBT364 were potently active and showed IC_{50} values < 10 µg/ml after 48 h and 72h incubation.

Table 2.3 Biological activities of 46 selected bacterial crude extracts

Sample ID	AUC (100 µg/mL)	Antimicrobial (inhibition zone, mm)		Antitrypanosomal (IC_{50} µg/mL)	
		***Bacillus* sp.**	***Aspergillus* sp.**	**48h**	**72h**
SBT344				<10	<10
SBT345	1323				
SBT348	1284	12	7	16.52	20.50
SBT349	1033				
SBT357	952				
SBT362				19.34	21.28
SBT363				<10	<10
SBT364				<10	<10
SBT367				19.97	22.37
SBT381				18.60	21.36
SBT686	994				
SBT687				14.87	19.95
SBT692	875				

Out of the 18 different sponges collected from Mediterranean Sea belonging to 12 different species in the current study, a total of 64 actinomycetes was recovered representing 23 different genera including four putatively new species compared to their closest strains and type strains. To our knowledge, the genera *Geodermatophilus*, *Microlunatus*, *Actinomycetospora*, *Modestobacter*, and *Promicromonospora*were were isolated from marine sponges for the first time. Among these 64 isolates, *Streptomyces* sp. SBT348 displayed antioxidant activity, inhibitory properties against *Bacillus* sp., *Aspergillus* sp. and *Trypanosma brucei brucei* TC221. Another five isolates belonging to the genera *Streptomyces* (3), *Micromonospora* (1), and *Kocuria* (1) exhibited antioxidant activity. As for antitrypanosomal bioassay, inhibitory effects were observed from another seven isolates belonging to the genera *Modestobacter* (2), *Streptomyces* (1), *Micromonospora* (1), *Nonomuraea* (1), *Geodermatophilus* (1), and *Rhodococcus* (1). The results also highlight marine sponges as a rich source of new and bioactive actinomycetes as well as the importance of using new cultivation approaches to access novel actinomycete diversity.

2.3 References

Abdelmohsen, U.R., Pimentel-Elardo, S.M., Hanora, A., Radwan, M., Abou-El-Ela, S.H., Ahmed, S., Hentschel, U., 2010. Isolation, phylogenetic analysis and anti-infective activity screening of marine sponge-associated actinomycetes. Marine Drugs 8, 399-412.

Ahn, J., Park, J.W., McConnell, J.A., Ahn, Y.B., Haggblom, M.M., 2011. *Kangiella spongicola* sp. nov., a halophilic marine bacterium isolated from the sponge *Chondrilla nucula*. International journal of systematic and evolutionary microbiology 61, 961-964.

Altschul, S.F., Gish, W., Miller, W., Myers, E.W., Lipman, D.J., 1990. Basic local alignment search tool. Journal of molecular biology 215, 403-410.

Danovaro, R., Company, J.B., Corinaldesi, C., D'Onghia, G., Galil, B., Gambi, C., Gooday, A.J., Lampadariou, N., Luna, G.M., Morigi, C., Olu, K., Polymenakou, P., Ramirez-Llodra, E., Sabbatini, A., Sarda, F., Sibuet, M., Tselepides, A., 2010. Deep-sea biodiversity in the Mediterranean Sea: the known, the unknown, and the unknowable. PloS one 5, e11832.

Edgar, R.C., 2004. MUSCLE: multiple sequence alignment with high accuracy and high throughput. Nucleic acids research 32, 1792-1797.

Ganske, F., Dell, E.J., 2006. ORAC assay on the fluorstar optima to determine antioxidant capacity. Application note of BMG labtech 148.

Hentschel, U., Schmid, M., Wagner, M., Fieseler, L., Gernert, C., Hacker, J., 2001. Isolation and phylogenetic analysis of bacteria with antimicrobial activities from the Mediterranean sponges *Aplysina aerophoba* and *Aplysina cavernicola*. FEMS microbiology ecology 35, 305-312.

Hoffmann, M., Monday, S.R., Allard, M.W., Strain, E.A., Whittaker, P., Naum, M., McCarthy, P.J., Lopez, J.V., Fischer, M., Brown, E.W., 2012. *Vibrio caribbeanicus* sp. nov., isolated from the marine sponge *Scleritoderma cyanea*. International journal of systematic and evolutionary microbiology 62, 1736-1743.

Huang, D.J., Ou, B.X., Hampsch-Woodill, M., Flanagan, J.A., Prior, R.L., 2002. High-throughput assay of oxygen radical absorbance capacity (ORAC) using a multichannel liquid handling system coupled with a microplate flourescence reader in 96-well format. Journal of agricultural and food chemistry 50, 4437-4444.

Huber, W., Koella, J.C., 1993. A comparison of three methods of estimating EC_{50} in studies of drug resistance of malaria parasites. Acta Tropica 55, 257-261.

Inderlied, C.B., Salfinger, M., 1995. Antimicrobial agents and susceptibility tests: *Mycobacteria*, in: Murray, P.R., Baron, E.J., Pfaller, M.A., Tenover, F.C., Yolken, R.H. (Eds.), Manual of Clinical Microbiology. American Society for Microbiology, Washington D.C.,USA, p 1385-1404.

Kaur, I., Das, A.P., Acharya, M., Klenk, H.P., Sree, A., Mayilraj, S., 2012. *Planococcus plakortidis* sp. nov., isolated from the marine sponge *Plakortis simplex (Schulze)*. International journal of systematic and evolutionary microbiology 62, 883-889.

Letunic, I., Bork, P., 2007. Interactive Tree Of Life (iTOL): an online tool for phylogenetic tree display and annotation. Bioinformatics 23, 127-128.

Li, H., Durbin, R., 2009. Fast and accurate short read alignment with Burrows-Wheeler transform. Bioinformatics 25, 1754-1760.

Menezes, C.B., Ferreira-Tonin, M., Silva, L.J., Souza, W.R., Parma, M., Melo, I.S., Zucchi, T.D., Destefano, S.A., Fantinatti-Garboggini, F., 2015. *Marmoricola aquaticus* sp. nov. an

actinomycete isolated from marine sponge. International journal of systematic and evolutionary microbiology, International journal of systematic and evolutionary microbiology 65, 2286-2291.

Mincer, T.J., Fenical, W., Jensen, P.R., 2005. Culture-dependent and culture-independent diversity within the obligate marine actinomycete genus *Salinispora*. Applied and environmental microbiology 71, 7019-7028.

Olson, J.B., Lord, C.C., McCarthy, P.J., 2000. Improved Recoverability of Microbial Colonies from Marine Sponge Samples. Microbial ecology 40, 139-147.

Pruesse, E., Peplies, J., Glockner, F.O., 2012. SINA: accurate high-throughput multiple sequence alignment of ribosomal RNA genes. Bioinformatics 28, 1823-1829.

Reasoner, D.J., Geldreich, E.E., 1985. A new medium for the enumeration and subculture of bacteria from potable water. Applied and environmental microbiology 49, 1-7.

Shirling, E.B., Gottlieb, D., 1966. Methods for characterization of Streptomyces species. International journal of systematic microbiology 16, 313-340.

Stamatakis, A., 2014. RAxML version 8: a tool for phylogenetic analysis and post-analysis of large phylogenies. Bioinformatics 30, 1312-1313.

Wright, E.S., Yilmaz, L.S., Noguera, D.R., 2012. DECIPHER, a search-based approach to chimera identification for 16S rRNA sequences. Applied and environmental microbiology 78, 717-725.

Zhang, H., Lee, Y.K., Zhang, W., Lee, H.K., 2006. Culturable actinobacteria from the marine sponge *Hymeniacidon perleve*: isolation and phylogenetic diversity by 16S rRNA gene-RFLP analysis. Antonie van Leeuwenhoek 90, 159-169.

Chapter 3
Metabolomics and dereplication-based strain prioritization

3.1 Materials and methods

3.1.1 Metabolomics analysis using NMR data

Five mg of the crude bacterial EtOAc extracts were prepared in 500 µL DMSO-d_6 and transferred into NMR tubes (NORELL, US). 1D experiment of ^{1}H and presaturated ^{1}H (improve the suppression of solvent or water signal) NMR spectra, as well as 2D experiment of COSY proton correlation spectroscopy) NMR spectrum were obtained from Fourier Transform NMR spectrometer JNM LA-400 400 MHz instruments (JEOL, Japan) at the University of Strathclyde. Mnova (Mestrelab Research SL, US) was used to process spectral data.

The ^{1}H NMR spectrum was preprocessed with three general steps in Mnova: baseline correction, apodization to enhance the spectral resolution and phase correction to reduce negative signals and adjust signal symmetry. In order to transform the spectral data to digital data for multivariate analysis, all the preprocessed ^{1}H NMR spectra including the medium control were stacked into one plot, binned using average sum and the integral region at 0.01 ppm and finally normalized the intensity of the spectrum by the largest peak (value 100). The binned spectral data from δ 0.5 ppm to δ 12.5 ppm were transported into Excel of ASCII format followed by medium effect removal and solvent peak removal (DMSO-d_6 at H_δ 2.50 ppm, H_2O at H_δ 3.33 ppm). The resulting peak list was imported into SIMCA 13.0.3 for further metabolomics analysis.

3.1.2 Metabolomics analysis using LC-MS data

The bacterial crude EtOAc extracts of 1 mg/mL in MeOH were applied on an Accela HPLC from Thermo Scientific (Bremen, Germany) combined with Accela UV/VIS and Exactive (Orbitrap) mass spectrometer from Thermo Fisher Scientific (Bremen, Germany). The column attached to the HPLC was HiChrom, ACE (Berkshire, UK) C18, 75 mm × 3.0 mm, 5 µm column. The mobile phase consisted of purified water (A) and acetonitrile (B) with 0.1% formic acid in each solvent. The gradient started at a flow rate of 300 µL/min with 10% B linearly increased to 100% B within 30 min and remained isocratic for the next 5 min before linearly decreasing back to 10% B for the following 1 min. The mobile phase was then equilibrated for 9 min before the next injection. The injection volume was 10 µL and the tray temperature was maintained at 4 ˚C with the column oven controlled at 20 ˚C. High Resolution Mass Spectrometry was carried out in both positive and negative ionization modes with a spray voltage at 4.5 kV and

capillary temperature at 320 ˚C. The mass range was set from *m/z* 100-2000 for ESI-MS (Electrospray Mass Spectrometry) using in-source CID (Collision-Induced Dissociation) mechanism and *m/z* 50-1000 for MS/MS using untargeted HCD (High Energy Collision Dissociation).

Raw LC-MS data were initially sliced by MassConverz tool ProteoWizard (online: and http://proteowizard.sourceforge.net/) into negtive or positive files in mzML format. The sliced data sets were imported into MZmine 2.12, a framework for the differential analysis of mass spectrometry data. Peak detection in MZmine 2.12 was executed following noise removal, chromatogram construction, and peak deconvolution. First, the mass values were detected using the centroid mode in each spectrum and the peaks below 1×10^4 of the height were discarded as noise. In the second step, chromatograms were constructed for each of the mass values which span over a certain time range. The minimum time span over the same ion was set as 0.2 min and the error of the ion *m/z* value was allowed within 5 ppm. The minimum intensity of the highest data point in the chromatogram was set at 1×10^4. Finally, a deconvolution algorithm was applied to each constructed chromatogram of each mass ion to recognize the actual chromatographic peaks. The “local minimum search” algorithm which searches for local minima in the chromatogram and separates individual peaks at minimal points was used. The settings to separate individual peaks were as follows: the chromatographic threshold at 95%; search minimum in RT range of 0.4 min; minimum relative height at 5%; minimum absolute height of 3×10^4; a minimum ratio of peak top/edge 3 and peak duration range from 0.2 to 5.0 min. The separated peaks were then deisotoped using the function of isotopic peaks grouper in which the *m/z* tolerance was set at 0.001 m/z or 5.0 ppm; retention time tolerance at 0.1 absolute (min); maximum charge of 2; and representative isotope being most intense. Retention time normalizer was also used after deisotoping to reduce inter-batch variation by setting *m/z* tolerance at 0.001 *m/z* or 5.0 ppm; retention time tolerance at 0.5 absolute (min), and minimum standard intensity: 5.0×10^3. The remained peaks in different samples were aligned based on the mass and retention time of each peak. The ion m/z tolerance for alignment was set at 5 ppm, retention time was 5 relative (%), and weight for m/z and Rt were 20 respectively. Following alignment, the resulting peak list was gap-filled with missing peaks using the intensity tolerance of 25% and retention time tolerance of 0.5 min. The solvent peaks were subtracted from samples by peak intensity at a level above 1×10^5. All the mass ions were finally formula predicted and searched by the adduct mode and complex mode. The medium effects were then cleaned up by using an Excel macros program which was written to subtract of medium peaks but remained features which are 20 times greater in the samples than in the medium. Data were then dereplicated by the AntiMarin

database 2013 and imported to SIMCA 13.0.3 (Umetrics, USA) for further multivariate analysis (Macintyre et al., 2014).

3.1.3 Dereplication study using LC-MS/MS data

Data-dependent MS^2 and MS^3 experiments were carried out using a Finnigan LTQ Orbitrap coupled to a Surveyor Plus HPLC pump (Thermo Scientific, Bremen, Germany) and autosampler (Thermo Fisher, Bremen, Germany) in negative and positive ionization modes using a mass range of *m/z* 100–2000 and 30,000 resolution. The capillary temperature 270 °C, the capillary voltage 35 V, the ion spray voltage 4.5 kV, the tube lens voltage 110 V, and the auxiliary and sheath gas flow rates 15 and 50 (units not specified by the manufacturer) respectively were used. Multi-fragmentation (MS^n) experiments were performed on an Orbitrap analyzer, CID (collision-induced dissociation) which was utilized with a normalized collision energy of 35%, activation time of 30,000 ms and activation Q of 0.250 ms applied on ions of the most intense, the 2nd most intense, and the 3rd most intense peaks for MS^2 and MS^3, respectively, at an isolation width of 3 microns with 5 microscans. The minimum ion signal threshold was set to 500, while the resolution was at 15,000 m/Δm50%. Mass tolerance for molecular formula composition was set at ±5 ppm (Macintyre et al., 2014).

3.1.4 HPLC profiling

HPLC chromatography was performed on Hewlett-Packard series 1100 (QuatPump, degasser, DAD, Colcomp, Iterface 35900E) and Agilent Technologies series 1100 (ALS, UV Detect00719) combined HPLC system on a phenomenx RP-C18 column (4.6 x 250 mm, Merck). The mobile phase consisted of purified water (A) and acetoneitrile (B) with 0.1% trifluoroacetic acid in each solvent. Fifty µL (10 mg/mL in MeOH) of each bacterial crude extract was injected, and the UV wavelength was set to 220, 280, 254, and 366 nm. The gradient started with 5% B for 5 min, and then linearly increased to 100% B within 25 min and remained isocratic for the next 5 min before linearly decreasing back to 5% B within 0.01 min at a flow rate of 1 mL/min. The mobile phase was then equilibrated for 5 min before the next injection and the total analysis time for each sample was 30 min.

3.2 Results

3.2.1 Milos collection

3.2.1.1 Metabolomics analysis

LC-MS data of 34 crude bacterial extracts were subjected to PCA analysis which was generated from 4 components, an R2 (coefficient of determination) value at 0.524 was obtained using the Pareto scaling mode, suggesting a good mode for the data to fit (R2 > 0.5). The two outlying strains, *Streptomyces* sp. SBT348 and *Brachybacterium* sp. SBT376 were uncovered in the scores plot (**Fig. 1A**), thus indicating their chemical uniqueness. The loadings plot (**Fig. 3.1B**) showed the molecular ion masses of all detected secondary metabolites. The ion masses at the same quadrant position as the outliers represented the significant secondary metabolites contributing to the specific observations in the scores plot (**Fig. 3.1A**). From the loadings plot, the outlying feature of SBT348 was attributed by a group of small metabolites from 100 to 250 Da, while SBT376 showed metabolites with molecular weights between 550 and 720 Da (**Fig. 3.1B**). Compared to the results of bioassay screening, only SBT348 showed bioactivities including antitrypanosomal, antioxidant, antimicrobial activities (**Table 2.3 Chapter 2**). The outlying mass ion peak at *m/z* 153.020 $[M-H]^-$ with the predicted molecular formula $C_7H_6O_4$ was dereplicated as 2,3-dihydroxybenzoic acid (Dyer et al., 1964) earlier described as a streptomycete metabolite. This outlying mass ion was also highlighted as a major compound in the extract shown in the total ion chromatogram (TIC) in negative mass spectrometry (**Fig. 3.3**). Outlying mass ion peak at *m/z* 152.035 $[M-H]^-$, with the predicted molecular formula $C_7H_7NO_3$, was dereplicated as maleimycin (Elstner et al., 1973; Ghiringhelli et al., 1981), 3-amino-4-hydroxybenzoic acid (Li et al., 2000), or 2,3-dihydroxybenzamide (Sugiyama and Hirota, 2009), all of which were previously reported as actinomycete metabolites (**Fig. 3.2B**). The outlying mass ion peaks at *m/z* 178.015 $[M-H]^-$ and 195.014 $[M-H]^-$, were dereplicated as benadrostin (Aoyagi et al., 1988; Yoshida et al., 1988) and N-carbamoyl-2,3-dihydroxybenzamide (Sugiyama and Hirota, 2009), respectively, both isolated from *Streptomyces* sp. Ank132 (**Fig. 3.2C**). Due to low peak intensity at *m/z* 153.020, 152.035, 178.015 and 195.014, it was not possible to obtain any MS^2 data. To validate the dereplication data for the low-intensity ion peaks, SBT348 extract was again performed on higher-energy collisional dissociation on the Orbitrap. As illustrated in **Fig 3.2B** and **3.2C**, respectively, the loss of an amide group was verified to *m/z* 152.035 for 2,3-dihydroxybenzamide that gave a fragment ion at *m/z* 109.03 $[C_6H_5O_2]$ and *m/z* 178.015 for benadrostin as indicated by the fragment ion at *m/z* 137.02 $[C_7H_5O_3]$. For *m/z* 195.041, the MS^2 and MS^3 data did not match the dereplicated metabolite as shown at *m/z* 166.05 [-CHO] and 151.04 [-NH] respectively which indicated the occurrence of a formamide moiety but not a *N*-carbamoyl-amide moiety (**Fig 3.2C**). However, LC-MS/MS analysis of *Streptomyces* sp. SBT348 extract exhibited significant MS^2 and MS^3 data for molecular ion peaks between 200 and 600 Da (**Table 3.1**),

which interestingly did not get any matching hit from the dereplication study. It can be observed that the predicted molecular formula from the high resolution data were highly oxygenated showing a good lead for the biological activity of the projected secondary metabolites produced by *Streptomyces* sp. SBT348.

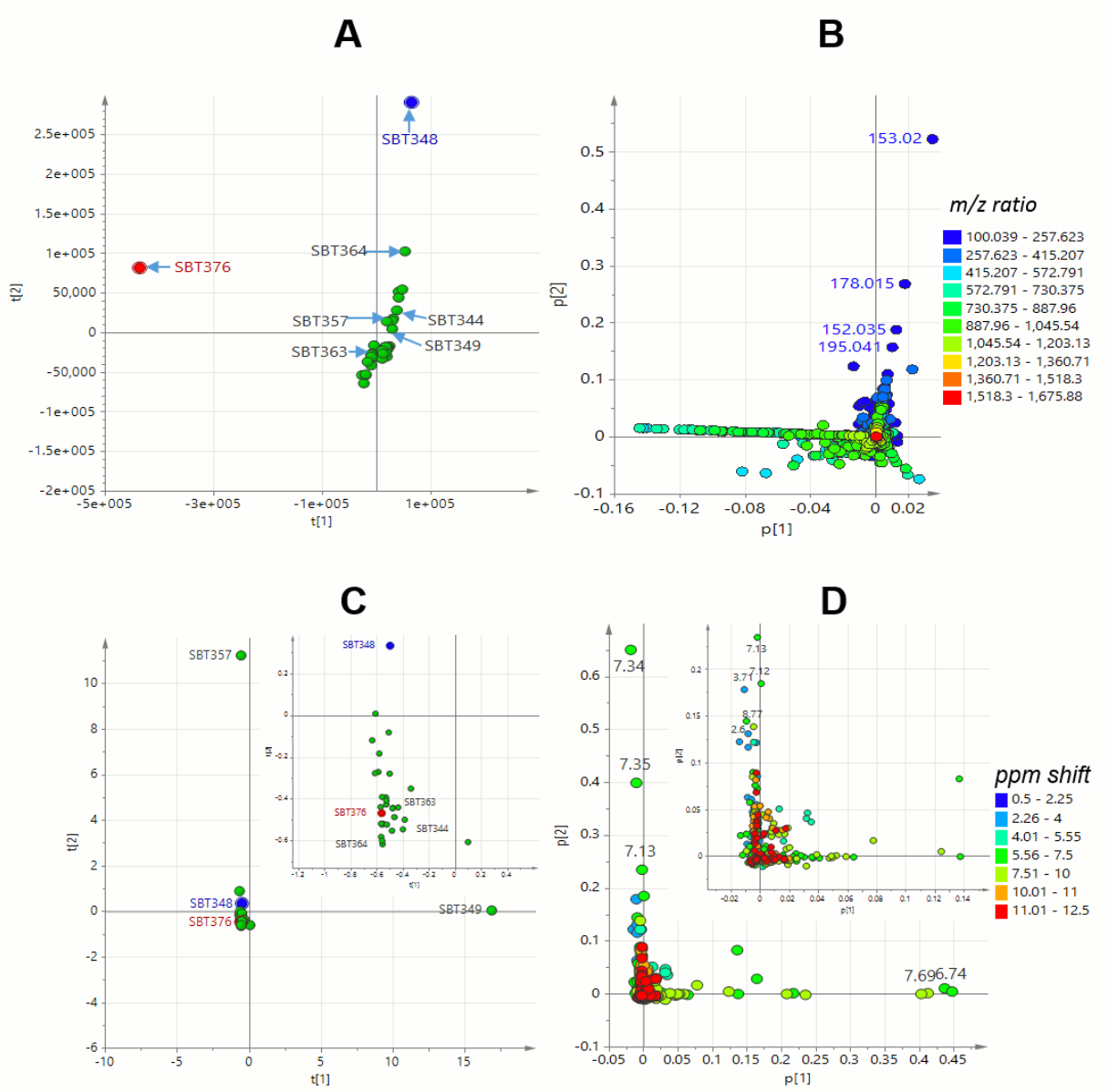

Fig. 3.1 PCA analysis of 34 extracts from Milos collection. Scores plot (A) and loadings plot (B) of LC-HRMS data; scores plot (C) and loadings plot (D) of ^{1}H NMR data of 34 extracts. For the scores plot (A and C), the outmost PCA outliers for the HRMS data were colored blue for the antitrypanosomal active extract and red for the inactive extract.

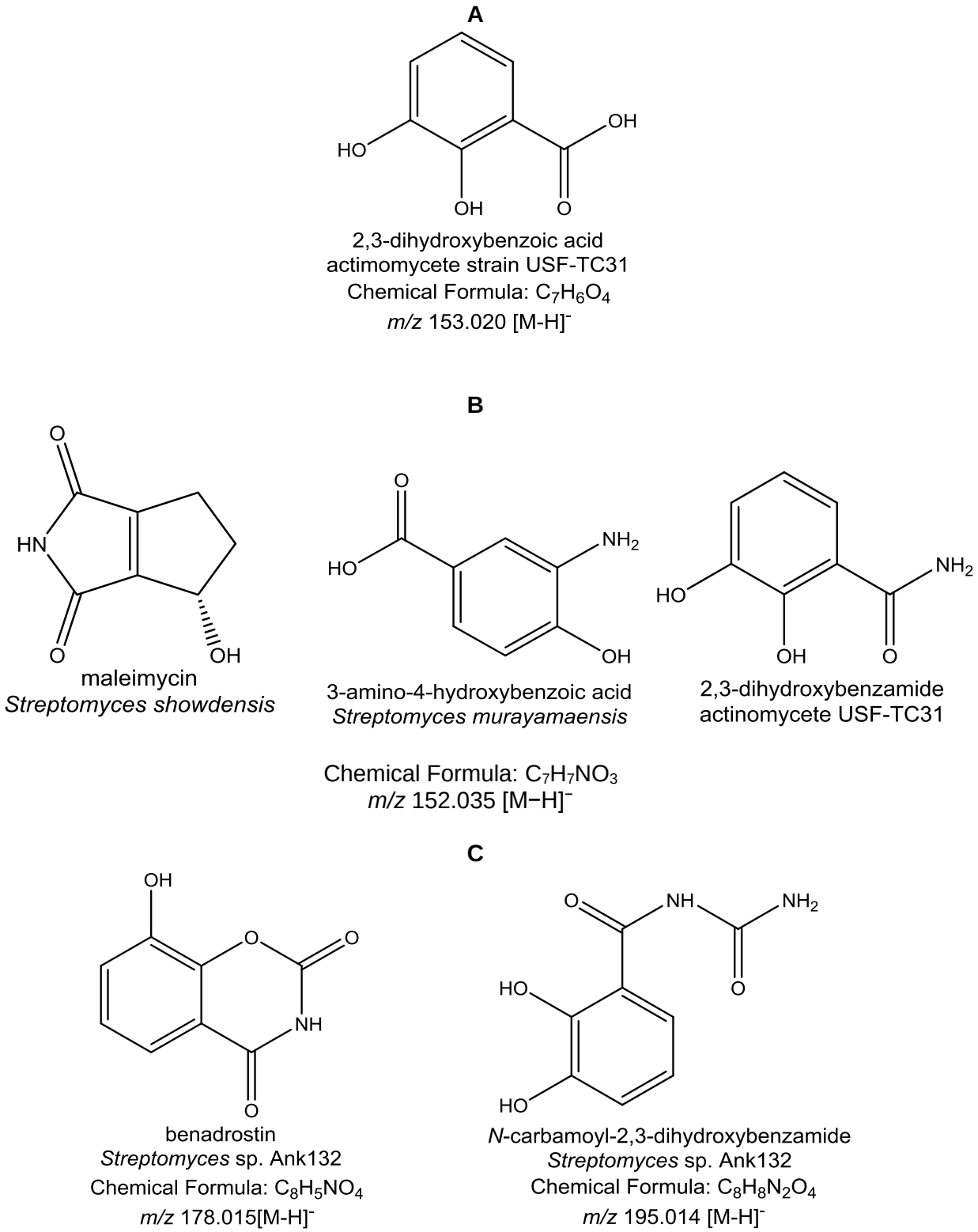

Fig. 3.2 Dereplicated metabolites for the outlying mass ion peaks for *Streptomyces* SBT348. (A) Compound "hits" for *m/z* 153.020 $[M-H]^-$, (B) compound "hits" for *m/z* 152.035 $[M-H]^-$, and (C) *m/z* 178.015 $[M-H]^-$, and 195.014 $[M-H]^-$.

Table 3.1 Selected major metabolites found in positive and negative ionization modes in *Streptomyces* SBT348. (P = positive mode; N = negative mode)

Peak ID	ESI Mode	Molcular ion MS (m/z)	Rt (min)	Molecular Formula	MW	RDB	Hits	Fragment ion MS^2 (m/z)	Fragment Formula (+/-)	RDBE	Fragment ion MS^3 (m/z)	Fragment Formula (+/-)	RDBE
1	N	289.0683	1.5	$C_{10}H_{14}O_8N_2$	290.0756	5	No hits	243.0626	$C_9H_{11}O_6N_2$	5	200.0566	$C_8H_{10}O_5N$	4
2	N	251.0565	3.8	$C_{12}H_{12}O_6$	252.0638	7	No hits	191.0353	$C_{10}H_7O_4$	7	147.0454	$C_9H_7O_2$	6
3	P	242.1023	4.0	$C_{11}H_{15}O_5N$	241.095	5	No hits	225.0750	$C_{11}H_{14}O_5$	6	163.0750	$C_{10}H_{11}O_2$	6
								207.0649	$C_{11}H_{12}O_4$	7	133.0646	C_9H_9O	6
4	N	241.1198	4.2	$C_{11}H_{18}O_4N_2$	242.1271	4	No hits	197.1298	$C_{10}H_{17}O_2N_2$	3			
								181.0985	$C_9H_{13}O_2N_2$	4			
								154.1239	$C_9H_{16}ON$	2			
5	P	219.1129	5.4	$C_{12}H_{14}O_2N_2$	218.1056	5	No hits	191.1177	$C_{11}H_{16}ON_2$	6	159.0918	$C_{10}H_{11}N_2$	7
								174.0914	$C_{11}H_{13}ON$	7	130.0653	C_9H_8N	7
								120.0809	$C_8H_{11}N$	5			
6	N	319.1766	7.0	$C_{15}H_{28}O_7$	320.1839	2	No hits	125.0973	$C_8H_{13}O$	2	97.06588	C_6H_9O	2
7	N	347.2079	10.3	$C_{19}H_{28}O_4N_2$	348.2152	7	No hits	311.2233	$C_{18}H_{31}O_4$	3			
8	P	271.0963	11.1	$C_{12}H_{15}O_6N$	270.0890	6	No hits	252.0862	$C_{12}H_{15}O_5N$	7			
								126.0549	$C_6H_9O_2N$	4			
								108.0444	C_6H_7ON	5			
9	P	325.2275	11.3	$C_{21}H_{28}ON_2$	324.2202	9	No hits	233.1639	$C_{14}H_{22}ON_2$	6	160.1117	$C_{11}H_{14}N$	6
											148.1118	$C_{10}H_{14}N$	5
											84.0807	$C_5H_{20}N$	2
10	N	206.0826	11.7	$C_{11}H_{13}O_3N$	207.0899	6	No hits	164.0718	$C_9H_{10}O_2N$	5			
								147.0454	$C_9H_7O_2$	6			
11	N	399.2758	12.4	$C_{22}H_{40}O_6$	400.2831	3	No hits	313.2017	$C_{17}H_{29}O_5$	3			
12	P	423.2717	12.4	$C_{25}H_{34}O_2N_4$	422.2644	10	No hits	406.2481	$C_{25}H_{32}O_2N_3$	12			
13	P	250.1437	14.3	$C_{14}H_{19}O_3N$	249.1365	6	No hits	232.1327	$C_{14}H_{19}O_2N$	7			
								204.1379	$C_{13}H_{19}ON$	6			
								166.0858	$C_9H_{13}O_2N$	5			
								120.0807	$C_8H_{11}N$	5			
14	N	583.3497	15.2	$C_{29}H_{44}O_5N_8$	584.357	12	No hits	329.1664	$C_{22}H_{21}ON_2$	13			

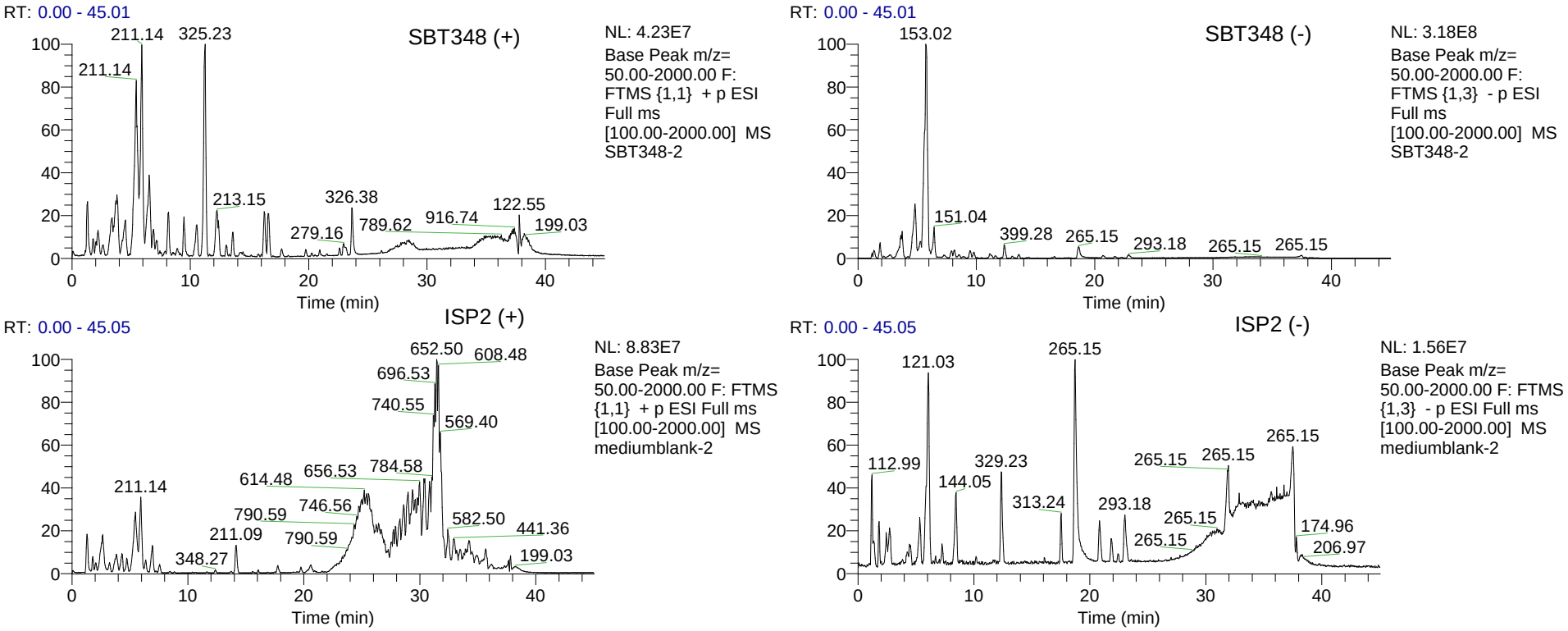

Fig. 3.3 LCMS chromatograms of SBT348 and ISP2 medium blank in positive and negative modes with mass ions label

PCA analysis was also performed on proton NMR data of the 34 strains from Milos collection (**Fig. 3.1C**) and generated from a two-components model achieving an R2 value at 0.719 using the Pareto scaling mode. Two strains, *Streptomyces* sp. SBT349 and *Kocuria* sp. SBT357, which both exhibited antioxidant activities, were revealed distantly as two outliers from the main cluster (**Fig. 3.1C**). For SBT349, the outlying chemical shifts were observed in the aromatic region. By analyzing the ^{1}H, COSY and HMBC spectra, an ABCD aromatic system was elucidated by the coupling constant at 8 Hz and the signal correlation between a doublet-triplet-triple-doublet resonances (**Fig. 3.4**). Anthranilic acid (**Fig. 3.4**) was therefore confirmed by the mass ion peak found in LC-HRMS data at 3.47 min and m/z 138.0551 $[M+H]^+$ which was established as $C_7H_8NO_2$. Anthranilic acid was previously isolated and characterized from *Nocardio opaca* as an intermediate in the metabolism of anthranilate. It was also discovered from marine sediment-derived fungus *Penicillium paneum* SD-44 (Cain, 1968; Hurley and Gairola, 1979; Li et al., 2013; Orlova et al., 1973). For SBT357, the unique chemical shifts at δ_H 7.34 and 7.35 also indicated the presence of an aromatic moiety which is usually of chemical interest. The outliers, SBT348 and SBT376, revealed by PCA analysis of HRMS data were both located at the center of the scores plot (**Fig. 3.1C**). Expansion of the central field of the loadings plot (**Fig. 3.1D**) revealed a clustering of resonances between 10.0 and 12.5 ppm indicating the existence of highly deshielded exchangeable protons found in aromatic/olefinic-bound N*H*$_2$s, phenolic O*H* substituents, and amide moieties. This verified the dereplication result of the HRMS data and indicated the presence of such structures (**Fig. 3.2**) described above. The COSY spectrum (**Fig. 3.5**) also displayed correlations between resonances at 6.50 to 7.50 ppm which were expected to be observed in 3-amino-4-hydroxybenzoic acid, 2,3-dihydroxybenzamide, benadrostin, and N-carbamoyl-2,3-dihydroxybenzamide (**Fig. 3.2**).

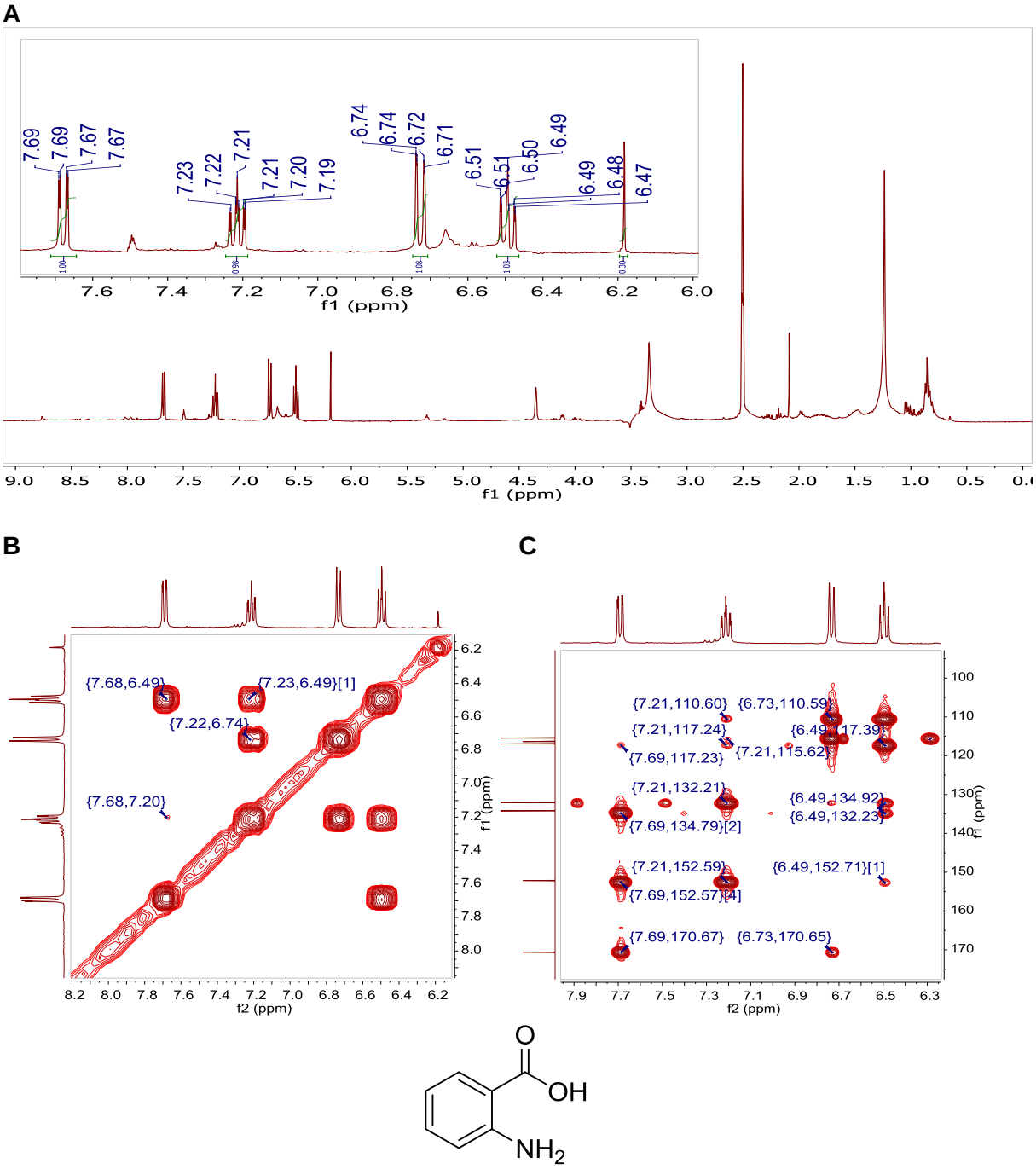

Chemical Formula: $C_7H_7NO_2$

Exact Mass: 137.0477

Found: 138.0551 $[M+H]^+$

D ppm = 0.83722

RT: 3.47 min

Fig. 3.4 ^{1}H NMR (A), COSY (B) and HMBC (C) of ethyl acetate extract of bacterial isolate SBT349 showing anthranilic acid as the major component

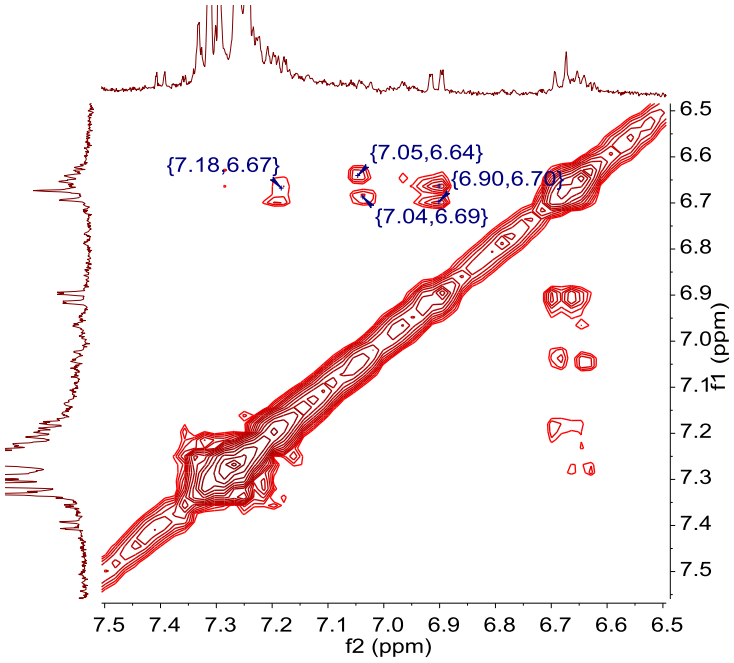

Fig 3.5 COSY spectrum of ethyl acetate extract of bacterial isolate SBT348 in DMSO-d_6

To be able to predict and investigate the type of compounds that would be responsible for the antitrypanosomal bioactivity of the 7 extracts obtained from the Milos sponges (**Table 2.2**), a supervised multivariate analysis was performed by subjecting both the LC-MS (**Figs. 3.6A** and **3.6B**) and ^{1}H NMR (**Figs. 3.6C** and **3.6D**) data sets to OPLS-DA. The sample extracts were divided into two classes: active vs. inactive (Y variables) and by using an S-plot, individual metabolites (LC-MS data) and functional groups (NMR data) can be pinpointed to be responsible for the bioactivity. This statistical model would help to target the potential bioactive compounds for further isolation work (Abdelmohsen et al., 2014). Remarkably, SBT348 was highlighted as the typical outlier from both the HRMS (**Fig. 3.6A**) and NMR (**Fig**. **3.6C**) data sets. The end-point metabolites (circled in **Fig. 3.6B**) in the active quadrant were suspected to be responsible for the antitrypanosomal activity. They belong to *Streptomyces* sp. SBT348 found with molecular weights from 100 to 200 Da or *Nonomuraea* sp. SBT364 found with molecular weights 900 to 990 Da (**Fig. 3.6B**). Strains of the genus *Nonomuraea* sp. were reported to produce anti-tumor cyclic tetrapeptides, glycopeptide antibiotics, and trehalose-derived metabolites (Igarashi et al., 2009; Stinchi et al., 2003; Terui et al., 2008), which were compatible with the dereplication results of the HRMS data. The active quadrant was also populated with mass ion peaks between 200 and 600 Da found in SBT348 as shown in **Fig. 3.6B** and further included in **Table 3.1**. A majority (12 out of 14) of these major compounds listed in **Table 3.1** bear aromatic structures as indicated by their RDBE (Ring Double Bond Equivalents) values ≥ 4. Moreover, the outlying chemical shifts revealed from the ^{1}H NMR data (**Fig. 3.6D**) also validated the presence of the compounds dereplicated from SBT348 in the HRMS data, which included the shielded *ortho* protons adjacent to the OH substituent from 6.0

to 6.9 ppm, along with the phenolic proton (O*H*) chemical shifts observed at 10 to 12 ppm. Expansion of the active quadrant of NMR data (**Fig. 3.6D**) revealed not only a higher distribution of resonances typical of phenolic or aniline natural products, but also α protons of amino acids from 4.01 to 5.55 ppm and their corresponding amide protons from 7.51 to 10 ppm for a peptide structure. Comparing to the dereplication results, these chemical shifts were compatible with the peptide metabolites found in the other outlier *Rhodococcus* sp. SBT367 shown in the OPLS-DA scores plot using ^{1}H NMR data (**Fig. 3.6C**). *Rhodococcus* strains have also been reported to yield peptides in literature, such as the cyclic peptide lariatins isolated from a soil-derived *Rhodococcus* sp. K01-B0171 (Iwatsuki et al., 2006; Iwatsuki et al., 2007).

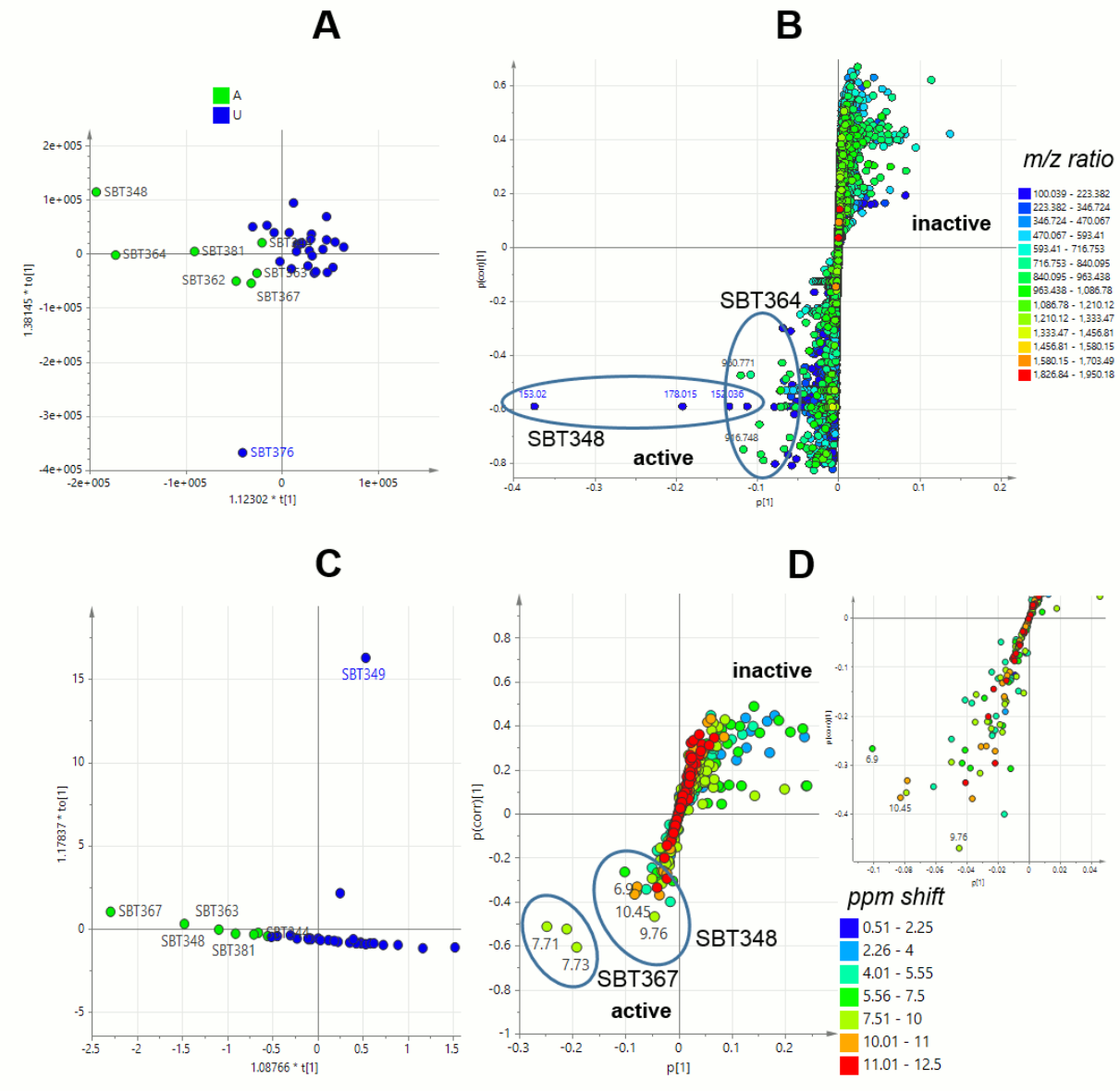

Fig. 3.6 OPLS-DA analysis of 34 extracts from Milos collection. Scores plot (A) and S plot (B) of LC-HRMS data; scores plot (C) and S plot (D) of ^{1}H NMR data of 34 extracts.

3.2.1.2 HPLC profiling of broth extracts of 34 Milos isolates

Since compounds isolation and purification would mainly be performed by HPLC in this study, HPLC profiling also plays a crucial role in the strain prioritization. Among the 46 broth extracts, only two isolates *Streptomyces* sp. SBT348 and SBT349 showed rich HPLC profiling at 254 nm (**Fig. 3.7**). Both of them were revealed as outliers in LC-MS and NMR PCA analysis respectively. SBT348 showed a group of compounds during the early middle retention time, indicating the moderate hydrophilicity of this set of compounds, which was also compatible with the dereplication results that showed the presence of phenolic, aniline or amide moieties (**Table 3.1**; **Fig. 3.1C**, **3.1D**, **3.6C**, and **3.6D**). SBT349 revealed a group of compounds that share very similar and polar properties since they were almost eluded together at the early retention time. The above compound anthranilic acid confirmed by NMR and LC-HRMS analysis was also suspected to be corresponding to in this significant peak by its dominance showed in NMR (**Fig. 3.4**), and polarity showed in HPLC (**Fig. 3.7**).

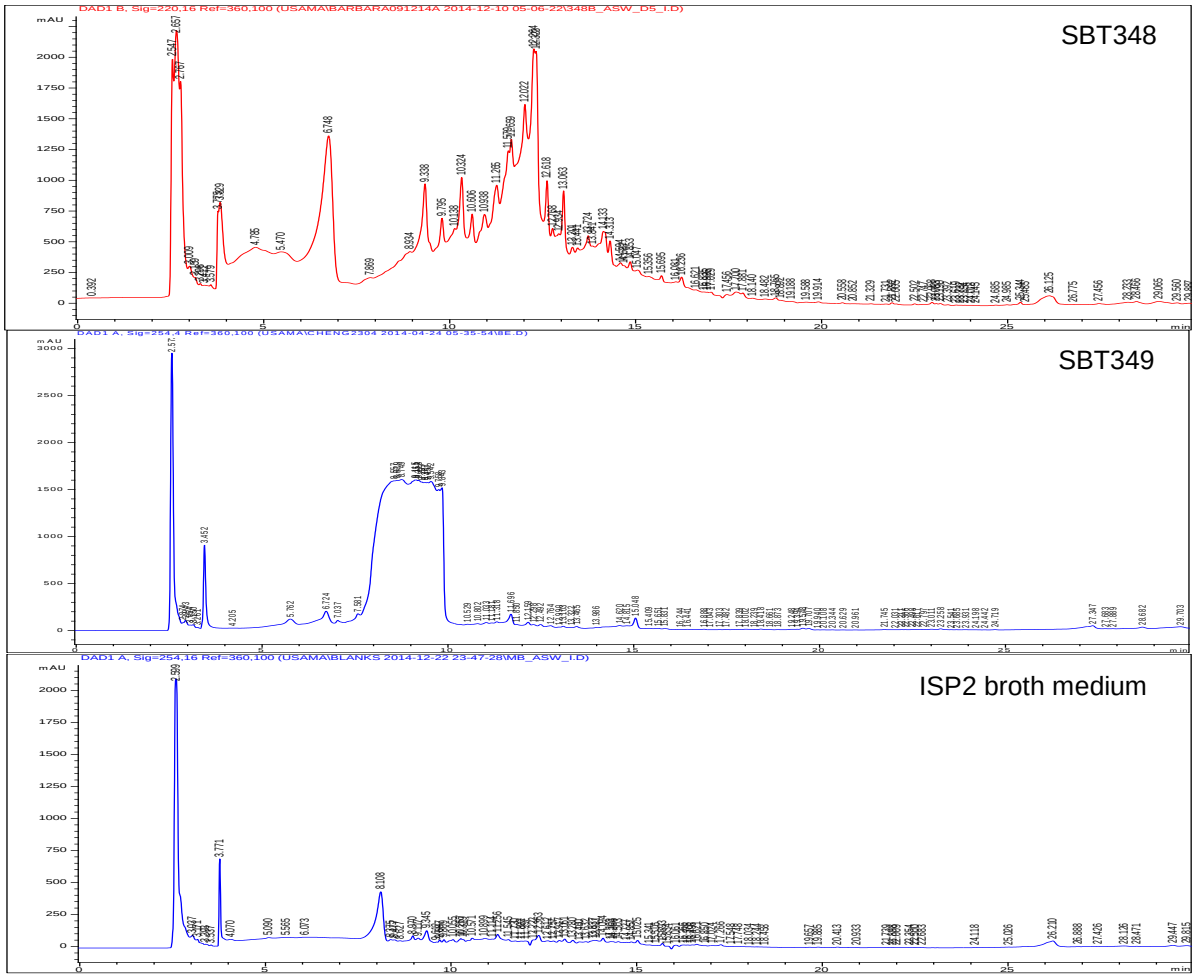

Fig. 3.7 HPLC chromatogram of broth extracts of SBT348, SBT349, and ISP2 medium at 254 nm

3.2.1.2 HPLC profiling of solid extracts of 13 selected Milos isolates

Considering to make some backup candidates, HPLC profiling was also investigated on a group of solid extracts obtained from the bacterial isolates that belonging to genera *Streptomyces*, *Micromonospora*, *Nocardiopsis*, and *Nonomuraea*, which are experientially rich in biological compounds. The solid extracts of SBT345, SBT348, and SBT349 showed prolific HPLC profiling, in which SBT348, SBT349 were comparative rich to their broth extracts. However, SBT349 takes two weeks to go into the logarithmic phase in broth and more than three weeks on solid plates. As for the strain *Streptomyces* sp. SBT345, its solid extract showed similar HPLC chromatogram at the late retention time with SBT348 which is of the same genus *Streptomyces* and similar morphology (**Fig. 3.8**). Due to the fast growth period of SBT345 (5 days to the stationary phase), this strain was considered to be prioritized than SBT349 for further compounds isolation.

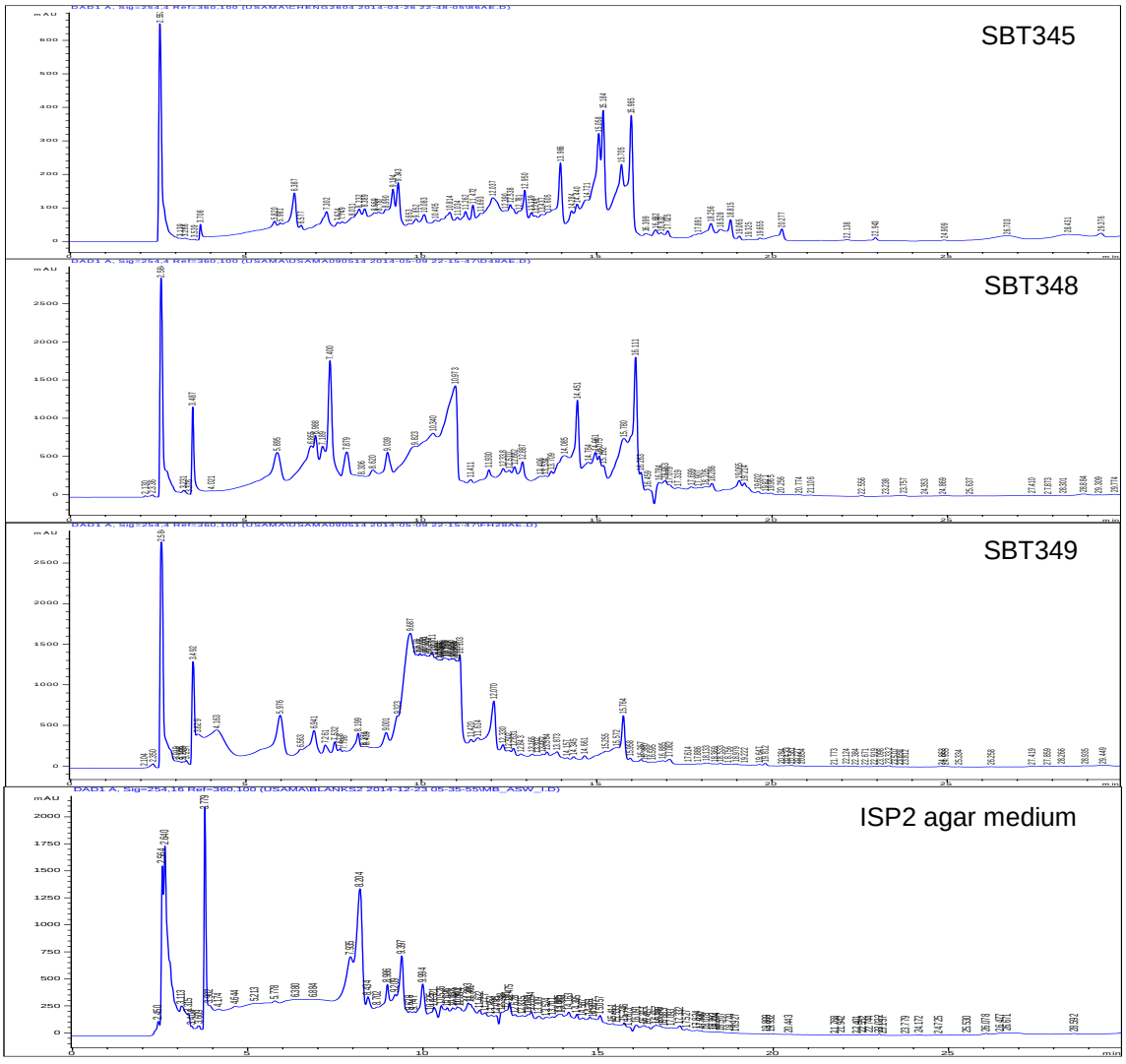

Fig. 3.8 HPLC chromatogram of solid extracts of SBT345, SBT348, SBT349, and ISP2 medium at 254 nm

3.2.2 Crete collection

3.2.2.1 Metabolomics analysis

The 12 Crete isolates were also subjected to PCA analysis using their LC-MS and NMR data (**Fig. 3.9**). Using a two-components model, PCA analysis of both the NMR and LC-MS data gave R2 values of 0.564 and 0.538, respectively. The Crete and Milos collections were subjected to similar metabolomics profiling procedures. The metabolomics analyses were performed separately in order to avoid instrument errors (large shifting of *m/z* values) from different running batches by LC-HRMS. In the LC-HRMS PCA scores plot, *Streptomyces* sp. SBT691, *Micromonospora* sp. SBT687 and *Micromonospora* sp. SBT693 were revealed as outliers (**Fig. 3.9A**). Only SBT687 was found active against *T. b. brucei* strain TC 221 (**Table 2.2**). From the loadings plot (**Fig. 3.9B**), the outlying mass ion peaks for SBT687 were revealed at *m/z* 178.087 $[M-H]^-$ for $C_{10}H_{13}NO_2$, 218.14 $[M+H]^+$ for $C_{11}H_{15}N_5$, 274.131 $[M-H]^-$ for $C_{13}H_{17}N_5O_2$, and 276.146 $[M+H]^+$ for $C_{13}H_{17}N_5O_2$ or $C_{12}H_{21}NO_6$. All these enumerated mass ion peaks were not dereplicated from AntiMarine databases 2013, except for the mass ion peak at *m/z* 178.087 $[M-H]^-$, which was found as 3-(4-hydroxyphenyl)-N-methylpropanamide, earlier isolated from a *Micromonospora* species (Gutierrez-Lugo et al., 2005). An extended list of the major secondary metabolites for SBT 687 and their mass fragments were tabulated in **Table 3.2**. SBT687 produced a set of secondary metabolites with molecular weights ranging from 250 to 550 Da which are empirically chemically interesting (**Table 3.2**, **Fig. 3.9B**). The RDBEs of the metabolites were from 1 to 10, which was quite a wide range indicating a very diverse set of secondary metabolites produced by *Micromonospora* sp. SBT687. The MS^2 data along with the RDBE values suggested the presence of aromatic compounds mostly between 200 and 300 Da (peak ID nos. 1, 6, 7, 10, and 12) and adenine analogues (peak ID nos. 9 and 11, **Fig. 3.10**); as well as aliphatic type of compounds from 250 to 550 Da which included a sulfated compound (peak ID no. 2), three peptides (peak ID nos. 4, 13 and 18); and hydoxylated lipids, lactone, or polyketides (peak ID nos. 3, 15, 16, and 17). From the AntiMarin Database 2013, the mass ion peak at *m/z* 215.083 $[M-H]^-$ was dereplicated as N-acetyl-β-oxotryptamine as further implicated by the fragment mass ion at *m/z* 116.0506 $[M-H]^-$ (**Fig. 3.10**) which is characteristic of an indole moiety. This compound was previously isolated from marine bacterium *Bacillus pumilus* and exhibited inhibition activity against *Trypanosoma cruzi* with IC_{50} value of 19.4 μM (Martinez-Luis et al., 2012). While the mass ion peak at *m/z* 329.234 $[M-H]^-$ was dereplicated as penicitide B, (9*R*, 10*R*, *E*)-6, 9, 10-trihydroxyoctadec-7-enoic acid, and (*Z*)-9, 10, 11-trihydroxyoctadec-12-enoic acid, all of which are fungal metabolites. However, fragments ions found at *m/z* 171.103 and 211.134 were compatible to penicitide B in which the molecule underwent a rearrangement by losing two protons (**Fig. 3.10**). Penicitide B was previously described from the endophytic fungus *Penicillium chrysogenum* QEN-24S isolated from an algae of genus *Laurencia*, but there have been no report of its biological activities (Gao et al., 2011). *Micromonospora* sp. SBT695 and *Streptomyces* sp. SBT688 were

identified as the outliers in the PCA analysis of 12 Crete samples using ^{1}H NMR data (**Fig. 3.9C**). The unique chemical shifts of these two outliers (**Fig. 3.9D**) were shown by and heteroatom bound aliphatic (4.5 to 5.0 ppm) and aromatic (7.5 to 9.0 ppm) protons. The antitrypanosomal strain *Micromonospora* sp. SBT687 was situated in the middle of the scores plot with a cluster of exchangeable aromatic protons (10.0 to 12.5 ppm) presented by the loadings plot such as those of the phenolic O*H* in 3-(4-hydroxyphenyl)-N-methylpropanamide and the indolic N*H* found in N-acetyl-β-oxotryptamine. Similar to *Streptomyces* sp. SBT348, it seems that the observation of exchangeable aromatic protons plays a significant role on the antitrypanosomal activity found in the SBT687 extract.

Table 3.2 Selected major metabolites found in positive and negative ionization modes in *Micromonospora* sp. SBT687. (P = positive mode; N = negative mode)

Peak ID	ESI Mode	Molcular ion MS (*m/z*)	Rt (min)	Molecular Formula	MW	RDB	Hits	Fragment ion MS^2 (*m/z*)	Fragment Formula (+/-)	RDBE	Fragment ion MS^3 (*m/z*)	Fragment Formula (+/-)	RDB
1	N	279.0731	1.2	$C_{11}H_{12}O_5N_4$	280.0804	8	No hits	135.0314	$C_5H_2ON_4$	6			
								143.0351	$C_6H_7O_4$	3			
2	P	256.1754	2.4	$C_{14}H_{25}ONS$	255.1681	3	No hits	239.1482	$C_{14}H_{23}OS$	4			
3	P	283.1751	3.0	$C_{12}H_{26}O_7$	282.1678	1		133.0857	$C_6H_{13}O_3$	1			
								177.1118	$C_8H_{17}O_4$	1			
								89.0597	$C_4H_9O_2$	1			
								239.1484	$C_{10}H_{23}O_6$	0			
4	P	388.2543	4.1	$C_{17}H_{33}O_5N_5$	387.2470	4	No hits	371.2278	$C_{17}H_{31}O_5N_4$	5	353.2168	$C_{17}H_{29}O_4N_4$	6
											327.2011	$C_{15}H_{27}O_4N_4$	5
											309.1907	$C_{15}H_{25}O_3N_4$	6
5	P	432.2805	4.5	$C_{19}H_{37}O_6N_5$	431.2732	4	No hits	415.2527	$C_{19}H_{35}O_6N_4$	4	397.2434	$C_{19}H_{33}O_5N_4$	6
											371.2277	$C_{17}H_{32}O_5N_4$	5
											327.2015	$C_{15}H_{27}O_4N_4$	5
											309.1908	$C_{15}H_{25}O_3N_4$	6
											283.1752	$C_{13}H_{23}O_3N_4$	5
6	P	210.1124	4.6	$C_{11}H_{15}O_3N$	209.1052	4	No hits	151.0751	$C_9H_{11}O_2$	5	119.0494	C_8H_7O	6
								168.1015	$C_9H_{14}O_2N$	5	95.0494	C_6H_7O	4
								181.1333	$C_{10}H_{17}ON_2$	4	91.0545	C_7H_7	5
7	N	224.0932	5.1	$C_{11}H_{15}O_4N$	225.1004	5	No hits	178.0875	$C_{10}H_{12}O_2N$	5	136.0768	$C_8H_{10}ON$	4
											119.0523	C_8H_7O	5
8	P	520.3331	5.1	$C_{23}H_{45}O_8N_5$	519.3258	4	No hits	503.3055	$C_{23}H_{43}O_8N_4$	5	485.2954	$C_{23}H_{41}O_7N_4$	6
											459.2798	$C_{21}H_{39}O_{7N4}$	5
											415.2534	$C_{19}H_{35}O_6N_4$	5
											397.2430	$C_{19}H_{33}O_5N_4$	6
											371.2277	$C_{17}H_{31}O_5N_4$	5

Peak ID	ESI Mode	Molcular ion MS (*m/z*)	Rt (min)	Molecular Formula	MW	RDB	Hits	Fragment ion MS^2 (*m/z*)	Fragment Formula (+/-)	RDBE	Fragment ion MS^3 (*m/z*)	Fragment Formula (+/-)	RDB
											327.2013	$C_{15}H_{27}O_4N_4$	5
											309.1906	$C_{15}H_{25}O_3N_4$	6
											283.1751	$C_{13}H_{23}O_3N_4$	5
											177.1122	$C_8H_{17}O_4$	1
9	P	218.1399	5.7	$C_{11}H_{15}N_5$	217.1327	7	No hits	162.0770	$C_7H_8N_5$	7			
								150.0771	$C_6H_8N_5$	6			
10	N	215.0829	6.5	$C_{12}H_{12}O_2N_2$	216.0902	8	N-acetyl-□-oxotryptamine	116.0506	C8H6N	6			
11	N	274.1312	6.8	$C_{13}H_{17}O_2N_5$	275.1385	8	No hits	217.1098	$C_{11}H_{13}ON_4$	7	202.0864	$C_{12}H_{12}O_2N$	7
12	P	284.1393	6.8	$C_{16}H_{17}O_2N_3$	283.1320	10	No hits	267.1122	$C_{16}H_{15}O_2N_2$	11			
								170.0597	$C_{11}H_8ON$	8			
								130.0650	C_9H_8N	7			
								132.0806	$C_9H_{10}N$	6			
13	P	227.1753	8.2	$C_{12}H_{22}O_2N_2$	226.1681	3	No hits	199.1800	$C_{11}H_{23}ON_2$	2	154.1587	$C_{10}H_{20}N$	2
								182.1536	$C_{11}H_{20}ON$	3	86.0964	$C_5H_{12}N$	1
14	N	329.2340	12.0	$C_{18}H_{34}O_5$	330.2413	2	penicitide B	229.1448	$C_{12}H_{21}O_4$	2			
								211.1342	$C_{12}H_{19}O_3$	3			
								171.1029	$C_9H_{15}O_3$	2			
15	N	525.3806	13.4	$C_{30}H_{54}O_7$	526.3879	4	No hits	311.2589	$C_{19}H_{35}O_3$	2	293.2490	$C_{19}H_{33}O_2$	3
16	N	523.3650	15.0	$C_{30}H_{52}O_7$	524.3722	5	No hits	309.2434	$C_{19}H_{33}O_3$	3	291.2332	$C_{19}H_{31}O_2$	4
											233.1914	$C_{16}H_{25}O$	4
17	P	509.3840	17.0	$C_{30}H_{52}O_6$	508.3767	5	No hits	491.3731	$C_{30}H_{51}O_5$	6	311.1847	$C_{17}H_{27}O_5$	5
								473.3626	$C_{30}H_{49}O_4$	7	293.1749	$C_{17}H_{25}O_4$	6
								455.3521	$C_{30}H_{47}O_3$	8	259.2419	$C_{19}H_{31}$	5
								437.3415	$C_{30}H_{45}O_2$	9			
								295.2631	$C_{19}H_{35}O_2$	3			

Peak ID	ESI Mode	Molcular ion MS (*m/z*)	Rt (min)	Molecular Formula	MW	RDB	Hits	Fragment ion MS^2 (*m/z*)	Fragment Formula (+/-)	RDBE	Fragment ion MS^3 (*m/z*)	Fragment Formula (+/-)	RDB
	N	507.3686	17.0	$C_{30}H_{52}O_6$	508.3767	5	No hits	461.3639	$C_{29}H_{49}O_4$	5			
18	N	553.3755	17.1	$C_{27}H_{50}O_6N_6$	554.3828	6	No hits	405.3002	$C_{23}H_{39}O_3N_3$	6	311.2592	$C_{19}H_{35}O_3$	2
19	P	530.3547	23.3	$C_{25}H_{47}O_7N_5$	529.3474	5	No hits	513.3259	$C_{25}H_{45}O_7N_4$	6	495.3162	$C_{25}H_{43}O_6N_4$	7
											371.2273	$C_{17}H_{31}O_5N_4$	5
											187.1328	$C_{10}H_{19}O_3$	2

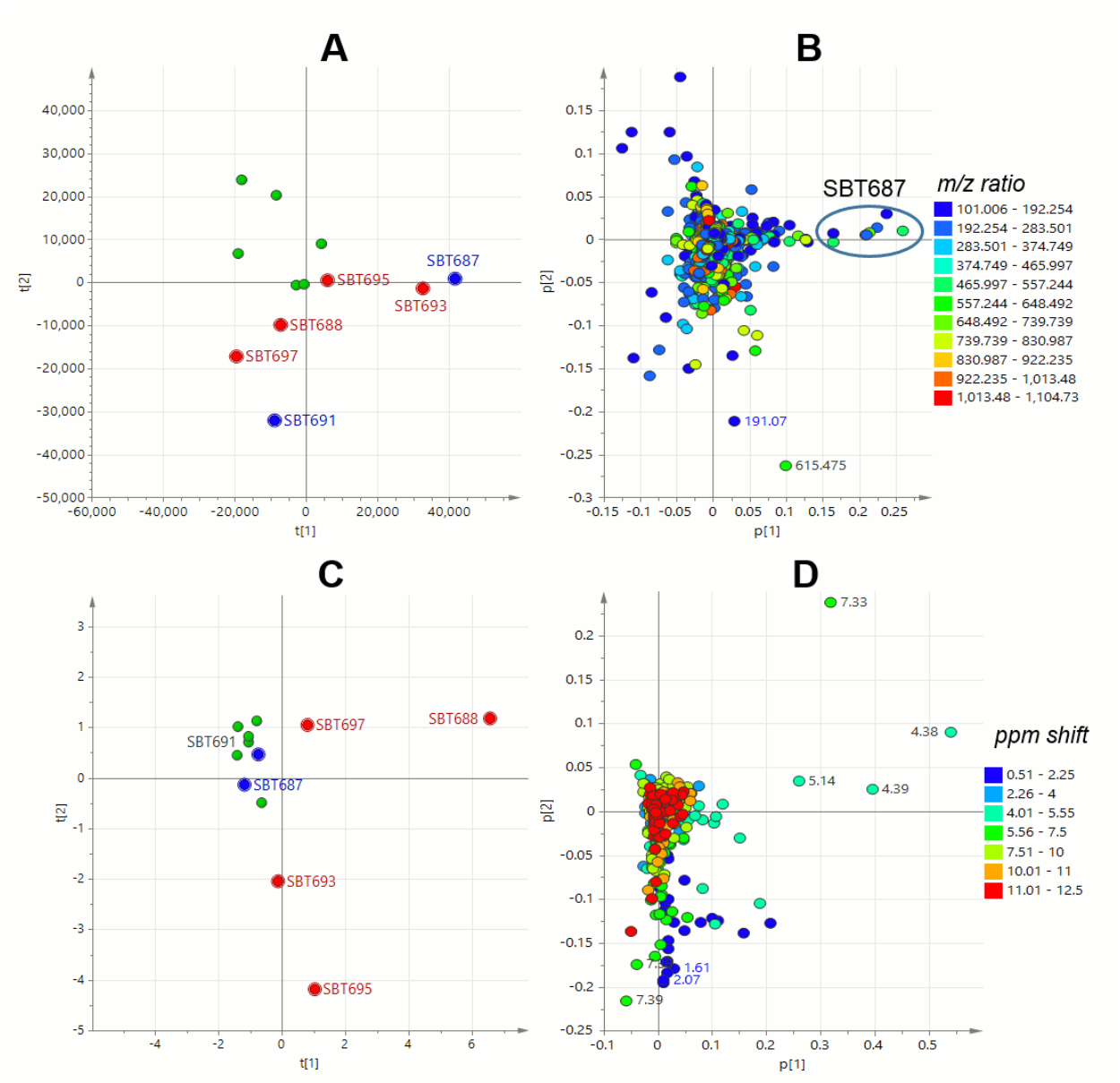

Fig. 3.9 PCA analysis of 12 extracts from Crete collection. Scores plot (A) and loadings plot (B) of LC-HRMS data; scores plot (C) and loadings plot (D) of ^{1}H NMR data of 12 extracts. For the scores plot (A and C), the outmost PCA outliers for the HRMS data were colored blue while those for the ^{1}H NMR data were colored red.

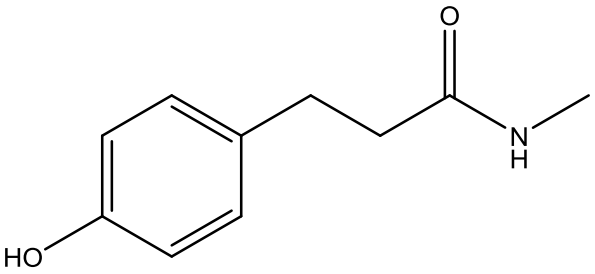

3-(4-hydroxyphenyl)-*N*-methylpropanamide
Micromonospora sp. P1068

Chemical Formula: $C_{10}H_{13}NO_2$
Exact Mass: 179.0946

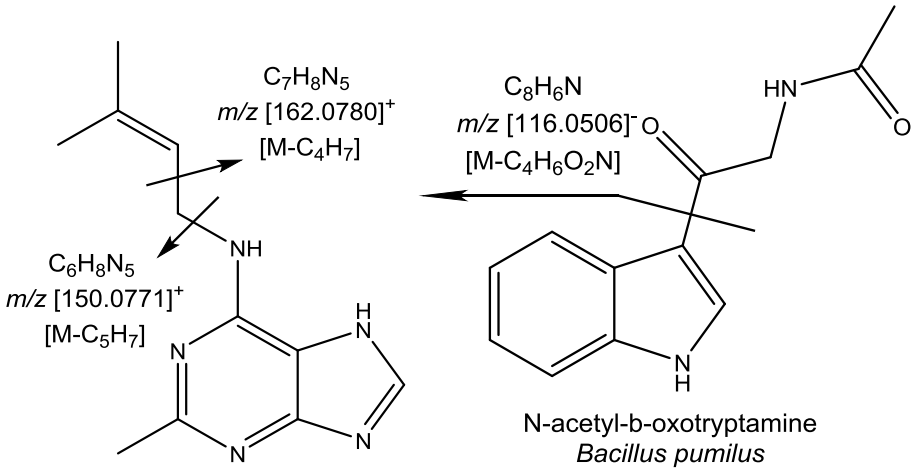

Chemical Formula: $C_{11}H_{15}N_5$
Exact Mass: 217.1327

N-acetyl-b-oxotryptamine
Bacillus pumilus

Chemical Formula: $C_{12}H_{12}N_2O_2$
Exact Mass: 216.0899

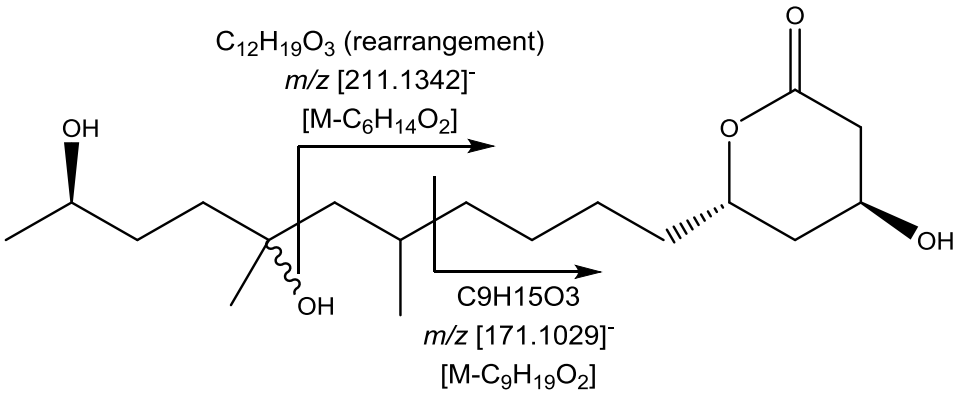

Penicitide B
Fungus *Penicillium chrysogenum* QEN-24S
Chemical Formula: $C_{18}H_{34}O_5$
Exact Mass: 330.2406

Fig. 3.10 Dereplicated metabolites for the outlying mass ion peaks for *Micromonospora* sp. SBT687.

3.2.2.2 HPLC and metabolomics profiling of 12 Crete solid extracts

As it mentioned above, further isolation work will mainly be carried out on HPLC, therefore all the Crete broth extracts were also subjected to HPLC chromatography to verify the results from metabolomics analysis. Unfortunately, none of the broth extracts displayed a rich HPLC profiling under the 4 different UV wavelengths (220 nm, 254nm, 280 nm, and 360 nm). Therefore, the solid cultivation of the 12 Crete isolates was carried out, and the EtOAc extracts were also subjected to LC-HRMS for dereplication and PCA analysis. Isolates from different genera were well separated in the PCA scores plot (**Fig. 3.11A**) with one exception of the genus *Nocardia* which clustered with the genus *Micromonospora* (**Fig. 3.11B**). The genus *Promicromonospora* was revealed as an outlier (**Fig. 3.11A**) indicating a significant chemical difference compared to the others. One of the duplicate extracts from SBT688 was also outlized (**Fig. 3.11A**), therefore the total ion chromatograph of both duplicates of SBT688 was investigated (**Fig. 3.12**). The outlying duplicate SBT688A_2 showed more intensive major peaks at the same retention time and more diverse small peaks compared to the other duplicate, but entirely different profiling compared to the medium blank. The variance therefore was speculated from some inevitably uncertain factors during the cultivation or different growing stages on different culture plates (e.g. different moisture), rather than an artificial mistake. Unfortunately, SBT688 didn't exhibit any activities in the bioassay screening. To better investigate the inner relationships among the other clustering strains, the outlying isolates belonging the genus *Promicromonospora* sp. SBT697 were removed. The new PCA scores plot after removal of the effect of the preliminary outlier *Promicromonospora* sp. SBT697 (**Fig. 3.11C)** also well separated the strains from different genera and in this case SBT689 representing the genus *Nocardia* was apparently distinguished. The broth outliers SBT687 and SBT693 also showed a leaving tendency to the other *Micromonospora* sp. strains in the solid PCA analysis (**Fig. 3.11D**), which indicated their distinctness in the secondary metabolites in both broth and solid cultivation (**Fig. 3.9A**). However, the major secondary metabolites detected from broth and solid extracts of SBT687 only showed the overlaps of 2 compounds 17 and 18 (**Table 3.2**), which indicated a great change in the secondary metabolites production from different cultivation methods. However, none of the broth or solid cultivation of SBT687 showed a rich HPLC profiling, a short growth period or even a high yield of the organic extract, which made it difficult to process further up-scaling cultivation and compounds isolation. Due to the limited amount obtained from each solid extracts, NMR measurement of the 12 Crete isolates was not performed.

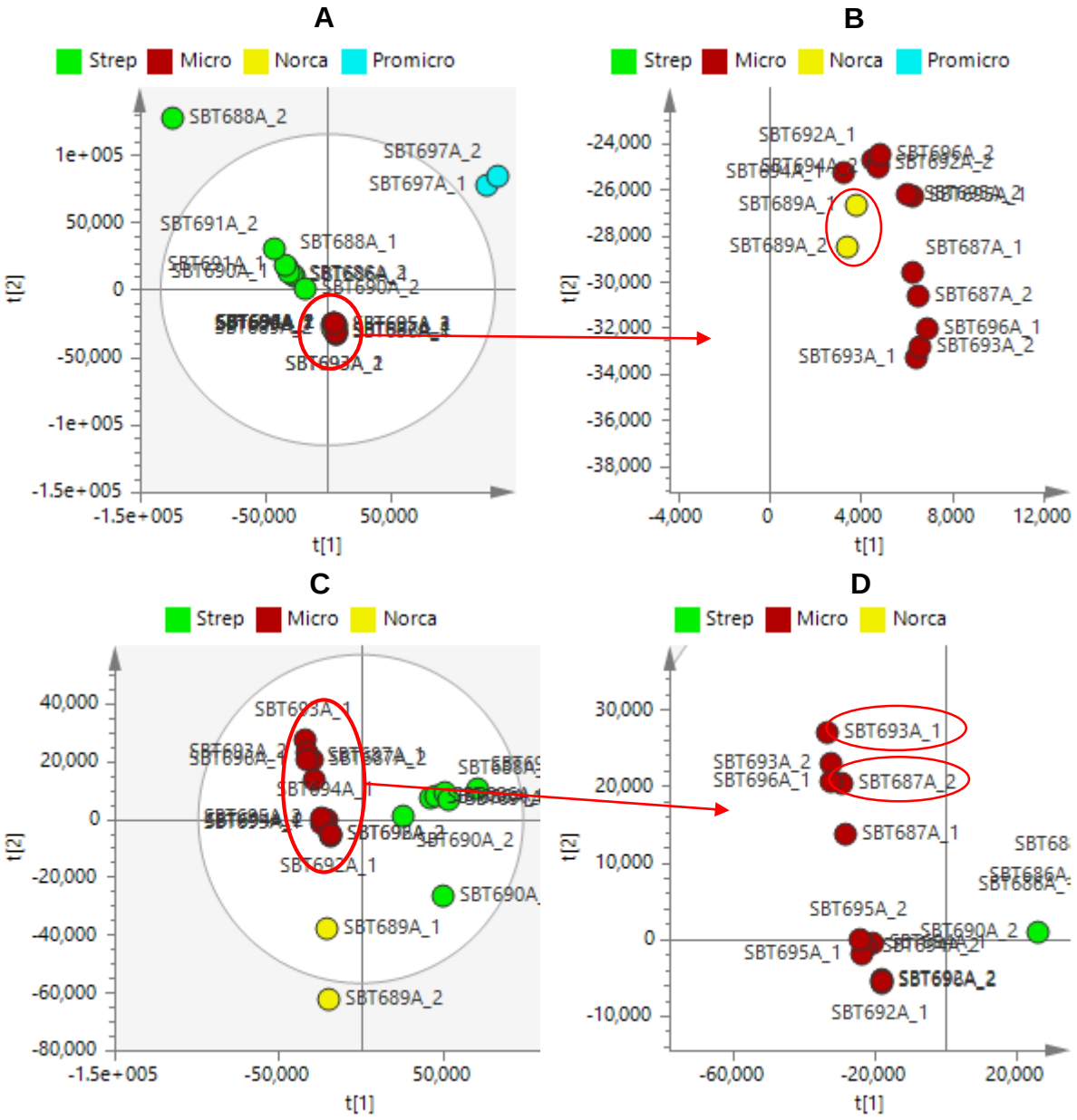

Fig. 3.11 PCA scores plot of 12 Crete bacterial extracts (in duplicate) from solid medium. Scores plot (A) and zoom-in scores plot (B) of LC-HRMS data of all Crete bacterial extracts, scores plot (C) and zoom-in scores plot (D) of LC-HRMS data of Crete bacterial extracts by removing *Promicromonospora* sp. SBT697

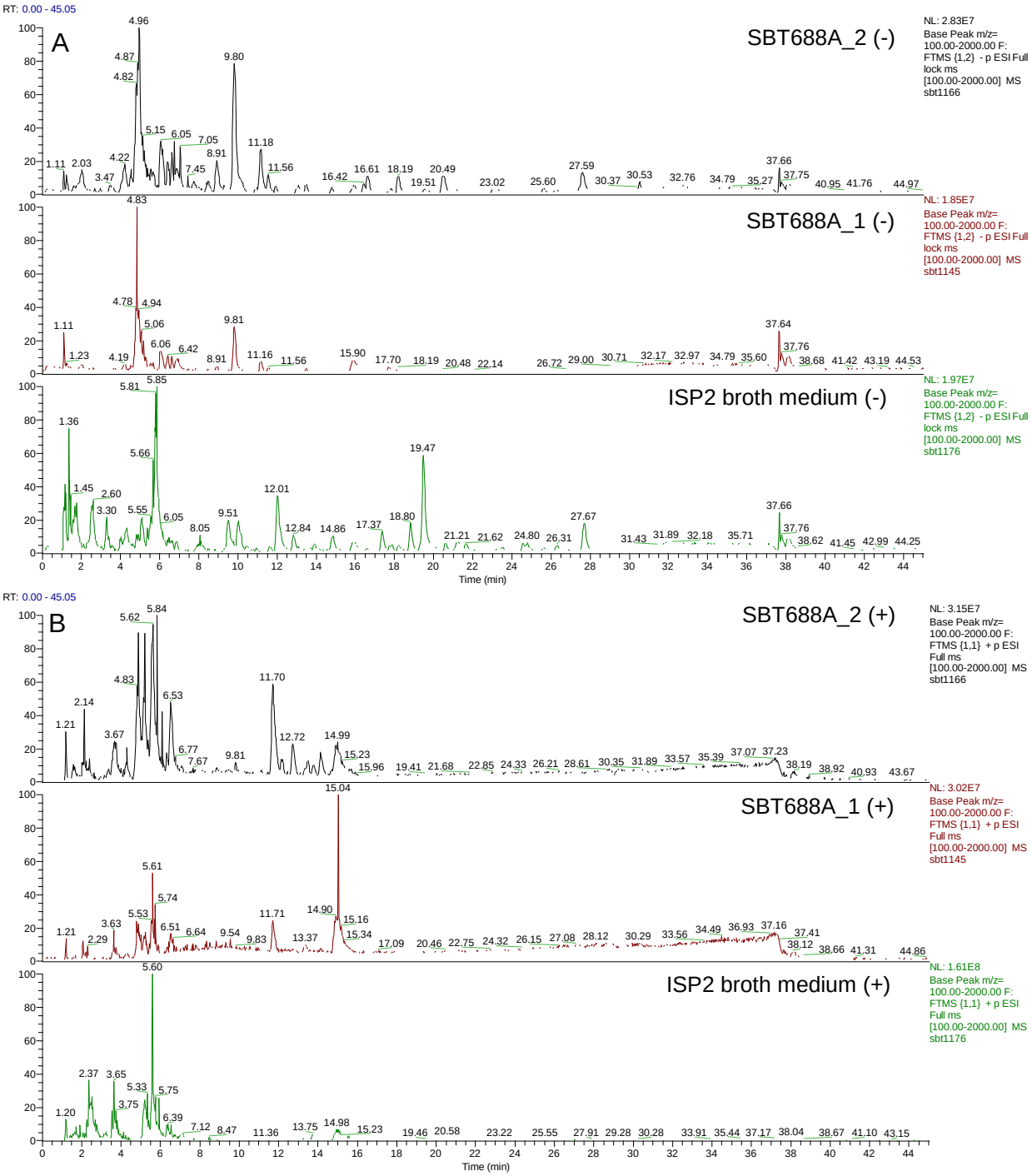

Fig. 3.12 Total ion chromatography of SBT688B_1, SBT688B_2, and ISP2 agar medium blank in negative (A) and positive ionization (B) modes.

3.3 Strain prioritization for up-scaling cultivation and compounds isolation

For the purpose of prioritizing the candidate strains for further up-scaling cultivation and compounds isolation, four evaluation criteria were established in this study including the taxonomic novelty, biological activity, metabolomics distinction, and HPLC profiling richness. All the strains that accord with at least one of the criteria were listed in **Table 3.3**. As it was discussed above, *Streptomyces* sp. SBT348 was revealed as a unique strain that produced distinct secondary metabolites in the PCA and OPLS-DA analyses of both LC-MS and NMR data, as well as a rich HPLC profiling. In addition to its antioxidant, anti-*Bacillus* sp., anti-*Aspergillus* sp., and antitrypanosomal bioactivities, *Streptomyces* sp. SBT348 stood out from the other strains, therefore, was prioritized as the best candidate for further up-scaling cultivation and compounds isolation. As for the other two HPLC-rich strains *Streptomyces* sp. SBT345 and *Streptomyces* sp. SBT349, SBT349 takes at least three weeks to grow to the exponential phase and therefore was considered as a backup candidate and SBT345 was considered as the second priority for further compounds isolation due to its fast growing period, rich HPLC chromatogram, and antioxidant activity.

The metabolomics analysis and antitrypanosomal activities of the selected 46 isolates were published in the journal PLoS One (Cheng et al., 2015).

Table 3.3 Strain prioritization based on four evaluation criteria

Sample	Taxonomic Novelty	Bioassay Screening	Metabolomics outliers	HPLC Profiling
SBT344		3		
SBT345		1		Solid rich
SBT348		1, 2, 3	LC-MS, NMR	Solid & liquid rich
SBT349		1	NMR	Solid & liquid rich
SBT350	√			
SBT357		1		
SBT362		3		
SBT363		3		
SBT364		3		
SBT365	√			
SBT367	√	3		
SBT374	√			
SBT376			LC-MS	
SBT381		3		
SBT686		1		
SBT687		3	LC-MS	
SBT688			LC-MS	
SBT692		1		

1. Antioxidant assay; 2. Antimicrobial disc diffusion assay; 3. Antitrypanosomal bioassay.

3.4 References

Abdelmohsen, U.R., Cheng, C., Viegelmann, C., Zhang, T., Grkovic, T., Ahmed, S., Quinn, R.J., Hentschel, U., Edrada-Ebel, R., 2014. Dereplication strategies for targeted isolation of new antitrypanosomal actinosporins A and B from a marine sponge associated-*Actinokineospora* sp. EG49. Marine drugs 12, 1220-1244.

Aoyagi, T., Yoshida, S., Harada, S., Okuyama, A., Nakayama, C., Yoshida, T., Hamada, M., Takeuchi, T., Umezawa, H., 1988. Benadrostin, new inhibitor of poly(ADP-ribose) synthetase, produced by actinomycetes. I. Taxonomy, production, isolation, physico-chemical properties and biological activities. Jounal of antibiotics (Tokyo) 41, 1009-1014.

Cain, R.B., 1968. Anthranilic acid metabolism by microorganisms. Formation of 5-hydroxyanthranilate as an intermediate in anthranilate metabolism by *Norcardia opaca*. Antonie van Leeuwenhoek 34, 17-32.

Cheng, C., MacIntyre, L., Abdelmohsen, U.R., Horn, H., Polymenakou, P.N., Edrada-Ebel, R., Hentschel, U., 2015. Biodiversity, anti-trypanosomal activity screening, and metabolomic profiling of actinomycetes isolated from Mediterranean sponges. PloS one 10, e0138528.

Dyer, J.R., Heding, H., Schaffner, C.P., 1964. Phenolic metabolite of “low-iron fermentation” of *Streptomyces griseus*. Characterization of 2,3-dihydroxybenzoic acid. Journal of Organic Chemistry 29, 2802-2803.

Elstner, E.F., Carnes, D.M., Suhadolnik, R.J., Kreishman, G.P., Schweizer, M.P., Robins, R.K., 1973. Isolation, structural elucidation, biological properties, and biosynthesis of maleimycin, a new bicyclic maleimide antibiotic isolated from the culture filtrates of *Streptomyces showdoensis*. Biochemistry 12, 4992-4997.

Gao, S.S., Li, X.M., Du, F.Y., Li, C.S., Proksch, P., Wang, B.G., 2011. Secondary metabolites from a marine-derived endophytic fungus *Penicillium chrysogenum* QEN-24S. Marine drugs 9, 59-70.

Ghiringhelli, D., Griffini, A., Traldi, P., 1981. Electron impact mass spectrometry of maleimycin. Biomedical & environmental mass spectrometry 8, 155-159.

Gutierrez-Lugo, M.T., Woldemichael, G.M., Singh, M.P., Suarez, P.A., Maiese, W.M., Montenegro, G., Timmermann, B.N., 2005. Isolation of three new naturally occurring compounds from the culture of *Micromonospora* sp. P1068. Nature Product Research 19, 645-652.

Hurley, L.H., Gairola, C., 1979. Pyrrolo (1,4) benzodiazepine antitumor antibiotics: biosynthetic studies on the conversion of tryptophan to the anthranilic acid moieties of sibiromycin and tomaymycin. Antimicrobial Agents and Chemotherapy 15, 42-45.

Igarashi, Y., Mogi, T., Yanase, S., Miyanaga, S., Fujita, T., Sakurai, H., Saiki, I., Ohsaki, A., 2009. Brartemicin, an inhibitor of tumor cell invasion from the actinomycete *Nonomuraea* sp. Journal of natural products 72, 980-982.

Iwatsuki, M., Tomoda, H., Uchida, R., Gouda, H., Hirono, S., Omura, S., 2006. Lariatins, antimycobacterial peptides produced by *Rhodococcus* sp. K01-B0171, have a lasso structure. Journal of the American Chemical Society 128, 7486-7491.

Iwatsuki, M., Uchida, R., Takakusagi, Y., Matsumoto, A., Jiang, C.L., Takahashi, Y., Arai, M., Kobayashi, S., Matsumoto, M., Inokoshi, J., Tomoda, H., Omura, S., 2007. Lariatins, novel anti-mycobacterial peptides with a lasso structure, produced by *Rhodococcus jostii* K01-B0171. Journal of antibiotics 60, 357-363.

Li, C.S., Li, X.M., Gao, S.S., Lu, Y.H., Wang, B.G., 2013. Cytotoxic anthranilic acid derivatives from deep sea sediment-derived fungus *Penicillium paneum* SD-44. Marine drugs 11, 3068-3076.

Li, Y.F., Gould, S.J., Proteau, P.J., 2000. Biosynthesis of 3-amino-4-hydroxybenzoic acid in *Streptomyces murayamaensis*: incorporation of [4-13C]oxalacetate. Tetrahedron letters 41, 5181-5185.

Macintyre, L., Zhang, T., Viegelmann, C., Martinez, I.J., Cheng, C., Dowdells, C., Abdelmohsen, U.R., Gernert, C., Hentschel, U., Edrada-Ebel, R., 2014. Metabolomic tools for secondary metabolite discovery from marine microbial symbionts. Marine drugs 12, 3416-3448.

Martinez-Luis, S., Gomez, J.F., Spadafora, C., Guzman, H.M., Gutierrez, M., 2012. Antitrypanosomal alkaloids from the marine bacterium *Bacillus pumilus*. Molecules 17, 11146-11155.

online:, A.S.F.P.H.A., http://proteowizard.sourceforge.net/.

Orlova, T.I., Sorokina, N.V., Silaev, A.B., 1973. Formation of N-acetyl-4-methyl-3-oxy-anthranilic acid by actinomycete producers of various types of actinomycins. Antibiotiki 18, 500-503.

Stinchi, S., Azimonti, S., Donadio, S., Sosio, M., 2003. A gene transfer system for the glycopeptide producer *Nonomuraea* sp. ATCC39727. FEMS Microbiology letters 225, 53-57.

Sugiyama, Y., Hirota, A., 2009. New potent DPPH radical scavengers from a marine-derived actinomycete strain USF-TC31. Bioscience, biotechnology, and biochemistry 73, 2731-2734.

Terui, Y.C., Chu, Y., Li, J., Ando, T., Fukunaga, T., Aoki, T., Toda, Y., 2008. New cyclic tetrapeptides from *Nonomuraea* sp. TA-0426 that inhibit glycine transporter type 1 (GlyT1). Bioorganic & medicinal chemistry letters 18, 6321-6323.

Yoshida, S., Naganawa, H., Aoyagi, T., Takeuchi, T., Umezawa, H., 1988. Benadrostin, new inhibitor of poly(ADP-ribose) synthetase, produced by actinomycetes. II. Structure determination. Journal of antibiotics 41, 1015-1018.

Chapter 4
Compounds purification, structure elucidation, and testing of their biological activities

4.1 Materials and methods

4.1.1 General procedure for compounds purification

Column chromatography was performed using Sephadex LH20 (32-64 µm, Merck). TLC analysis was carried out using pre-coated silica gel 60 F254 plates (Merck, Germany). Preparative HPLC separation and purification were performed on Hewlett-Packard series 1100 (QuatPump, degasser, DAD, Colcomp, Iterface 35900E) and Agilent Technologies Series 1100 (ALS, UV Detect00719) on a Semip-rep RP-C18 column (5 µm, 10×250 mm, Waters XBridge, Germany) and Onyx Monolithic semi-prep RP-C18 column (5 µm, 10×100 mm, Phenomenex, Germany) respectively, while the analytical detection was carried out using an analytical Gemini-NX RP-C18 column (5 µm, 4.60x100 mm, Phenomenex, Germany). Accurate electrospray ionization mass spectra (ESI) were obtained by a Synapt G2 HDMS qTOF-Mass Spectrometer (Waters, Germany). The ESI was operated in the positive and negative ionization modes. The capillary voltage was set to 0.8 kV and nitrogen (at 350 °C, the flow rate of 800 L/h) was used as desolvation gas. The molecular ion was determined by quadrupole in a wide-band RF mode, and data was acquired over the mass range of 50−1200 Da. Product ion scan was optimized for different analyses using different collision voltage from 10 to 25 eV. MassLynx (version 4.1, Waters) was utilized to acquire and process mass spectrum. ^{1}H NMR (400 MHz, 600 MHz) and ^{13}C NMR (150 MHz) spectra were recorded on Bruker Avance III HD 400 and 600 instruments. Heteronuclear correlations were measured using HSQC (optimized for $^{1}J_{HC}$ = 145 Hz) and HMBC (optimized for $^{n}J_{HC}$ = 8.3 Hz or $^{n}J_{HC}$ = 4.0 Hz) pulse sequences. NOE effects were measured using a standard pulse sequence from the standard Bruker pulse program library. The samples were prepared in deuterated solvents (e.g. DMSO-d_6 and MeOD-d_4) and degassed by ultrasonic water bath (Branson 3800 Ultrasonic Cleaner, Branson, Germany) for 20 min before measurements. Solvent signals of DMSO-d_6 (δ_H 2.5 ppm and δ_C 39.5 ppm) and MeOD-d_4 (δ_H 3.3 ppm and δ_C 49.0 ppm) were considered as the internal reference signal for calibration. The observed chemical shift values (δ) were recorded in ppm and the coupling constants (J) in Hz.

4.1.2 Fermentation and extraction of candidate actinomycetes

Three hundreds of ISP2 agar plates (square 120×120 mm), each inoculated with 100 µL of 5 days liquid culture of *Streptomyces* sp. SBT345 and *Streptomyces* sp. SBT348 respectively were incubated at 30 °C for 7 days. The agar media with bacterial biomass were scalped into small pieces and transferred to 1 L Erlenmeyer flasks. Five hundred mL of ethyl acetate/flask were added to submerge the agar pieces and macerated the medium culture under shaking at 175 rpm for overnight. The macerations were subsequently filtered by gravity using filter paper (A. Hartenstein, Germany). The filtrates were combined and evaporated by rotavapor (Büchi, Germany).

4.1.3 Compounds isolation from *Streptomyces* sp. SBT348

Three hundred and seventy mg of the dried crude EtOAc extract obtained from the solid culture of strain *Streptomyces* sp. SBT348 was extracted with 50 mL hexane under ultrasonic water bath for 10 min. The remaining EtOAc extract was fractionated by semi-preparative HPLC (Agilent, Germany) using H_2O/ACN (95:5%) initially for 5 min, then a linear gradient to 100 % ACN within 40 min, which was followed by an isocratic condition of 100% ACN for a further 5 min on the Prep C18 column (5 µm, 10×250 mm, Waters XBridge), with a flow rate of 3.0 mL/min to yield 15 fractions. Fractions were collected based on time slot which was set at 2 min and combined into 5 fractions according to the peaks shown in the HPLC chromatogram which showed similar peak pattern. Compounds were purified from combined factions by semi-preparative HPLC using Onyx Monolithic semi-prep RP-C18 column (5 µm, 10×100 mm, Phenomenex). The hexane extract was conducted on the Monolithic semi-prep RP-C18 column (5 µm, 10×100 mm, Phenomenex) and directly led to the pure compounds (**3-4**).

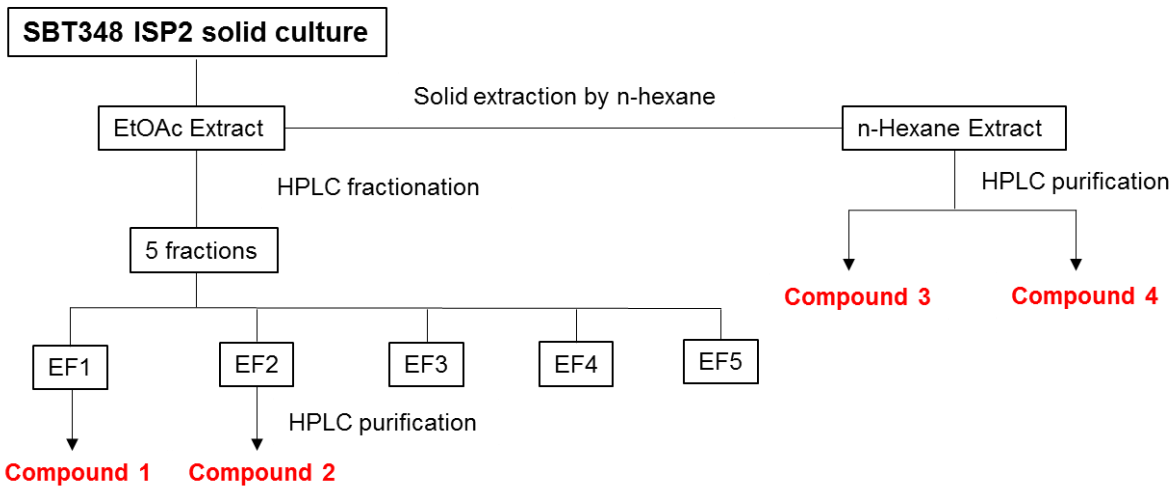

Fig. 4.1 Isolation scheme of compounds from the crude solid extract of *Streptomyces* sp. SBT348

2,3- dihydroxybenzoic acid (**1**) 2.7 mg; white powder (R_t = 12.30 min); UV (EtOH) λ_{max} 220, 247, 310 nm; IR (KBr) v_{max} 3571, 2014, 1868, 1458, 1227 cm^{-1}; ^1H NMR (DMSO-d_6, 600 MHz,): δ = 6.98 (1H, dd, *J* = 7.8, 1.6 Hz, H-4), 6.71 (1H, t, *J* = 7.8, 15.8 Hz, H-5), 7.24 (1H, dd, *J* = 7.8, 1.6 Hz, H-6); ^{13}C NMR (DMSO-d_6, 150 MHz,): δ = 113.5 (C, C-1), 150.5 (C, C-2), 145.9 (C, C-3), 120.5 (CH, C-4), 118.4 (CH, C-5), 120.0 (CH, C-6), 172.5 (C, C-7); EI 154.0 Dalton, $C_7H_6O_4$ (calcd. 154.0266); Anal. Calcd. for $C_7H_6O_4$: C, 54.55; H, 3.92; O, 41.52.

2,3-dihydroxybenzamide (**2**) 2.3 mg; white powder (R_t = 9.94 min); UV (EtOH) λ_{max} 220, 254, 320 nm; IR (KBr) v_{max} 3664, 1980, 1506, 1035 cm^{-1}; ^1H NMR (MeOD-d_4, 600 MHz,): δ = 6.95 (1H, dd, *J* = 7.9, 1.5 Hz, H-4), 6.71 (1H, t, H-5), 7.24 (3H, dd, *J* = 7.9, 1.5 Hz, H-6); ^{13}C NMR (MeOD-*d4*, 150 MHz,): δ = 115.9 (C, C-1), 151.1 (C, C-2), 147.3 (C, C-3), 120.0 (CH, C-4), 119.5 (CH, C-5), 119.4 (CH, C-6), 174.5 (C, C-7); EI 153.0 Dalton, $C_7H_7NO_3$ (calcd. 153.0426); Anal. Calcd. for $C_7H_7NO_3$: C, 54.90; H, 4.61; N, 9.15; O, 34.31.

Maltol (**3**) 1.6 mg; colorless solid (R_t = 11.72 min); UV (EtOH) λ_{max} 220, 260, 284 nm; IR (KBr) v_{max} 3928, 1936, 1313, 293 cm^{-1}; ^1H NMR (MeOD-d_4, 600 MHz,): δ = 6.38 (1H, d, *J* = 5.5 Hz, H-5), 7.94 (1H, d, *J* = 5.5 Hz, H-6), 2.35 (3H, s, H-7); ^{13}C NMR (MeOD-d_4, 150 MHz,): δ = 152.2 (C, C-2), 144.6 (C, C-3), 175.3 (C, C-4), 114.4 (CH, C-5), 156.3 (CH, C-6), 14.2 (CH_3, C-7); EI 126.0 Dalton, $C_6H_6O_3$ (calcd. 126.0317); Anal. Calcd. for $C_6H_6O_3$: C, 57.14; H, 4.80; O, 38.06.

Petrocidin A (**4**) 1.8 mg; colorless solid (R_t = 14.72 min); UV (EtOH) λ_{max} 220, 254, 320 nm; IR (KBr) v_{max} 4376, 4203, 3353, 1859, 1616, 1500, 1204 cm^{-1}; ^1H NMR (MeOD-d_4, 600 MHz,): δ = 6.98 (1H, d, *J* = 7.8 Hz, H-4), 6.71 (1H, t, *J* = 7.8, 15.8 Hz, H-5), 7.23 (1H, d, *J* = 7.8 Hz, H-6), 4.26 (1H, t, Orn α-proton), 2.30 (1H, m, Orn β-proton), 2.01 (1H, m, Orn β-proton), 2.02 (1H, m, Orn γ-proton), 1.94 (1H, m, Orn γ-proton), 3.51 (2H, t, Orn δ-proton), 4.13 (1H, t, Leu α-proton), 1.52 (1H, m, Leu β-proton), 1.91 (1H, m, , Leu β-proton), 1.89 (1H, m, Leu γ-proton), 0.96 (3H, d, *J* = 3.7 Hz, Leu δ-proton), 0.95 (3H, d, *J* = 3.7 Hz, Leu δ-proton) ppm. ^1H NMR (DMSO-d_6, 600 MHz,): 8.02 (1H, s, Leu NH). ^{13}C NMR (MeOD-d_4, 150 MHz,): δ = 114.7 (C, C-1), 151.7 (C, C-2), 147.0 (C, C-3), 121.3 (CH, C-4), 119.6 (CH, C-5), 121.9 (CH, C-6), 174.2 (C, C-7), 172.8 (C, Orn CO), 60.3 (1C, Orn α-carbon), 29.1 (1C, Orn β-carbon), 23.7 (1C, Orn γ-carbon), 46.4 (1C, Orn δ-carbon), 168.9 (1C, Leu CO), 54.6 (1C, Leu α-carbon), 39.4 (1C, β-carbon), 25.8 (1C, γ-carbon), 22.2 (1C, δ-carbon), 23.2 (1C, δ-carbon). ESI-HRMS *m/z* 383.1692 $[M+Na]^+$, $C_{18}H_{25}N_3O_5Na$ (calcd. 383.1691); Anal. Calcd. for $C_{18}H_{25}N_3O_5$: C, 59.49; H, 6.93; N, 11.56; O, 22.01.

4.1.4 Compounds isolation from *Streptomyces* sp. SBT345

Six hundred and thirty mg of the dried crude EtOAc extract obtained from the solid culture of strain *Streptomyces* sp. SBT345 was fractionated on a Sephadex LH20 (GE Healthcare, Germany; 100 x 10 mm) column eluting with H_2O/MeOH (90:10%) to MeOH (100%) with 100 mL for each decimal portion to yield 14 fractions. Fourteen fractions were generated and combined into 3 fractions based on their HPLC chromatogram which showed similar peak pattern. Compounds were purified from combined factions by Monolithic semi-prep RP-C18 column (5 µm, 10×100 mm, Phenomenex). The agar macerations of strain *Streptomyces* sp. SBT345 were also macerated with 500 mL acetone and shaked at 175 rpm for overnight to extract polar compounds. The acetone macerations were filtered using filter paper (A. Hartenstein, Germany), and the filtrates were combined and evaporated by rotavapor (Büchi, Germany). Due to the difficulty of water evaporation which was absorbed by acetone during the extraction procedure, one g of resin (Amberlite® XAD16N, Merck, Germany) was added to the water phase (acetone extracts) followed by the EtOAc and DCM extraction and shaked at 175 rpm overnight to absorb the rest compounds from water phase as much as possible. The resin carrying compounds from acetone extracts were filtered by filter paper and macerated in 250 mL acetone and shaked at 175 rpm for 3 hours. The acetone filtrate was evaporated by rotavapor and subjected to a Sephadex LH20 (GE Healthcare, Germany; 100 x 10 mm) column eluting with 100% MeOH to H_2O/MeOH (60:40%) with 100 mL for each decimal portion to yield 12 fractions. Fractions were combined into 3 fractions based on HPLC chromatogram which showed similar peak pattern. Compounds were purified from combined factions by Monolithic semi-prep RP-C18 column (5 µm, 10×100 mm, Phenomenex).

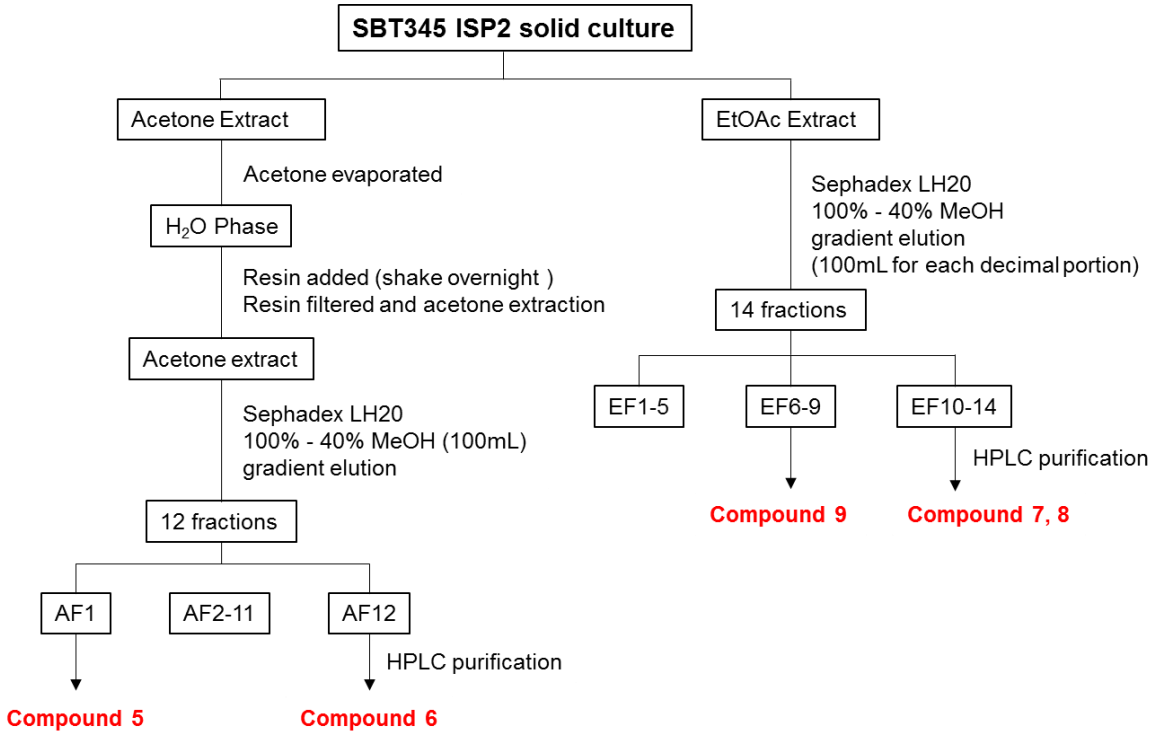

Fig. 4.2 Isolation scheme of compounds from the crude solid extract of *Streptomyces* sp. SBT345

Strepthonium A (**5**) 1.7 mg; white powder (R_t = 16.99 min); UV (EtOH) λ_{max} 280 nm; IR (KBr) ν_{max} 2734，2542 cm^{-1}; ^1H NMR (MeOD-d_4, 600 MHz,): δ = 7.50 (1H, m, H-4), 7.55 (2H, m, H-2 and H-6), 7.53 (2H, m, H-3 and H-5), 4.62 (2H, s, H-7), 3.60 (2H, m, H-8), 4.13 (2H, m, H-9), 3.96 (2H, m, H-10), 4.24 (2H, m, H-11), 7.35 (1H, d, *J* = 2.4 Hz, H-14), 7.27 (1H, dd, *J* = 2.4, 8.7 Hz, H-16), 7.00 (1H, d, *J* = 8.7 Hz, H-17), 1.73 (2H, s, H-19), 0.71 (9H, s, H-21, H-26, and H-27), 3.12 (6H, s, H-22 and H-23), and 1.33 (6H, s, H-24 and H-25); ^{13}C NMR (MeOD-d_4, 150 MHz,): δ = 128.9 (C, C-1), 134.4 (2CH, C-2 and C-6), 131.9 (CH, C-4), 130.3 (2CH, C-3 and C-5), 70.4 (CH_2, C-7), 64.6 (CH_2, C-8), 66.1 (CH_2, C-9), 70.7 (CH_2, C-10), 69.5 (CH_2, C-11), 153.2 (C, C-12), 122.8 (C, C-13), 129.3 (CH, C-14), 145.2 (C, C-15), 126.9 (CH, C-16), 113.9 (CH, C-17), 39.0 (C, C-18), 57.8 (CH_2, C-19), 33.2 (C, C-20), 32.2 ($3CH_3$, C-21, C-26 and C-27), 51.4 ($2CH_3$, C-22 and C-23), and 32.1 ($2CH_3$, C-24 and C-25); ESI-HRMS *m/z* 446.2878 $[M]^+$, $C_{27}H_{41}ClNO_2^+$ (calcd. 446.2826); Anal. Calcd. for $C_{27}H_{41}ClNO_2^+$: C, 72.54; H, 9.24; Cl, 7.93; N, 3.13; O, 7.16.

Ageloline A (**6**) 2.3 mg; yellowish powder (R_t = 17.75 min); UV (EtOH) λ_{max} 220, 258, 340 nm; IR (KBr) ν_{max} 3612, 3319, 2026, 1917, 1788, 1643, 1601, 1435, 1274, 905 cm^{-1}; ^1H NMR (MeOD-d_4, 600 MHz,): δ = 6.93 (1H, s, H-3), 8.19 (1H, d, *J* = 8.7 Hz, H-5), 7.36 (1H, dd, *J* = 8.7, 1.9 Hz, H-6), 7.90 (1H, d, *J* = 1.9 Hz, H-8), ^{13}C NMR (MeOD-d_4, 150 MHz,): δ = 148.4 (C, C-2), 110.0 (CH, C-3), 181.5 (C, C-4), 128.0 (CH, C-5), 125.7 (CH, C-6), 139.7 (C, C-7), 119.6 (CH, C-8), 141.7 (C, C-9), 125.0 (C, C-10), 166.6 (C, C-11); HRESI-MS *m/z* 224.0113 $[M+H]^+$,

$C_{10}H_7ClNO_3$ (calcd. 224.0114); Anal. Calcd. for $C_{10}H_6ClNO_3$: C, 53.71; H, 2.70; Cl, 15.87; N, 6.26; O, 21.46.

Phencomycin (**7**) 2.6 mg; yellowish powder (R_t = 21.14 min); UV (EtOH) λ_{max} 254, 380 nm; IR (KBr) v_{max} 3228, 2957, 1698, 1543, 1432, 1359, 1285, 750 cm^{-1}; ^1H NMR (DMSO-d_6, 400 MHz,): δ = 7.67 (1, d, *J* = 8.7 Hz, H-2), 7.88 (1H, t, *J* = 8.7, 15.4 Hz, H-3), 8.02 (1H, d, *J* = 8.7 Hz, H-4), 8.19 (1H, d, *J* = 8.7 Hz, H-7), 7.97 (1H, t, *J* = 8.7, 15.6 Hz, H-8), 8.38 (1H, d, *J* = 8.7 Hz, H-9), and 4.01 (3H, s, H-13) ppm; ^{13}C NMR (DMSO-d_6,150 MHz,): δ = 125.9 (1C, C-2), 127.3 (1C, C-4), 142.0 (1C, C-4a), 139.1 (1C, C-5a), 132.1 (1C, C-6), 131.1 (1C, C-7), 132.0 (1C, C-9), 142.1 (1C, C-9a), 140.4 (1C, C-10a), 170.5 (1C, C-11), and 167.8 (1C, C-12) ppm; HRESI-MS *m/z* 283.0710 $[M+H]^+$, $C_{15}H_{11}N_2O_4$ (calcd. 283.0719); Anal. Calcd. for $C_{15}H_{10}N_2O_4$: C, 63.83; H, 3.57; N, 9.93; O, 22.67.

Tubermycin B (**8**) 1.2 mg; yellowish powder (R_t = 21.40 min); UV (EtOH) λ_{max} 254, 380 nm; IR (KBr) v_{max} 3529, 1976, 1445, 916, 863, 729 cm^{-1}; ^1H NMR (DMSO-d_6, 400 MHz,): δ = 8.72 (1H, d, *J* = 8.8 H, H-2), 8.12 (1H, m, H-3), 8.53 (1H, d, *J* = 8.8 Hz, H-4), 8.37 (1H, d, *J* = 8.3 Hz, H-6), 8.08 (1H, m, H-7), 8.10 (1H, m, H-8), 8.34 (1H, d, *J* = 8.3 Hz, H-9); ^{13}C NMR (DMSO-d_6, 150 MHz,): δ = 133.3 (1C, C-2), 143.2 (1C, C-5a), 129.7 (1C, C-6), 132.2 (1C, C-7), 131.6 (1C, C-8), 129.7 (1C, C-9), 143.2 (1C, C-9a), and 140.1 (1C, C-10a); HRESI-MS *m/z* 225.0655 $[M+H]^+$, $C_{13}H_9N_2O_2$ (calcd. 225.0664); Anal. Calcd. for $C_{13}H_8N_2O_2$: C, 69.64; H, 3.60; N, 12.49; O,14.27.

Strepoxazine A (**9**) 1.3 mg; yellowish powder (R_t = 17.01 min); UV (EtOH) λ_{max} 220, 258, 290, 350 nm; IR (KBr) v_{max} 3436, 3044, 2816, 2270, 2137, 1877, 1767, 1415, 1114 cm^{-1}; ^1H NMR (MeOD-d_4, 600 MHz,): δ = 7.38 (1H, brs, H-1), 7.01 (1H, t, *J* = 7.9, 15.7 Hz, H-2), 7.93 (1H, d, *J* = 7.9 Hz, H-3), 7.19 (1H, d, *J* = 7.7 Hz, H-6), 7.24 (1H, t, *J* = 7.7, 15.4 Hz, H-7), 7.43 (1H, brs, H-8), 3.88 (3H, s, H-15); ^{13}C NMR (MeOD-d_4, 150 MHz,): δ = 127.8 (CH, C-1), 120.6 (CH, C-2), 131.3 (CH, C-3), 126.1 (C, C-4), 144.2 (C, C-4a), 142.5 (C, C-5a), 119.6 (CH, C-6), 127.9 (CH, C-7), 122.9 (CH, C-8), 129.4 (C, C-9), 125.0 (C, C-9a), 121.5 (C, C-10a), 173.3 (C, C-11), 133.7 (C, C-12), 134.1 (C, C-13), 168.5 (C, C-14), 52.8 (CH3, C-15); HRESI-MS *m/z* 341.0766 $[M-H]^-$, $C_{17}H_{13}N_2O_6$ (calcd. 341.0774); *m/z* 365.0757 $[M+Na]^+$, $C_{17}H_{14}N_2O_6Na$ (cald. 365.0750); Anal. Calcd. for $C_{17}H_{14}N_2O_6$: C, 59.65; H, 4.12; N, 8.18; O, 28.04.

4.1.5 Marfey's derivatization

The absolute configuration of α-H that presented in compound **4** was performed by Marfey's derivatization and compared to the purchased amino acid with D and L configurations (Sigma, Germany) by HPLC. Compound **4** (0.5 mg) was initially hydrolyzed with 6 M HCl (2 ml) in the water bath at 100 °C for 24 h. The hydrolysate was cooled to room temperature, dried using vacuum evaporator and finally dissolved in 100 µL of water. The Marfey's derivatization was carried out by adding 100 µL of 1% Marfey's reagent (1-fluoro-2,4-dinitrophenyl-5-L-alanine amid) dissolved in acetone and 20 µL of 1 M $NaHCO_3$ (H_2O) to 50 µL of the hydrolysate of compound **4,** as well as 50 mM standard amino acid (D-Leu, L-Leu, D-Orn, and L-Orn) respectively , and incubated at 40 °C for 1 h with frequently shaking. The reaction was stopped by adding 10 µL of 2 M HCl after cooling. The Marfey's derivatization products were finally dried and prepared in MeOH for further HPLC analysis. The HPLC chromatography was carried out on Gemini-NX RP-C18 column by eluting with H_2O/CH_3CN (95:5%) for the first 5 min, linearly gradient to 100% CH_3CN within 25 min, and stayed at 100% CH_3CN for a further 5 min with a flow rate at 1 mL/min and UV detection at 340 nm. The configuration was eventually determined with the observation of the same retention times compared to the purchased standard enantiomeric amino acids (Bhushan and Bruckner, 2004; Kochhar and Christen, 1989; Marfey, 1984).

4.1.6 Bioactivity assays

4.1.6.1 Antimicrobial disc diffusion assay

The antimicrobial disc diffusion assay was performed as described in **Chapter 2** where it was used for the screening of crude extracts. The concentration used for each compound in this section was in a series of 4, 6, and 10 µg/Ø 6 mm disc.

4.1.6.2 Anti-Shiga toxin bioassay

Enterohemorrhagic *Escherichia coli* (EHEC) O157:H7 strain EDL933 producing both Stx1 and Stx2 was provided by Ulrich Dobrindt (University of Münster, Germany), and the probiotic control *E. coli* Nissle 1917 (EcN) was obtained from Ardeypharm GmbH (Herdecke, Germany). Both *E. coli* strains were grown in LB medium (10 g/l tryptone, 5 g/l yeast extract, and 5 g/l NaCl) at 37 °C. The Shiga toxin (Stx) production of the EHEC strain EDL933, in the presence and absence of the tested compounds, was assessed using the commercial Ridascreen ® Verotoxin ELISA kit (R-biopharm, Darmstadt, Germany). Briefly, bacterial cultures in LB medium (OD_{600}=0.05) were added to a 24 well plate in quadruplicate (with/without tested compounds). Cultures were statically incubated at 37° C for 24 hours and then, were filtered with a low protein binding sterile-filter (Millex-GV, Millipore, Tullagreen, Ireland) and the ELISA was performed with the filtered supernatant according to the manufacturer's specifications.

The ELISA output ($OD_{450\ nm}$) was compared to evaluate the extent of inhibition of Stx production. Positive control (PC) was included in the kit, whereas LB medium without EDL933, LB medium supplemented with 1.6% DMSO, and the probiotic strain EcN served as negative controls. Co-cultures of EDL933 and the probiotic EcN (EDL933:EcN, 1:1 and 1:10) were used as positive controls for inhibition of Stx production. The growth of EHEC O157:H7 was evaluated by measuring the $OD_{620\,nm}$ of the bacterial cultures after 24 hours of static incubation at 37° C. This step was performed before the samples were filtered for ELISA. Mitomycin C at a concentration of 2 µg/mL was used as a positive control for inhibition of growth in EHEC O157:H7 strain EDL933 and for inducing increased Shiga toxin production. Experiments were repeated at least three times in quadruplicates and the data were expressed as mean±standard error mean. The Student's t-test was used to assess the statistical significance with $p<0.05$ considered as statistically significant. This experiment was performed by Srikkanth Balasubramanian (Würzburg University, Germany).

4.1.6.3 Antioxidant assay

Cell Culture

The human promyelocytic cell line HL-60 was subcultured three times per week at 37 °C and at 5% (v/v) CO_2 in RPMI 1640 medium, supplemented with 10% (v/v) fetal bovine serum (FBS), 1% (w/v) L-glutamine and 0.4% (w/v) antibiotics (50 U/mL penicillin, 50 mg/mL streptomycin). The human human kidney 2 cells HK-2 was cultured in RPMI-1640 (Gibco/Life technologies, Paisley, UK) media supplemented with 10% (v/v) FBS (Biochrom, Berlin, Germany) at 37 °C under 5% CO_2.

Antibodies

The Phalloidin555, an F-actin probe conjugated to red fluorescent dye, was obtained from Life Technologies (Carlsbad, CA, USA) and DAPI (4´,6-diamidino-2-phenylindole) was purchased from Sigma-Aldrich Co. (St. Louis, MO, USA).

Ferric reducing antioxidant power (FRAP) assay

Total antioxidant activity was measured according to Benzie and Strain (Benzie and Strain, 1999). Briefly, different concentrations of compound (1-50 µM) were mixed with 600 µL of freshly prepared FRAP solution (25 mL of 300 mM acetate buffer, pH 3.6, 2.5 mL of 20 mM ferric chloride hexahydrate dissolved in distilled water, and 2.5 mL of 10 mM 2,4,6-tripyridyl-s-triazine (TPTZ) dissolved in 40 mM HCl) and the volume was filled up to 800 µl with water. Absorbance was measured at 595 nm after 10 min of incubation at room temperature by use of a spectrophotometer (Bio-Tek, Model Uvikon XL) against a blank using distilled water. Fifty µM Tempol was used as a positive control. FRAP values were obtained by comparing the

absorbance change at 595 nm in test reaction mixtures with those containing ferrous ions at known concentrations.

Vitality Test

The vitality test (Schmitt et al., 2002) was modified in that ethidium bromide was replaced with Gel Red (Biotrend, Köln, Germany). Vitality staining was applied to the cells in parallel to all experiments. After treatment of the cells for 24 h with the tested compound, cells were collected, and 70 µL of the cell suspension were mixed with 30 µL staining solution (Gel Red and Fluorescein Diacetate (FDA)**.** 20 µl of this mixture was applied to the slide, and the fractions of green and red cells in a total of 200 cells were counted at a 500-fold magnification with a fluorescence microscope.

Flow cytometric analysis of oxidative stress

10^6 HeLa cells were subjected to the test substances in 5 mL culture medium for 16 h and in the last 30 min 5 µg/ml 4-Nitroquinoline 1-oxide (NQO) was added while 20 µM 2,7-dichlorodihydrofluorescein diacetate (H2DCF-DA) was added in the last 10 min. The cells were harvested and washed once with phosphate buffer (PBS)/1% bovine serum albumin (BSA), 3×10^4 cells per sample were analyzed by using a FACS LSR I at λ_{exc} 475 nm and λ_{em} 525 nm (Becton-Dickinson, Mountain View, CA). Medians of the histograms were assessed (Abdelmohsen et al., 2012).

Microscopic analysis of the reactive oxygen species

To evaluate the formation of ROS, the cell-permeable fluorogenic probe dihydroethidium (DHE) was used. Five x 10^5 cells were seeded in 6-well plates in 3 ml medium. The cells were preincubated with ageloline A for 1h, 5 µg/ml NQO and 10 µM DHE, were added to the cells and incubated in dark at 37°C for 30 min. After washing with PBS, the cells were observed under an Eclipse 55i microscope (Nikon GmbH, Düsseldorf, Germany) and a Fluoro Pro MP 5000 camera (Intas Science Imaging Instruments GmbH, Göttingen, Germany) at 200-fold magnification. All images of the DHE staining were taken using the same exposure time. Quantification was done by measuring grey values of 200 cells per treatment with ImageJ 1.40g (http://rsb.info.nih.gov/ij/).

Statistical Analysis

Statistical calculations were performed using Statistica 8 (StatSoft (Europe) GmbH, Hamburg, Germany). Data were shown as averages ± standard deviation of three independent experiments. Individual treatments were tested using the Mann Whitney U-test and results were considered significant if the *p*-value was ≤ 0.05.

The antioxidant assays were performed by Dr. Eman Maher Othman (Würzburg University, Germany).

4.1.6.4 Antichlamydial bioassay

Chlamydia trachomatis C2 (L2/434/BU), a green fluorescent protein-expressing strain, was generated essentially as described in Wang et al. (Wang et al., 2011).The human cervix carcinoma cell line HeLa was cultured in RPMI-1640 (Gibco/Life Technologies, Paisley, UK) media supplemented with 10% (v/v) FBS (Biochrom, Berlin, Germany) at 37 °C under 5% CO2. The assay was carried out in black bottom 96-well plates (Greiner/Sigma-Aldrich Co., St. Louis, MO, USA) which had been seeded with 1.2×10^4 HeLa cells per well. The compounds were solubilized in DMSO and were added to final concentrations ranging from 0.5 µM to 40 µM. The control samples were added with the same amount of DMSO and 11.25 µM tetracycline. After 1 h incubation, cells were infected with *C. trachomatis* at a multiplicity of infection (MOI) for 24 h at 35 °C under 5% CO_2 in media supplemented with 5% h.i. FBS in the presence of the compounds. The cells were then washed with phosphate-buffered saline (PBS) and fixed with 4% PFA. After washing, cell nuclei were stained with DAPI (0.2 ng/ml) and the actin cytoskeleton with Phalloidin555. The analysis was carried out with the Operetta High Content Imaging System (Perkin Elmer, Waltham, MA, USA) at six pictures per well and × 20 magnification. The ratio between the cell surface of HeLa and *C. trachomatis* inclusion area was calculated by the system. A total of 11×10^3 cells were analyzed on average. For the illustration of the bioactivity of the compound, the infection was performed on glass slides. After fixation and staining, the slides were mounted in mowiol and visualized by a Leica TCS SPE confocal microscope with an HCxPL APO 63x oil objective (Leica Microsystems CMS GmbH, Mannheim, Germany). The antichlamydial bioassays were performed by Ms. Anastasija Reimer (Würzburg University, Germany).

4.1.6.5 Cytotoxic bioassays

Cell Line

The human promyelocytic leukemia cells HL-60 were sub-cultured three times per week at 37 °C, 5% (v/v) CO_2 in RPMI 1640 medium, supplemented with 10% (v/v) FBS, 1% (w/v) L-glutamine and 0.4% (w/v) antibiotics (50 U/mL penicillin, and 50 mg/mL streptomycin). The human breast adenocarcinoma cells MCF-7 were sub-cultured twice per week at 37 °C, 5% (v/v) CO_2 in RPMI1640 medium, supplemented with 5% (v/v) FBS, 1% (w/v) L-glutamine, 1% sodium pyruvate and 0.4% (w/v) antibiotics (50 U/ml penicillin, 50 mg/ml streptomycin). HL-60 cells and MCF-7 cells were obtained from the American Type Culture Collection (ATCC, Rockville, MD; HPACC, Salisbury, UK).

Vitality Test
The same as used in the antioxidant assays.

MTT (3-(4,5-Dimethylthiazol-2-yl)-2,5-Diphenyltetrazolium Bromide) assay
Cell proliferation was evaluated in cell lines by the MTT assay. Briefly, cells were plated in a 96-well microtiter plate at a density of 1×10^4 cells per well in a final volume of 100 µl of culture medium. These cells were treated for 24 h with tested compounds at 37 °C with 5% CO_2. After treatment, the cells were immediately incubated with 10 µl MTT (5.0 mg/ml) for 4 h at 37 °C. The medium was then carefully removed, and the cells were lysed in 100 µl of lysis buffer (isopropanol, conc. HCl and Triton X-100) for 10 min at room temperature and 300 rpm shaking. The enzymatic reduction of MTT to formazan crystals that dissolved in DMSO was quantified by photometry at 570 nm.

4.2 Results

4.2.1 Compounds from *Streptomyces* sp. SBT348

4.2.1.1 2,3-dihydroxybenzoic acid

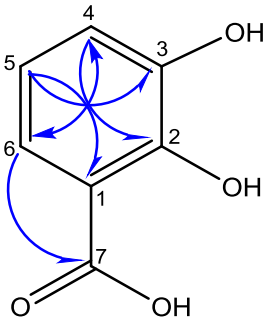

2,3-dihydroxybenzoic acid (**1**)

Fig. 4.3 Structure of 2,3- dihydroxybenzoic acid (**1**) with HMBC key correlations (arrows from H to C)

Structure elucidation
Compound **1** (2.7 mg, yield 0.73%) was purified as a white powder from fraction EF1 of the EtOAc extract. The molecular formula was determined to be $C_7H_7O_4$ by the EI mass spectrum found at 154.0 Da (**Fig. S1**) with 5 degrees of unsaturation. The following NMR spectral data were acquired using a 600 MHz instrument: ^{1}H, ^{13}C, ^{13}C-DEPT135, ^{1}H-^{1}H COSY, ^{1}H-^{1}H NOESY, ^{1}H-^{13}C HSQC, ^{1}H-^{13}C HMBC (optimized to J = 8.3 Hz) in DMSO-d_6 and were tabulated in **Table 4.1**. The ^{1}H NMR spectrum exhibited three aromatic protons at δ_H 6.98 (1H, dd, J = 7.8, 1.6 Hz), 6.70 (1H, t, J = 7.8, 15.8 Hz), and 7.23 (1H, dd, J = 7.8, 1.6 Hz), as well as one active proton at δ_H 9.24 (1H, s) ppm. The ^{13}C NMR spectrum revealed six aromatic carbon resonances at δ_C 113.5, 150.5, 145.9, 120.5, 118.4, and 120.0 ppm, as well as one carboxylic carbon at δ_C 172.5 ppm. The HSQC spectrum assigned three aromatic resonances

at δ_C 120.5, 120.0, and 118.4 ppm to C-4, C-5, and C-6, respectively. Two phenyl carbon resonances at δ_C 150.5 ppm and 145.9 ppm, the other aromatic carbon at δ_C 113.5 ppm, as well as the carboxylic carbon at δ_C 172.5 ppm were assigned C-2, C-3, C-1, and C-7, respectively by the analysis of COSY and HMBC spectra. The NMR spectral data were compared to the literature (Corbin and Bulen, 1969) and AIST: Integrated Spectral Database System of Organic Compounds where the data were obtained from the National Institute of Advanced Industrial Science and Technology (Japan). The structure was determined as a known compound 2,3- dihydroxybenzoic acid based on the NMR elucidation and comparison to the literature. Additionally, the EI spectral data were compared with AIST: Integrated Spectral Database System of Organic Compounds and showed the consistent results as compound 2,3- dihydroxybenzoic acid by displaying the same major fragments at 136.0, 108.0, 80.0, and 52.1 Da (**Fig. S1**).

Table 4.1 NMR-spectroscopic data of 2,3-dihydroxybenzoic acid (**1**) in DMSO-d_6 (^{1}H: 600 MHz; ^{13}C: 150 MHz).

Position C/H No.	**δH, Mult**	**COSY**	**δC, Mult**	**^{13}C-DEPT135**	**HMBC (C-H *J* = 8.3 Hz)**
1			113.5 (1C)		
2			150.5 (1C)		
3	9.24 (1H, brs, -O*H*)		145.9 (1C)		
4	6.98 (1H, dd, *J* = 7.8, 1.6 Hz)	7.23, 6.70	120.5 (1C)	CH	118.4, 145.9, 150.5
5	6.70 (1H, t, *J* = 7.8, 15.8 Hz)	7.23, 6.98	118.4 (1C)	CH	113.5, 120.0, 120.5, 145.9, 150.5, 172.5
6	7.23 (1H, dd, *J* = 7.8, 1.6 Hz)	6.98, 6.70	120.0 (1C)	CH	120.5, 145.9, 150.5, 172.5
7			172.5 (1C)		

Biological activity of 2,3- dihydroxybenzoic acid

The antimicrobial capacity of 2,3- dihydroxybenzoic acid (**1**) was investigated against *Bacillus* sp. and *Aspergillus* sp. by following the positive results found in the crude extract. However, 2,3- dihydroxybenzoic acid (**1**) did not show any inhibition zones in the disc diffusion assay.

4.2.1.2 2,3-dihydroxybenzamide

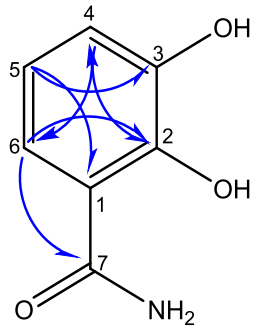

2,3-dihydroxybenzamide (**2**)

Fig. 4.4 Structure of 2,3-dihydroxybenzamide (**2**) with HMBC key correlations (arrows from H to C)

Structure elucidation

Compound **2** (2.3 mg, yield 0.62%) was purified as a white powder from fraction EF2 of the EtOAc extract. The molecular formula was determined to be $C_7H_7NO_3$ from the EI mass spectrum found at 153.0 Da (**Fig. S2**) with 5 degrees of unsaturation. The following NMR spectral data were acquired using a 600 MHz instrument: ^{1}H, ^{13}C, ^{13}C-DEPT135, ^{1}H-^{1}H COSY, ^{1}H-^{1}H NOESY, ^{1}H-^{13}C HSQC, ^{1}H-^{13}C HMBC (optimized to J = 8.3 Hz) in MeOD-d_4, as well as ^{1}H spectrum in DMSO-d_6 (^{1}H: 400 MHz). All the NMR spectral data were tabulated in **Table 4.2**. The ^{1}H NMR spectrum exhibited three aromatic protons at δ_H 6.94 (1H, dd, J = 7.9, 1.5 Hz), 6.71 (1H, t), and 7.23 (1H, dd, J = 7.9, 1.5 Hz) ppm. The ^{13}C NMR spectrum revealed seven signal resonances at δ_C 115.9, 151.0, 147.3, 120.0, 119.5, 119.4, and 174.5 ppm. The HSQC spectrum assigned three aromatic resonances at δ_C 120.0, 119.5, and 119.4 ppm to C-4, C-5, and C-6, respectively. Two phenyl carbon resonances at δ_C 151.0 and 147.3 ppm, aromatic carbon at δ_C 115.9 ppm, as well as the carboxylic carbon at δ_C 174.5 ppm were assigned C-2, C-3, C-1, and C-7, respectively by the analysis of HMBC spectrum. Furthermore, ^{1}H spectrum using DMSO-d_6 (**Table 4.2**) was also performed and exhibited three -O*H*/NH_2 active protons at δ_H 7.87, 8.34, and 9.12 ppm which can be assigned to the two phenolic protons at C-2 and C-4, as well as amide proton at C-7, respectively. The NMR spectral data were compared to the literature (Sugiyama and Hirota, 2009) and the structure was determined as a known compound 2,3-dihydroxybenzamide. Additionally, the EI spectral data was searched in the NIST 14 mass spectral library and showed the consistent result as compound 2,3-dihydroxybenzamide by displaying the same major fragments at 136.0, 108.0, 80.1, 52.1, and 44.0 Da (**Fig. S2**).

Table 4.2 NMR-spectroscopic data of 2,3-dihydroxybenzamide (**2**) in MeOD-d_4 (^{1}H: 600 MHz; ^{13}C: 150 MHz) and DMSO-d_6 (^{1}H: 400 MHz).

Position C/H No.	δH, Mult	COSY	δC, Mult	^{13}C-DEPT135	HMBC (C-H *J* = 8.3 Hz)
1			115.9 (1C)		
2	7.87 (1H, s, -O*H*, DMSO-d_6)		151.0 (1C)		
3	8.34 (1H, s, -O*H*, DMSO-d_6)		147.3 (1C)		
4	6.94 (1H, dd, *J* = 7.9, 1.5 Hz)	7.23, 6.71	120.0 (1C)	CH	119.4, 151.0, 147.3
5	6.71 (2H, t)	7.23, 6.94	119.5 (1C)	CH	115.9, 147.3,151.0, 120.0, 195.4
6	7.23 (1H, dd, *J* = 7.9, 1.5 Hz)	6.94, 6.71	119.4 (1C)	CH	120.0, 151.0, 174.5
7	9.12 (2H, brs, -N*H*$_2$, DMSO-d_6)		174.5 (1C)		

Biological activity of 2,3-dihydroxybenzamide

The anti-microbial capacity of 2,3-dihydroxybenzamide (**2**) was also investigated against *Bacillus* sp. and *Aspergillus* sp. using disc diffusion assy. However, 2,3- dihydroxybenzoic acid (**2**) did not show any inhibitory effects agaisnt these two strains as the crude extract showed.

4.2.1.3 Maltol

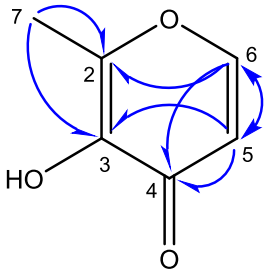

Matol (**3**)

Fig. 4.5 Structure of maltol (**3**) with HMBC key correlations (arrows from H to C)

Structure elucidation

Compound **3** (1.6 mg, yield 0.43%) was purified as a colorless solid from the hexane extract. The molecular formula was determined to be $C_6H_6O_3$ from the EI mass spectrum found at 126.0 Dalton (**Fig. S3**) with 4 degrees of unsaturation. The following NMR spectral data were acquired using a 600 MHz instrument: ^{1}H, ^{13}C, ^{13}C-DEPT135, ^{1}H-^{1}H COSY, ^{1}H-^{1}H NOESY, ^{1}H-^{13}C HSQC, ^{1}H-^{13}C HMBC (optimized to J = 8.3 Hz) in MeOD-d_4 and were tabulated in **Table 4.3**. The ^{1}H NMR spectrum exhibited two olefinic protons at δ_H 7.94 (1H, d, J = 5.5 Hz) and 6.39 (1H, d, J = 5.5 Hz) ppm, as well as three protons at δ_H 2.35 ppm (3H, s) belonging to a methyl group. The ^{13}C NMR spectrum revealed six signal resonances at δ_C 175.3, 156.3, 152.2, 144.6, 114.4, and 14.2 ppm. The HSQC spectrum assigned three resonances at δ_C 156.3, 114.4, and 14.2 ppm to C-6, C-5, and C-7, respectively. C-4, C-3, and C-2 were assigned by the carbon resonances at δ_C 175.3, 144.6, and 152.2 ppm, respectively with the analysis of HSQC and HMBC spectra. The structure was determined as 3-hydroxy-2-methyl-(4H)-4-one, a known compound named maltol. Additionally, the EI spectrum was compared to the reported literature (Samejo et al., 2009) and showed compatible fragments at 55.1, 71.1, 77.1, 97.0 and 126.0 Da (**Fig. S3**).

Table 4.3 NMR-spectroscopic data of maltol (**3**) in MeOD-d_4 (^{1}H: 600 MHz; ^{13}C: 150 MHz).

Position C/H No.	δ_H, Mult	COSY	δ_C, Mult	^{13}C-DEPT135	HMBC (C-H J = 8.3 Hz)
2			152.2 (1C)		
3			144.6 (1C)		
4			175.3 (1C)		
5	6.39 (1H, d, J = 5.5 Hz)	7.94	114.4 (1C)	CH	144.6, 156.3, 175.3
6	7.94 (1H, d, J = 5.5 Hz)	6.38	156.3 (1C)	CH	114.4, 152.2, 175.3
7	2.35		14.2 (1C)	CH_3	144.6, 152.2

Biological activity of maltol

In the anti-*Bacillus* sp. and anti-*Aspergillus* sp. disc diffusion assay, maltol (**3**) did not display any activates against these two pathogen strains.

4.2.1.4 Petrocidin A

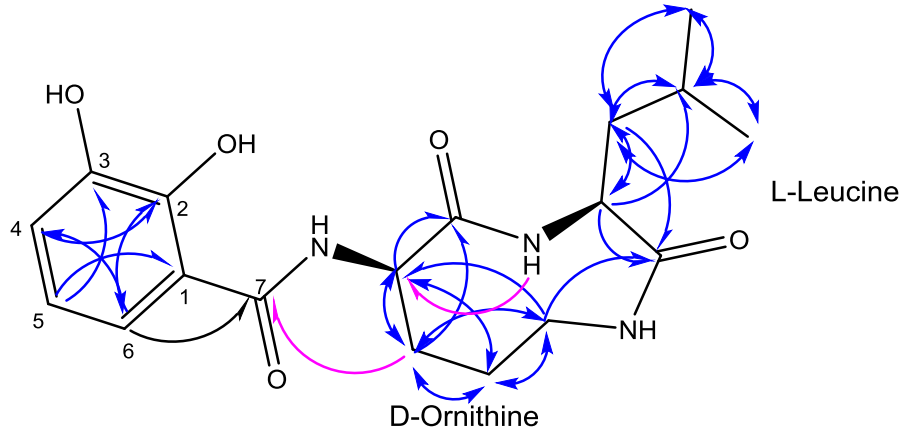

Petrocidin A(**4**)

Fig. 4.6 Structure of petrocidin A (**4**) with HMBC key correlations (blue, arrows from H to C in MeOD-d_4; Purple, key arrows from H to C in DMSO-d_6)

Structure elucidation

Compound **4** (1.8 mg, yield 0.49%) was purified as a colorless solid from the hexane extract. The following NMR spectral data were acquired using a 600 MHz instrument: ^{1}H, ^{13}C, ^{13}C-DEPT135, ^{1}H-^{1}H COSY, ^{1}H-^{1}H NOESY, ^{1}H-^{13}C HSQC, and ^{1}H-^{13}C HMBC (optimized to J = 8.3 Hz) in MeOD-d_4, as well as ^{1}H-^{13}C HMBC (optimized to J = 8.3 Hz) in DMSO-d_6 and tabulated in **Table 4.4**. The molecular formula was determined to be $C_{18}H_{25}N_3O_5$ from its HRESI-MS (*m/z* 386.1692 $[M+Na]^+$ calcd. for $C_{18}H_{25}N_3O_5Na$) (**Fig. S4**) indicating 8 degrees of unsaturation. The ^{1}H spectrum displayed three aromatic protons at δ_H 6.98 (1H, d, J = 7.8 Hz), 6.71 (1H, t, J =7.8, 15.8 Hz), and 7.34 (1H, d, J = 7.8 Hz) ppm, three methine protons at δ_H 1.89 (1H, m), 4.13 (1H, t), and 4.26 (1H, t), eight methylene protons at δ_H 3.51 (2H, t), 2.30 (1H, m), 2.02(1H, m), 2.01 (1H, m), 1.94 (1H, m), 1.91 (1H, m), and 1.52 (1H, m) ppm, and six methyl protons at δ_H 0.96 (3H, d, J = 3.7 Hz) and 0.95 (3H, d, J = 3.7 Hz) ppm. ^{13}C, ^{3}C-DEPT135 and HSQC spectra displayed six aromatic carbons at δ_C 114.7, 119.6, 121.3, 121.9, 147.0, and 151.7ppm, three ester/amide-type carbonyls at δ_C 168.3, 172.8, and 174. 2ppm, three methine carbons at δ_C 60.3, 54.6, and 25.8 ppm, four methylene carbons at δ_C 23.7, 29.1, 39.4, and 46.4 ppm, and two methyl carbons at δ_C 22.2 and 23.2 ppm. The three aromatic protons at δ_H 6.98, 6.71, and 7.34 ppm were assigned to H-4, H-5, and H-6, respectively by COSY spectrum and indicated an adjacent three-substitution aromatic system as part of the structure. The deshielded carbon resonances at δ_C 151.7 and 147.0 ppm suggested two hydroxyl substitutions on the aromatic ring, and were assigned to C-2 and C-3 respectively, with the correlations observed amongst H-4, H-5, and H-6 in the HMBC spectrum. The other aromatic carbon resonances at δ_C 114.7, 121.3, 119.6, 121.9 ppm were attributed to C-1, C-4, C-5, C-6, respectively according to the cross-peaks observed in the HMBC and HSQC

spectra. The strong correlation observed in the HMBC spectrum between H-6 and one of the ester/amide-type carbonyls at δ_C 174.2 ppm has assigned δ_C 174.2 to C-7. The HSQC and HMBC spectra also exhibited standard resonance signals for amino acids by the observation of two α-methines signals at δ_H 4.26 (1H, m), 4.13 (1H, m) with their connected deshielded carbons at δ_C 60.3 and 54.6 ppm, respectively, as well as HMBC cross-peaks between the α-protons and ester/amide-type carbonyls at δ_C 172.8 and 168.3 ppm. Analysis of the COSY, HSQC, and HMBC data, as well as degrees of unsaturation assigned one ornithine and one leucine moiety presented in a cyclic nature. The connection between the aromatic part and the cyclic peptide moiety was confirmed by the correlation displayed in HMBC (using DMSO-d_6 as solvent) between Orn β-H and C-7. The proton and carbon resonances were also compared to the human metabolites database (HMDB) with ornithine and leucine individually, as well as 2,3-dihydroxybenzamide- scaffold with compound **2** and literature (Sugiyama and Hirota, 2009), and showed consistent results. The absolute configuration of leucine and ornithine was determined by acid hydrolysis followed by Marfey's derivatization and comparison to their analogues of the authentic amino acids by HPLC analysis. The Marfey's derivatization revealed the L-leucine and D-ornithine in compound **4** by the observation of the same retention times to the reference analogues at 25.639 min and 14.513 min, respectively. Compound **4** was identified as 2,3-dihydroxy-N-((3S,6R)-3-isobutyl-2,5-dioxo-1,4-diazonan-6-yl)benzamide, a new cyclic dipeptide, and given the name as petrocidin A.

Biological activity of petrocidin A

The antimicrobial disc diffusion assay was performed on petrocidin A (**4**) against *Bacillus* sp. and *Aspergillus* sp. However, petrocidin A (**4**) did not exhibit inhibitory effects against these two strains.

Table 4.4 NMR-spectroscopic data of petrocidin A (**4**) in MeOD-d_4 and DMSO-d_6 (^{1}H: 600 MHz; ^{13}C: 150 MHz).

Position C/H No.	**δ_H, Mult**	**COSY**	**δ_C, Mult**	**^{13}C-DEPT135**	**HMBC (C-H *J* = 8.3 Hz) in MeOD-d_4**	**HMBC (C-H *J* = 8.3 Hz) in** DMSO-d_6
1			114.7 (1C)			
2			151.7 (1C)			
3			147.0 (1C)			
4	6.98 (1H, d, *J* = 7.8 Hz)	6.71, 7.34	121.3 (1C)	CH	151.7, 147.0, 121.9	
5	6.71 (1H, t, *J* = 7.8, 15.8 Hz)	6.98, 7.34	119.6 (1C)	CH	147.0, 114.7, 121.3, 151.7, 174.2	
6	7.34 (1H, d, *J* = 7.8 Hz)	6.98, 6.71	121.9 (1C)	CH	174.2, 151.7, 121.3, 147.0	
7			174.2 (1C)			
Orn						
CO			172.8 (1C)			
α	4.26 (1H, t)	4.13, 2.30, 2.02, 3.51	60.3 (1C)	CH	172.8, 29.1, 23.7	
β	2.30 (1H, m), 2.01 (1H, m)	2.03, 1.94	29.1 (1C)	CH2	46.4, 23.7, 60.3, 172.8	171.9 (C-7)
γ	2.02 (1H, m), 1.94 (1H, m)		23.7 (1C)	CH2	172.8, 29.1, 60.3, 46.4	
δ	3.51 (2H, t)	2.30,2.01,1.94	46.4 (1C)	CH	168.9, 60.3, 29.1, 23.7	
Leu						
NH	8.02 (1H, s, DMSO-d_6)					37.8 (Leu β-C), 52.6 (Leu α-C), 58.5 (Orn α-C), 166.6 (Leu CO)
CO			168.9 (1C)			
α	4.13 (1H, t)	1.91, 1.52, 0.96	54.6 (1C)	CH	168.9, 39.4, 25.8	
β	1.52 (1H, m), 1.91 (1H, m)	0.96, 0.95	39.4 (1C)	CH2	168.9, 54.6, 25.8, 23.2, 22.2	
γ	1.89 (1H, m)	0.96, 0.95	25.8 (1C)	CH	39.4	
δ	0.96 (3H, d), 0.95 (3H, d)	1.53, 1.50	22.2, 23.2 (2C)	CH3	25.8, 39.4	

4.2.2 Compounds from *Streptomyces* sp. SBT345

4.2.2.1 Strepthonium A

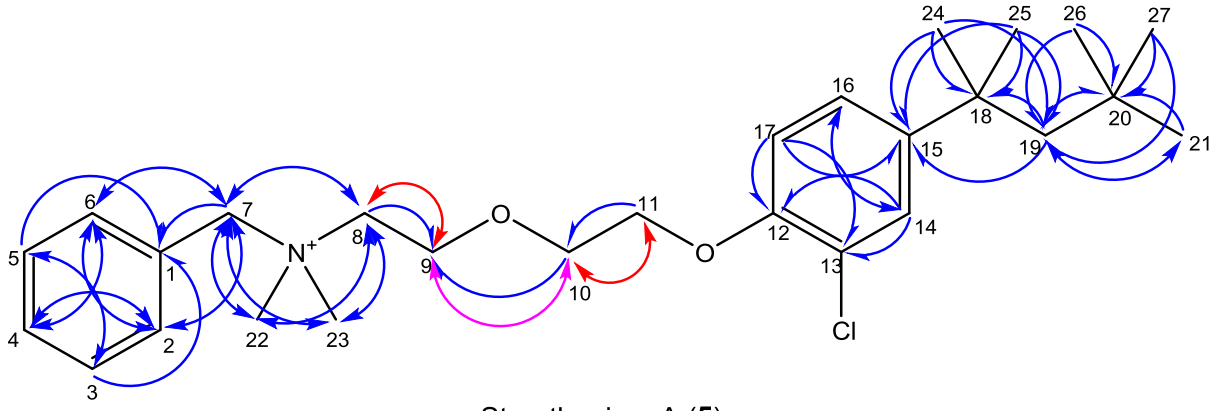

Strepthonium A (**5**)

Fig. 4.7 Structure of strepthonium A (**5**) with Key correlations of HMBC (blue, arrows from H to C), COSY (red arrows), NOESY (purple arrow)

Structure Elucidation

Compound **5** (1.7 mg, yield 0.27%) was obtained as a white powder from fraction AF1 of the acetone extract. The molecular formula was determined to be $C_{27}H_{41}ClNO_2^+$ from the HRESI-MS (*m/z* 446.2878 $[M]^+$ calcd for $C_{27}H_{41}ClNO_2^+$, 446.2826 with chlorine isotopic pattern) which indicated 8 degrees of unsaturation (**Fig. S5a**). The following NMR spectral data were acquired using a 600 MHz instrument: ^{1}H, ^{13}C, ^{13}C-DEPT135, ^{1}H-^{1}H COSY, ^{1}H-^{1}H NOESY, ^{1}H-^{13}C HSQC, ^{1}H-^{13}C HMBC (optimized to J = 8.3 Hz) in MeOD-d_4 and were tabulated in **Table 4.5**. The ^{1}H NMR spectrum exhibited eight aromatic protons δ_H 7.50 (1H, m, H-4), 7.53 (2H, ddd, H-3 and H-5), 7.55 (2H, ddd, H-2 and H-6), and protons δ_H 7.27 (1H, dd, J = 2.4 and 8.7 Hz, H-16), 7.35 (1H, d, J = 2.4 Hz, H-14), 7.00 (1H, d, J = 8.7 Hz, H-17) in two different rings, six methylene multiplets at δ_H 1.73 (2H, s, H-19), 3.60 (2H, m, H-8), 3.96 (2H, m, H-10), 4.13 (2H, m, H-9), 4.24 (2H, m, H-11), and 4.62 (2H, s, H-7). Other signals were attributed to seven methyl groups at δ_H 0.71 (9H, s, H-21, 26, and 27), 1.33 (6H, s, H-24 and H-25), and 3.12 (6H, s, H-22 and H-23), which were further confirmed by the proton integrations and their carbon chemical shifts displayed in the HSQC spectrum. The ^{13}C and ^{13}C-DEPT135 spectra displayed 27 carbon resonances including twelve aromatic carbons at δ_C 128.9, 134.4 (2C), 131.9, 130.3 (2CH), 153.2, 122.8, 129.3, 145.2, 126.9, and 113.9 ppm, seven methyls 32.2 (3C), 51.4 (2C), and 32.1 (2C) ppm, six methylenes at 70.4, 64.6, 66.1, 70.7, 69.5, and 57.8 ppm which might be attached to oxygen or nitrogen, and two quaternary carbons at 39.0 and 33.2 ppm. In HMBC spectrum (**Table 4.2.2.1**), δ_H 3.12 (6H, s, H-22 and H-23) were equivalent, which indicated that both methyl groups were connected to the same heteroatom. In addition, these two methyl groups were also correlated with δ_C 64.6 and 70.4 ppm which unveiled the presence of a quaternary amine in its structure. Analysis of COSY and HMBC data indicated a structure of two different phenyl rings attached by a hetero aliphatic chain which was

interrupted by a dimethylammonium group and two oxo-bridged oxygens. An aliphatic chain was assigned to C-15, in the phenoxy ring based on HMBC correlations from the methyl groups (H-24 and H-25) and the methylene proton (H-19) to C-15. The remaining aromatic carbon at C-13 was substituted by chlorine. To confirm the structure elucidation, fragmentation pattern of compound **5** was determined using product ion scan and a mechanistic pathway for the fragmentations was proposed. Isotope pattern of the fragments at *m/z* of 267.1520 and *m/z* of 354.2220 revealed presence of chlorine with the determined elemental composition of $C_{16}H_{24}ClO$ and $C_{20}H_{33}ClNO_2$ respectively (**Fig. S5b**). The fragment at *m/z* 354.2220 might be formed through rearrangement by substituting one of the aromatic protons via the charged quaternary nitrogen (**Fig. S6**). Other product ions at collision voltage of 25 eV were detected at *m/z* 91.0550 with elemental composition of C_7H_7 which was the phenethyl group cleavaged at C-8, *m/z* 135.1032 with elemental composition of $C_9H_{13}N$ which was cleavaged at C-8, as well as *m/z* 72.0809 with elemental composition of $C_4H_{10}N$ and *m/z* 116.1085 with the elemental composition of $C_6H_{14}NO$ which might be cleaved from fragment ion of *m/z* 354.2220 at C-9 and C-10, respectively (**Fig. S6**). The structure of compound **5** was determined as *N*-benzyl-2-(2-(2-chloro-4-(2,4,4-trimethylpentan-2-yl)phenoxy)ethoxy)-N,N-dimethylethan-1-aminium and proposed its new name as strepthonium A.

Table 4.5 NMR-spectroscopic data of strepthonium A (**5**) in MeOD-d_4 (^{1}H: 600 MHz; ^{13}C: 150 MHz).

Position C/H No.	δ_H, Mult	COSY	NOESY	δ_C, Mult	^{13}C-DEPT135	HMBC (C-H *J* = 8.3 Hz)
1				128.9 (1C)		
2, 6	7.55 (2H, ddd)	7.53, 7.50, 4.62	4.62, 3.12, 3.60	134.4 (2C)	CH	134.4, 131.9, 70.4
3, 5	7.53 (1H, m)	7.50, 7.55		131.9 (1C)	CH	134.4
4	7.50 (2H, m)	7.53, 7.55, 4.62		130.3 (2C)	CH	130.3, 128.9
7	4.62 (2H, s)	7.55, 3.12	7.55, 4.13, 3.60, 3.12	70.4 (1C)	CH_2	134.4, 128.9, 64.6, 51.4
8	3.60 (2H, m)	4.13, 3.12	7.55, 4.62, 4.13, 3.12	64.6 (1C)	CH_2	70.4, 66.1, 51.4
9	4.13 (2H, m)	3.60	4.62, 3.96, 3,60, 3.12	66.1 (1C)	CH_2	
10	3.96 (2H, m)	4.24	4.24, 4.13	70.7 (1C)	CH_2	66.1
11	4.24 (2H, m)	7.00, 3.96	7.00, 3.96	69.5 (1C)	CH_2	70.7
12				153.2 (1C)		
13				122.8 (1C)		
14	7.35 (1H,d, *J* = 2.4 Hz)	7.27	1.73, 1.33, 0.71	129.3 (1C)	CH	153.2, 126.9, 122.8, 39.0
15				145.2 (1C)		
16	7.27 (1H, dd, *J* = 8.7, 2.4 Hz)	7.35, 7.00	7.00, 1.73, 1.32, 0.71	126.9 (1C)	CH	153.2, 129.3, 122.8, 39.0
17	7.00 (1H, d, *J* = 8.7 Hz)	7.27, 4.24	7.27, 4.24	113.9 (1C)	CH	153.2, 145.2, 122.8
18				39.0 (1C)		
19	1.73 (2H, s)	1.33, 0.71	7.35, 7.27, 1.33, 0.71	57.8 (1C)	CH_2	145.2, 39.0, 33.2, 32.2
20				33.2 (1C)		
21, 26, 27	0.71 (9H, s)	1.73	1.73, 1.33	32.2 (3C)	CH_3	57.8, 33.2
22, 23	3.12 (6H, s)	4.62, 3.60	7.55, 4.62, 4.13, 3.60	51.4 (2C)	CH_3	70.4, 64.6, 51.4
24, 25	1.33 (6H, s)	1.73	7.35, 7.27, 1.73, 0.71	32.1 (2C)	CH_3	145.2, 57.8, 39.0, 32.1

Biological activity of strepthonium A

*Influence of strepthonium A (**5**) on Shiga toxin production of EHEC O157:H7 strain EDL933*

The effect of compound **5** on inhibiting the Stx production in EHEC O157:H7 strain EDL933 was tested. In order to assess the effect on the Stx release, EHEC was incubated in the presence of 80 µM compound **5** for 24 hours and Stx levels were determined with the Verotoxin-ELISA assay. Results showed that incubation of EHEC O157:H7 strain EDL933 with strepthonium A reduced the Stx levels by 68%. The positive control using the probiotic strain EcN in co-cultures with EDL933 in two different ratios (EDL933: EcN (1:1 and 1:10)) reduced the Stx levels by 50 and 89%, respectively. The antibiotic mitomycin C was known to trigger an SOS response activating the Stx expression (Pacheco and Sperandio, 2012). The addition of mitomycin C (2 µg/ml) enhanced the Stx production by 138.32% compared to the control (**Fig. 4.8A** and **Table 4.6**).

*Effect of strepthonium A (**5**) on the growth of EHEC O157:H7 strain EDL933*

Antibiotics are preferably not used to treat EHEC infections because of possible antibiotic resistance development and the risk of HUS development resulting from Stx release from dead/dying bacteria. Strepthonium A (**5**) at the tested concentration did not display inhibitory effect on the growth of EHEC O157:H7 strain EDL933, however the antibiotic mitomycin C (used here as the positive control) severely impaired the bacterial growth (**Fig. 4.8B**).

Table 4.6 Effect on Stx production in terms of percentage

Sample name	Stx production
Strepthonium A (80 µM)	62.79%R
EDL933:EcN (1:1)	49.72%R
EDL933:EcN (1:10)	88.67%R
Mitomycin C (2 µg/ml)	138.32%I

EHEC O157:H7 strain EDL933 treated with 1.6% (v/v) DMSO was assigned 100% in terms of Stx production. Since, DMSO at this concentration did not affect the Stx production and bacterial cell viability. R, reduction; I, increase.

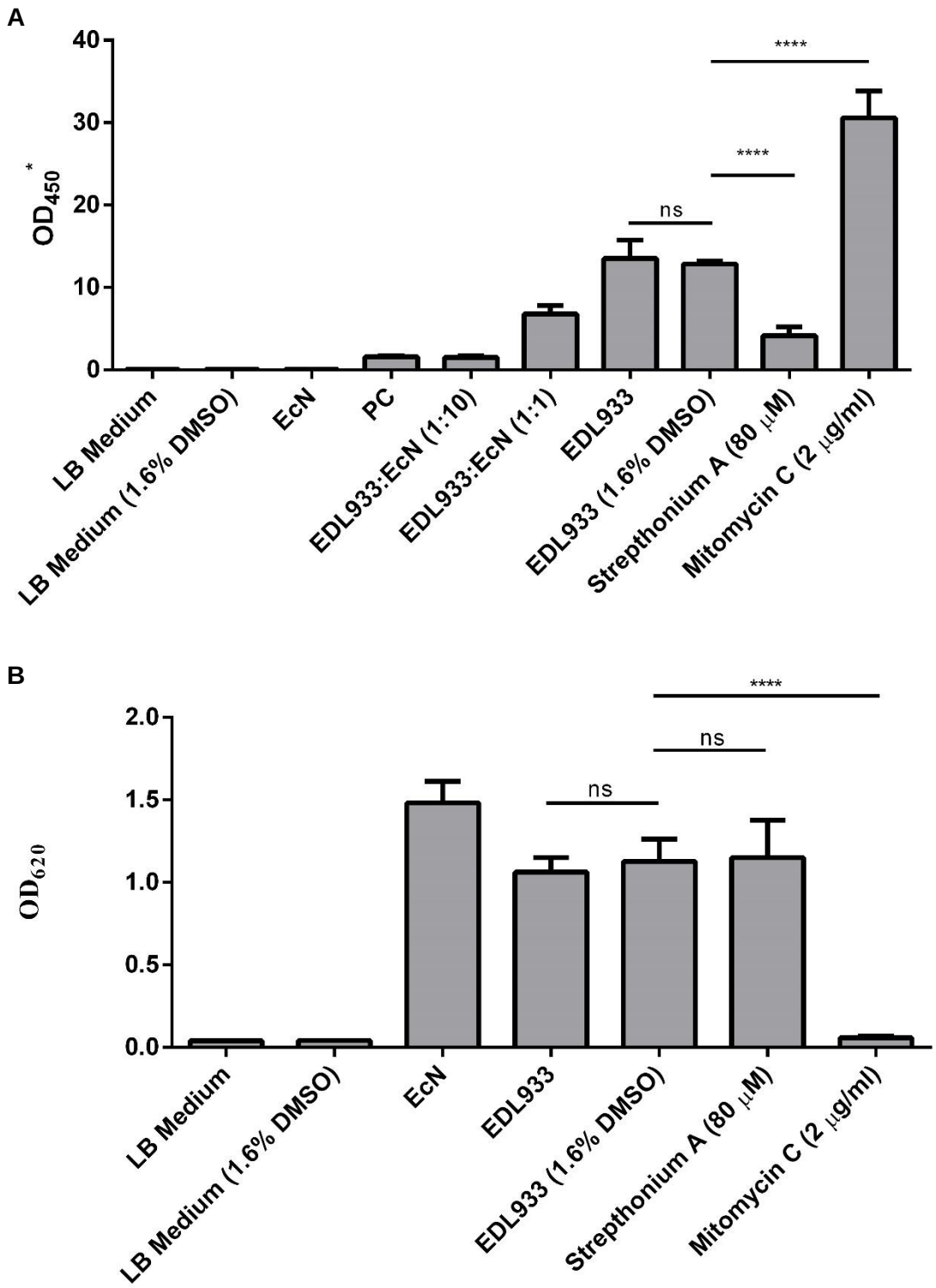

Fig. 4.8 Strepthonium A (**5**) inhibited the Stx production in EHEC O157:H7 without affecting the growth. A) Effect on Stx production, B) Effect on growth. The graphs represent mean values ± SEM from three independent repetitions of the experiment done in quadruplicates. *Samples were diluted 1:10 before the Verotoxin ELISA was performed (ns: not significant, ****p<0.0001)

4.2.2.2 Ageloline A

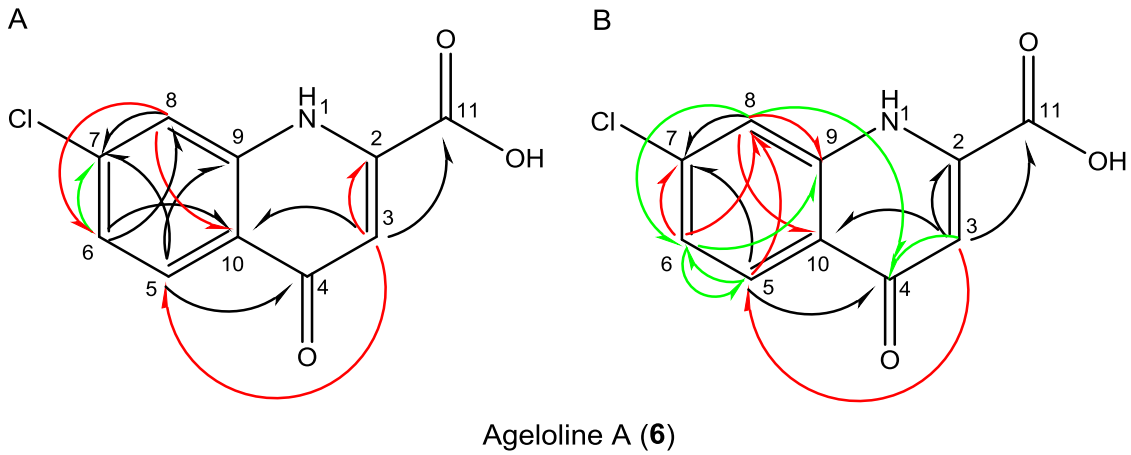

Ageloline A (**6**)

Fig. 4.9 Structure and key HMBC correlations of ageloline A (**6**) measured by 8.3 Hz (A) and 4.0 Hz (B) (arrows from H to C, Black: Strong; Red: Medium; Green: Weak Arrows)

Structure elucidation

Compound **6** (2.3 mg, yield 0.35%) was obtained as a yellowish powder from fraction AF12 of the aceton extract and the molecular formula was established as $C_{10}H_6ClNO_3$ with 8 degrees of unsaturation by ESI-HR-MS determination (**Fig. S7** found at m/z 224.01261 $[M+H]^+$ with chlorine isotopic pattern). The following NMR spectral data were acquired using a 600 MHz instrument: ^1H, ^{13}C, ^{13}C-DEPT135, ^1H-^1H COSY, ^1H-^1H NOESY, ^1H-^{13}C HSQC, ^1H-^{13}C HMBC (optimized to J = 8.3 Hz and 4.0 Hz) in MeOD-d_4 and were tabulated in **Table 4.7**. The NMR data suggested the structure of an olefinic ring adjacent to one aromatic ring. The aromatic part includes three protons at δ_H 7.36 (H-6, dd, J = 8.7, 1.9 Hz), 7.90 ppm (H-8, d, J = 1.9 Hz), and 8.19 ppm (H-5, d, J = 8.7 Hz) ppm. Their adjacent carbons were assigned by the HSQC spectrum to δ_C 125.7 (C-6), 119.6 (C-8), and 128.0 (C-5), respectively. The carbon signals at 141.7 ppm and 139.7 ppm were assigned to C-9 and C-7 by their cross peaks observed with protons H-5, H-6, and H-8 in the HMBC spectra optimized to the coupling constants of 4.0 Hz and 8.3 Hz. C-10 was assigned with δ_C 125.0 ppm by the strong correlations in the HMBC spectrum with protons H-3, H-6, and H-8 at J = 8.3 Hz. The deshielded aromatic carbon at δ_C 141.7 ppm was assigned to C-9 which is next to the nitrogen atom. The last proton at δ_H 6.93 ppm was assigned to H-3 according to the strong correlation with C-10 observed in the HBMC spectrum at J = 8.3 Hz and verified by COSY spectrum in which δ_H 6.93 did not show any correlations with other aromatic protons. The ^{13}C NMR spectrum showed two carbonyl signals at 181.5 ppm and 166.6 ppm which were assigned to C-4 and C-11 according to the correlations observed with H-5 and H-3, respectively, in the HMBC spectra optimized for J = 4.0 Hz and 8.3 Hz. C-2 was assigned with the second olefinic carbon resonance at 148.4 ppm according to the moderate correlation with H-3 for J = 8.3 Hz and the strong correlation for J

= 4.0 Hz shown in the HMBC spectra. The chlorine atom was determined to link to C-7 which is consistent with the deshielded chemical shift at 139.7 ppm.

Table 4.7 NMR-spectroscopic data of ageloline A (**6**) in MeOD-d_4 (^{1}H: 600 MHz; ^{13}C: 150 MHz).

Position C/H No.	δ_H, Mult	COSY	δ_C/ δ_N, Mult	^{13}C-DEPT135	HMBC (δ_H to δ_C *J* = 8.3 Hz)	HMBC (δ_H to δ_C *J* = 4.0 Hz)
2			148.4 (1C)			
3	6.93 (1H, s)		110.0 (1C)	CH	125.0, 128.0, 166.6, 148.4	125.0, 128.0, 166.6, 148.4, 181.5
4			181.5 (1C)			
5	8.19 (1H, d, *J* = 8.7 Hz)	7.36, 7.90	128.0 (1C)	CH	181.5, 139.7, 141.7	181.5, 139.7, 119.6, 125.7
6	7.36 (1H, dd, *J* = 8.7, 1.9 Hz)	8.20, 7.90	125.7 (1C)	CH	125.0, 139.7, 119.6	119.6, 128.0, 139.7, 141.7
7			139.7 (1C)			
8	7.90 (1H, d, *J* = 1.9 Hz)	7.36, 8.19	119.6 (1C)	CH	125.0, 125.7, 139.7	125.0, 139.7, 141.7, 181.5
9			141.7 (1C)			
10			125.0 (1C)			
11			166.6 (1C)			

Biological activity of ageloline A

Antioxidant activity

HK-2 cells were treated with the concentrations from 1-50 µM of ageloline A for 16 h. A small and non-significant ($p > 0.05$) decrease in cell viability of less than 5% was observed, indicating that ageloline A is not toxic towards HK-2 cells. In the ferric reducing antioxidant power (FRAP) assay, ageloline A was tested in the cell free system and the compound displayed antioxidant activity in a dose dependent manner (**Fig. 4.10**).

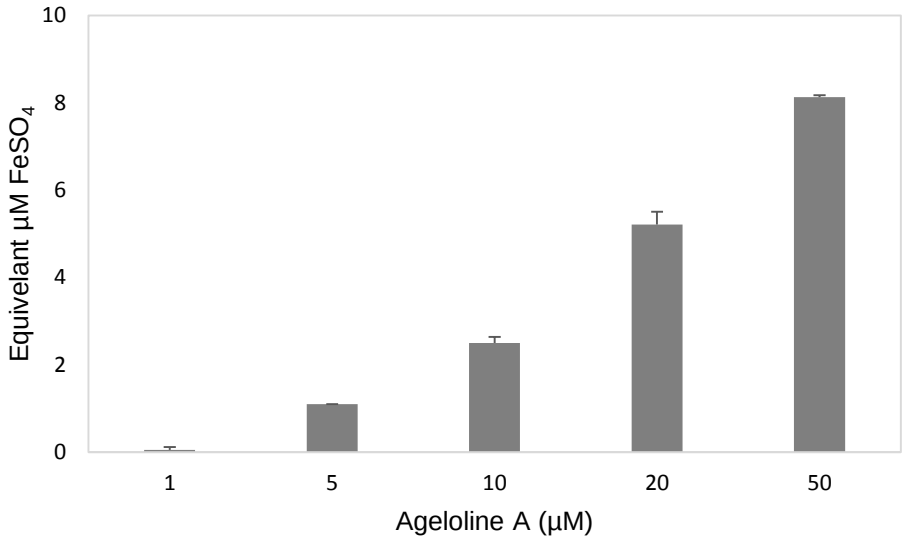

Fig. 4.10 Measurement of the intrinsic antioxidant activity of different concentrations of ageloline A in a cell free system using the FRAP assay.

Induction of oxidative stress in the in vitro experiments was accomplished by adding the known mutagen 4-nitroquinoline-1-oxide (NQO), which has been shown to form 8-hydroxydeoxyguanosine (8-oxodG) by reactive oxygen species (Arima et al., 2006). Short and long preincubation of the cells with ageloline A protected the cells from the oxidative stress mediated by NQO which was detected by two different assays. First, HL-60 cells were preincubated for 1 h with ageloline A then fowllowed by the treatment with NQO and the superoxide sensitive, the cell-permeable fluorogenic probe dihydroethidium (DHE). The cells treated with NQO exhibited a high level of ROS production which was attenuated by the preincubation with ageloline A. Twenty µM of ageloline A alone did not decrease the ROS production in the treated cells (**Fig. 4.11**).

To investigate the antioxidant effect of ageloline A after long incubation time, HL-60 cells were pretreated with ageloline A for 16 h, when the oxidative stress was induced by addition of NQO and detected by using the oxidative stress-sensitive dye H_2DCF-DA (2',7'-dichlorodihydrofluorescein diacetate). The oxidative stress induced by NQO was significantly reduced by ageloline A at 10 µM and 20 µM (**Fig. 4.12**), while ageloline A at 20 µM alone did not alter the background level of oxidative stress in the treated cells.

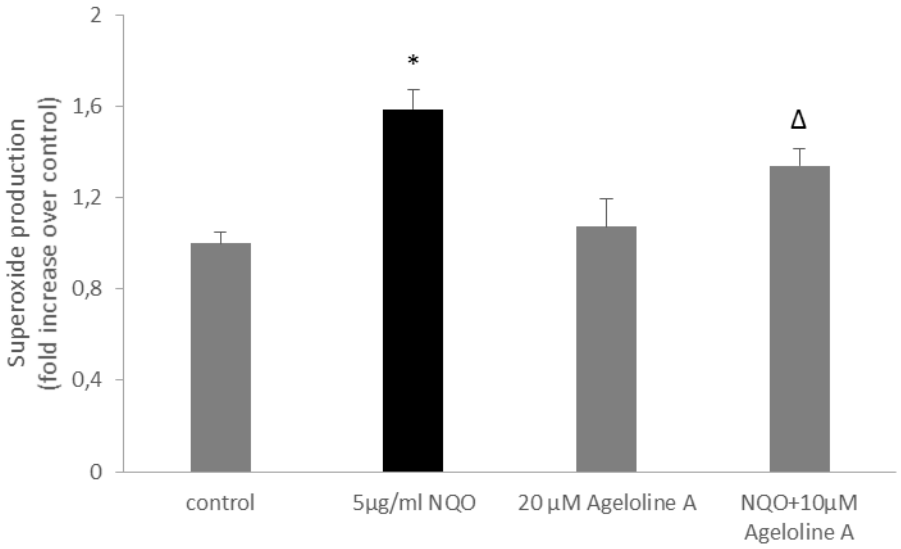

Fig. 4.11 Microscopic detection of superoxide formation using the dye DHE in HL-60 cells treated for 1 h with different concentrations of ageloline A, 5 µg/ml NQO (30 min) and 10 µM DHE (30 min). * significantly different from control; Δ significantly different from NQO.

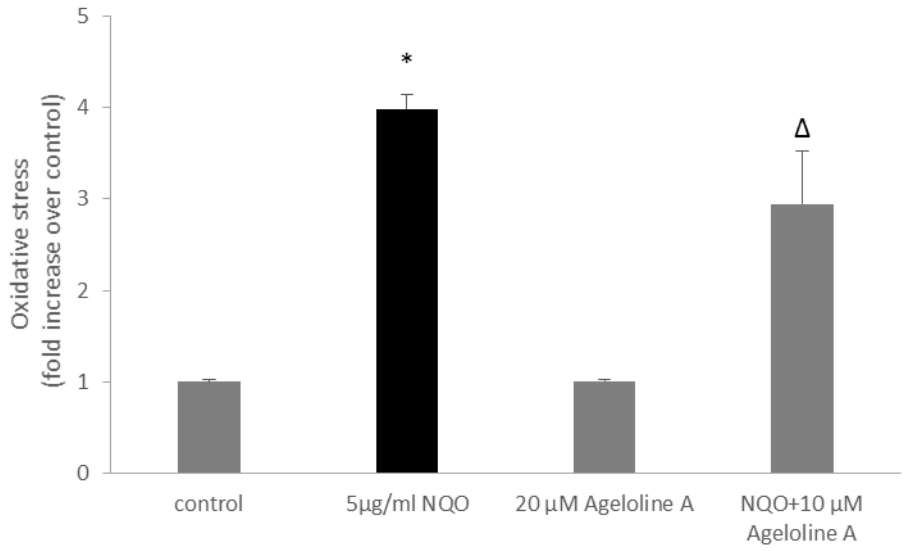

Fig. 4.12 Flow cytometric oxidative stress measurement using the dye H_2DCF-DA in HL-60 cells treated for 16 h with different concentrations of ageloline A, 5 µM NQO and 10 min 20 µM H_2DCF-DA.* significantly different from control; Δ significantly different from NQO.

Anti-Chlamydia trachomatis activity

The production of reactive oxygen species (ROS) in epithelial cells was shown to play an important role during *Chlamydia trachomatis* infection in previous studies (Abdul-Sater et al., 2009). The ROS levels were increased in the first hours of chlamydial infection and were decreased to basal levels 9 h post-infection (Boncompain et al., 2010). The reactive oxygen species were required along with K^+ efflux for activation of NLRP3-dependent pro-inflammatory cysteine protease caspase-1. It could be shown that treatment of infected cells with antioxidants blocks caspase-1 production. Furthermore, inhibition of caspase-1 by inhibitors showed to decrease chlamydial infection by 60% (Abdul-Sater et al., 2009). Therefore ageloline A, which was identified to exhibit antioxidant activity, was analyzed towards anti-infective properties against *Chlamydia trachomatis*.

Ageloline A was applied at a concentration range from 0.5-40 µM on infected epithelial HeLa cells. The size of the chlamydial inclusions was determined by an automated microscopy assay. To confirm the reliability of the assay, tetracycline was used at the concentration of 11.25 µM, at which very few or no chlamydial inclusions should be present. Ageloline A inhibited the formation and growth of the bacterial inclusions in a dose-dependent manner (**Fig. 4.13A**). The inclusion size further decreased in a dose-dependent manner. At the concentration of 20 µM, almost no inclusions could be observed, resembling the tetracycline effect. The determined IC_{50} value, defined as the concentration at which the size of chlamydial inclusion relative to the cell surface was reduced by 50%, was 9.54 ± 0.36 µM (**Fig. 4.13B**).

This data was published in the journal *Tetrahedron Letters* (Cheng et al. 2016)

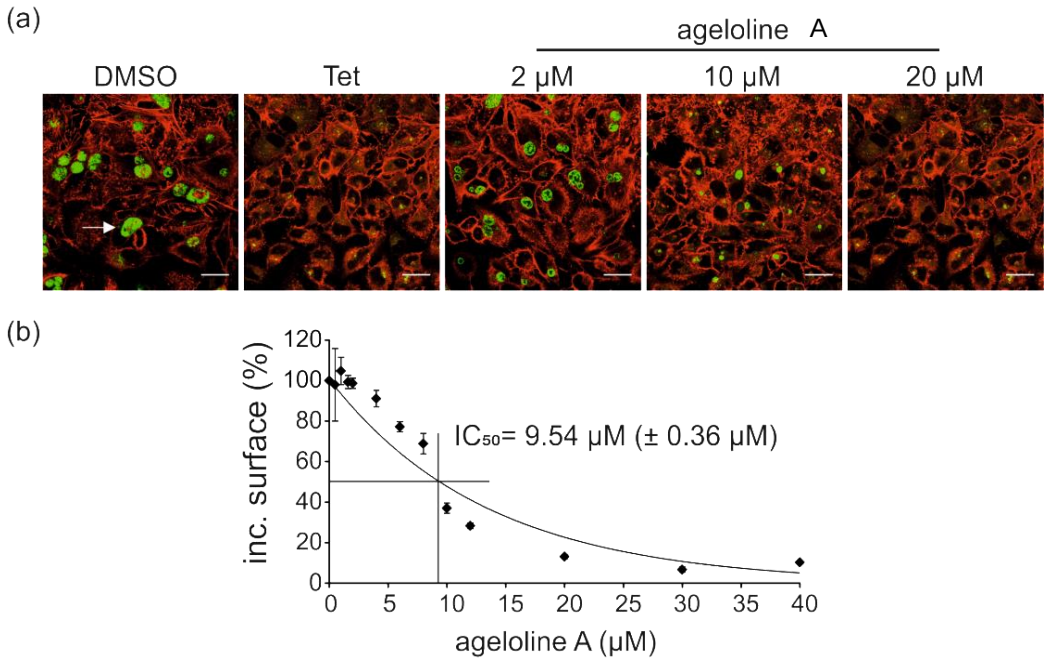

Fig. 4.13 Ageloline A inhibited chlamydial infection in a dose-dependent manner. (A) HeLa cells were infected with *C. trachomatis*, expressing green fluorescent protein (GFP) at an MOI of 1 for 24 h in the presence of 2, 10 and 20 µM ageloline A. DMSO was used as the negative control, and tetracycline (Tet) as the positive control at 11.25 µM. The chlamydial inclusions appear in the green channel (arrow) and the actin cytoskeleton was stained with Phalloidin555 (red channel). Scale bars are 25 µm. (B) HeLa cells were infected with *C. trachomatis* for 24 h in the presence of ageloline A, ranging in concentration between 0.5 µM and 40 µM. The graph represents mean values±SD of the surface of inclusions relative to the cell surface from at least three independent repetitions of the experiment of the bioactivity assay. The values refer to the DMSO control which was set to 100%. A logarithmic trend line was used to calculate the agent concentration at 50% inclusion surface (IC_{50}).

4.2.2.3 Phencomycin

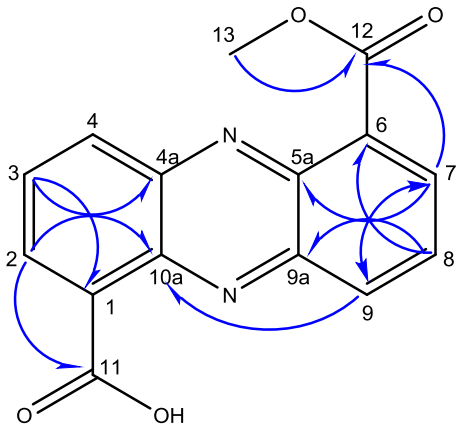

phencomycin (**7**)

Fig. 4.14 Structure of phencomycin with key HMBC correlations (arrows from H to C)

Structure elucidation

Compound **7** (2.6 mg, yield 0.41%) was isolated as a yellow oil from fraction EF10-14 of the EtOAc extract of *Streptomyces* sp. SBT345. The molecular formula was established as $C_{15}H_{10}N_2O_4$ with 11 degrees of unsaturation by HRESI-MS determination (**Fig. S8**, found at *m/z* 283.0710 $[M+H]^+$). The following NMR spectra data were acquired using a 400 MHz instrument (DMSO-d_6): ^{1}H, ^{1}H-^{1}H COSY, ^{1}H-^{13}C HMBC (optimized to *J* = 8.3 Hz) and were tabulated in **Table 4.8**. The ^{1}H NMR revealed the presence of 6 aromatic protons at δ_H 7.67 (1, d, *J* = 6.6, 1.4 Hz, H-2), 7.88 (1H, t, *J* = 8.7, 15.4 Hz, H-3), 8.02 (1H, dd, *J* = 8.7, 1.4 Hz, H-4), 8.19 (1H, dd, *J* = 6.9, 1.4 Hz, H-7), 7.96 (1H, t, *J* = 8.7, 15.6 Hz, H-8), 8.38 (1H, dd, *J* = 8.7, 1.4 Hz, H-9) in two different aromatic rings and three methoxy protons at δ_H 4.01 (3H, s, H-13). The ^{1}H-^{13}C HMBC spectrum assigned the aromatic carbons C-1 (δ_C 146.4), C-2 (δ_C 125.9), C-4 (δ_C 127.3), C-4a (δ_C 142.0), C-5a (δ_C 139.1), C-6 (δ_C 132.1), C-7 (δ_C 131.1), C-9 (δ_C 132.0), C-9a (δ_C142.1), and C-10a (δ_C 140.4). The chemical shifts of carbons C-4a, C-5a, C-9a, and C-10a indicated a phenazine based structure. Two carbonyl carbons at δ_C 170.48 and 167.47 were assigned to C-11 and C-12 which adjacent to oxygen. A search in Database of Natural Products based on the exact mass resulted in a phenazine compound phencomycin as the hit. The spectral data were compared to the literature (Chatterjee et al., 1995; Pusecker et al., 1997) and compound (**7**) was identified as phencomycin.

Table 4.8 NMR-spectroscopic data of phencomycin (**7**) in DMSO-d_6 (^{1}H: 600 MHz; ^{13}C: 150 MHz).

Position C/H No.	δ_H, Mult	COSY	δ_C, Mult	HMBC (δ_H to δ_C)
1			146.4 (1C)	
2	7.67 (1H, dd, *J* = 6.6, 1.4 Hz)	7.88	125.9 (1C)	127.3, 140.4, 170.5
3	7.88 (1H, t, *J* = 8.7, 15.4 Hz)	7.67, 8.02		142.0, 146.4
4	8.02 (1H, dd, *J* = 8.7, 1.4 Hz)	7.88	127.3 (1C)	125.9
4a			142.0 (1C)	
5a			139.1 (1C)	
6			132.1 (1C)	
7	8.19 (1H, dd, *J* = 6.9, 1.4 Hz)	7.96	131.1 (1C)	132.0, 139.1, 167.8
8	7.96 (1H, t, *J* = 8.7, 15.4 Hz)	8.19, 8.38		132.1, 142.1
9	8.38 (1H, dd, *J* = 8.7, 1.4 Hz)	7.96	132.0 (1C)	131.1, 140.4
9a			142.1 (1C)	
10a			140.4 (1C)	
11			170.5 (1C)	
12			167.5 (1C)	
13	4.01 (1H, s)			167.4

Biological activity of phencomycin

The apoptotic effects of phencomycin (**7**) were investigated towards the HL-60 and MCF-7 cell lines but did not display any antiproliferative effects.

4.2.2.4 Tubermycin B

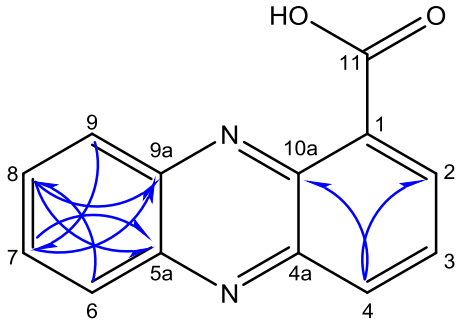

Tubermycin B (**8**)

Fig. 4.15 Structure of tubermycin B (**8**) with key HMBC correlations (arrows from H to C)

Structure elucidation

Compound **8** (1.2 mg, yield 0.19%) was isolated as a yellow oil from fraction EF10-14 of the EtOAc extract of *Streptomyces* sp. SBT345. The molecular formula was established as $C_{13}H_9N_2O_2$ with 10 degrees of unsaturation by ESI-HRMS determination (**Fig. S9**, found at *m/z* 225.0655 $[M+H]^+$. The following NMR spectral data were acquired using a 400 MHz instrument (DMSO-d_6): ^{1}H, ^{1}H-^{1}H COSY, ^{1}H-^{13}C HMBC (optimized to *J* = 8.3 Hz) and were tabulated in **Table 4.9**. The ^{1}H NMR and COSY spectrum revealed the presence of 7 aromatic

protons at δ_H 8.72 (1H, d, *J* = 8.8 Hz, H-2), 8.12 (1H, m, H-3), 8.53 (1H, d, *J* = 8.8 Hz, H-4), 8.37 (1H, d, *J* = 8.3 Hz, H-6), 8.08 (1H, m, H-7), 8.10 (1H, m, H-8), 8.34 (1H, d, *J* = 8.3 Hz, H-9) ppm in two different aromatic rings. The ^{1}H-^{13}C HMBC spectrum assigned the aromatic carbons δ_C 133.3 (1C, C-2), 147.5 (1C, C-5a), 132.2 (1C, C-7), 131.6 (1C, C-8), 143.2 (1C, C-9a), and 140.1 (1C, C-10a). A search in Database of Natural Products based on the exact mass resulted in a phenazine compound tubermycin B. The spectral data were compared to literature (Gebhardt et al., 2002; Geiger et al., 1988) and compound **9** was identified as tubermycin B.

Table 4.9 NMR-spectroscopic data of tubermycin B (**8**) in DMSO-d_6 (^{1}H: 600 MHz; ^{13}C: 150 MHz).

Position C/H No.	δ_H, Mult	δ_C, Mult	HMBC (δ_H to δ_C)
2	8.72 (1H, d, *J* = 8.8 Hz)	133.3 (1C)	
3	8.12 (1H, m)		
4	8.53 (1H, d, *J* = 8.8 Hz)		133.3, 140.1
4a			
5a		147.5 (1C)	
6	8.37 (1H, d, *J* = 8.3 Hz)		131.6
7	8.08 (1H, m)	132.2 (1C)	129.7, 143.2
8	8.10 (1H, m)	131.6 (1C)	129.7, 143.2
9	8.34 (1H, d, *J* = 8.3 Hz)		132.2
9a		143.2 (1C)	
10a		140.1 (1C)	

Biological activity of tubermycin B

Tubermycin B (**8**) was tested in the antiproliferative bioassay against HL-60 and MCF-7 cell lines but did not show any antiproliferative effects against these two tumor cell lines.

4.2.2.5 Strepoxazine A

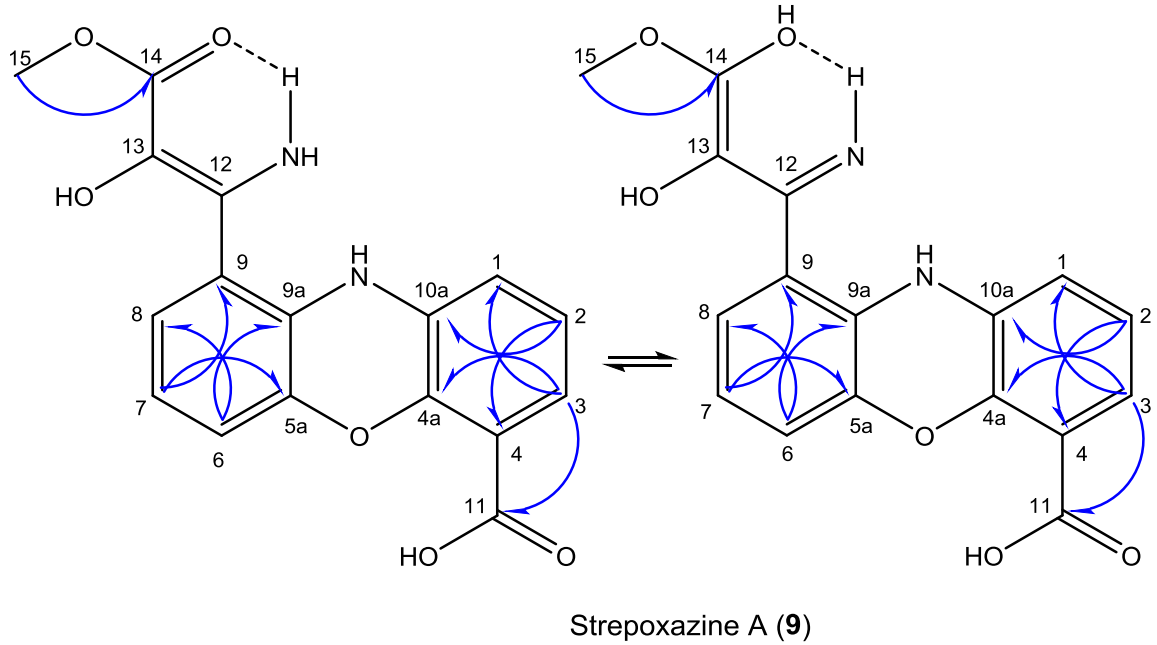

Strepoxazine A (**9**)

Fig. 4.16 Structure of strepoxazine A (**9**) with key HMBC correlation (arrows from H to C)

Structure elucidation

Compound **9** (1.3 mg, yield 0.21%) was obtained as a yellowish powder from fraction EF6-9 of the EtOAc extract and the molecular formula was established as $C_{17}H_{14}N_2O_6$ by ESI-HR-MS (**Fig. S10,** molecular ion mass found at *m/z* 341.0766 $[M-H]^-$, cald. 341.0774; and *m/z* 365.0757 $[M + Na]^+$, cald. 365.0750) requiring 11 degrees of unsaturation. The following NMR spectral data were acquired using a 600 MHz instrument: ^1H, ^{13}C, ^{13}C-DEPT135, ^1H-^1H COSY, ^1H-^1H NOESY, ^1H-^{13}C HSQC, ^1H-^{13}C HMBC (optimized to J = 8.3 Hz and 4.0 Hz) in MeOD-d_4 and were tabulated in **Table 4.10**. The ^1H NMR spectrum exhibited the resonances for six sp^2 aromatic proton signals at δ_H 7.38 (1H, brs, H-1), 7.01 (1H, t, *J* = 7.9, 15.7 Hz, H-2), 7.93 (1H, d, *J* = 7.9 Hz, H-3), 7.19 (1H, d, *J* = 7.7 Hz, H-6), 7.24 (1H, t, *J* = 7.7, 15.4 Hz, H-7), 7.43 (1H, brs, H-8) ppm, of which two independent aromatic systems were observed based on the analysis of COSY spectrum. The HMBC cross-peaks from the aromatic protons of H-2 to δ_C 121.5 (1C, C-10a) ppm, H-3 to δ_C 144.2 (1C, C-4a) ppm, H-7 to δ_C 142.5 (1C, C-5a) ppm, and H-6 to δ_C 125.0 (1C, C-9a) ppm led to the assignment of a phenoxazin nucleus in which the carbon resonance of C-4a, C-5a, C-9a and C-10a were consistent with the other analogues in the literature exemplified by venezueline C and venezueline D (Ren et al., 2013). Additional NMR data conducted to assign one carboxylic acid group to C-4 by correlation observed between H-3 and a carboxylic carbon at δ_C 173.3 (1C, C-11) ppm, and one methoxyl ester by correlation observed between the methoxyl protons at δ_H 3.88 (3H, H-15) ppm to the other carbonyl at δ_C 168.5 (1C, C-14) ppm in the HMBC spectrum. The presence of the carboxylic acid group was further verified in ESI-HRMS/MS spectra (collision voltage of 20 eV) by the

loss mass of 43.9898 Da (cald. for COO) from the molecular ion mass *m/z* 341.0766 (cald. for $C_{17}H_{13}N_2O_6^-$) to fragment ion mass *m/z* 297.0867 (cald. for $C_{16}H_{13}N_2O_4^-$) (**Fig. S11**). The presence of the methoxyl ester was also verified by the loss mass of 59. 0234 Da (cald. for $C_2H_3O_2$) in both negative and positive ionization modes from the molecular ion mass *m/z* 341.0766 (cald. for $C_{17}H_{13}N_2O_6^-$) to fragment ion mass *m/z* 282.0639 (cald. for $C_{15}H_{10}N_2O_4^-$) (**Fig. S11**), as well as the molecular ion mass *m/z* 365.0757 (cald. for $C_{17}H_{14}N_2O_6Na^+$) to fragment ion mass *m/z* 306.0619 (cald. for $C_{15}H_{11}N_2O_4Na^+$) (**Fig. S12**) respectively. The fragment ion mass *m/z* 265.0611 (cald. for $C_{15}H_9N_2O_3^-$) in negative ionization mode (**Fig. S11**), and *m/z* 288.0515 (cald. for $C_{15}H_9N_2O_3Na^+$) in the positive ionization mode (**Fig. S12**) were deduced by losing the carboxylic acid and methoxyl groups from the parent molecule. Furthermore, *m/z* 237.0662 (cald. for $C_{14}H_9N_2O_2^-$) and *m/z* 260.0564 (cald. for $C_{14}H_9N_2O_2Na^+$) were the products of losing both carboxylic acid group and methoxyl ester side chain (**Fig. S11** and **S12**). The high-resolution fragment ion masses and the NMR data assigned the phenoxazine based structure, one carboxylic acid, and one methoxyl ester side chain which established a partial elementary composition as $C_{15}H_{11}NO_5$. The remaining elements C_2H_3NO were deduced as an olefinic structure that substituted by a hydroxyl and an amine group, and connects between the methoxyl ester and the aromatic carbon C-9. The enamino proton was speculated to form the the intramolecular hydrogen bond with the ketone oxygen at C-14 to form a keto-enamine structure, which makes the whole structure more stable than the presence of single enol or enamino group (hKikta and Bieron, 1976; Isaac et al., 2008). Additionally, the fragment ion mass *m/z* 209.0710 (cald. for $C_{13}H_9N_2O^-$) presented in the negative mass spectrum was interpreted as the structure shown in **Fig. S11** by the web server named as CFM-ID designed for annotation, spectrum prediction and metabolite identification from tandem mass spectra using the data from HMDB, MassBank, and Metlin databases (Allen et al., 2014). The deprotonated imine at C-12 (**Fig. S11**) further demonstrated the elucidation of enamino part.

Table 4.10 NMR-spectroscopic data of strepoxazine A (**9**) in MeOD-d_4 (^{1}H: 600 MHz; ^{13}C: 150 MHz).

Position C/H No.	δ_H, Mult	COSY	NOESY	δ_C, Mult	HMBC
1	7.38 (1H, s, br)	7.01		127.8 (1C)	
2	7.01 (1H, t)	7.93, 7.38		120.6 (1C)	121.5, 126.1, 127.8, 131.3, 144.3
3	7.93 (1H, d)	7.38, 7.01		131.3 (1C)	127.8, 144.2, 173.3
4				126.1 (1C)	
4a				144.2 (1C)	
5a				142.5 (1C)	
6	7.18 (1H, d)	7.24		119.6 (1C)	125.0, 122.9
7	7.24 (1H, t)	7.18		127.9 (1C)	129.4, 142.5
8	7.43 (1H, s, br)	7.24		122.9 (1C)	
9				129.4 (1C)	
9a				125.0 (1C)	
10a				121.5 (1C)	
11				173.3 (1C)	
12				133.7 (1C)	
13				134.1 (1C)	
14				168.5 (1C)	
15	3.88 (3H, s)			52.8 (1C)	168.5

Biological activity of phencomycin

The apoptotic effects of phenoxazine A (**9**) were also tested towards HL-60 and MCF-7 cell lines. Strepoxazine A (**9**) displayed antiproliferative effects against HL-60 cell line with the IC_{50} value of 16 µg/ml, and MCF-7 cell line with the IC_{50} value of 48 µg/ml.

4.3 References

Abdelmohsen, U.R., Szesny, M., Othman, E.M., Schirmeister, T., Grond, S., Stopper, H., Hentschel, U., 2012. Antioxidant and anti-protease activities of diazepinomicin from the sponge-associated *Micromonospora* Strain RV115. Marine drugs 10, 2208-2221.

Abdul-Sater, A.A., Koo, E., Hacker, G., Ojcius, D.M., 2009. Inflammasome-dependent caspase-1 activation in cervical epithelial cells stimulates growth of the intracellular pathogen *Chlamydia trachomatis*. Journal of biological chemistry 284, 26789-26796.

Allen, F., Pon, A., Wilson, M., Greiner, R., Wishart, D., 2014. CFM-ID: a web server for annotation, spectrum prediction and metabolite identification from tandem mass spectra. Nucleic acids research 42, 94-99.

Arima, Y., Nishigori, C., Takeuchi, T., Oka, S., Morimoto, K., Utani, A., Miyachi, Y., 2006. 4-Nitroquinoline 1-oxide forms 8-hydroxydeoxyguanosine in human fibroblasts through reactive oxygen species. Toxicological sciences: an official journal of the Society of Toxicology 91, 382-392.

Benzie, I.F., Strain, J.J., 1999. Ferric reducing/antioxidant power assay: direct measure of total antioxidant activity of biological fluids and modified version for simultaneous measurement of total antioxidant power and ascorbic acid concentration. Methods enzymology 299, 15-27.

Bhushan, R., Bruckner, H., 2004. Marfey's reagent for chiral amino acid analysis: a review. Amino acids 27, 231-247.

Boncompain, G., Schneider, B., Delevoye, C., Kellermann, O., Dautry-Varsat, A., Subtil, A., 2010. Production of reactive oxygen species is turned on and rapidly shut down in epithelial cells infected with *Chlamydia trachomatis*. Infection and immunity 78, 80-87.

Chatterjee, S., Vijayakumar, E.K., Franco, C.M., Maurya, R., Blumbach, J., Ganguli, B.N., 1995. Phencomycin, a new antibiotic from a *Streptomyces* species HIL Y-9031725. Journal of antibiotics 48, 1353-1354.

Cheng, C., Othman, E.M., Reimer, A., Grüne, M., Kozjak-Pavlovic, V., Stopper, H., Hentschel, U., Abdelmohsen, U.R., 2016. Ageloline A, new antioxidant and antichlamydial quinolone from the marine sponge-derived bacterium *Streptomyces* sp. SBT345. Tetrahedron letters 57, 2786–2789.

Corbin, J.L., Bulen, W.A., 1969. The isolation and identification of 2,3-dihydroxybenzoic acid and 2-N,6-N-di-92,3-dihydroxybenzoyl)-L-lysine formed by iron-deficient *Azotobacter vinelandii*. Biochemistry 8, 757-762.

Gebhardt, K., Schimana, J., Krastel, P., Dettner, K., Rheinheimer, J., Zeeck, A., Fiedler, H.P., 2002. Endophenazines A-D, new phenazine antibiotics from the arthropod associated endosymbiont *Streptomyces anulatus*. I. Taxonomy, fermentation, isolation and biological activities. Journal of antibiotics 55, 794-800.

Geiger, A., Keller-Schierlein, W., Brandl, M., Zahner, H., 1988. Metabolites of microorganisms. 247. Phenazines from *Streptomyces antibioticus*, strain Tu 2706. Journal of antibiotics 41, 1542-1551.

hKikta, E.J., Bieron, J.F., 1976. The enol-imine to keto-enamine tautomerization involved in the formation of 3-benzylamino-5,5-dimethylcyclohex-2-enone. Organic magnetic resonance 8, 192-197.

Isaac, J.F., Jalbout, A.F., Effat, M., Heidar, R., 2008. β-Aminoacrolein: An ab initio, AIM and NBO study. International journal of quantum chemistry 108, 383-390.

Kochhar, S., Christen, P., 1989. Amino acid analysis by high-performance liquid chromatography after derivatization with 1-fluoro-2,4-dinitrophenyl-5-L-alanine amide. Analytical biochemistry 178, 17-21.

Marfey, P., 1984. Determination ofD-amino acids. II. Use of a bifunctional reagent, 1,5-difluoro-2,4-dinitrobenzene. Carlsberg research communications 49, 591-596.

Pacheco, A.R., Sperandio, V., 2012. Shiga toxin in enterohemorrhagic *E.coli*: regulation and novel anti-virulence strategies. Frontiers in cellular and infection microbiology 2, 81.

Pusecker, K., Laatsch, H., Helmke, E., Weyland, H., 1997. Dihydrophencomycin methyl ester, a new phenazine derivative from a marine Streptomycete. Journal of antibiotics 50, 479-483.

Ren, J., Liu, D., Tian, L., Wei, Y., Proksch, P., Zeng, J., Lin, W., 2013. Venezuelines A-G, new phenoxazine-based alkaloids and aminophenols from *Streptomyces venezuelae* and the regulation of gene target Nur77. Bioorganic & medicinal chemistry letters 23, 301-304.

Samejo, M.Q., Ndukwe, G.I., Burdi, D.K., Bhanger, M.I., Khan, K.M., 2009. Isolation and crystal structure of maltol from Abies pindrow. Journal of medicinal plants research 3, 55-60.

Schmitt, E., Lehmann, L., Metzler, M., Stopper, H., 2002. Hormonal and genotoxic activity of resveratrol. Toxicology letters 136, 133-142.

Sugiyama, Y., Hirota, A., 2009. New potent DPPH radical scavengers from a marine-derived actinomycete strain USF-TC31. Bioscience, biotechnology, and biochemistry 73, 2731-2734.

Wang, Y., Kahane, S., Cutcliffe, L.T., Skilton, R.J., Lambden, P.R., Clarke, I.N., 2011. Development of a transformation system for *Chlamydia trachomatis*: restoration of glycogen biosynthesis by acquisition of a plasmid shuttle vector. PLoS pathogens 7, e1002258.

Chapter 5
General discussion

5.1 Actinomycete diversity and bioactivities

5.1.1 Different sponges

Marine sponges are abundant in dense and diverse microorganism communities (Hentschel et al., 2003; Hentschel et al., 2012; Taylor et al., 2007; Webster and Thomas, 2016). Extensive efforts have been made within the last two decades (Sun et al., 2015) to isolate microbes, especially actinomycetes from marine sponges for pharmaceutical development (Abdelmohsen et al., 2010; Abdelmohsen et al., 2014b; Cheng et al., 2015). Our study recovered a total of 64 actinomycetes represented by 23 genera from 12 different sponge species collected from the Mediterranean Sea. A group of studies focusing on the actinomycete collection from marine sponges for the sake of biological use were tabulated in **Table 5.1**. Comparing to the previous studies, our efforts exhibited the highest diversity rate of culture-dependent actinomycetes at the genus level. It can also be seen from the table that marine sponge-associated actinomycetes have increasingly drawn scientists' attention since 2010 and considerable isolation efforts for actinomycetes have been carried out within the past five years. This could be attributed to the rising number of novel biologically active compounds isolated from marine sponge-associated actinomycetes (Abdelmohsen et al., 2014b). Our attempt in seeking new chemical entities with diverse biological properties was also inspired by the richness of marine-sponge-associated actinomycetes. To enrich the diversity and the collective number of actinomycetes, two expeditions for sponge collections have been made in the Mediterranean area and eventually obtained a total of 18 sponge specimens.

In our study, the most actinomycetes were recovered from the marine sponge *Sarcotragus spinosulus* from which the isolation of many novel biologically active compounds was reported (Abed et al., 2011; Bisio et al., 2014; Liu et al., 2011; Wang et al., 2008; Watjen et al., 2009). The phylum *Proteobacteria* was reported as one of the dominant phyla among the isolated bacteria from *Sarcotragus spinosulus* which was collected from the southern coast of Portugal in Esteves et al.'s study (Esteves et al., 2013). This sponge species was also described with the isolation of a novel *Vibrio* sp. which belongs to the phylum *Proteobacteria* (Goncalves et al., 2015). However, our study exhibited 15 actinomycetes from this sponge species with 10 different genera recovered. This could be attributed to the effort of using 12 diverse media and pre-heating of the bacterial extract at 90 °C so that the undesirable fast growing bacteria were

killed in advance and the growth of the slowly growing actinomycetes on the culture plate was facilitated. In Esteves et al.'s study, only marine agar was used for the whole bacterial reviving process without any heating pre-treatment (Esteves et al., 2013). The different cultivation methods used in these two studies may explain the big difference observed in each microorganism collection.

Table 5.1 Diversity of sponge-associated actinomycetes from different collections

Actino-mycete Nr.	Genus Nr.	Sponge individual Nr.	Location	Ref
106	7	1	Yellow Sea	(Zhang et al., 2006)
90	18	11	Red Sea	(Abdelmohsen et al., 2010)
79	20	18	Caribbean Sea	(Tabares et al., 2011)
327	13	8	Yellow Sea	(Xi et al., 2012)
130	7	16	Caribbean Sea	(Vicente et al., 2013)
77	20	15	China Sea	(Sun et al., 2015)
64	23	12	Mediterranean Sea	(Cheng et al., 2015)

The sponge *Petrosia ficiformis*, which was notable for the isolation of 5 *Streptomyces* sp. in this study, also yielded a new *Actinomycetospora* sp. SBT374. Two other new bacterial isolates, *Microlunatus* sp. SBT365 and *Rhodococcus* sp. SBT367, were recovered from the sponge *Spirastrella cunctatrix*. The sponge *Chondrilla nucula*, which was reported with the cultivation of a novel halophilic bacterium belonging to the genus *Kangiella* sp. (Ahn et al., 2011), also yielded a new actinomycete *Geodermatophilus* sp. SBT350 in this study. To our knowledge, the sponges *Petrosia ficiformis* and *Spirastrella cunctatrix* were described for the first time with the isolation of novel actinomycetes.

5.1.2 Effect of different cultivation methods

In order to maximize the recovery of actinomycetes, I designed 12 different media to facilitate the growth and try to enrich the diversity of actinomycetes. M1 and ISP2 media, including the modified ones, unsurprisingly recovered the highest number of actinomycetes, which was consistent with previous studies (Abdelmohsen et al., 2010; Abdelmohsen et al., 2014b; Macintyre et al., 2014; Vicente et al., 2013), and provided three putatively novel species: *Microlunatus* sp. SBT365, *Rhodococcus* sp. SBT367, and *Actinomycetospora* sp. SBT374. The other putatively new species *Geodermatophilus* sp. SBT350 was retrieved from Agar_NSW, which was only prepared with agar and natural seawater. This founding rationally matches with the nature of the genus *Geodermatophilus*, which was mostly isolated from a desert area and prefers to grow under low-nutrient conditions (Mohammadipanah and Wink, 2015). Furthermore, our collection enclosed two naturally rare genera, *Knoellia* and *Nonomuraea*, from M1_F and ISP2 media, respectively. In addition to the diverse media

introduced in **Chapter 2**, I tried the sponge bacterial extracts in four dilution series to estimate the environmental growth concentrations in order to optimally retrieve the actinomycetes. Each dilution was further treated with heating and non-heating prior to the final inoculation. A total of 3456 plates were generated for reviving actinomycetes from 18 different sponges affiliating 12 species in our study and resulted in the isolation of 23 genera belonging to 15 families. To our knowledge so far, our collection in this study exhibited the highest rate of cultivable diversity of actinomycetes from marine sponges.

Besides the conventional plating approach, the diffusion chamber (Kaeberlein et al., 2002), which was initially applied to soil samples, was also successfully applied by Steinert et al. on living marine sponges and resulted in the isolation of 255 bacterial isolated from the marine sponge *Rhabdastrella globostellata*, 15 of which were putatively novel species (Steinert et al., 2014). However, actinobacteria only took up 14.5% of the whole collection and no new actinomycetes were recovered. Another innovative approach termed “I-tip” developed by Jung et al. uses an *in* situ cultivation device to improve the recovery of the novel and diverse microorganisms from sponges. In this method, glass beads and medium were prepared in pipette tips and inserted into different parts of the sponge specimen. This method led to the isolation of 34 species affiliating 5 major phyla, including *Actinobacteria*, *Alphaproteobacteria*, *Betaproteobacteria*, *Firmicutes*, and *Gammaproteobacteria*, more than two times more diverse in the phyla lever compared to the standard plate cultivation (Jung et al., 2014). The application of a diffusion chamber and I-tip provided promising approaches for the extensive cultivation of previously uncultured microorganisms from marine sponges. The combination of those recent tools with the conventional cultivation methods using specific media was strongly suggested in the future exploration of microorganisms from marine sponges or other invertebrates.

5.1.3 Putatively novel actinomycetes

Our strain collection identified four putatively novel actinomycetes based upon the 16S rRNA gene sequencing with < 98.5 % similarities compared to those available in the NCBI database. These four actinomycetes belong to the genus *Geodermatophilus*, *Microlunatus*, *Rhodococcus*, and *Actinomycetospora* and tabulated in **Table 5.2**.

Table 5.2 Putatively new species isolated from marine sponges

Isolate Code	Sponge Source	Medium Source	Closest Relative by BLAST	% Sequence Identity
***Geodermatophilus* sp. SBT350**	*Chondrilla nucula*	Agar_NSW	*Geodermatophilus obscurus* strain DSM 43160	98.41
***Microlunatus* sp. SBT365**	*Spirastrella cunctatrix*	ISP2	*Microlunatus soli* strain CC-012602	97.97
***Rhodococcus* sp. SBT367**	*Spirastrella cunctatrix*	M1_SE	*Rhodococcus opacus* strain S106	98.40
***Actinomycetospora* sp. SBT374**	*Petrosia ficiformis*	M1	*Actinomycetospora atypica* strain NEAU-st4	98.46

The putatively novel *Geodermatophilus* sp. SBT350 was isolated from marine sponge *Chondrilla nucula* from the nutrition restricted Agar_NSW medium. The genus *Geodermatophilus*, which was first reported by Luedemann in 1968 from soil samples (Luedemann, 1968) exhibited novel species from the terrestrial area, such as arid habitats (Hezbri et al., 2015; Montero-Calasanz Mdel et al., 2013), sediment (Qu et al., 2013) and soils (Jin et al., 2013; Zhang et al., 2011). However, no record from marine invertebrates has been found so far. *Geodermatophilus* prefers to grow in an arid environment with at least three-fifth of the 15 species being isolated from a desert area (Mohammadipanah and Wink, 2015). Our discovery of the novel *Geodermatophilus* sp. SBT350 from the marine sponge association in the marine environment enriched the diversity discovery of the genus *Geodermatophilus*.

Microlunatus sp. SBT365 was cultivated from the sponge *Spirastrella cunctatrix* from ISP2 medium. This genus belongs to the family *Propionibacteriaceae* and was described with a group of novel species from bark (Tuo et al., 2016), soil (Cheng et al., 2013; Lee and Kim, 2012) and sediment (Yuan et al., 2014). A recent study from Sun et al. extended the observation of *Microlunatus* sp. to the marine sponge (Sun et al., 2010). Our collection showed the first isolation of a novel *Microlunatus* sp. from marine sponge. However, biological activity was not reported from this genus so far.

The sponge *Spirastrella cunctatrix* also derived another putatively new spices *Rhodococcus* sp. SBT367 which was isolated from the sponge tissue sparked M1_SE medium. The genus *Rhodococcus* was best known by its catabolic capacities for a variety of organic compounds, such as polychlorinated biphenyls, aliphatic and aromatic hydrocarbons (Armstrong and Patel, 1993; Kaminski et al., 1983; Yang et al., 2016). A recent ecological study reported the isolation of *Rhodococcus* sp. from an industry area and demonstrated its ability in depredating phenolic

compounds, which may support the bioremediation studies in phenol-contaminated environments (Wang et al., 2016). Some marine sediment-derived *Rhodococcus* sp. also displayed significant bio-remediate roles and was proposed to apply in the petroleum-contaminated marine areas dealing with the degradation of oil contamination (Iwabuchi et al., 2002; Urai et al., 2006; Urai et al., 2007). Moreover, they have been shown as good biocatalysts in cell engineering, such as being used to improve biotransformation of steroids (van der Geize and Dijkhuizen, 2004). As for their potential in pharmaceutical use, a group of antibiotics have been isolated from this genus, such as rhodostreptomycins A and B (Kurosawa et al., 2008), lariatins A and B (Iwatsuki et al., 2006) and quinolone antibiotic (Kitagawa and Tamura, 2008), highlighting a potential of discovering new antibiotics from this new *Rhodococcus* sp. SBT367. As for the habitat and distribution, *Rhodococcus* sp. has exhibited a wide diversity and abundance in terrestrial and marine environments (Colquhoun et al., 1998). This genus was also frequently reported from the marine sponge specification (Abdelmohsen et al., 2014b; Karuppiah et al., 2015; Zhang et al., 2006). Three new species of this genus have been isolated from Saudi Arabia marine sponges in Abdelmohsen et al.'s study and exhibited antifungal and antiviral activities (Abdelmohsen et al., 2014b). Here I reported a novel species of *Rhodococcus* sp. SBT367 from the Mediterranean sponge *Spirastrella cunctatrix* exhibiting antitrypanosomal activity (**Table 2.3, Chapter 2**).

The strain *Actinomycetospora* sp. SBT374 was isolated from the marine sponge *Petrosia ficiformis* using M1 medium. The genus *Actinomycetospora* was first described by Jiang et al. following the isolation of the species *Actinomycetospora chiangmaiensis* from soil obtained from a tropical rainforest in northern Thailand (Jiang et al., 2008). This genus belongs to the family *Pseudonocardiaceae* and was recorded mostly with a number of novel species from terrestrial environment, such as bark (Tamura et al., 2011), soil (He et al., 2015; Zhang et al., 2014) and lichen (Yamamura et al., 2011a, b). A recent study by Peng et al. derived *Actinomycetospora chlora* from marine sediment from a mangrove swamp in Vava'u, Tonga and reported three new cytotoxic thiazoles thiasporine A-C produced by this strain (Fu and MacMillan, 2015). To our knowledge, this is the first time that a new *Actinomycetospora* sp. was described from marine sponge.

5.1.4 Biological activities

Twenty percentage of the isolated actinomycetes displayed different biological activities in our bioassay screening. The biologically active stains were dominated by the genus *Streptomyces*, which was eminent in producing secondary metabolites with various pharmacological properties (Abdelmohsen et al., 2014b; Clardy et al., 2006; Rutledge and Challis, 2015). *Streptomyces* sp. SBT348 exhibited activities in all the assays; thus, apparently standing out

amongst the other active ones. Interestingly, this strain was also revealed as an outlier in the following metabolomics analysis, indicating its chemical uniqueness and possible novelty of the secondary metabolites towards the aforementioned biological activities. In addition, the putatively novel species *Rhodococcus* sp. SBT367 and *Geodermatophilus* sp. SBT350, as well as the naturally rare *Nonomuraea* sp. SBT364 were shown to have antitrypanosomal activity, further highlighting the profit of exploring novel biological and chemical entities from marine sponges.

5.2 Metabolomics and dereplication-based natural products discovery

Metabolomics coupled chemometric analyses have been well developed and widely utilized in various fields, which all involve disease diagnosis (Madsen et al., 2010), human toxicology (Robertson, 2005) and plant metabolism (Jansen et al., 2012). However, a very limited number of studies have been reported to employ statistically-based metabolomics approaches to execute a rapid determination of candidate entities, such as chemically distinct microbes or bioactive extracts, for further natural product discovery. The first application was described in the study of Hou et al. where the feasibility of the metabolomics approach was evaluated by three experiments (Hou et al., 2012). They first assessed 47 broth cultures of marine invertebrate-associated strains of different genus' on the LC-MS coupled PCA analysis and exhibited finer resolution amongst different genera compared to the phylogenetic analysis. The same procedure was further carried out on solid cultures of 50 marine-derived streptomycetes and resulted in the prioritization of one chemically distinct candidate, along with the identification of three new polyenepyrones from the same strain. They also demonstrated LC-MS-coupled PCA as a valuable tool for the investigation of the biosynthesis process of certain compounds, which was exemplified by the regulation of desferrioxamine produced by *Micromonospora* sp. WMMB-224 under 30 different conditions. The benefit of utilizing metabolomics tools for candidate prioritization was also extensively demonstrated in other natural product studies where a large scale of samples was involved. Macintyre et al. subjected the LC-MS data of 77 marine sponge-associated strains to PCA analysis and identified 4 chemically distinct strains for further chemical profiling using tandem mass and NMR spectroscopy to gain deeper insight into the compound structure. They also developed an Excel Macro program that can rapidly filter and dereplicate the "top 20" secondary metabolites which were dominantly presented in each extract (Macintyre et al., 2014). A search for photosensitizers from 278 photocytotoxic plant extracts, which were used for photodynamic therapy in anti-cancer treatment, was assisted with the application of the same metabolomics method in Samat et al.'s study utilizing PCA analysis on LC-MS data. Twenty-

seven candidate extracts were prioritized along with the identification of two new photosensitizers presenting cyclic tetrapyrrolic structures (Samat et al., 2014). Abdelmohsen et al. also tried the unsupervised multivariate analysis (OPLS-DA) and 2D-scattering plot to investigate the diversity and production of biologically active metabolites in different cultivation and extraction methods on a Red Sea sponge associated-*Actinokineospora* sp. EG49 which showed significant antitrypanosomal activity. Two new antitrypanosomal actinosporins A and B were eventually isolated according to the metabolomics analyses in which the two compounds were initially speculated as the potentially active compounds (Abdelmohsen et al., 2014a). Wu et al also reviewed the utilization of NMR-based metabolomics for the prioritization of antibiotic compounds (Wu et al., 2016).

In the course of my Ph.D. thesis, I subjected both LC-MS and ^{1}H NMR data to metabolomics techniques to complementarily investigate the chemical profiling of the selected bacterial extracts. Some overlapping was observed between the two spectroscopy data sets in the PCA analyses, where *Streptomyces* sp.SBT348 was apparently highlighted by both LC-MS and ^{1}H NMR profiling. This evidence indicated the chemical uniqueness of this strain compared to the others. The significance was further illustrated by its activities in all the bioassays tested (**Chapter 2**). The compelling connection observed between the metabolomics analysis and biological capacities illustrated by this stain marked PCA based metabolomics as a confidential approach in candidate prioritization. The supervised multivariate analysis OPLS-DA was also tried on both LC-MS and ^{1}H NMR data of the strains obtained from Milos collection to facilitate the understanding or discovery of potential relevance between the antitrypanosomal activity and the metabolites that possibly attributed to the activity. The further up-scaling cultivation of our first candidate strain *Streptomyces* sp. SBT348 has led to the isolation of one of the outlying compounds (*m/z* 153.020 $[M-H]^-$), shown in the antitrypanosomal quadrant in the S-plot (**Fig. 3.5B, Chapter 3**). This compound was elucidated as 2,3-dihydroxybenzoic acid (compound **1**) by MS and NMR spectral data and has been previously reported with weak toxicity towards the trypanocidal effect (Grady et al., 1986; Merschjohann and Steverding, 2006), which again demonstrated a living instance of showing the link between the metabolite and biological activity by the chemometrics couple metabolomics method.

Furthermore, the compound represented by the ion mass *m/z* 152.035 $[M-H]^-$, which was visualized as one of the outlying secondary metabolites in the LC-MS-PCA analysis (**Fig. 3.1B, Chapter 3**) was isolated from the candidate strain *Streptomyces* sp. SBT348 and identified as 2,3-dihydroxybenzamide (compound **2**). One of the undereplicated major secondary metabolites shown in the dereplication study was also isolated and elucidated as the new

compound petrocidin A (compound **4**). The isolation of the three secondary metabolites highlighted by metabolomics manifested a good feasibility and a confidential means of using metabolomics approaches in the discovery of novel natural products. This methodology also offered an effective method for the prioritization of promising candidates from a large-scale sample set and may efficiently reduce redundancy in drug discovery programs.

5.3 Marine actinomycetes as source for novel bioactive compounds

Both of the candidate strains prioritized for further compounds isolation and purification are streptomycetes. A vast number of novel biologically active compounds were derived from this genus, which was dominated by antibiotics (Chater, 2006; Subramani and Aalbersberg, 2012), as well as various anticancer (Cimmino et al., 2012; Olano et al., 2009), anti-parasite agents (McKerrow, 2015; Pimentel-Elardo et al., 2011) and enzyme inhibitors (Manivasagan et al., 2015).

5.3.1 Compounds from *Streptomyces* sp. SBT348

Two structurally similar compounds 2,3-dihydroxybenzoic acid (compound **1**), 2,3-dihydroxybenzamide (compound **2**), and a new 2,3-dihydroxybenzamide conjoint cyclic dipeptide petrocidin A (compound **3**), as well as a known compound maltol (compound **4**), were isolated from the metabolomics outlier *Streptomyces* sp. SBT348 (**Fig. 5.1**).

2,3-dihydroxybenzoic acid and 2,3-dihydroxybenzamide were both previously isolated from a marine alga-derived actinomycete strain USF-TC31 and exhibited potent antioxidant activity in DPPH (2,2-Diphenyl-1-picrylhydrazyl) radical scavenging assay (Sugiyama and Hirota, 2009). An antimicrobial study from Anatharackal et al.in 2011 also identified 2,3-dihydroxybenzoic acid from the fruit extract of *Flacourtia inermis* and demonstrated its antibiotic potential against a group of multidrug resistant bacterial strains, such as *Serratia marcescens, Escherichia coli*, *Pseudomonas aeruginosa, Staphylococcus aureus* and *Klebsiella pneumoniae* (Anatharackal et al., 2011). 2,3-dihydroxybenzoic acid was additionally found to display weak inhibitory activity against *Trypanosoma brucei brucei* in mice (Grady et al., 1986; Merschjohann and Steverding, 2006).

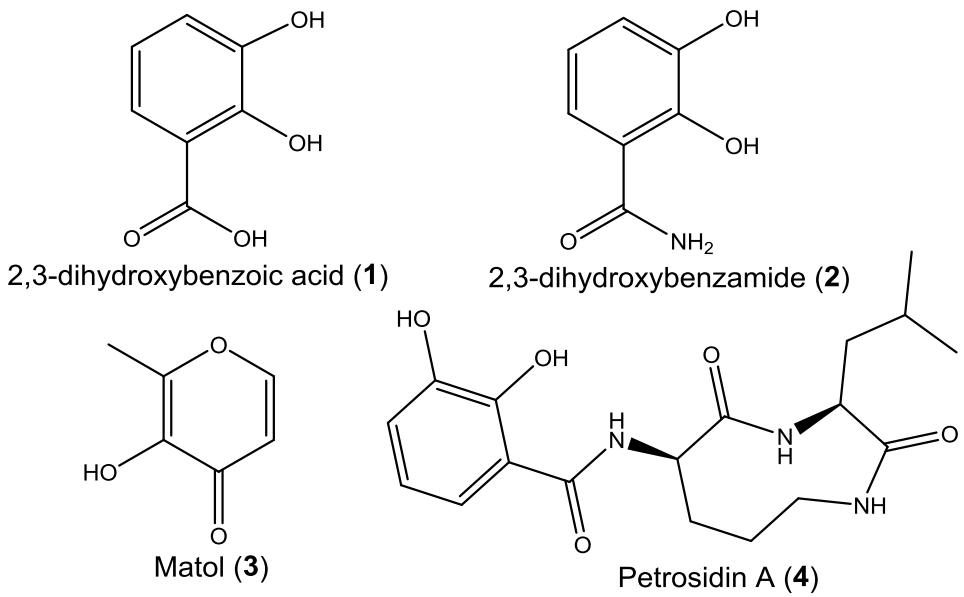

Fig. 5.1 Compounds isolated from *Streptomyces* sp. SBT348

Furthermore, 2,3-dihydroxybenzoic acid was considered as an intermediate derivative involved in the biosynthesis of streptomycin and isolated from the iron-deficient fermentation culture of *Streptomyces griseus* strain 2-38 (Dyer et al., 1964). It was also described as a product in the tryptophan metabolism by *Claviceps Paspali* (Tyler et al., 1964). More early in 1958, the glycine conjugated 2,3-dihydroxybenzoic acid was identified as the first catecholate siderophore, which is also the specific iron chelator used by bacteria for the acquisition of environmental iron (Hider and Kong, 2010), from *Bacillus subtilis* (Ito and Neilands, 1958) in its “low-iron fermentation” culture broth. Following the discovery of more siderophores from other pathogenic bacteria, a number of biosynthesis studies of siderophores, such as enterobactin (Pollack et al., 1970), anguibactin (Actis et al., 1986) and vancrobactin (Soengas et al., 2006) have been carried out and identified 2,3-dihydroxybenzoic acid as the precursor of these siderophores (Balado et al., 2006; Chen et al., 1994; Pollack et al., 1970; Soengas et al., 2006). Interestingly, the new compound petrocidin A, which encloses 2,3-dihydroxybenzamide as part of the structure, was simultaneously isolated with 2,3-dihydroxybenzoic acid from the same strain *Streptomyces* sp. SBT348, indicating that 2,3-dihydroxybenzoic acid might be the direct precursor of petrocidin A.

More literature has been reviewed whilst examining the function of the substructures of 2,3-dihydroxybenzamide- and cyclodipeptide of petrocidin A for their potential biological properties. The catechol and salicylic groups in 2,3-dihydroxybenzamide- moiety were generally considered as the chelating sites for ferric ions in a group of catecholate siderophores (Iglesias et al., 2011). Siderophore was found to play a causative role in the pathogenicity of the

pathogenic bacteria and fungi (Miethke and Marahiel, 2007). However, the siderophore-mediated iron-acquisition system was also utilized as a “Trojan Horse” approach, where the antibiotic molecule was modified to conjugate to a siderophore and expected to be passively taken up by pathogenic bacteria through the iron transport pathway (Souto et al., 2013). A group of siderophore-antibiotic conjugates was synthesized, one of which linked β-lactam antibiotics to the catecholate siderophores exhibiting inhibitory effects towards resistant *E. coli* strains without any observation of cross-resistance (Miller and Malouin, 1993). Additionally, 2,3-dihydroxybenzamide was identified as an active scaffold for synthesizing HIV-1 integrase (IN) inhibitors in HIV-1 resistant strains which display resistance to strand transfer specific inhibitors (Fan et al., 2011). In this case, the inhibitory effect was hypothesized to attribute to the metal-chelating property of the salicylic and catechol pharmacophores of 2,3-dihydroxybenzamide (Fan et al., 2011). Moreover, the same moiety of 2,3-dihydroxybenzamide was also proposed in the search for new microsomal prostaglandin E2 synthase-1 inhibitors which are involved in anti-inflammatory and anticancer process’ (Lauro et al., 2016). 2,3-dihydroxybenzamide-scaffold offers a significant prospect of petrocidin A for future research due to its ability to act as a real active pharmacophore or to assist in the transportation of drug molecules.

Regarding the cyclodipeptide substructure, there are numbers of cyclic dipeptides reported exhibiting antifungal and antibacterial activities (Graz et al., 1999; Huang et al., 2010; Patel et al., 2015). To track the compound(s) who contribute(s) to the antimicrobial activity of *Streptomyces* sp. SBT348 which was found in the bioassay screening, the four isolated metabolites were tested against *Bacillus* sp. and *Aspergillus* sp. using our in-house disc diffusion assay. However, neither petrocidin A, 2,3-dihydroxybenzamide, or 2,3-dihydroxybenzoic acid showed positive results against these two pathogens. Nonetheless, the limited amount obtained and insufficient loads to the paper disc should be taken into consideration as one of the possible reasons that led to the negative results in this assay.

Maltol is primarily known as a plant metabolite found in the plant bark (Dean, 1963; Ushanova et al., 1998), pine needles (Samejo et al., 2008) and roasted malt (Ochiai et al., 2012; Salmeron et al., 2014), from which it gets its name. It was widely used as a flavor enhancer in food production (Ma et al., 2014) and beverages (Qin et al., 2011; Salmeron et al., 2014), as well as an intermediate in pharmaceutical formulations (Kontoghiorghe and Kontoghiorghes, 2016; Thompson et al., 2009). A study on the maypop *Passiflora incarnata* has led to the isolation of maltol from its dry extract and exhibited a depressant effect in mice (Aoyagi et al., 1974). Maltol was also isolated as a microbial metabolite from fungi, such as *Scytalidium uredinicola* (Cunningham and Pickard, 1985), and bacteria, such as *Streptomyces* sp.

GW3/1538 (Maskey et al., 2004). It was found to inhibit the spore germination of the pine tree pathogen fungus *Endocronartium harknessii* (Cunningham and Pickard, 1985). However, in our in-house disc diffusion assay, maltol didn't show any inhibitory effect against *Bacillus* sp. or *Aspergillus* sp.. The use of malt extracts in the culture medium ISP2 also raised a question to maltol's real origin, of it originates from the medium or if it is being produced by *Streptomyces* sp. SBT348. When checking the mass spectra, maltol was not detected in either the bacterial or medium control extracts. This is likely due to maltol's hard-ionized chemical character in the electrospray ionization mode which was routinely used in the measurement of crude extracts.

5.3.2 Compounds from *Streptomyces* sp. SBT345

The up-scaling cultivation and chromatographic process of *Streptomyces* sp. SBT345 resulted in the isolation of three new compounds termed strepthonium A (compound **5**), ageloline A (compound **6**) and strepoxazine A (compound **9**), as well as two known phenazines phencomycin (compound **7**) and tubermycin B (compound **8**) (**Fig. 5.2**).

Strepthonium A is a chlorinated quaternary ammonium compound and is structurally similar to the synthesized non-chlorinated quaternary ammonium surfactant benzethonium, which has been widely used as a bactericide and antiseptic in medications (Hikiba et al., 2005), deodorants (Sugimoto et al., 2008), mouthwashes (Oyanagi et al., 2012), cosmetics (Oztekin and Erim, 2005) etc. However, unlike the inhibitory properties of benzethonium to the growth of bacteria, Strepthonium A did not specifically interfere with the growth of EHEC O157:H7 but rather selectively inhibited the production of Stx at a concentration of 80 µM. This observation indicated that the induction of resistance to this compound is less likely. Strepthonium A has a permanent cation and is therefore likely not to be membrane permeable. However, this could be treated as an advantage as no systemic effects are expected following oral uptake. In addition, a group of strepthonium A-similar compounds which were chlorinated at different positions in the aromatic rings was found to possess less toxic and less irritating properties than the previously investigated non-chlorinated quaternary ammonium compounds (Weiss et al., 1951). This comparison explores the effect of ring chlorination on benzyldimethylammonium chlorides (Weiss et al., 1951). Therefore, a low toxicity of strepthonium A was suspected and the chlorination in the 2-position of the phenoxy group may possibly contribute to the lower cytotoxicity. However, further experiments are needed to evaluate the cytotoxicity, and the possible induction of resistance with strepthonium A.

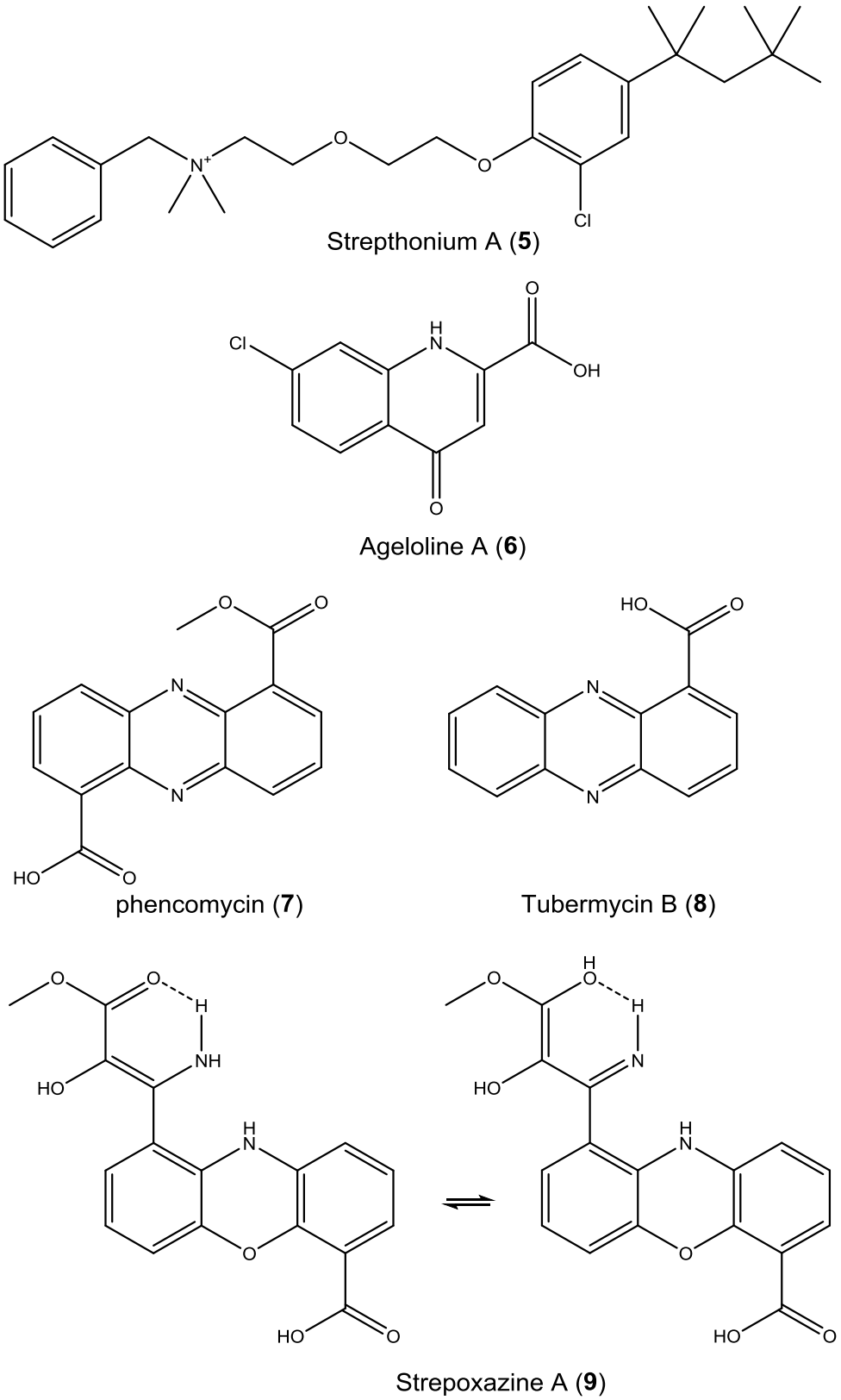

Fig. 5.2 Compounds isolated from *Streptomyces* sp. SBT345

Ageloline A is a new chlorinated quinolone isolated as a natural product. The nucleus of quinoline and quinolone were frequently utilized by chemists to design and synthesize novel and biologically active molecules, especially in the synthesis of anti-malarial (Thota and Yerra, 2016), antitrypanosomal (Hiltensperger et al., 2016), antimicrobial (Chung et al., 2015; Savarino and Shytaj, 2015) and antichlamydial (Smelov et al., 2004; Tartaglione and Hooton, 1993) derivatives. Ageloline A was initially tested in antioxidant assays to track the antioxidant effect shown in the crude extract of *Streptomyces* sp. SBT345 and ageloline A did exhibited antioxidant activity without any cytotoxicity against human kidney 2 cells. Due to the fact that antioxidants block caspase-1 production and the inhibition of caspase-1 by inhibitors demonstrated a decrease in chlamydial infection by 60% (Abdul-Sater et al., 2009), ageloline A was tested towards anti-infective activity against *Chlamydia trachomatis* and fortunately showed a significantly inhibitory effect on the formation and growth of the bacterial inclusions with IC_{50} value of 9.54 ± 0.36 μM. Some reports have described the multiple drug-resistance of floroguinolone compounds in the treatment of Chlamydial infections (Sandoz and Rockey, 2010; Somani et al., 2000). However, our results implied that the chlorinated quinolone ageloline A, which was shown to attenuate oxidative stress mediated by NQO, might influence the increasing cellular ROS production in the early phase of chlamydial infection and may thus have an impact on the establishment of the infection.

The fractionation and purification of EtOAc extract of *Streptomyces* sp. SBT345 also led to the isolation of two phenazines phencomycin, tubermycin B and one phenoxazine, strepoxazine A. Phenazine- and phenoxazine-constructed compounds have been extensively studied and synthesised due to their diverse biomedical properties, antibiotic activity (Katsamakas et al., 2016; Li et al., 2009) and biotechnological applications, such as their possible use as asorganic light emitting devices (Li et al., 2009), and bio-sensors to detect pH (Ryazanova et al., 2007) and amperometric variations (Shobha Jeykumari and Sriman Narayanan, 2007). They were solely known as bacterial metabolites (Pierson and Pierson, 2010). A group of novel compounds consisting of phenoxazine and phenazine chromophores has been reported from marine sponge derived bacteria, such as *Streptomyces* sp. (Khan et al., 2010; Kunz et al., 2014), *Norcardiopsis* sp. (Karuppiah et al., 2015), and *Brevibacterium* sp. (Choi et al., 2009). They were also reported with various anticancer activities against a panel of tumor cell lines, including intestinal adenocarcinoma (Gao et al., 2012; Ren et al., 2013), gastric cancer (Kasuga et al., 2007; McLuckie et al., 2011; Tomoda et al., 2013), pancreatic cancer cell lines (Kato et al., 2006; Nisr et al., 2011), lung tumor (Che et al., 2011; Kennedy et al., 2015a; Kennedy et al., 2015b), breast cancer (Kennedy et al., 2015a; Kennedy et al., 2015b; Thimmaiah et al., 1998), human hepatoma (Ren et al., 2013; Thuy et al., 2013; Zhao et al., 2014), multiple myeloma (Shirato et al., 2008; Takasaki et al., 2009) and human promyelocytic

leukemia (Kondratyuk et al., 2012; Li et al., 2007; Pettit et al., 1998) cells, *etc*. To evaluate the diversity of the possible biological properties of phenoxazines and phenazines, compounds **7-9** were extensively evaluated for the antiproliferative potential against human promyelocytic leukemia cells HL-60 and human breast adenocarcinoma cells MCF-7 using the Vitality Test and MTT assay in our study. The new phenoxazine strepoxazine A exhibited significant cytotoxic property against HL-60 with IC_{50} at 16 µg/ml (47 µM) and moderate against with IC_{50} at 64 µg/ml (188 µM). However, the other two phenazines, phencomycin and tubermycin B, did not display any activity. Suzuki et al. synthesized a group of phenoxazine-based analogues and investigated their cytotoxicity towards human promyelocytic leukemia cells (Ishihara et al., 2007; Suzuki et al., 2007). Five out of the 24 synthesized phenoxazines exhibited significant cytotoxicity against HL-60 cells with IC_{50} values ≤ 1.6 µM (Ishihara et al., 2007; Suzuki et al., 2007). 2-Amino-4,4alpha-dihydro-4alpha,7-dimethyl-3H-phenoxazine-3-one was another synthesized phenoxazine displaying an inhibitory effect towards HL-60 cells proliferation with IC_{50} value at 81 µM (Shimamoto et al., 2001). However, this is the first report of a new natural phenoxazine analogue isolated from marine sponge-associated microorganism and exhibiting anti-proliferative activity towards HL-60 cells.

5.4 Outlook

The in vivo devices developed by Steinert et al. and Jung et al. (Steinert et al., 2014; Jung et al., 2014) are highly recommended to be used parallel with the conventional plate cultivation in the future attempt to pursue more novel and "uncultured" sponge-associated microorganisms. It is also suggested to further investigate the phenotypic and genotypic characteristics of the four putatively novel isolates *Geodermatophilus* sp. SBT350, *Microlunatus* sp. SBT365, *Rhodococcus* sp. SBT367, and *Actinomycetospora* sp. SBT374 using, for example, the microscopy and whole genome sequencing to confirm their phylogenetic affiliations.

Further genomes of the candidate actinomycetes *Streptomyces* sp. SBT348 and *Streptomyces* sp. SBT345 should be sequenced so as to gain more insights into the secondary metabolism, such as determining the possible gene clusters (e.g. polyketide synthase and nonribosomal peptide genes) and biosynthetic pathways of the isolated bioactive secondary metabolites. Elicitation experiments will also be proposed for these two strains trying to facilitate the production of new compounds by adding different elicitors such as microbial lysates, microbial cell components, and inorganic compounds *etc.*, or co-cultivation with other microorganisms to activate or induce the activator of the silent gene clusters (Abdelmohsen et al., 2015).

Due to the inhibitory effect towards *Trypanosoma brucei brucei* strain TC 221 observed in the crude extract of *Streptomyces* sp. SBT348, antitrypanosomal bioassays should be pursued for the the four compounds (2,3-dihydroxybenzoic acid, 2,3-dihydroxybenzamide, maltol, petrocidin A) isolated from *Streptomyces* sp. SBT348. Additionally, further cytotoxic evaluation and possible resistance induction of strepthonium A are expected to perform and investigate in the further research.

The interdisciplinary approaches as suggested above using the new microorganism-reviving techniques and compound-facilitating methods from the genomic level are expected to pave the way for future drug discovery.

5.5 References

Abdelmohsen, U.R., Cheng, C., Viegelmann, C., Zhang, T., Grkovic, T., Ahmed, S., Quinn, R.J., Hentschel, U., Edrada-Ebel, R., 2014a. Dereplication strategies for targeted isolation of new antitrypanosomal actinosporins A and B from a marine sponge associated-*Actinokineospora* sp. EG49. Marine drugs 12, 1220-1244.

Abdelmohsen, U.R., Grkovic, T., Balasubramanian, S., Kamel, M.S., Quinn, R.J., Hentschel, U., 2015. Elicitation of secondary metabolism in actinomycetes. Biotechnology advances 33, 798-811.

Abdelmohsen, U.R., Pimentel-Elardo, S.M., Hanora, A., Radwan, M., Abou-El-Ela, S.H., Ahmed, S., Hentschel, U., 2010. Isolation, phylogenetic analysis and anti-infective activity screening of marine sponge-associated actinomycetes. Marine drugs 8, 399-412.

Abdelmohsen, U.R., Yang, C., Horn, H., Hajjar, D., Ravasi, T., Hentschel, U., 2014b. Actinomycetes from Red Sea sponges: sources for chemical and phylogenetic diversity. Marine drugs 12, 2771-2789.

Abdul-Sater, A.A., Koo, E., Hacker, G., Ojcius, D.M., 2009. Inflammasome-dependent caspase-1 activation in cervical epithelial cells stimulates growth of the intracellular pathogen *Chlamydia trachomatis*. Journal of biological chemistry 284, 26789-26796.

Abed, C., Legrave, N., Dufies, M., Robert, G., Guerineau, V., Vacelet, J., Auberger, P., Amade, P., Mehiri, M., 2011. A new hydroxylated nonaprenylhydroquinone from the Mediterranean marine sponge *Sarcotragus spinosulus*. Marine drugs 9, 1210-1219.

Actis, L.A., Fish, W., Crosa, J.H., Kellerman, K., Ellenberger, S.R., Hauser, F.M., Sanders-Loehr, J., 1986. Characterization of anguibactin, a novel siderophore from *Vibrio anguillarum* 775(pJM1). Journal of bacteriology 167, 57-65.

Ahn, J., Park, J.W., McConnell, J.A., Ahn, Y.B., Haggblom, M.M., 2011. *Kangiella spongicola* sp. nov., a halophilic marine bacterium isolated from the sponge *Chondrilla nucula*. International journal of systematic and evolutionary microbiology 61, 961-964.

Anatharackal, S.G., Benny, P.V., Kuriakose, S., George, C., 2011. Antibiotic activity of 2, 3-dihydroxybenzoic acid isolated from *Flacourtia inermis* fruit against multidrug resistant bacteria. Asian journal of pharmaceutical sciences 4, 126-130.

Aoyagi, N., Kimura, R., Murata, T., 1974. Studies on *passiflora incarnata* dry extract. I. Isolation of maltol and pharmacological action of maltol and ethyl maltol. Chemical & pharmaceutical bulletin 22, 1008-1013.

Armstrong, S., Patel, T.R., 1993. 1,3,5-Trihydroxybenzene biodegradation by *Rhodococcus* sp. BPG-8. Canadian journal of microbiology 39, 175-179.

Balado, M., Osorio, C.R., Lemos, M.L., 2006. A gene cluster involved in the biosynthesis of vanchrobactin, a chromosome-encoded siderophore produced by *Vibrio anguillarum*. Microbiology 152, 3517-3528.

Bisio, A., Fedele, E., Pittaluga, A., Olivero, G., Grilli, M., Chen, J., Mele, G., Malafronte, N., De Tommasi, N., Leddae, F., Manconi, R., Pronzato, R., Marchi, M., 2014. Isolation of hydroxyoctaprenyl-1',4'-hydroquinone, a new octaprenylhydroquinone from the marine sponge *Sarcotragus spinosulus* and evaluation of its pharmacological activity on acetylcholine and glutamate release in the rat central nervous system. Natural product communications 9, 1581-1584.

Chater, K.F., 2006. *Streptomyces* inside-out: a new perspective on the bacteria that provide us with antibiotics. Philosophical transactions of the Royal Society of London. Series B, Biological sciences 361, 761-768.

Che, X.F., Zheng, C.L., Akiyama, S., Tomoda, A., 2011. 2-Aminophenoxazine-3-one and 2-amino-4,4alpha-dihydro-4alpha,7-dimethyl-3H-phenoxazine-3-one cause cellular apoptosis by reducing higher intracellular pH in cancer cells. Proceedings of the Japan Academy. Series B, Physical and biological sciences 87, 199-213.

Chen, Q., Actis, L.A., Tolmasky, M.E., Crosa, J.H., 1994. Chromosome-mediated 2,3-dihydroxybenzoic acid is a precursor in the biosynthesis of the plasmid-mediated siderophore anguibactin in *Vibrio anguillarum*. Journal of bacteriology 176, 4226-4234.

Cheng, C., MacIntyre, L., Abdelmohsen, U.R., Horn, H., Polymenakou, P.N., Edrada-Ebel, R., Hentschel, U., 2015. Biodiversity, anti-trypanosomal activity screening, and metabolomic profiling of actinomycetes isolated from Mediterranean sponges. PloS one 10, e0138528.

Cheng, J., Chen, W., Huo-Zhang, B., Nimaichand, S., Zhou, E.M., Lu, X.H., Klenk, H.P., Li, W.J., 2013. *Microlunatus cavernae* sp. nov., a novel actinobacterium isolated from Alu ancient cave, Yunnan, South-West China. Antonie van Leeuwenhoek 104, 95-101.

Choi, E.J., Kwon, H.C., Ham, J., Yang, H.O., 2009. 6-Hydroxymethyl-1-phenazine-carboxamide and 1,6-phenazinedimethanol from a marine bacterium, *Brevibacterium* sp. KMD 003, associated with marine purple vase sponge. Journal of antibiotics 62, 621-624.

Chung, P.Y., Bian, Z.X., Pun, H.Y., Chan, D., Chan, A.S., Chui, C.H., Tang, J.C., Lam, K.H., 2015. Recent advances in research of natural and synthetic bioactive quinolines. Future medicinal chemistry 7, 947-967.

Cimmino, A., Evidente, A., Mathieu, V., Andolfi, A., Lefranc, F., Kornienko, A., Kiss, R., 2012. Phenazines and cancer. Natural product reports 29, 487-501.

Clardy, J., Fischbach, M.A., Walsh, C.T., 2006. New antibiotics from bacterial natural products. Nature biotechnology 24, 1541-1550.

Colquhoun, J.A., Heald, S.C., Li, L., Tamaoka, J., Kato, C., Horikoshi, K., Bull, A.T., 1998. Taxonomy and biotransformation activities of some deep-sea actinomycetes. Extremophiles: life under extreme conditions 2, 269-277.

Cunningham, J.E., Pickard, M.A., 1985. Maltol, a metabolite of *Scytalidium uredinicola* which inhibits spore germination of *Endocronartium harknessii*, the western gall rust. Canadian journal of microbiology 31, 1051-1055.

Dean, F.M., 1963. Naturally Occuring Oxygen Ring Compounds. Chem. Abstr 59, 640.

Dyer, J.R., Heding, H., Schaffner, C.P., 1964. Phenolic metabolite of “low-iron fermentation” of *Streptomyces griseus*. Characterization of 2,3-dihydroxybenzoic acid. Journal of organic chemistry 29, 2802-2803.

Esteves, A.I., Hardoim, C.C., Xavier, J.R., Goncalves, J.M., Costa, R., 2013. Molecular richness and biotechnological potential of bacteria cultured from *Irciniidae* sponges in the north-east Atlantic. FEMS microbiology ecology 85, 519-536.

Fan, X., Zhang, F.H., Al-Safi, R.I., Zeng, L.F., Shabaik, Y., Debnath, B., Sanchez, T.W., Odde, S., Neamati, N., Long, Y.Q., 2011. Design of HIV-1 integrase inhibitors targeting the catalytic domain as well as its interaction with LEDGF/p75: a scaffold hopping approach using salicylate and catechol groups. Bioorganic & medicinal chemistry 19, 4935-4952.

Fu, P., MacMillan, J.B., 2015. Thiasporines A-C, thiazine and thiazole derivatives from a marine-derived *Actinomycetospora chlora*. Journal of natural products 78, 548-551.

Gao, X., Lu, Y., Xing, Y., Ma, Y., Lu, J., Bao, W., Wang, Y., Xi, T., 2012. A novel anticancer and antifungus phenazine derivative from a marine actinomycete BM-17. Microbiological research 167, 616-622.

Goncalves, A.C., Franco, T., Califano, G., Dowd, S.E., Pohnert, G., Costa, R., 2015. Draft genome sequence of *Vibrio* sp. strain Vb278, an antagonistic bacterium isolated from the marine sponge *Sarcotragus spinosulus*. Genome announcements 3, pii: e00521-00515.

Grady, R.W., Bienen, E.J., Clarkson, A.B., Jr., 1986. Esters of 3,4-dihydroxybenzoic acid, highly effective inhibitors of the sn-glycerol-3-phosphate oxidase of *Trypanosoma brucei brucei*. Molecular and biochemical parasitology 21, 55-63.

Graz, M., Hunt, A., Jamie, H., Grant, G., Milne, P., 1999. Antimicrobial activity of selected cyclic dipeptides. Die Pharmazie 54, 772-775.

He, H., Zhang, Y., Ma, Z., Li, C., Liu, C., Zhou, Y., Li, L., Wang, X., Xiang, W., 2015. *Actinomycetospora rhizophila* sp. nov., an actinomycete isolated from rhizosphere soil of a peace lily (*Spathi phyllum Kochii*). International journal of systematic and evolutionary microbiology 65, 1520-1524.

Hentschel, U., Fieseler, L., Wehrl, M., Gernert, C., Steinert, M., Hacker, J., Horn, M., 2003. Microbial diversity of marine sponges. In: Müller, W.E.G. (Ed.), Sponges (Porifera). Springer Berlin, Germany, p 59-88.

Hentschel, U., Piel, J., Degnan, S.M., Taylor, M.W., 2012. Genomic insights into the marine sponge microbiome. Nature reviews microbiology 10, 641-654.

Hezbri, K., Ghodhbane-Gtari, F., Montero-Calasanz Mdel, C., Sghaier, H., Rohde, M., Schumann, P., Klenk, H.P., Gtari, M., 2015. *Geodermatophilus sabuli* sp. nov., a gamma-radiation-resistant actinobacterium isolated from desert limestone. International journal of systematic and evolutionary microbiology 65, 3365-3372.

Hider, R.C., Kong, X., 2010. Chemistry and biology of siderophores. Natural product reports 27, 637-657.

Hikiba, H., Watanabe, E., Barrett, J.C., Tsutsui, T., 2005. Ability of fourteen chemical agents used in dental practice to induce chromosome aberrations in Syrian hamster embryo cells. Journal of pharmacological sciences 97, 146-152.

Hiltensperger, G., Hecht, N., Kaiser, M., Rybak, J.C., Hoerst, A., Dannenbauer, N., Muller-Buschbaum, K., Bruhn, H., Esch, H., Lehmann, L., Meinel, L., Holzgrabe, U., 2016. Quinolone amides as anti-trypanosomal lead compounds with in vivo activity. Antimicrobial agents and chemotherapy, pii: AAC.01757-01715.

Hou, Y., Braun, D.R., Michel, C.R., Klassen, J.L., Adnani, N., Wyche, T.P., Bugni, T.S., 2012. Microbial strain prioritization using metabolomics tools for the discovery of natural products. Analytical chemistry 84, 4277-4283.

Huang, R., Zhou, X., Xu, T., Yang, X., Liu, Y., 2010. Diketopiperazines from marine organisms. Chemistry & biodiversity 7, 2809-2829.

Iglesias, E., Brandariz, I., Jimenez, C., Soengas, R.G., 2011. Iron(III) complexation by Vanchrobactin, a siderophore of the bacterial fish pathogen *Vibrio anguillarum*. Metallomics: integrated biometal science 3, 521-528.

Ishihara, M., Kawase, M., Westman, G., Samuelsson, K., Motohashi, N., Sakagami, H., 2007. Quantitative structure-cytotoxicity relationship analysis of phenoxazine derivatives by semiempirical molecular-orbital method. Anticancer research 27, 4053-4057.

Ito, T., Neilands, J.B., 1958. Products of “low-iron fermentation” with *Bacillus subilis*: isolation, characterization and synthesis of 2,3-dihydroxybenzoylglycine1,2. Journal of the American Chemical Society 80, 4645-4647.

Iwabuchi, N., Sunairi, M., Urai, M., Itoh, C., Anzai, H., Nakajima, M., Harayama, S., 2002. Extracellular polysaccharides of *Rhodococcus rhodochrous* S-2 stimulate the degradation of aromatic components in crude oil by indigenous marine bacteria. Applied and environmental microbiology 68, 2337-2343.

Iwatsuki, M., Tomoda, H., Uchida, R., Gouda, H., Hirono, S., Omura, S., 2006. Lariatins, antimycobacterial peptides produced by *Rhodococcus* sp. K01-B0171, have a lasso structure. Journal of the American Chemical Society 128, 7486-7491.

Jansen, J.J., Szymańska, E., Hoefsloot, H.C.J., Smilde, A.K., 2012. Individual differences in metabolomics: individualised responses and between-metabolite relationships. Metabolomics 8, 94-104.

Jiang, Y., Wiese, J., Tang, S.K., Xu, L.H., Imhoff, J.F., Jiang, C.L., 2008. *Actinomycetospora chiangmaiensis* gen. nov., sp. nov., a new member of the family Pseudonocardiaceae. International journal of systematic and evolutionary microbiology 58, 408-413.

Jin, L., Lee, H.G., Kim, H.S., Ahn, C.Y., Oh, H.M., 2013. *Geodermatophilus soli* sp. nov. and *Geodermatophilus terrae* sp. nov., two actinobacteria isolated from grass soil. International journal of systematic and evolutionary microbiology 63, 2625-2629.

Jung, D., Seo, E.Y., Epstein, S.S., Joung, Y., Han, J., Parfenova, V.V., Belykh, O.I., Gladkikh, A.S., Ahn, T.S., 2014. Application of a new cultivation technology, I-tip, for studying microbial diversity in freshwater sponges of Lake Baikal, Russia. FEMS microbiology ecology 90, 417-423.

Kaeberlein, T., Lewis, K., Epstein, S.S., 2002. Isolating "uncultivable" microorganisms in pure culture in a simulated natural environment. Science 296, 1127-1129.

Kaminski, U., Janke, D., Prauser, H., Fritsche, W., 1983. Degradation of aniline and monochloroanilines by *Rhodococcus* sp. An 117 and a *pseudomonad*: a comparative study. Zeitschrift fur allgemeine Mikrobiologie 23, 235-246.

Karuppiah, V., Li, Y., Sun, W., Feng, G., Li, Z., 2015. Functional gene-based discovery of phenazines from the actinobacteria associated with marine sponges in the South China Sea. Applied microbiology and biotechnology 99, 5939-5950.

Kasuga, T., Tabuchi, T., Shirato, K., Imaizumi, K., Tomoda, A., 2007. Caspase-independent cell death revealed in human gastric cancer cell lines, MKN45 and KATO III treated with phenoxazine derivatives. Oncology reports 17, 409-415.

Kato, S., Shirato, K., Imaizumi, K., Toyota, H., Mizuguchi, J., Odawara, M., Che, X.F., Akiyama, S., Abe, A., Tomoda, A., 2006. Anticancer effects of phenoxazine derivatives combined with tumor necrosis factor-related apoptosis-inducing ligand on pancreatic cancer cell lines, KLM-1 and MIA-PaCa-2. Oncology reports 15, 843-848.

Katsamakas, S., Zografos, A.L., Sarli, V., 2016. Advances of phenoxazines: synthesis, reactivity and their medicinal applications. Current medicinal chemistry 23.

Kennedy, R.K., Naik, P.R., Veena, V., Lakshmi, B.S., Lakshmi, P., Krishna, R., Sakthivel, N., 2015a. 5-Methyl phenazine-1-carboxylic acid: a novel bioactive metabolite by a rhizosphere soil bacterium that exhibits potent antimicrobial and anticancer activities. Chemico-biological interactions 231, 71-82.

Kennedy, R.K., Veena, V., Naik, P.R., Lakshmi, P., Krishna, R., Sudharani, S., Sakthivel, N., 2015b. Phenazine-1-carboxamide (PCN) from *Pseudomonas* sp. strain PUP6 selectively induced apoptosis in lung (A549) and breast (MDA MB-231) cancer cells by inhibition of antiapoptotic Bcl-2 family proteins. Apoptosis: an international journal on programmed cell death 20, 858-868.

Khan, S.T., Izumikawa, M., Motohashi, K., Mukai, A., Takagi, M., Shin-Ya, K., 2010. Distribution of the 3-hydroxyl-3-methylglutaryl coenzyme A reductase gene and isoprenoid production in marine-derived *Actinobacteria*. FEMS microbiology letters 304, 89-96.

Kitagawa, W., Tamura, T., 2008. A quinoline antibiotic from *Rhodococcus erythropolis* JCM 6824. Journal of antibiotics 61, 680-682.

Kondratyuk, T.P., Park, E.J., Yu, R., van Breemen, R.B., Asolkar, R.N., Murphy, B.T., Fenical, W., Pezzuto, J.M., 2012. Novel marine phenazines as potential cancer chemopreventive and anti-inflammatory agents. Marine drugs 10, 451-464.

Kontoghiorghe, C.N., Kontoghiorghes, G.J., 2016. New developments and controversies in iron metabolism and iron chelation therapy. World journal of methodology 6, 1-19.

Kunz, A.L., Labes, A., Wiese, J., Bruhn, T., Bringmann, G., Imhoff, J.F., 2014. Nature's lab for derivatization: new and revised structures of a variety of streptophenazines produced by a sponge-derived *Streptomyces* strain. Marine drugs 12, 1699-1714.

Kurosawa, K., Ghiviriga, I., Sambandan, T.G., Lessard, P.A., Barbara, J.E., Rha, C., Sinskey, A.J., 2008. Rhodostreptomycins, antibiotics biosynthesized following horizontal gene transfer from *Streptomyces padanus* to *Rhodococcus fascians*. Journal of the American Chemical Society 130, 1126-1127.

Lauro, G., Tortorella, P., Bertamino, A., Ostacolo, C., Koeberle, A., Fischer, K., Bruno, I., Terracciano, S., Gomez-Monterrey, I.M., Tauro, M., Loiodice, F., Novellino, E., Riccio, R., Werz, O., Campiglia, P., Bifulco, G., 2016. Structure-based design of microsomal prostaglandin E2 Synthase-1 (mPGES-1) inhibitors using a virtual fragment growing optimization scheme. ChemMedChem 11, 612-619.

Lee, J.J., Kim, M.K., 2012. *Microlunatus terrae* sp. nov., a bacterium isolated from soil. Journal of microbiology 50, 547-552.

Li, D., Wang, F., Xiao, X., Zeng, X., Gu, Q.Q., Zhu, W., 2007. A new cytotoxic phenazine derivative from a deep sea bacterium *Bacillus* sp. Archives of pharmacal research 30, 552-555.

Li, X.N., Wu, Z.J., Si, Z.J., Liang, Z., Liu, X.J., Zhang, H.J., 2009. Effect of secondary ligands' size on energy transfer and electroluminescent efficiencies for a series of europium(III) complexes, a density functional theory study. Physical chemistry chemical physics: PCCP 11, 9687-9695.

Liu, Y., Jung, J.H., Xu, T., Long, L., Lin, X., Yin, H., Yang, B., Zhou, X.F., Yang, X., 2011. New cyclitol derivative from a sponge *Sarcotragus* species. Natural product research 25, 648-652.

Luedemann, G.M., 1968. *Geodermatophilus*, a new genus of the Dermatophilaceae (Actinomycetales). Journal of bacteriology 96, 1848-1858.

Ma, J., Zhang, B., Wang, Y., Hou, X., He, L., 2014. Determination of flavor enhancers in milk powder by one-step sample preparation and two-dimensional liquid chromatography. Journal of separation science 37, 920-926.

Macintyre, L., Zhang, T., Viegelmann, C., Martinez, I.J., Cheng, C., Dowdells, C., Abdelmohsen, U.R., Gernert, C., Hentschel, U., Edrada-Ebel, R., 2014. Metabolomic tools for secondary metabolite discovery from marine microbial symbionts. Marine drugs 12, 3416-3448.

Madsen, R., Lundstedt, T., Trygg, J., 2010. Chemometrics in metabolomics-a review in human disease diagnosis. Analytica Chimica Acta 659, 23-33.

Manivasagan, P., Venkatesan, J., Sivakumar, K., Kim, S.K., 2015. Actinobacterial enzyme inhibitors-a review. Critical reviews in microbiology 41, 261-272.

Maskey, R.P., Shaaban, M., Grun-Wollny, I., Laatsch, H., 2004. Quinazolin-4-one derivatives from *Streptomyces* isolates. Journal of natural products 67, 1131-1134.

McKerrow, J.H., 2015. Recognition of the role of Natural Products as drugs to treat neglected tropical diseases by the 2015 Nobel prize in physiology or medicine. Natural product reports 32, 1610-1611.

McLuckie, K.I., Waller, Z.A., Sanders, D.A., Alves, D., Rodriguez, R., Dash, J., McKenzie, G.J., Venkitaraman, A.R., Balasubramanian, S., 2011. G-quadruplex-binding benzo[a]phenoxazines down-regulate c-KIT expression in human gastric carcinoma cells. Journal of the American Chemical Society 133, 2658-2663.

Merschjohann, K., Steverding, D., 2006. In vitro growth inhibition of bloodstream forms of Trypanosoma *brucei* and *Trypanosoma congolense* by iron chelators. Kinetoplastid biology and disease 5, 3.

Miethke, M., Marahiel, M.A., 2007. Siderophore-based Iron acquisition and pathogen control. Microbiology and molecular biology reviews 71, 413-451.

Miller, M.J., Malouin, F., 1993. Microbial iron chelators as drug delivery agents: the rational design and synthesis of siderophore-drug conjugates. Accounts of chemical research 26, 241-249.

Mohammadipanah, F., Wink, J., 2015. Actinobacteria from arid and Ddesert habitats: diversity and biological activity. Frontiers in microbiology 6, 1541.

Montero-Calasanz Mdel, C., Goker, M., Potter, G., Rohde, M., Sproer, C., Schumann, P., Gorbushina, A.A., Klenk, H.P., 2013. *Geodermatophilus africanus* sp. nov., a halotolerant actinomycete isolated from Saharan desert sand. Antonie van Leeuwenhoek 104, 207-216.

Nisr, R.B., Russell, M.A., Chrachri, A., John Moody, A., Gilpin, M.L., 2011. Effects of the microbial secondary metabolites pyrrolnitrin, phenazine and patulin on INS-1 rat pancreatic β-cells. FEMS immunology & medical microbiology 63, 217–227.

Ochiai, N., Sasamoto, K., Hoffmann, A., Okanoya, K., 2012. Full evaporation dynamic headspace and gas chromatography-mass spectrometry for uniform enrichment of odor compounds in aqueous samples. Journal of chromatography. A 1240, 59-68.

Olano, C., Mendez, C., Salas, J.A., 2009. Antitumor compounds from actinomycetes: from gene clusters to new derivatives by combinatorial biosynthesis. Natural product reports 26, 628-660.

Oyanagi, T., Tagami, J., Matin, K., 2012. Potentials of mouthwashes in disinfecting cariogenic bacteria and biofilms leading to inhibition of caries. The open dentistry journal 6, 23-30.

Oztekin, N., Erim, F.B., 2005. Determination of cationic surfactants as the preservatives in an oral solution and a cosmetic product by capillary electrophoresis. Journal of pharmaceutical and biomedical analysis 37, 1121-1124.

Patel, S., Ahmed, S., Eswari, J.S., 2015. Therapeutic cyclic lipopeptides mining from microbes: latest strides and hurdles. World journal of microbiology & biotechnology 31, 1177-1193.

Pettit, G.R., Tan, R., Xu, J., Ichihara, Y., Williams, M.D., Boyd, M.R., 1998. Antineoplastic agents. 398. Isolation and structure elucidation of cephalostatins 18 and 19. Journal of natural products 61, 955-958.

Pierson, L.S., Pierson, E.A., 2010. Metabolism and function of phenazines in bacteria: impacts on the behavior of bacteria in the environment and biotechnological processes. Applied microbiology and biotechnology 86, 1659-1670.

Pimentel-Elardo, S.M., Buback, V., Gulder, T.A., Bugni, T.S., Reppart, J., Bringmann, G., Ireland, C.M., Schirmeister, T., Hentschel, U., 2011. New tetromycin derivatives with anti-trypanosomal and protease inhibitory activities. Marine drugs 9, 1682-1697.

Pollack, J.R., Ames, B.N., Neilands, J.B., 1970. Iron transport in *Salmonella typhimurium*: mutants blocked in the biosynthesis of enterobactin. Journal of bacteriology 104, 635-639.

Qin, P., Ma, T., Wu, L., Shan, F., Ren, G., 2011. Identification of tartary buckwheat tea aroma compounds with gas chromatography-mass spectrometry. Journal of food science 76, 401-407.

Qu, J.H., Hui, M., Qu, J.Y., Wang, F.F., Li, H.F., Hu, Y.S., Luo, Y., Cai, J.P., 2013. *Geodermatophilus taihuensis* sp. nov., isolated from the interfacial sediment of a eutrophic lake. International journal of systematic and evolutionary microbiology 63, 4108-4112.

Ren, J., Liu, D., Tian, L., Wei, Y., Proksch, P., Zeng, J., Lin, W., 2013. Venezuelines A-G, new phenoxazine-based alkaloids and aminophenols from *Streptomyces venezuelae* and the regulation of gene target Nur77. Bioorganic & medicinal chemistry letters 23, 301-304.

Robertson, D.G., 2005. Metabonomics in toxicology: a review. Toxicological sciences: an official journal of the Society of Toxicology 85, 809-822.

Rutledge, P.J., Challis, G.L., 2015. Discovery of microbial natural products by activation of silent biosynthetic gene clusters. Nature reviews microbiology 13, 509-523.

Ryazanova, O.A., Voloshin, I.M., Makitruk, V.L., Zozulya, V.N., Karachevtsev, V.A., 2007. pH-induced changes in electronic absorption and fluorescence spectra of phenazine derivatives. Spectrochimica acta. Part A, Molecular and biomolecular spectroscopy 66, 849-859.

Salmeron, I., Rozada, R., Thomas, K., Ortega-Rivas, E., Pandiella, S.S., 2014. Sensory characteristics and volatile composition of a cereal beverage fermented with *Bifidobacterium breve* NCIMB 702257. Food science and technology international/Ciencia y tecnologia de los alimentos internacional 20, 205-213.

Samat, N., Tan, P.J., Shaari, K., Abas, F., Lee, H.B., 2014. Prioritization of natural extracts by LC-MS-PCA for the identification of new photosensitizers for photodynamic therapy. Analytical chemistry 86, 1324-1331.

Samejo, M.Q., Ndukwe, G.I., Burdi, D.K., Bhanger, M.I., Khan, K.M., 2008. Isolation and crystal structure of maltol from *Abies pindrow*. Journal of medicinal plant research 3, 55-60.

Sandoz, K.M., Rockey, D.D., 2010. Antibiotic resistance in Chlamydiae. Future microbiology 5, 1427-1442.

Savarino, A., Shytaj, I.L., 2015. Chloroquine and beyond: exploring anti-rheumatic drugs to reduce immune hyperactivation in HIV/AIDS. Retrovirology 12, 51.

Shimamoto, T., Tomoda, A., Ishida, R., Ohyashiki, K., 2001. Antitumor effects of a novel phenoxazine derivative on human leukemia cell lines in vitro and in vivo. Clinical cancer research: an official journal of the American Association for Cancer Research 7, 704-708.

Shirato, K., Imaizumi, K., Miyazawa, K., Takasaki, A., Mizuguchi, J., Che, X.F., Akiyama, S., Tomoda, A., 2008. Apoptosis induction preceded by mitochondrial depolarization in multiple myeloma cell line U266 by 2-aminophenoxazine-3-one. Biological & pharmaceutical bulletin 31, 62-67.

Shobha Jeykumari, D.R., Sriman Narayanan, S., 2007. Covalent modification of multiwalled carbon nanotubes with neutral red for the fabrication of an amperometric hydrogen peroxide sensor. Nanotechnology 18, 125501.

Smelov, V., Perekalina, T., Gorelov, A., Smelova, N., Artemenko, N., Norman, L., 2004. In vitro activity of fluoroquinolones, azithromycin and doxycycline against *chlamydia trachomatis* cultured from men with chronic lower urinary tract symptoms. European urology 46, 647-650.

Soengas, R.G., Anta, C., Espada, A., Paz, V., Ares, I.R., Balado, M., Rodríguez, J., Lemos, M.L., Jiménez, C., 2006. Structural characterization of vanchrobactin, a new catechol siderophore produced by the fish pathogen *Vibrio anguillarum* serotype O2. Tetrahedron letters 47, 7113-7116.

Somani, J., Bhullar, V.B., Workowski, K.A., Farshy, C.E., Black, C.M., 2000. Multiple drug-resistant *Chlamydia trachomatis* associated with clinical treatment failure. The Journal of infectious diseases 181, 1421-1427.

Souto, A., Montaos, M.A., Balado, M., Osorio, C.R., Rodriguez, J., Lemos, M.L., Jimenez, C., 2013. Synthesis and antibacterial activity of conjugates between norfloxacin and analogues of the siderophore vanchrobactin. Bioorganic & medicinal chemistry 21, 295-302.

Steinert, G., Whitfield, S., Taylor, M.W., Thoms, C., Schupp, P.J., 2014. Application of diffusion growth chambers for the cultivation of marine sponge-associated bacteria. Marine biotechnology 16, 594-603.

Subramani, R., Aalbersberg, W., 2012. Marine actinomycetes: an ongoing source of novel bioactive metabolites. Microbiological research 167, 571-580.

Sugimoto, N., Tada, A., Kuroyanagi, M., Yoneda, Y., Yun, Y.S., Kunugi, A., Sato, K., Yamazaki, T., Tanamoto, K., 2008. Survey of synthetic disinfectants in grapefruit seed extract and its compounded products. Shokuhin eiseigaku zasshi. Journal of the Food Hygienic Society of Japan 49, 56-62.

Sugiyama, Y., Hirota, A., 2009. New potent DPPH radical scavengers from a marine-derived actinomycete strain USF-TC31. Bioscience, biotechnology, and biochemistry 73, 2731-2734.

Sun, W., Dai, S., Jiang, S., Wang, G., Liu, G., Wu, H., Li, X., 2010. Culture-dependent and culture-independent diversity of Actinobacteria associated with the marine sponge *Hymeniacidon perleve* from the South China Sea. Antonie van Leeuwenhoek 98, 65-75.

Sun, W., Zhang, F., He, L., Karthik, L., Li, Z., 2015. Actinomycetes from the South China Sea sponges: isolation, diversity, and potential for aromatic polyketides discovery. Frontiers in microbiology 6, 1048.

Suzuki, F., Hashimoto, K., Ishihara, M., Westman, G., Samuelsson, K., Kawase, M., Motohashi, N., Sakagami, H., 2007. Tumor-specificity and type of cell death induced by phenoxazines. Anticancer research 27, 4233-4238.

Tabares, P., Pimentel-Elardo, S.M., Schirmeister, T., Hunig, T., Hentschel, U., 2011. Anti-protease and immunomodulatory activities of bacteria associated with Caribbean sponges. Marine biotechnology 13, 883-892.

Takasaki, A., Hanyu, H., Iwamoto, T., Shirato, K., Izumi, R., Toyota, H., Mizuguchi, J., Miyazawa, K., Tomoda, A., 2009. Mitochondrial depolarization and apoptosis associated with sustained activation of c-jun-N-terminal kinasein the human multiple myeloma cell line U266 induced by 2-aminophenoxazine-3-one. Molecular medicine reports 2, 199-203.

Tamura, T., Ishida, Y., Hamada, M., Otoguro, M., Yamamura, H., Hayakawa, M., Suzuki, K., 2011. Description of *Actinomycetospora chibensis* sp. nov., *Actinomycetospora chlora* sp. nov., *Actinomycetospora cinnamomea* sp. nov., *Actinomycetospora corticicola* sp. nov., *Actinomycetospora lutea* sp. nov., *Actinomycetospora straminea* sp. nov. and *Actinomycetospora succinea* sp. nov. and emended description of the genus Actinomycetospora. International journal of systematic and evolutionary microbiology 61, 1275-1280.

Tartaglione, T.A., Hooton, T.M., 1993. The role of fluoroquinolones in sexually transmitted diseases. Pharmacotherapy 13, 189-201.

Taylor, M.W., Radax, R., Steger, D., Wagner, M., 2007. Sponge-associated microorganisms: evolution, ecology, and biotechnological potential. Microbiology and molecular biology reviews 71, 295-347.

Thimmaiah, K.N., Jayashree, B.S., Germain, G.S., Houghton, P.J., Horton, J.K., 1998. Characterization of 2-chloro-N10-substituted phenoxazines for reversing multidrug resistance in cancer cells. Oncology research 10, 29-41.

Thompson, K.H., Lichter, J., LeBel, C., Scaife, M.C., McNeill, J.H., Orvig, C., 2009. Vanadium treatment of type 2 diabetes: a view to the future. Journal of inorganic biochemistry 103, 554-558.

Thota, S., Yerra, R., 2016. Drug discovery and development of antimalarial agents: recent advances. Current protein & peptide science 17, 275-279.

Thuy, T.T., Huong, N.T., Nhung le, T.H., Ninh, P.T., Delfino, D.V., Van Sung, T., 2013. Isolation, characterisation and biological evaluation of a phenoxazine, a natural dyestuff isolated from leaves of *Peristrophe bivalvis*. Natural product research 27, 771-774.

Tomoda, A., Miyazawa, K., Tabuchi, T., 2013. Prevention of carcinogenesis and development of gastric and colon cancers by 2-aminophenoxazine-3-one (Phx-3): direct and indirect anti-cancer activity of Phx-3. International journal of molecular sciences 14, 17573-17583.

Tuo, L., Li, J., Liu, S.W., Liu, Y., Hu, L., Chen, L., Jiang, M.G., Sun, C.H., 2016. *Microlunatus endophyticus* sp. nov., an endophytic actinobacterium isolated from bark of *Bruguiera sexangula*. International journal of systematic and evolutionary microbiology 66, 481-486.

Tyler, V.E.J., Mothes, K., Groeger, D., 1964. Conversion of tryptophan to 2,3-dihydroxybenzoic acid by *Claviceps Paspali* Tetrahydron letters 11, 593-598.

Urai, M., Anzai, H., Ogihara, J., Iwabuchi, N., Harayama, S., Sunairi, M., Nakajima, M., 2006. Structural analysis of an extracellular polysaccharide produced by *Rhodococcus rhodochrous* strain S-2. Carbohydrate research 341, 766-775.

Urai, M., Yoshizaki, H., Anzai, H., Ogihara, J., Iwabuchi, N., Harayama, S., Sunairi, M., Nakajima, M., 2007. Structural analysis of an acidic, fatty acid ester-bonded extracellular polysaccharide produced by a pristane-assimilating marine bacterium, *Rhodococcus erythropolis* PR4. Carbohydrate research 342, 933-942.

Ushanova, V.M., Ziganshin, A.V., Repyakh, S.M., 1998. Isolation of maltol from *Siberian fir* bark by the carbon dioxide method. Chemistry of Natural Compounds 34, 104-105.

van der Geize, R., Dijkhuizen, L., 2004. Harnessing the catabolic diversity of rhodococci for environmental and biotechnological applications. Current opinion in microbiology 7, 255-261.

Vicente, J., Stewart, A., Song, B., Hill, R.T., Wright, J.L., 2013. Biodiversity of actinomycetes associated with Caribbean sponges and their potential for natural product discovery. Marine biotechnology 15, 413-424.

Wang, L., Li, Y., Niu, L., Dai, Y., Wu, Y., Wang, Q., 2016. Isolation and growth kinetics of a novel phenol-degrading bacterium *Microbacterium oxydans* from the sediment of Taihu Lake (China). Water science and technology: a journal of the International Association on Water Pollution Research 73, 1882-1890.

Wang, N., Song, J., Jang, K.H., Lee, H.S., Li, X., Oh, K.B., Shin, J., 2008. Sesterterpenoids from the sponge *Sarcotragus* sp. Journal of natural products 71, 551-557.

Watjen, W., Putz, A., Chovolou, Y., Kampkotter, A., Totzke, F., Kubbutat, M.H., Proksch, P., Konuklugil, B., 2009. Hexa-, hepta- and nonaprenylhydroquinones isolated from marine sponges *Sarcotragus muscarum* and *Ircinia fasciculata* inhibit NF-kappaB signalling in H4IIE cells. Journal of pharmacy and pharmacology 61, 919-924.

Webster, N.S., Thomas, T., 2016. The sponge hologenome. mBio 7, e00135-00116.

Weiss, P., Cordasco, M.G., Carman, W., Reiner, L., 1951. The effect of ring chlorination on the antibacterial action of (aryloxyethoxyethyl) benzyldimethylammonium chlorides. Journal of the American Pharmaceutical Association (1912-1977) 40, 267-272.

Wu, C., Choi, Y.H., van Wezel, G.P., 2016. Metabolic profiling as a tool for prioritizing antimicrobial compounds. Journal of industrial microbiology & biotechnology 43, 299-312.

Xi, L., Ruan, J., Huang, Y., 2012. Diversity and biosynthetic potential of culturable actinomycetes associated with marine sponges in the China Seas. International journal of molecular sciences 13, 5917-5932.

Yamamura, H., Ashizawa, H., Nakagawa, Y., Hamada, M., Ishida, Y., Otoguro, M., Tamura, T., Hayakawa, M., 2011a. *Actinomycetospora iriomotensis* sp. nov., a novel actinomycete isolated from a lichen sample. Journal of antibiotics 64, 289-292.

Yamamura, H., Ashizawa, H., Nakagawa, Y., Hamada, M., Ishida, Y., Otoguro, M., Tamura, T., Hayakawa, M., 2011b. *Actinomycetospora rishiriensis* sp. nov., isolated from a lichen. International journal of systematic and evolutionary microbiology 61, 2621-2625.

Yang, G.C., Huang, S.C., Jen, Y.S., Tsai, P.S., 2016. Remediation of phthalates in river sediment by integrated enhanced bioremediation and electrokinetic process. Chemosphere 150, 576-585.

Yuan, M., Yu, Y., Li, H.R., Dong, N., Zhang, X.H., 2014. Phylogenetic diversity and biological activity of actinobacteria isolated from the Chukchi Shelf marine sediments in the Arctic Ocean. Marine drugs 12, 1281-1297.

Zhang, H., Lee, Y.K., Zhang, W., Lee, H.K., 2006. Culturable actinobacteria from the marine sponge *Hymeniacidon perleve*: isolation and phylogenetic diversity by 16S rRNA gene-RFLP analysis. Antonie van Leeuwenhoek 90, 159-169.

Zhang, Y., Liu, C., Zhang, J., Shen, Y., Li, C., He, H., Wang, X., Xiang, W., 2014. *Actinomycetospora atypica* sp. nov., a novel soil actinomycete and emended description of the genus *Actinomycetospora*. Antonie van Leeuwenhoek 105, 891-897.

Zhang, Y.Q., Chen, J., Liu, H.Y., Zhang, Y.Q., Li, W.J., Yu, L.Y., 2011. *Geodermatophilus ruber* sp. nov., isolated from rhizosphere soil of a medicinal plant. International journal of systematic and evolutionary microbiology 61, 190-193.

Zhao, J., Wu, Y., Alfred, A.T., Wei, P., Yang, S., 2014. Anticancer effects of pyocyanin on HepG2 human hepatoma cells. Letters in applied microbiology 58, 541-548.

Annex

I. Abbreviations and Acronyms

δ_C	chemical shift (ppm), 13C NMR
δ_H	chemical shift (ppm), 1H NMR
°C	degree Celsius
ASW	artificial seawater
AUC	area under the fluorescence curve
BLAST	basic local alignment search tool
bp	base pair
br	broad
ca.	approximately
^{13}C	NMR correlation spectroscopy
COSY	correlation spectroscopy
d	(NMR) doublet
dd	(NMR) double doublet
dq	dq (NMR) double quartet
DMSO	Dimethylsulfoxide
DMSO-d_6	Deuterated dimethylsulfoxide
DNA	deoxyribonucleic acid
EtOH	Ethanol
EtOAc	ethyl acetate
g	Gram
h	Hour
HMBC	heteronuclear multiple bond correlation
^1H NMR	NMR proton nuclear magnetic resonance
HPLC	high performance liquid chromatography
HSQC	heteronuclear single quantum coherence
Hz	Hertz
IC_{50}	concentration required for 50% inhibition
J	coupling constant
Kb	Kilobase
L	Liter
M	Molar
m (NMR)	Multiplet
MHz	Megahertz
MeOH	Methanol

$MeOH\text{-}d_4$	Deuterated methanol
Mg	Milligram
MIC	minimum inhibitory concentration
min	Minute
Ml	Milliliter
mM	millimolar
MS	mass spectrometry
mult	multiplicity
NMR	nuclear magnetic resonance
NSW	Natural seawater
OD	optical density
PCR	polymerase chain reaction
PKS	polyketide synthase
ppm	parts per million
psu	practical salinity unit
rDNA	ribosomal DNA
rRNA	ribosomal RNA
RNA	ribonucleic acid
rpm	Round per minute
Rt	retention time
RT	room temperature
s	Second
s (NMR)	Singlet
sp.	Species
strainT	type strain
t (NMR)	Triplet
TFA	trifluoroacetic acid
µg	Microgram
µl	Microliter
µM	micromolar
UV	Ultraviolet
V	Volt
w/v	weight per volume
vol/vol	volume per volume

II. Recipes for different preparations

Media were sterilized by autoclaving. Components that are damaged by heat or whose pH or concentration are critical were sterilized by filtration through a 0.22 µm filter and added to autoclaved media after cooling to hand warm temperature. Media containing agar were aseptically poured into sterile disposable Petri dishes and allowed to solidify at room temperature.

A. Bacterial and fungal growth media

Artificial seawater	
NaCl	234.70 g
Na_2SO_4	39.20 g
$MgCl_2.6H_2O$	106.40 g
$CaCl_2$	11.00 g
$NaHCO_3$	1.92 g
KCl	6.64 g
KBr	0.96 g
H_3BO_3	0.26 g
$SrCl_2$	0.24 g
NaF	0.03 g
Distilled H_2O	10.00 L

Agar NSW	
Agar	18.0 g
NSW	1.0 L

ISP2	
Yeast extract	4.0 g
Malt extract	10.0 g
Glucose	4.0 g
Agar	18.0 g
ASW	1.0 L

ISP2_F	
Yeast extract	4.0 g
Malt extract	10.0 g
Glucose	4.0 g
Agar	18.0 g
ASW	1.0 L

LB (Luria-Bertani) agar	
Peptone 10.0 g	10.0 g
Yeast extract 5.0 g	5.0 g
NaCl 5.0 g	5.0 g
Agar 18.0 g	18.0 g
ASW	1.0 L

M1	
Soluble starch	10.0 g
Yeast extract	4.0 g
Peptone	2.0 g
Agar	18.0 g
ASW	1.0 L

M1_F	
Soluble starch	10.0 g
Yeast extract	4.0 g
Peptone	2.0 g
Agar	18.0 g
ASW	1.0 L

M1_SE	
Soluble starch	10.0 g
Yeast extract	4.0 g
Peptone	2.0 g
Sponge extract	1 g/mL
Agar	18.0 g
ASW	1.0 L

M5	
Polypeptone	10.0 g
Yeast extract	10.0 g
Na_2HPO_4 4.36 g	4.36 g
KH_2PO_4 0.25 g	0.25 g
Ammonium acetate 1.5 g	1.5 g
$MgSO_4 \cdot 7H_2O$	0.2 g
Agar	18.0 g
ASW	1.0 L

MA	
Ammonium acetate	1.5 mg
H_3BO_3	22.0 mg
$CaCl_2$	1.8 g
Ferric citrate	0.1 g
$MgCl_2$	5.9 g
$MgSO_4$	3.2 g
KBr	80.0 mg
KCl	0.5 g
NaCl	19.5 g
$NaHCO_3$	0.16 g
NaF	2.4 mg
$NaPO_3$	8.0 mg
$SrCl_2$	34.0 mg
Na_2O_3Si	4.0 mg
Starch	0.5 g
Yeast extract	1.0 g
Agar	18.0 g
ASW	1.0 L

R2A	
Casamino acids	0.5 g
Dextrose	0.5 g
Peptone	0.5 g
Potassium phosphate	0.3 g
Sodium pyruvate	1.0 g
Starch	0.5 g
Yeast extract	0.5 g
Agar	18.0 g
ASW	1.0 L

OLIGO	
Peptone	1.5 g
Yeast Extract	0.05 g
Sodium phosphate	0.08 g
Glycine	0.08 g
Agar	15 g
ASW	1.0 L

OLIGO_SE	
Peptone 1.5 g	1.5 g
Yeast Extract 0.05 g	0.05 g
Sodium phosphate 0.08 g	0.08 g
Glycine 0.08 g	0.08 g
Sponge extract 1 g/mL	15 g
Agar 15 g	1.0 L

B. Gel-loading buffer (5x)

Gel-loading buffer (5x)	
Bromphenol blue	25.0 mg
Xylene cyanol	25.0 mg
Ficoll (type 400)	1.5 g
Distilled	10.0 ml

C. Ferric reducing antioxidant power solution

Ferric reducing antioxidant power solution	
300 mM acetate buffer in H_2O	25 mL
20 mM ferric chloride hexahydrate (pH 3.6) in H_2O	2.5 mL
10 mM 2,4,6-tripyridyl-s-triazine (TPTZ) in 40 mM HCl	2.5 mL

III. Chemicals and bio-reagents

Name	Manufacturer
Acetic acid	AppliChem
Acetoneitrile	Sigma-Aldrich Co.-Aldrich Co.
Agar	granulated Difco
Agarose ultrapure	Gibco
Ammonium sulfate [$(NH_4)_2SO_4$]	AppliChem
Ampicillin	AppliChem
Arginine	Sigma-Aldrich Co.
Asparagine	Sigma-Aldrich Co.
Boric acid (H_3BO_3)	AppliChem
Bovine serum albumin	Sigma-Aldrich Co.
Bradford dye	BioRad
5-bromo-4-chloro-3-indolyl-β-D-galactoside (X-Gal)	Sigma-Aldrich Co.
Bromphenol blue	Merck
Calcium carbonate ($CaCO_3$)	AppliChem
Calcium chloride ($CaCl_2$)	AppliChem
Chloramphenicol	Sigma-Aldrich Co.
Chloroform	Roth
Cycloheximide	Sigma-Aldrich Co.
DAPI (4´,6-diamidino-2-phenylindole)	Sigma-Aldrich Co.
Diaion HP-20ss	Mitsubishi

Name	Manufacturer
2,7-dichlorodihydrofluorescein diacetate (H2DCF-DA)	Sigma-Aldrich Co.
Dihydroethidium	Sigma-Aldrich Co.
Dimethylsulfoxide	Sigma-Aldrich Co.
3-(4,5-Dimethylthiazol-2-yl)-2,5-Diphenyltetrazolium Bromide	Sigma-Aldrich Co.
Deuterated chloroform	Sigma-Aldrich Co.
D-Leu	Sigma-Aldrich Co.
D-Orn	Sigma-Aldrich Co.
Ethanol absolute (EtOH)	Merck
Ethanol denatured (EtOH)	Roth
Ethyl acetate	Roth
Ferric chloride hexahydrate ($FeCl_3$. $6H_2O$)	Sigma-Aldrich Co.
Fetal bovine serum (FBS)	Sigma-Aldrich Co.
Fluorescein diacetate	Sigma-Aldrich Co.
1-fluoro-2,4-dinitrophenyl-5-L-alanine amid	Sigma-Aldrich Co.
GelRed	Biotrend
Glucose	AppliChem
Glycerin/ Glycerol	Roth
Hydrochloric acid (HCl)	AppliChem
Isopropanol	Roth
Lincomycin	Sigma-Aldrich Co.
L-glutamine	Sigma-Aldrich Co.
L-Leu	Sigma-Aldrich Co.
L-Orn	Sigma-Aldrich Co.
Malt extract	AppliChem
Magnesium chloride hexahydrate (MgCl2.6H2O)	AppliChem
Magnesium sulfate heptahydrate (MgSO4.7H2O)	AppliChem
Methanol	Sigma-Aldrich Co., Roth
Nalidixic acid	Sigma-Aldrich Co.
4-Nitroquinoline 1-oxide (NQO)	Sigma-Aldrich Co.
Nystatin	Sigma-Aldrich Co.
Penicillin	Sigma-Aldrich Co.
Peptone	Roth
Phalloidin555	Life Technologies
Phenol	AppliChem
Potassium acetate	AppliChem
Potassium acetate	AppliChem
Potassium bromide (KBr)	AppliChem
Potassium chloride (KCl)	Fluka
Potassium phosphate	Sigma-Aldrich Co.
Sodium bicarbonate (NaHCO3)	Merck
Sodium chloride (NaCl)	Roth
Sodium fluoride (NaF)	Fluka

Name	Manufacturer
Sodium pyruvate	Sigma-Aldrich Co.
Sodium sulfate (Na2SO4)	Merck
Starch	Roth
Streptomycin	Sigma-Aldrich Co.
Strontium chloride ($SrCl_2$)	Fluka
Tetracycline	Sigma-Aldrich Co.
Trifluoroacetic acid (TFA)	Sigma-Aldrich Co.
2,4,6-tripyridyl-s-triazine (TPTZ)	Sigma-Aldrich Co.
Tryptone	Roth
Yeast extract	Gibco

IV. Software

Software	Application	Reference
Align	Sequence alignment and editing	Hepperle 2002
Antimarin Database	Marine natural products database	University of Canterbury, New Zealand
Basic Local Alignment Search Tool (Blast)	Searching within the sequences stored in the database	http://www.ncbi.nlm.nih.gov/BLAST/
ChemDraw	Drawing of chemical structure	Chem Office 2014
Chemspider	Searching chemistry	http://www.chemspider.com/
Dictionary of Natural Products	Natural products database	
Geneious	Alignment of sequences	http://www.geneious.com/
GENtle	Sequences editing	University of Cologne
iTOL web	Phylogenetic tree builder	http://itol.embl.de/
MassConverz tool ProteoWizard	Mass data slicer	http://proteowizard.sourceforge.net/
Mnova	Visualisation and processing of spectral data	Mestrelab research
MzMine2.12	A framework for differential analysis of mass spectrometry data	http://mzmine.github.io/
SciFinder	natural products access tool	http://www.cas.org/products/scifinder
SIMCA	Metabolomics analysis	MKS
SINA web aligner		
Xcalibur	LC-MS data processing software	Thermo Fisher Scientific

V. Kits

Kit	Kit Manufacturer
FastDNA® spin kit for soil	Q-Biogene
Proteinase K	Sigma-Aldrich Co.
REDTaq® ReadyMixTM PCR reaction mix	Sigma-Aldrich Co.
GeneRulerTM 1kb DNA ladder	Fermentas
Ridascreen ® Verotoxin ELISA kit	R-biopharm

VI. Equipment and Supplies

Equipment	Manufacturer
Autoclave (Tec 120, 9191E, FV 3.3) (Varioklav 500, 135S)	Fedegari H+P Labortechnik
Benchtop centrifuge (Biofuge Frasco)	Hereaus Instruments
Distilling apparatus for H_2O_{dd} (Bi-Dest 2304)	GFL
Disposable cuvettes (halbmikro 1,5 ml)	Plastibrand
Gel documentation (Gel Doc 2000)	BioRad
Gel electrophoresis chamber	BioRad
Gel electrophoresis chamber	BioRad
Heat block (Digi-Block Jr.)	Laboratory Devices
HPLC	Angilent
HPLC columns (Chromolith RP18)	Phenomenex
Ice maker (AF-20)	Scotsman
Incubator (Kelvitron®t)	Heraeus
Incubator (TV 40b)	Memmert
Magnetic stirrer (L32)	Labinco
Micropipettes (MicroOne 0,5-10 µL)	Microlab
Micropipettes (MicroOne 2.0-20 µL)	Microlab
Micropipettes (MicroOne 20-200 µL)	Microlab
Micropipettes (MicroOne 100-1000 µL)	Microlab
Microwave (Micromat)	AEG
MS (Micromass Q-TOF, MicroTOF)	Bruker Daltonik
MS (Q-Extractive)	ThermoFisher Scientific
NMR (400, 600 MHz)	Bruker
PCR cycler (T3-Thermocycler)	Biometra
pH Meter (MultiLine P4, SenTix 41)	WTW
Rotary evaporator (Laborota 4010)	Heidolph
Spectrophotometer (Ultraspec 3000)	Pharmacia Biotech
Speedvac concentrator (Savant)	Thermo Scientific
Shakers (Certomat U)	Braun
Shakers (SM-30)	Edmund Bühler
Shakers (Rotationsmischer 3300)	Eppendorf
Shakers (HT)	Infors

VII. Microorganisms and cells

Microorganisms/cells	Application
***Bacillus* sp.**	Disc diffusion assay
***Aspergillus* sp.**	Disc diffusion assay
***Escherichia coli* ATCC 11229**	Anti-Stx bioassay
***Trypanosoma brucei brucei* 221**	Antitrypanosomal bioassay
Chlamydia trachomatis	Antichlamydial bioassay
Human cervix carcinoma cell line HeLa	Antichlamydial and antioxidant bioassays
Human breast adenocarcinoma cells MCF-7	Cytotoxic bioassay
Human promyelocytic cell line HL-60	Cytotoxic bioassay

VIII. Oligonucleotide primers

Oligonucleotide	Sequence 5' – 3'	Annealing (°C)	Specificity
27f	GAGTTTGATCCTGGCTCA	56	Bacterial 16S rRNA gene (universal)
1492r	TACGGCTACCTTGTTACGACTT	56	Bacterial 16S rRNA gene (universal)

IX. Special laboratory tools

Tool Manufacturer	Tool Manufacturer
Cryotubes (1.5 ml)	Greiner Bio-One
Eppendorf tubes	Sarstedt
Falkon tubes (50 ml)	Cell star
Filter paper discs (5 mm)	Roth
96-well plates	Greiner Bio-One
Parafilm	Pechiney
PCR tubes (0.5 ml) B.	Braun
Pipette tips	Sarstedt
Petri Dishes (145/20 mm)	Greiner Bio-One
Petri Dishes (60/20 mm)	Greiner Bio-One
Syringe filters (0.2 µm)	Schleicher & Schuell
Serological pipettes	Sarstedt

Supplementary information

Fig. S1 EI mass spectrum of 2,3-dihydroxybenzoic acid (**1**)

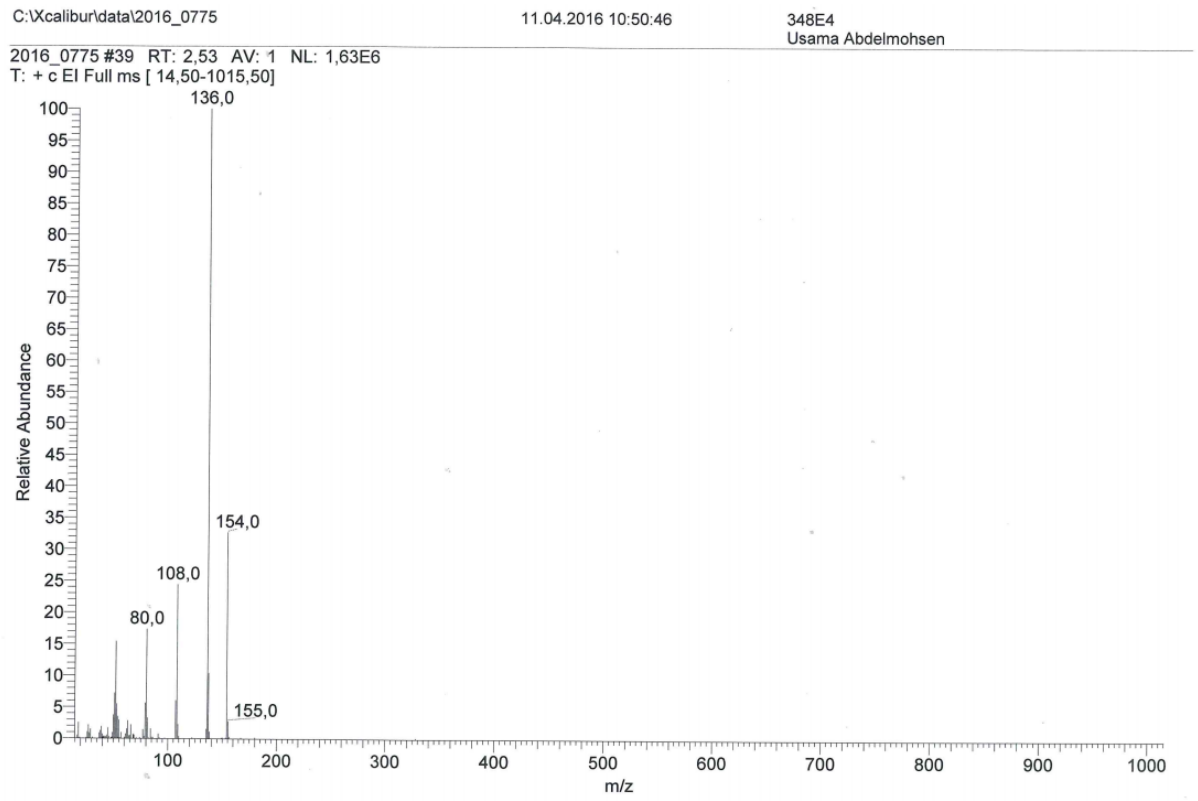

Fig. S2 EI mass spectrum of 2,3-dihydroxybenzamide (**2**)

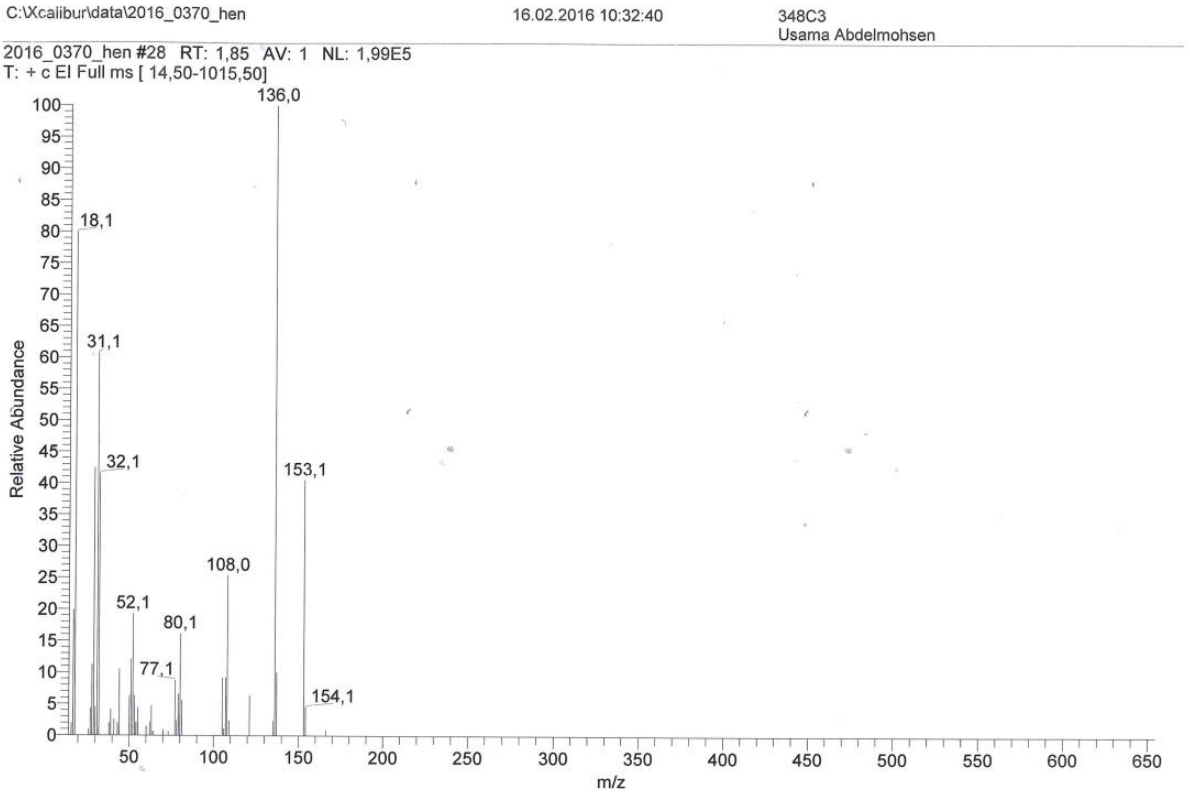

Fig. S3 EI mass spectrum of maltol (**3**)

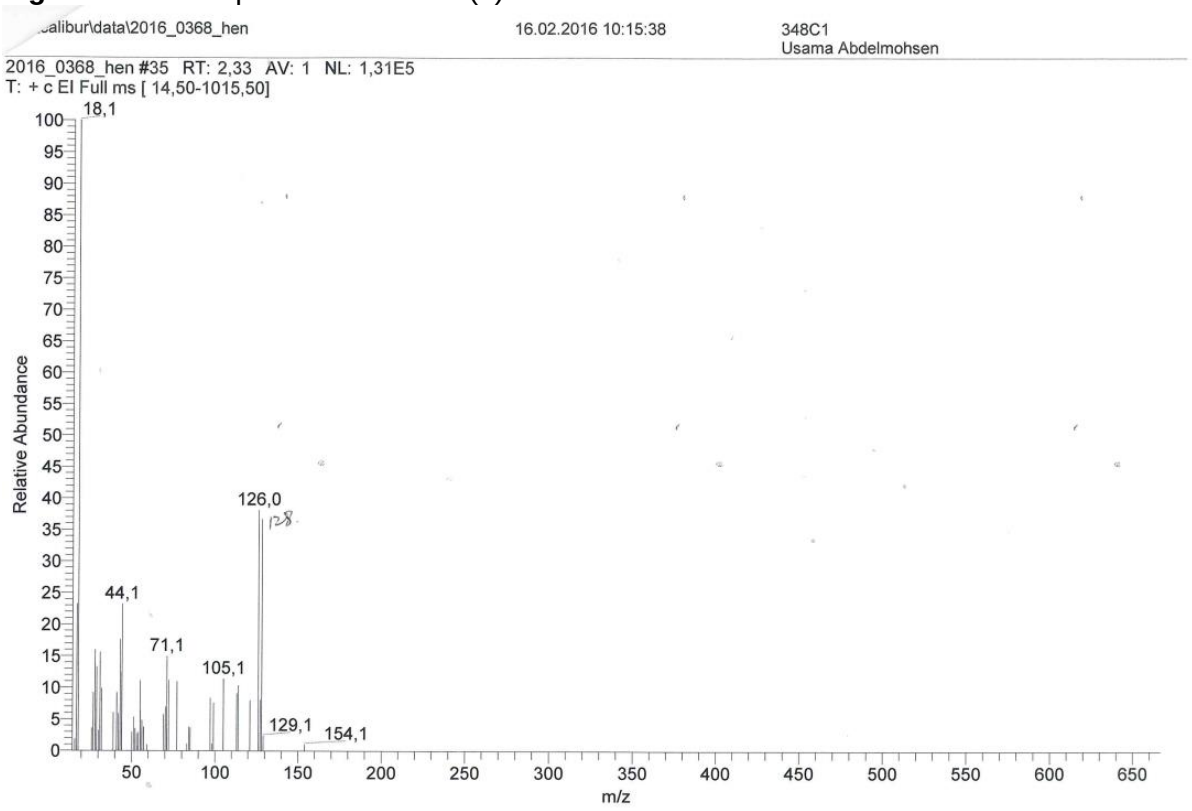

Fig. S3 ESI-HRMS spectrum of petrocidin A (**4**)

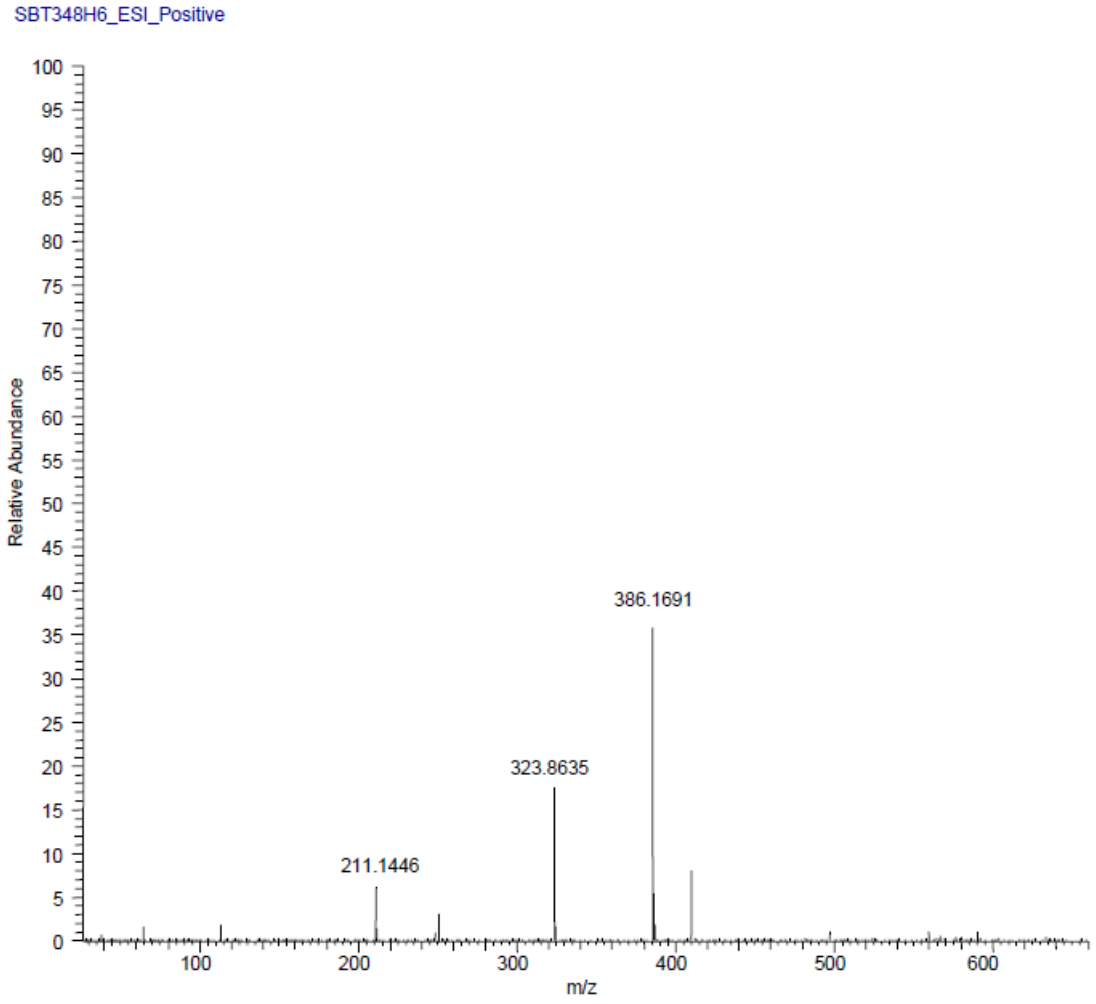

Fig. S5 ESI-HRMS (a) and ESI-HRMS^2 (b, 25eV) spectra of strepthonium A (**5**) positive ionization mode

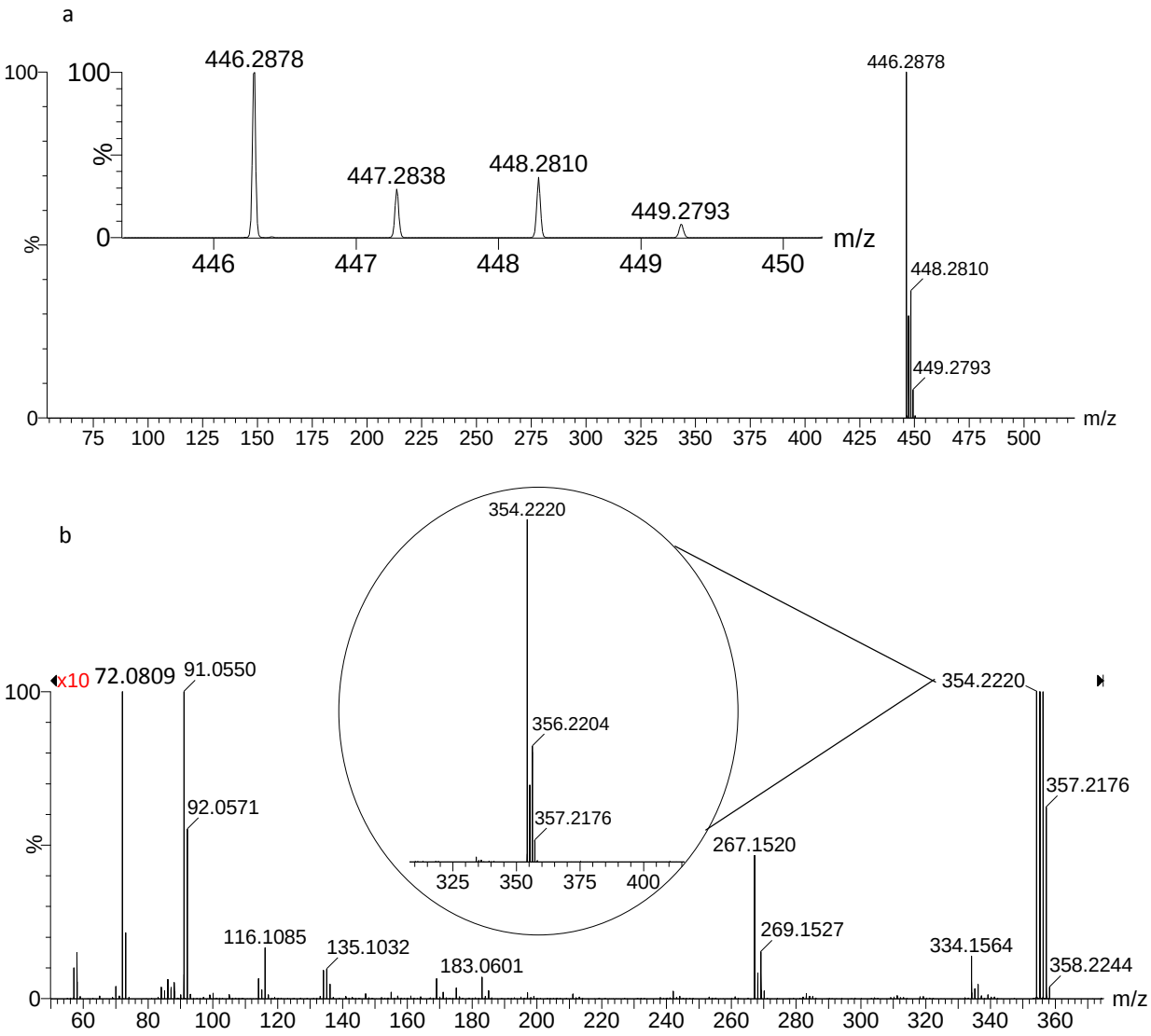

Fig. S6 Proposed mechanistic pathway for the fragmentations of strepthonium A (**5**) in positive ionization mode

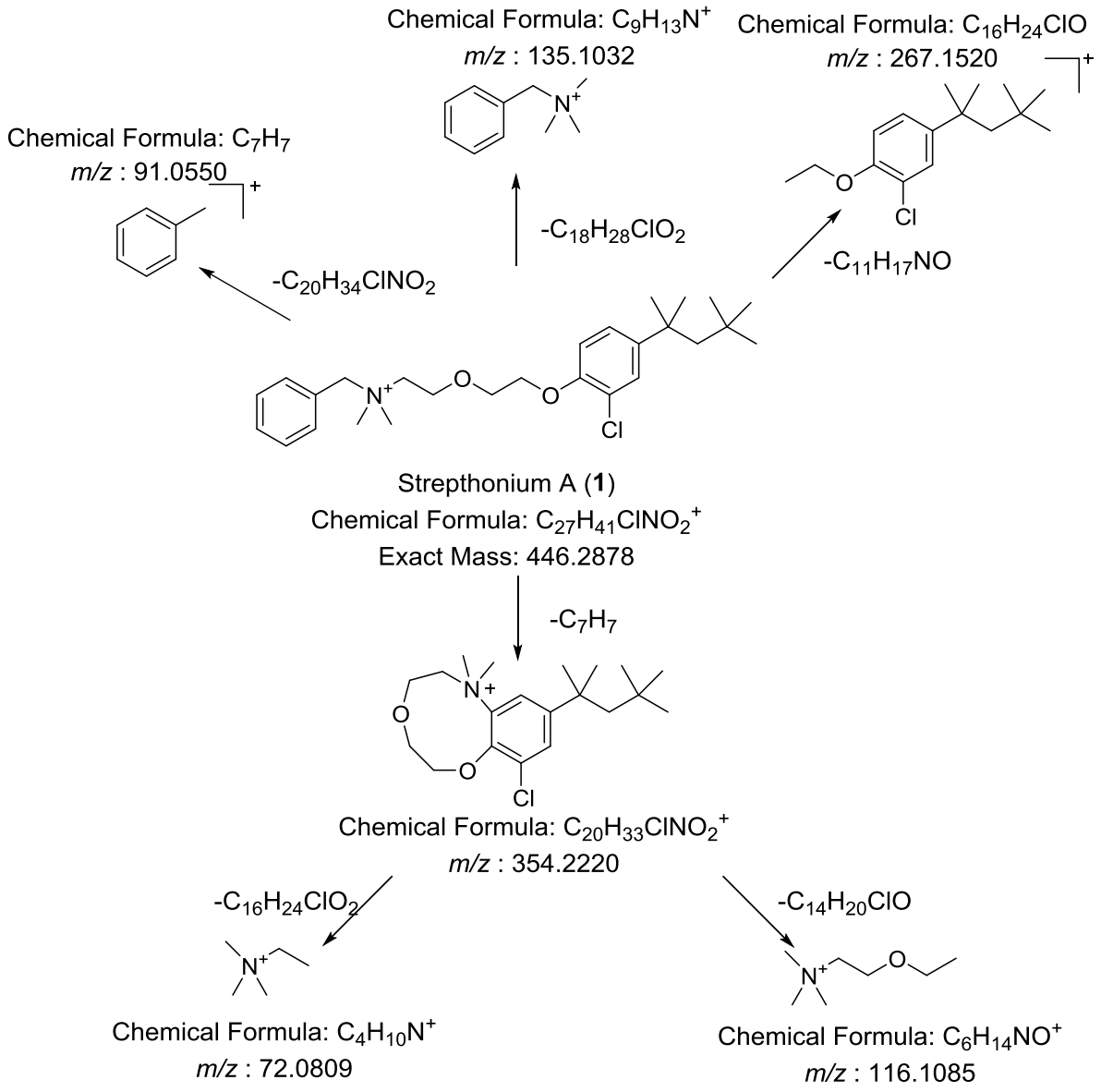

Fig. S7 ESI-HRMS spectrum of ageloline A (**6**) in positive ionization mode

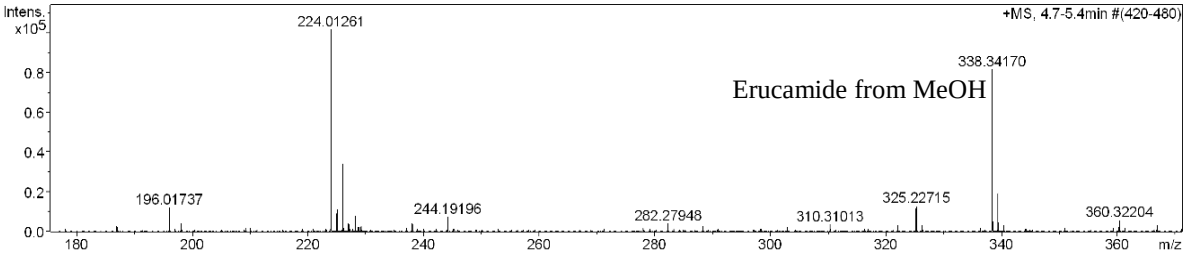

Fig. S8 ESI-HRMS spectrum of phencomycin (**7**) in positive ionization mode

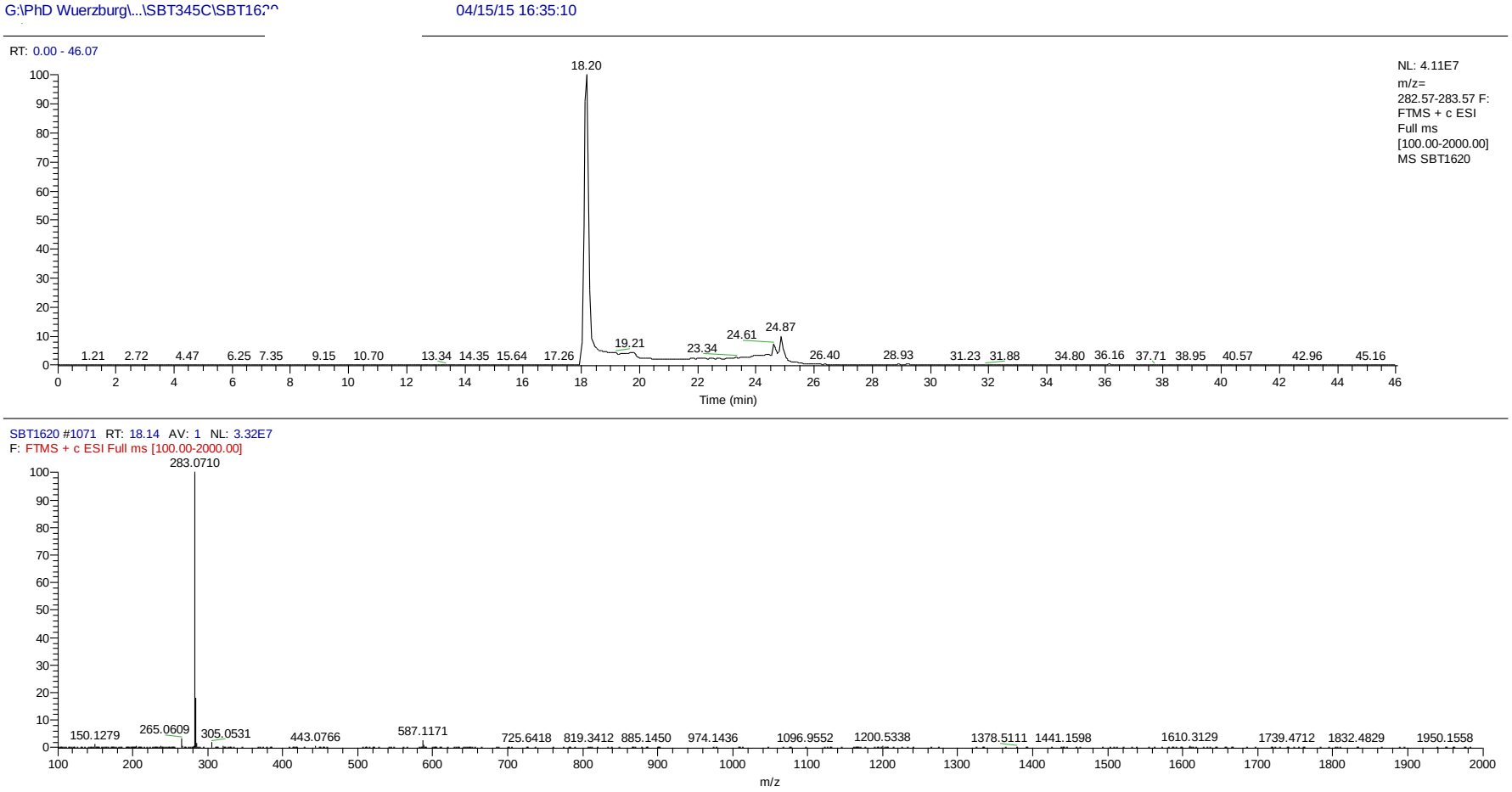

Fig. S9 ESI-HRMS spectrum of tubermycin B (**8**) in positive ionization mode

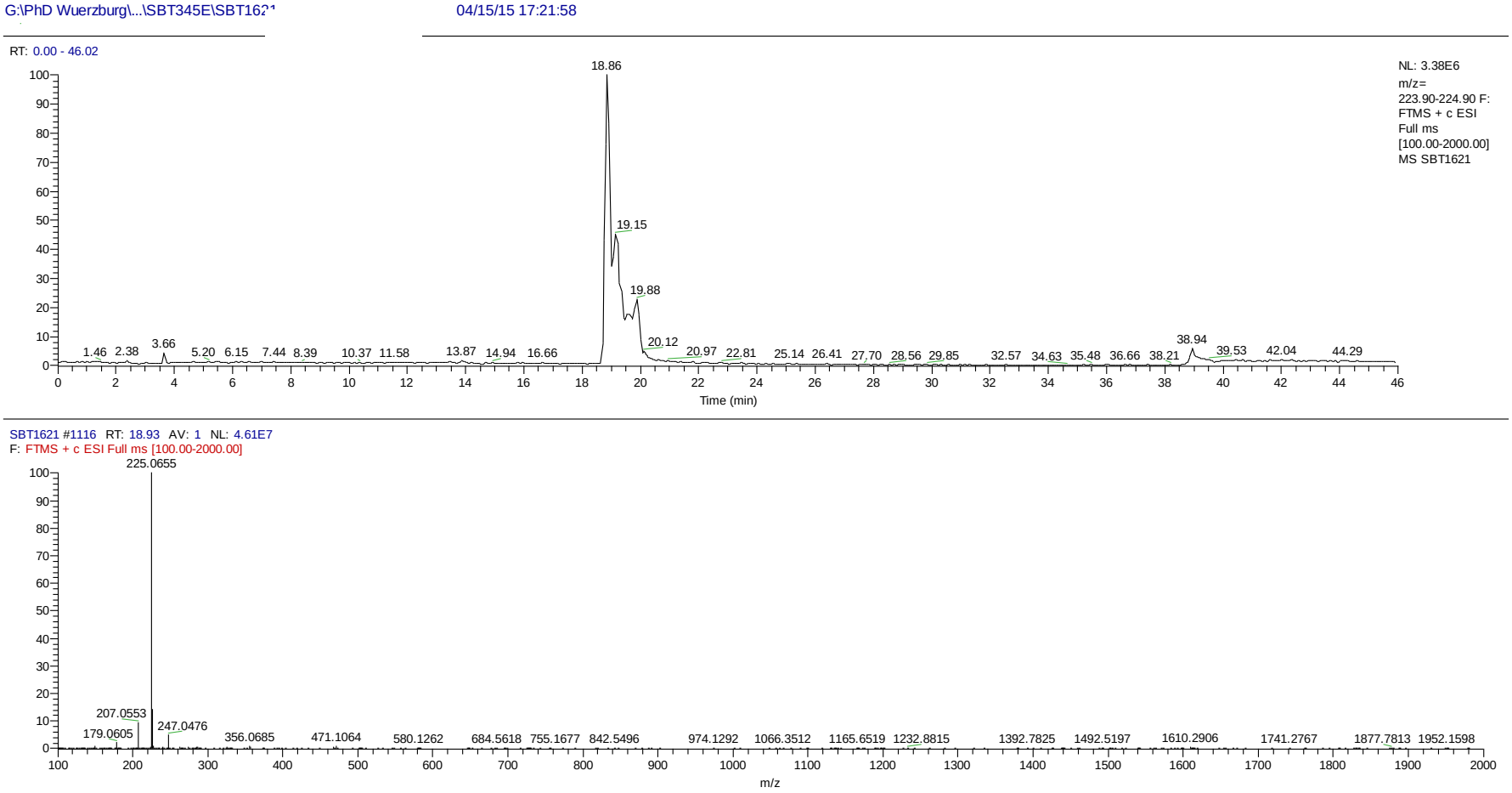

Fig. S10 ESI-HRMS^2 (10 eV) spectra of strepoxazine A (**9**), (a) negative ionization mode; (b) positive ionization mode

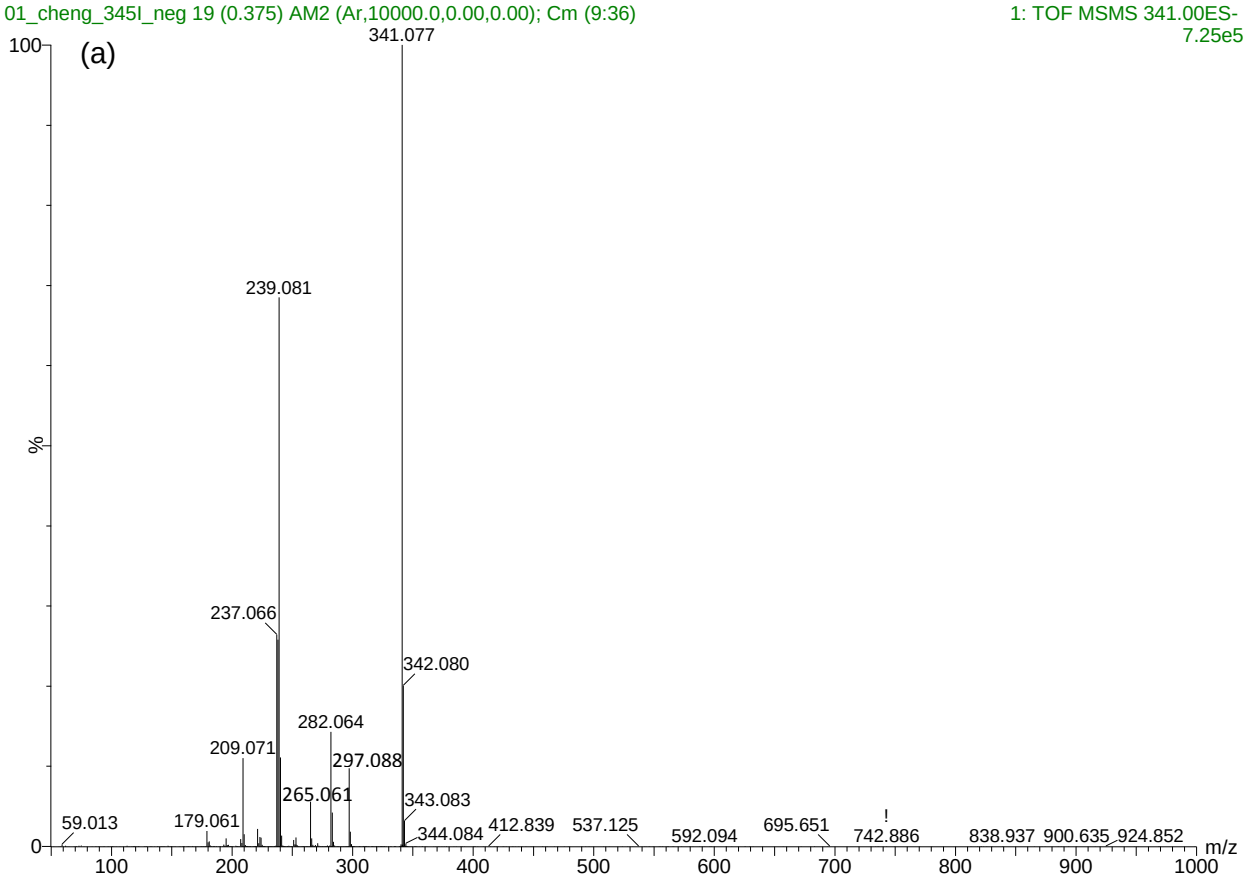

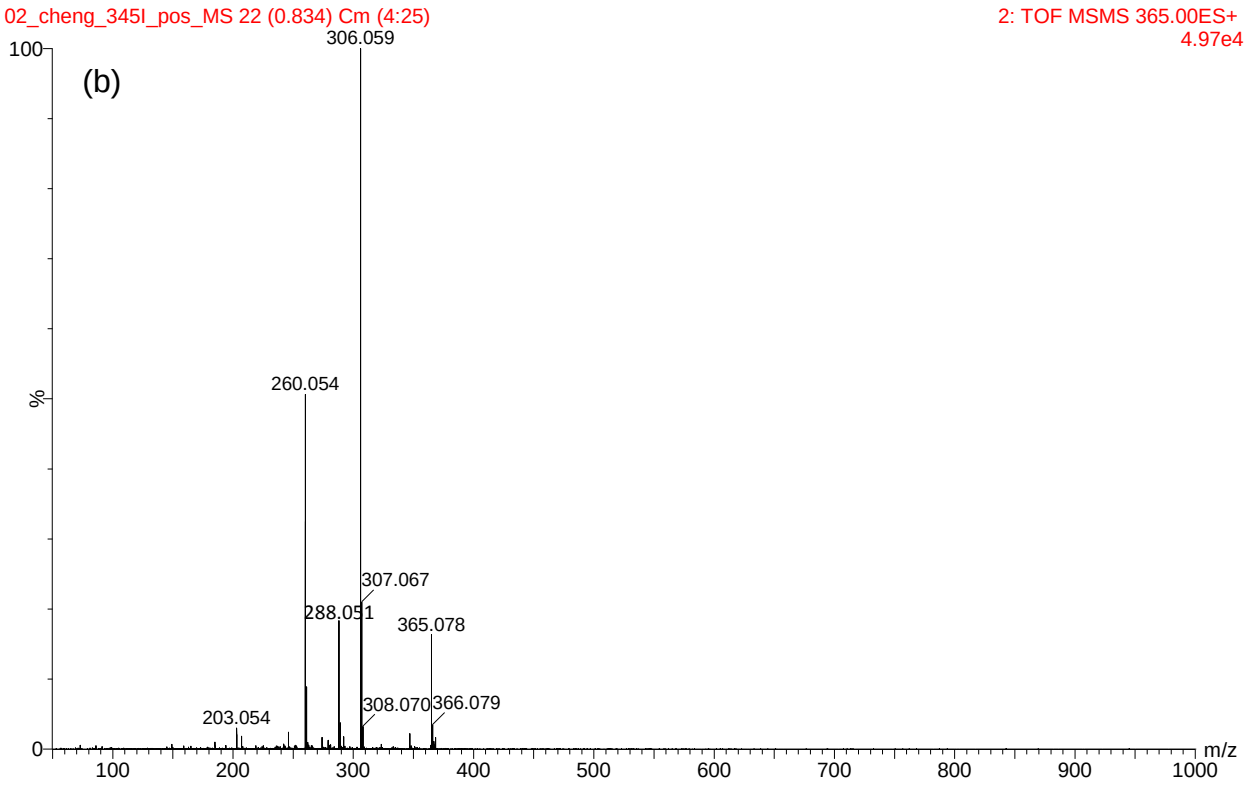

Fig. S11 ESI-HRMS^2 fragmentation of strepoxazine A (**9**) in negative ionization mode

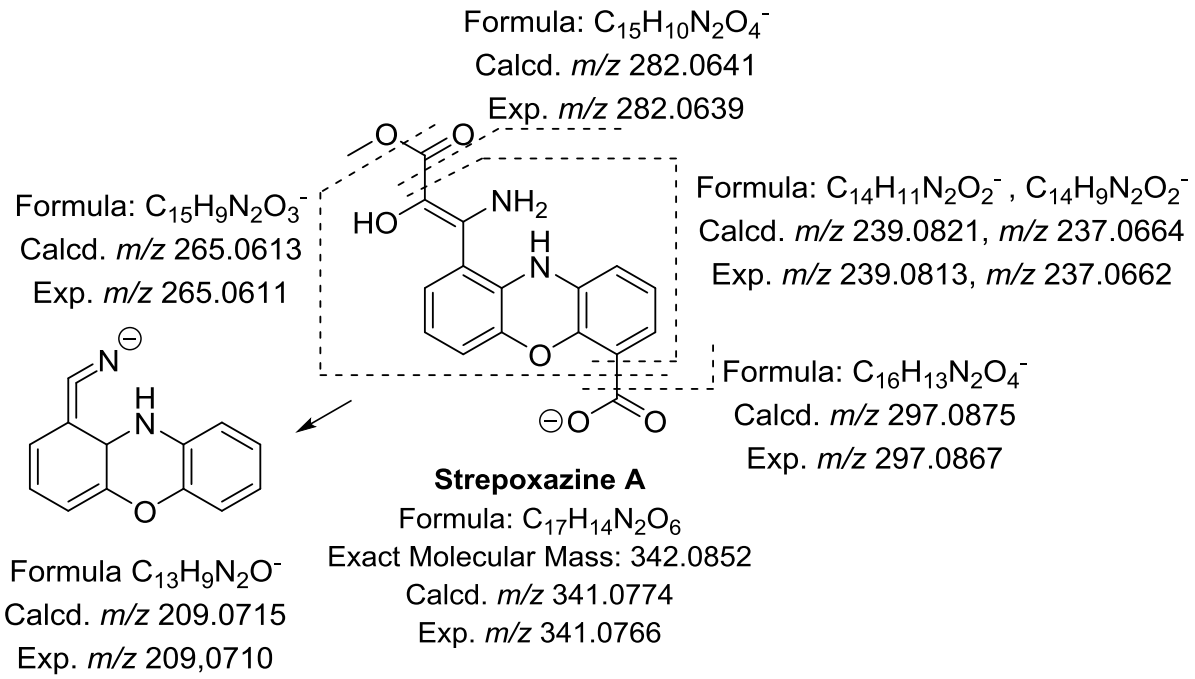

Fig. S12 ESI-HRMS^2 fragmentation of strepoxazine A (**9**) in positive ionization mode

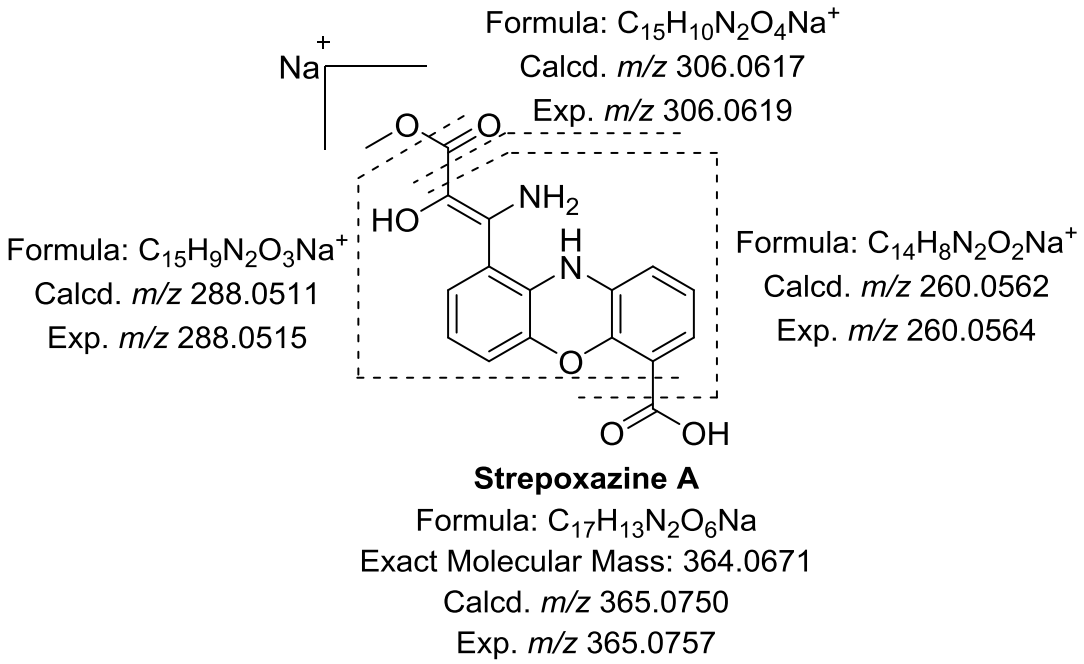

Publications

1. **Cheng, C.**, Othman, E.M., Fekete, A., Krischke, M., Stopper, H., Edrada-Ebel, R., Mueller, M.J., Hentschel, U., and Abdelmohsen, U.R.: Strepoxazine A, a new antiproliferative phenoxazine from the marine sponge-derived bacterium *Streptomyces* sp. SBT345. *J Antibiotics*, under review.
2. **Cheng, C.**, Balasubramanian, S., Fekete, A., Krischke, M., Mueller, M.J., Hentschel, U., Oelschlaeger, T.A., and Abdelmohsen, U.R.: Inhibitory potential of strepthonium A against Shiga toxin production in EHEC strain EDL933. *Int J Med Microbiol*, under review.
3. **Cheng, C.**, Othman, E.M., Reimer, A., Matthias, Grüne, Kozjak-Pavlovic, V., Stopper, H., Hentschel, U., and Abdelmohsen, U.R.: Ageloline A, new antioxidant and antichlamydial quinolone from the marine sponge-derived bacterium *Streptomyces* sp. SBT345. *Tetrhedron Lett*. 57, 2786-9 (**2016**).
4. Horn, H., **Cheng, C.**, Edrada-Ebel, R., Hentschel, U., and Abdelmohsen, U.R.: Draft genome sequences of three chemically rich actinomycetes isolated from Mediterranean sponges. *Mar Genomics* 3, 285-7 (**2015**).
5. Abdelmohsen, U.R., **Cheng, C.**, Reimer, A., Kozjak-Pavlovic, V., Ibrahim, A.K., Rudel, t., Hentschel, U., Edrada-Ebel, R., and Ahmed. S.: New antichlamydial sterol from the Red Sea sponge *Callyspongia aff. implexa*. *Planta Med*. 81, 382-7 (**2015**).
6. **Cheng, C.,** MacIntyre, L., Abdelmohsen, U.R., Horn, H., Polymenakou, P.N., Edrada-Ebel, R., Hentschel, U.: Biodiversity, antitrypanosomal activity screening, and metabolomics profiling of actinomycetes isolated from Mediterranean sponges. *PLoS One*. 10 (9): e0138528 (**2015**).
7. Macintyre, L., Zhang, T., Viegelmann, C., Martinez, I.J., **Cheng, C.**, Dowdells, C., Abdelmohsen, U.R., Gernert, C., Hentschel, U., and Edrada-Ebel, R.: Metabolomic tools for secondary metabolite discovery from marine microbial symbionts. *Mar Drugs*. 12, 3416-48 (**2015**).
8. Abdelmohsen, U.R., **Cheng, C.**, Viegelmann, C., Zhang, T., Grkovic, T., Quinn, R.J., Ahmed, S., Hentschel, U., and Edrada-Ebel, R.: Dereplication strategies for targeted isolation of new antitrypanosomal actinosporins A and B from a marine sponge associated-*Actinokineospora* sp. EG49. *Mar Drugs*. 12, 1220-44 (**2014**).

Symposia and conferences

09th – 10th Oct 2013, Würzburg, GSLS SCI Scientific Crosstalk

Poster Presentation: Micro Organism, Macro Function: the search for novel anti-infective secondary metabolites from marine sponge-associated actinomycetes

20th – 22nd Nov 2013, Würzburg, 3rd International Symposium of the SFB630

Poster Presentation: Novel agents against infectious diseases - an interdisciplinary approach

18th – 19th Aug 2014, Reykjavík, SeaBioTech Annual Meeting in Iceland

Oral Presentation: Metabolomics analysis and dereplication-based prioritization of selected actinomycete strains from the Milos sponge collection

08th Feb 2015, Würzburg, SFB630 Symposium

Oral Presentation: Biodiversity, anti-trypanosomal activity screening, and strain prioritization of sponge-associated actinomycetes

27th – 28th Aug. 2015, Glasgow, SeaBioTech Annual Meeting in Glasgow

Oral Presentation: Contribution to WP5 natural products - metabolomics

30th Aug – 02nd Sep 2015, Glasgow, 9th European Conference on Marine Natural Products

Poster Presentation: Discovery of biologically active compounds from marine sponge-associated actinomycetes

14th – 15th Oct 2015, Würzburg, GSLS Eureka 10th International Students Symposium

Poster Presentation: Biodiversity, antitrypanosomal activity screening, and candidate strain prioritization of actinomycetes isolated from Mediterranean sponges

06th – 11th Mar 2016, Los Angeles, Gordon Research Conference Marine Natural Products 2016

Poster Presentation: Metabolomics tools and dereplication-based isolation of novel bioactive natural products from marine sponge-associated actinomycetes

Workshops

16th May 2014, Würzburg, Missionsärtztliche Klinik

Seminar Title: Workshop zu Infektionen durch Kinetoplastiden

18th – 19th Dec 2014, Retzbach, 8th Joined Ph.D. Student Meeting: New Trends in Infectious Disease Research

Scientific course: R language

30th Aug 2015, Glasgow, PharmaSea

Seminar Title: ECMNP 2015 pre-conference workshop

Curriculum Vitae

Personal information

Name	Cheng Cheng
Date of birth	20th Oct 1987
Place of birth	Tianjin, China
Nationality	Chinese
Lanuguage	Chinese (mother tongue), English (fluent), German (basic)

Education

Apr 2013 ~ present	**University of Würzburg** Ph.D. dissertation “Metabolomics and dereplication-based isolation of novel bioactive natural products from marine sponge-associated actinomycetes”
Jan 2012 ~ Jan 2013	**University of Strathclyde** M.Phil. in Pharmaceutical Science
Sep 2010 ~ Sep 2011	**University of Strathclyde** M.Sc. in Pharmaceutical Analysis
Sep 2006 ~ Jul 2010	**Shanghai University of Traditional Chinese Medicine** BSc. (Honors) in Herbal Medicinal Science

Employment history

Mar 2012 ~ Dec 2012	Research assistant Strathclyde Institute of Pharmacy and Biomedical Science, University of Strathclyde, UK
May 2011 ~ Aug 2011	Placement student Process Research and Development site, AstraZeneca, UK